6. SITE 644: NORWEGIAN SEA[1]

Shipboard Scientific Party[2]

HOLE 644A

Date occupied: 8 August 1985

Date departed: 9 August 1985

Time on hole: 34.75 hr

Position: 66°40.7′N, 04°34.6′E

Water depth (sea level; corrected m, echo-sounding): 1227

Water depth (rig floor; corrected m, echo-sounding): 1216

Bottom felt (rig floor; m, drill pipe measurement): 1226.3

Distance between rig floor and sea level (m): 11.1

Total depth (rig floor; m): 1479.1

Penetration (m): 252.8

Number of cores (including cores with no recovery): 34

Total length of cored section (m): 252.8

Total core recovered (m): 238.4

Total recovery (%): 94

Oldest sediment cored:
Depth sub-bottom (m): 252.8
Nature: silty and siliceous muds
Age: Pliocene

HOLE 644B

Date occupied: 9 August 1985

Date departed: 10 August 1985

Time on hole: 20.25 hr

Position: 66°40.7′N, 04°34.6′E

Water depth (sea level; corrected m, echo-sounding): 1227

Water depth (rig floor; corrected m, echo-sounding): 1216

Bottom felt (rig floor; m, drill pipe measurement): 1225.9

Distance between rig floor and sea level (m): 11.1

Total depth (rig floor; m): 1353.6

Penetration (m): 127.7

Number of cores (including cores with no recovery): 15

Total length of cored section (m): 127.7

Total core recovered (m): 103.6

Total recovery (%): 81

Oldest sediment cored:
Depth sub-bottom (m): 127.7
Nature: siliceous ooze and mud
Age: Pleistocene

Principal Drilling Results: The upper Neogene and Quaternary sedimentary section of Hole 644A can be subdivided into two lithologic units:

Unit I. 0–230.9 m. Late Pliocene to Recent. Subunit IA. 0–49.9 m. Late Quaternary. Interbedded dark, carbonate-poor, glacial sandy muds and light, interglacial, calcareous muds. Subunit IB. 49.9–84.2 m. Mid- to late Quaternary. Interbedded dark, carbonate-poor and light, interglacial, calcareous muds, sandy calcareous muds, and marly foraminifer-nannofossil oozes. Subunit IC. 84.2–230.9 m. Late Pliocene to mid-Quaternary. Interbedded dark, carbonate-poor (glacial) muds and sandy muds and light (interglacial) siliceous muds, siliceous nannofossil muds, and nannofossil muds.

Unit II. 230.9–252.8 m. Mid–late Pliocene. Interbedded siliceous oozes and mixed siliceous nannofossil oozes.

Measurements of the remanent magnetic properties provided a complete late Neogene and Quaternary magnetostratigraphy that yielded an age of approximately 2.7 Ma at total depth. The sediments are also highly fossiliferous, which allows us to make detailed descriptions of the history and variability of the Norwegian Current system and the Northern Hemisphere late Cenozoic paleoclimates.

Significant quantities of methane were found, starting at depths below about 22 mbsf and continuing to the bottom of the hole. Large gas-expansion cracks were noted in the cores in the interval 73–159 mbsf. The gas within these cracks was composed of 45%–89% methane. Ethane, propane, and butane were present at low parts-per-million (ppm) levels, particularly toward the bottom of the hole. The composition of the gas mixtures indicates that the methane is of biological origin. The other hydrocarbon gases are probably products of low-temperature diagenesis. One maximum in methane concentration is associated with a sharp seismic marker at the base of lithologic Unit I (229 mbsf). These geochemical results at Site 644 contrast with findings at the two previous sites, where the maximum amount of methane measured was only 23 ppm.

PRINCIPAL RESULTS

ODP Site 644 represents the landward end of a transect of three drill sites across the Vøring Plateau in the Norwegian Sea. This transect was planned to study the variability of the Cenozoic depositional environment under the Norwegian Current. This current transports temperate water from the North Atlantic to the Arctic Ocean and has had an enormous impact on the Northern Hemisphere climate. Site 644 is located in the Vøring Basin close to the inner continental slope and overlies subsided, thinned continental crust. Drilling at Site 644 was limited to 250 mbsf because of safety concerns.

---

[1] Eldholm, O., Thiede, J., Taylor, E., et al., 1987. *Proc., Init. Repts. (Pt. A), ODP*, 104.

[2] Olav Eldholm, (Co-Chief Scientist), University of Oslo, Oslo, Norway; Jörn Thiede (Co-Chief Scientist), Christian-Albrechts-Universität, Kiel, FRG; Elliott Taylor (Staff Scientist), ODP, Texas A&M University, College Station, TX; Colleen Barton, Stanford University, Stanford, CA; Kjell Bjørklund, University of Oslo, Oslo, Norway; Ulrich Bleil, Universität Bremen, Bremen, FRG; Paul R. Ciesielski, University of Florida, Gainesville, FL; Alain Desprairies, Université de Paris Sud, Orsay, France; Diane Donnally, Amoco Production Co., New Orleans, LA; Claude Froget, Faculté des Sciences de Luminy, Marseille, France; Robert Goll, IKU/SINTEF, Trondheim, Norway; Rudiger Henrich, Christian-Albrechts-Universität, Kiel, FRG; Eystein Jansen, University of Bergen, Bergen, Norway; Larry Krissek, Ohio State University, Columbus, OH; Keith Kvenvolden, USGS, Menlo Park, CA; Anne LeHuray, Lamont-Doherty Geological Observatory, Palisades, NY; David Love, University of Waterloo, Ontario, Canada; Peter Lysne, Sandia National Laboratory, Albuquerque, NM; Thomas McDonald, Texas A&M University, College Station, TX; Peta Mudie, Geological Survey of Canada, Nova Scotia, Canada; Lisa Osterman, Smithsonian Institution, Washington, DC; Lindsay Parson, Institute of Oceanographic Sciences, Surrey, UK; Joseph Phillips, University of Texas, Austin, TX; Alan Pittenger, Texas A&M University, College Station, TX; Gunnbjørg Qvale, Norsk Hydro, Oslo, Norway; Günther Schönharting, University of Copenhagen, Copenhagen, Denmark; Lothar Viereck, Ruhr Universität, Bochum, FRG.

Hole 644A was double cored to 252.8 m using the advanced-piston-core (APC) technique. Thirty-four cores yielded a recovery of 94%. Hole 644B reached 127.7 m with 81% recovery in 15 cores. Drilling results are summarized in Figure 1.

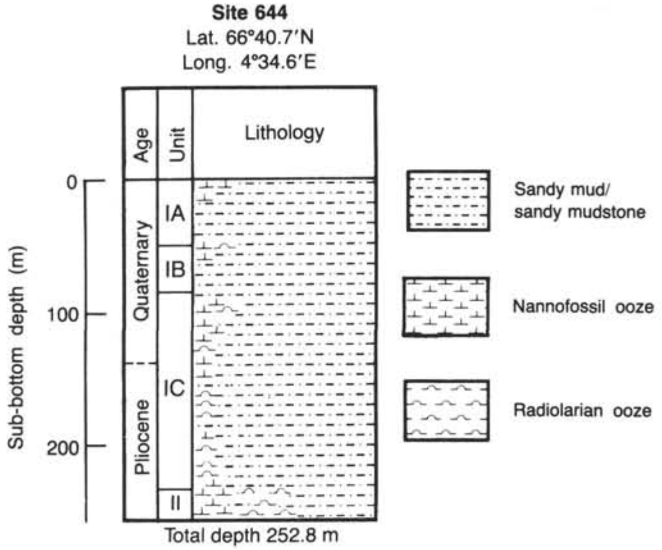

Figure 1. Core-summary column of Hole 644A.

SCIENTIFIC OBJECTIVES

Site 644 is located at the landward end of the paleoenvironmental transect (see Fig. 12b in Chapter 1, this volume). Because of safety concerns, Site 644 could be drilled to a maximum of 250 mbsf or to APC refusal. The site therefore is entirely devoted to the history of the paleoclimate and paleoceanography of the eastern Norwegian Sea during the later part of the Cenozoic.

Site 644 is located on the inner Vøring Plateau, close to the foot of the inner continental slope, in approximately 1200 m of water (Fig. 2). A thick, relatively undisturbed Quaternary to Miocene section was revealed in this region from earlier drilling (DSDP Leg 38) and in MCS line NH-1 (Fig. 3).

The main objectives for drilling Site 644 were:

1. To sample an upper Cenozoic high-sedimentation-rate depositional sequence to obtain a high temporal resolution of depositional history (by applying sophisticated micropaleontological, O-isotopic, paleomagnetic, and amino acid epimerization dating techniques).
2. To establish the paleoceanographic history of the eastern margin of the Norwegian Current, with particular emphasis on its glacial-interglacial fluctuations and its response to the late Neogene climates prior to the evolution of a glacial paleoclimate in the Northern Hemisphere.
3. To define the gradients that developed among the transect sites with increasing distance from shore and decreasing influence of terrigenous sediment components (including pollen).
4. To define source regions for the ice-rafted material in the glacial part of the upper Cenozoic sediment sequence.
5. To document the downcore lithostratigraphy and changes of physical properties when evaluating the stability of the sediment.

OPERATIONS

Holes 644A/B—Vøring Basin

The final drill site was at the landward end of the three-site transect of the Vøring Plateau area. The pipe trip at Hole 644A began just 9.5 hr after departure from the previous site. Water depth was only 1227 m (PDR), and Norwegian authorities had set a penetration limit of a maximum of 250 m or APC refusal, whichever came first. The site therefore was destined to be a quick double-APC effort that had to be completed in a little more than two days to meet the required departure time for Stavanger, Norway.

Because of the brief site time and the shallow water, no positioning beacon was free-dropped, but a single beacon was lowered on the rig's taut wire system. This tactic proved successful at Site 644 because no major change in environmental conditions forced a radical heading change with pipe below the seafloor. Had that occurred, we would have had to drop a second beacon for reference while the taut wire–deployed unit was raised and reset.

The first APC core established seafloor depth at 1226.3 m. Continuous APC cores then were taken until we reached the depth limitation (Table 1). The stiff glacial muds were far from ideal for hydraulic piston coring, but the section was recovered fairly completely. We experienced an inordinate number of core-liner failures, seal failures, and cores jamming in barrels. The plastic liner failures were caused partly by the nature of the sediment and partly by defects in the liners themselves. The pace at which the cores arrived on deck kept both the rig crew and the scientific staff struggling to keep up, which left no time for dealing with mechanical problems. The hole was spudded at 1540 hr, 8 August, and 110.5 m of core was received in the laboratory by midnight. By the second day, we had set aside several jammed core barrels and malfunctioning coring assemblies to make room for more core.

An additional complication to core handling and processing was the presence in the cores of a considerable amount of methane gas, which was not unexpected because of past experience in the area and the nature of the sediments. Gas was noted below about 50 mbsf, with the greatest amount present around 120 m. Expansion and pockets inside the liners contributed to jamming and caused significant core disturbance.

Overpull on retraction of the core barrels approached but did not reach the 100,000-lb figure that defines APC "refusal" on the basis of tensile strength of the coring assembly. Some short-stroke cores were recovered near the base of the mud section, but a marked improvement in penetration and recovery was noted when Pliocene biogenic oozes were reached below about 229 mbsf.

Because of the presence of hydrocarbon gas, we filled the hole with barite-weighted drilling mud before the core bit was pulled above the seafloor to spud the second hole.

When the seafloor had been cleared, an offset of 61 m was made to the south-southwest before respudding. The seafloor depth of the second hole, Hole 644B, was 1225.9 m.

Hole 644B was a virtual repetition of the coring operation (and problems) of 644A. The core intervals were staggered as much as feasible to provide overlap and to recover any intervals missing from the Hole 644A section. Operating time expired before the complete section could be recored, however, and coring was terminated at 127.7 mbsf. We also had to fill the second hole with heavy mud before the drill string could be recovered. A shipload of weary people departed the Vøring Plateau for the long-awaited port call at 1830 hr, 10 August.

SEDIMENT LITHOLOGY

Lithologic Summary

Site 644 was double-cored; because of time limitations, however, only the cores from Hole 644A were described aboard ship. The cores from Hole 644B were opened and described at shore-based facilities. Barrel sheets and summary diagrams for Hole 644B cores are included here. Because of this delay in obtaining

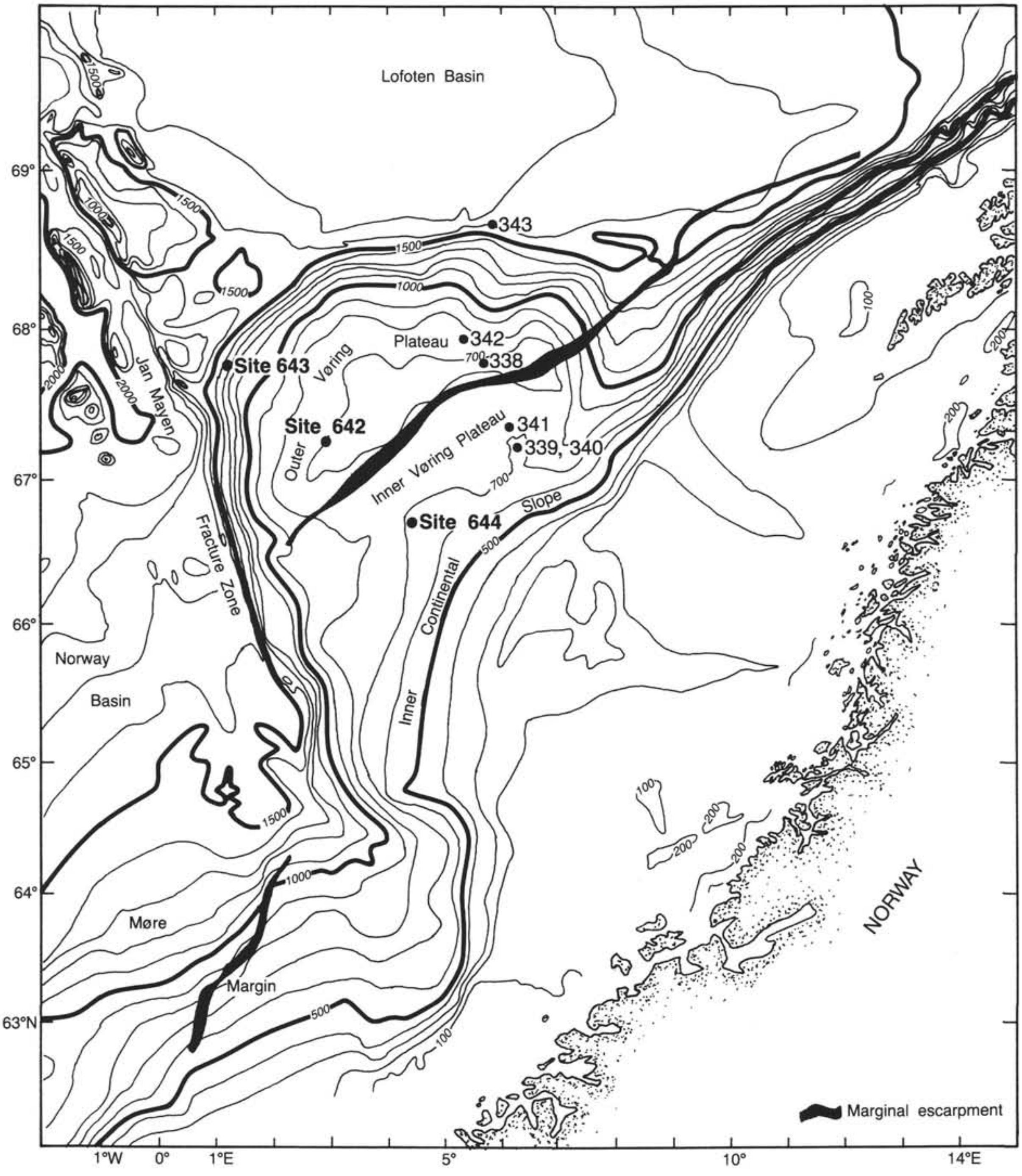

Figure 2. Vøring Plateau morphology and location of ODP Leg 104 drill sites.

information from Hole 644B, lithologic units for Site 644 have been identified on the basis of Hole 644A data; similar patterns of lithologic change can be identified at Hole 644B, although the boundaries around units may appear to vary because of differences in sampling density between Holes 644A and 644B.

The sedimentary sequence drilled at Site 644 has been subdivided into two units: Unit I is a terrigenous-dominated unit of glacial/interglacial depositional cycles, whereas Unit II contains a mixture of terrigenous/siliceous and biogenic deposits. On the basis of compositional differences, Unit I has been divided into three subunits: Subunit IA is almost entirely terrigenous dominated, Subunit IB contains minor amounts of biogenic silica, predominantly sponge spicules, and Subunit IC includes increasing amounts of biogenic silica (diatoms and radiolarians, in addition to sponge spicules), together with nannofossil oozes and muds. The lithologic divisions are summarized in Table 2 and Figure 4, whereas the smear-slide compositional data for these units are included in the barrel sheets (this chapter) and are summarized in Figure 5. Limited additional compositional data were obtained by semiquantitative X-ray-diffraction (XRD) analysis of pressed powders (see "Explanatory Notes," "Shipboard X-ray Diffraction Analysis" this volume, for a more complete

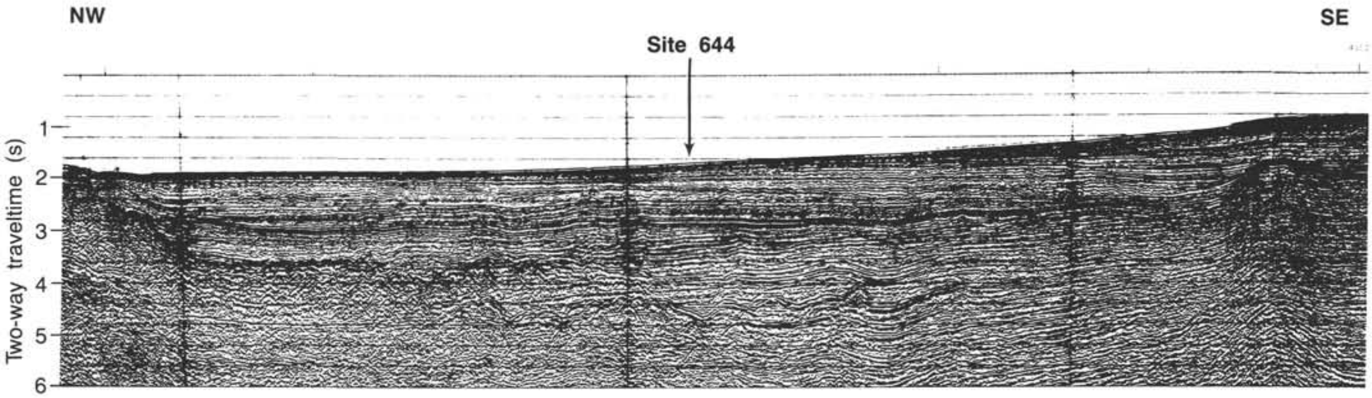

Figure 3. MCS line NH-1 with location of Site 644. Line is crossing the area in northwesterly direction.

explanation of this method); these results are shown in Figure 6. Several distal air-fall tephra deposits were recovered at Site 644; these are discussed separately later.

Lithologic Units

Unit I: Sections 104-644A-1H-1 to 104-644A-30H-4, 26 cm (0–230.86 cm sub-bottom)

Age: late Pliocene to Holocene.

Unit I is a 230-m-thick sequence of glacial/interglacial sedimentary cycles, characterized by repeated alternations of dark, relatively carbonate-poor layers, rich in coarse sandy ice-rafted debris, and light-colored, biogenic-rich layers. In the upper part of Unit I, the light layers are carbonate-rich, while the light layers in the lower part of Unit I are enriched in both carbonate and biogenic silica.

Unit I has been divided into three subunits on the basis of prominent changes in the compositional range, especially the biogenic opal content, of the sediments. Different criteria can be used to subdivide Unit I; these are discussed in more detail later. The major downcore changes in composition, which are evident regardless of the details of Unit I subdivision, are an increase in biogenic siliceous components and an overall decrease in carbonate. These trends are reflected in the graphic summary of smear-slide compositional data (Fig. 5), but are not apparent in the results of the XRD analysis (Fig. 6) because of the limited number of samples analyzed.

Each sedimentary component (clastics, clays, biogenic silica, and biogenic carbonate) exhibits a cyclic pattern of high and low abundances through Unit I, reflecting the alternation of dark and light layers to some extent. Correlations between layer color and carbonate abundance, however, are not as well developed at Site 644 as they were at Sites 642 and 643 because of the presence of detrital and reworked carbonates in Unit I at Site 644. Despite this effect, a strong inverse correlation does exist between calcareous and biogenic siliceous components and the clastic abundance. Variations in the abundance curve of the clastics indicate the episodic and fluctuating input of coarse ice-rafted debris, with major shifts in mean clastic content downcore. Mean clastic content generally increases from 0 to 100 m sub-bottom, decreases rapidly between 100 and approximately 140 m sub-bottom, and increases gradually, but less consistently, from 140 m to the base of Unit I.

On the basis of the compositional changes described earlier, Unit I can be divided into subunits in several different ways. One approach to subdivision is based on apparent changes in the importance of clastic inputs, as interpreted from the smear-slide data and the inversely correlated carbonate curve. This subdivision establishes boundaries at 100 and 142 m sub-bottom, as identified earlier. Sedimentation rates, calculated from shipboard paleomagnetic data, decrease within Unit I, from approximately 11 cm/1000 yr for the interval 0–85 m sub-bottom to approximately 8 cm/1000 yr for the interval 85–230 m sub-bottom. This change in sedimentation rate indicates that the higher clastic content above 110 m reflects an absolute increase in the input rate of clastics at that time and does not merely result from a decreased rate of dilution by other components.

An alternative subdivision, which will be employed in this discussion, is based upon changes in both the abundance of biogenic silica and the types of biogenic siliceous components present. We chose this subdivision because several potential problems, generally related to dilution effects, do exist for the clastic/carbonate ratio approach. A primary difficulty when using the clastic/carbonate ratio for subdivision of Unit I results from the presence of detrital carbonate within this interval (see core-barrel sheets, this chapter, for detailed data). Although the detrital carbonate can generally be distinguished from biogenic carbonate in smear slides, some reworked biogenic carbonate may also be present in these samples. Both of these carbonate sources can be confused with the autochthonous biogenic carbonate signal and can provide clastic/carbonate ratios that do not reflect the true balance of terrigenous and primary biogenic inputs. A second difficulty when using the clastic/carbonate ratio to establish subunits may result from the proximal location of Site 644 relative to the continental source, especially when compared with Sites 642 and 643. A comparison of the clastic content within the glacial/interglacial sequences at Sites 642 (Fig. 4, Site 642 chapter, this volume) and 644 (Fig. 5) indicates that the clastic content has a higher mean value and exhibits greater fluctuations about that mean at Site 644 than at Site 642. Because Site 644 is located at the base of the inner continental slope, changes in circulation patterns on the shelf or in shoreline position could have a significant effect on the clastic input at this site. As a result, changes in clastic/carbonate ratio at Site 644 may be strongly influenced by fluctuations in distance to the terrigenous source, in the inputs of ice-rafted debris (reflecting different compositions and amounts of terrigenous and carbonate constituents), and in the balance of physical and biological processes acting directly at Site 644. Despite these potential difficulties in subdividing Unit I on the basis of clastic/carbonate ratio, our general conclusions concerning environmental transitions through this interval are independent of the subdivisions made; only the physical boundaries of the subdivisions vary using these two approaches.

The biogenic siliceous content and the composition of the siliceous components were used to divide Unit I into three subunits at Hole 644A. The youngest occurrence of biogenic siliceous deposits marks the top of Subunit IB, while the top of

Table 1. Coring summary for Site 644, Leg 104.

Core no.	Core type[a]	Date	Time (LST)	Sub-bottom depths top (m)	Sub-bottom depths bottom (m)	Length cored (m)	Length recovered (m)	Amount recovered (%)
Hole 644A								
1	H	AUG-08-1985	1550	0	9.2	9.2	9.2	100.4
2	H	AUG-08-1985	1630	9.2	16.2	7.0	6.9	98.8
3	H	AUG-08-1985	1703	16.2	25.7	9.5	8.6	90.8
4	H	AUG-08-1985	1735	25.7	35.2	9.5	8.9	93.1
5	H	AUG-08-1985	1814	35.2	44.7	9.5	7.6	80.3
6	H	AUG-08-1985	1846	44.7	54.2	9.5	8.8	92.8
7	H	AUG-08-1985	1925	54.2	63.7	9.5	6.0	62.9
8	H	AUG-08-1985	1957	63.7	73.2	9.5	7.8	82.4
9	H	AUG-08-1985	2035	73.2	82.7	9.5	7.8	82.2
10	H	AUG-08-1985	2125	82.7	92.2	9.5	8.6	90.3
11	H	AUG-08-1985	2212	92.2	101.7	9.5	9.7	101.6
12	H	AUG-08-1985	2255	101.7	111.2	9.5	9.9	103.8
13	H	AUG-08-1985	2330	111.2	120.7	9.5	9.7	101.7
14	H	AUG-09-1985	0019	120.7	130.2	9.5	7.8	81.7
15	H	AUG-09-1985	0135	130.2	139.7	9.5	9.6	100.6
16	H	AUG-09-1985	0305	139.7	149.2	9.5	8.7	91.0
17	H	AUG-09-1985	0355	149.2	158.7	9.5	9.0	94.9
18	H	AUG-09-1985	0455	158.7	168.2	9.5	9.5	99.9
19	H	AUG-09-1985	0555	168.2	177.7	9.5	6.6	69.3
20	H	AUG-09-1985	0705	177.7	184.8	7.1	7.1	99.4
21	H	AUG-09-1985	0810	184.8	186.8	2.0	2.1	105.0
22	H	AUG-09-1985	0920	186.8	194.1	7.3	7.7	105.1
23	H	AUG-09-1985	1000	194.1	201.1	7.0	7.9	113.1
24	H	AUG-09-1985	1115	201.1	206.0	4.9	5.0	101.4
25	H	AUG-09-1985	1210	206.0	210.5	4.5	4.1	90.4
26	H	AUG-09-1985	1308	210.5	214.3	3.8	3.9	101.6
27	H	AUG-09-1985	1421	214.3	216.1	1.8	1.8	101.7
28	H	AUG-09-1985	1457	216.1	221.1	5.0	5.4	108.4
29	H	AUG-09-1985	1535	221.1	226.1	5.0	5.0	99.6
30	H	AUG-09-1985	1616	226.1	232.1	6.0	6.0	100.0
31	H	AUG-09-1985	1709	232.1	238.1	6.0	5.7	94.5
32	H	AUG-09-1985	1805	238.1	243.7	5.6	5.6	99.8
33	H	AUG-09-1985	1940	243.7	246.0	2.3	2.3	99.1
34	H	AUG-09-1985	2047	246.0	252.8	6.8	8.1	119.4
Hole 644B								
1	H	AUG-10-1985	0215	0	4.6	4.6	4.8	103.7
2	H	AUG-10-1985	0255	4.6	14.1	9.5	9.7	102.3
3	H	AUG-10-1985	0333	14.1	23.6	9.5	8.9	93.9
4	H	AUG-10-1985	0410	23.6	33.1	9.5	8.5	89.2
5	H	AUG-10-1985	0448	33.1	42.6	9.5	6.3	66.1
6	H	AUG-10-1985	0520	42.6	52.1	9.5	7.8	82.5
7	H	AUG-10-1985	0610	52.1	61.6	9.5	6.3	65.8
8	H	AUG-10-1985	0630	61.6	71.1	9.5	6.3	66.4
9	H	AUG-10-1985	0716	71.1	80.6	9.5	6.4	67.3
10	H	AUG-10-1985	0805	80.6	90.1	9.5	7.4	77.6
11	H	AUG-10-1985	0845	90.1	95.9	5.8	5.4	92.9
12	H	AUG-10-1985	0937	95.9	105.7	9.8	3.6	37.0
13	H	AUG-10-1985	1030	105.7	111.4	5.7	5.9	102.6
14	H	AUG-10-1985	1213	111.4	119.2	7.8	8.0	102.1
15	H	AUG-10-1985	1351	119.2	127.7	8.5	8.3	97.6

[a] H = hydraulic piston.

Subunit IC is characterized by a major upcore decrease in siliceous components and the youngest abundant appearance of diatoms and radiolarians. The base of Unit I is defined by the oldest occurrence of a discrete dark layer (Fig. 7). Subunits IA and IB are undifferentiated at Hole 644B, but the increased importance of biogenic silica does distinguish Subunit IC at Hole 644B (Fig. 5).

Subunit IA. Sections 104-644A-1H-1 to 104-644A-6H-4, 68 cm (0-49.88 m sub-bottom). Unit IA displays lithofacies similar to those observed at Sites 642 and 643, with alternating dark and light layers as the most prominent feature (Fig. 7). Three types of dark layers occur: dark gray (5Y 4/1) muds, some of them containing a few scattered small dropstones, very dark gray (5Y 3/1) sandy muds with numerous dropstones, and complex dark layers. The complex dark layers are the most diagnostic and consist of a basal, dark-gray (5Y 3/1) sandy mud with numerous dropstones that grades upward into a dark olive gray (5Y 3/2) laminated sandy mud with abundant dropstones and that commonly contains Fe/Mn impregnations. Tops of these complex dark layers are commonly bioturbated. Dark layers at Site 644 contain much more ice-rafted sand than dark layers at Sites 642 and 643, indicating a predominant ice drift along the Norwegian coast and a decrease offshore toward the outer Vøring Plateau. Larger dropstones include a wide spectrum of lithologies, such as basalt, various igneous and metamorphic rock types, and chalk.

The compositional range of the dark layers is 20%-40% quartz, 1%-10% feldspar, 1%-5% detrital carbonates, 1%-5%

Table 2. Summary of lithologic units.

Unit	Lithologic description	Interval (mbsf)	Age	Occurrence (core)
IA	Interbedded dark, carbonate-poor, glacial sandy mud and light, interglacial calcareous muds	0–49.88	Quaternary	104-644A-1H-1 to 104-644A-6H-4, 68 cm
IB	Interbedded dark, carbonate-poor glacial sandy muds and light, interglacial calcareous muds; sandy calcareous muds; and minor marly foraminifer-nannofossil oozes	49.88 to 84.20	Quaternary	104-644A-6H-4, 68 cm, to 104-644A-10H-1, 150 cm
IC	Interbedded dark, carbonate-poor glacial sandy muds/muds and light, interglacial, siliceous muds; siliceous nannofossil muds; and minor nannofossil muds	84.20 to 230.86	Quaternary to Pliocene	104-644A-10H-2, 0 cm, to 104-644A-30H-4, 26 cm
II	Interbedded siliceous oozes and mixed siliceous-nannofossil oozes	230.86 to 252.8	Pliocene	104-644A-30H-4, 26 cm, to 104-644A-34H-7, 27 cm

accessory minerals, and 1%–3% glauconite, as determined by smear-slide analysis. Light layers consist of olive gray (5Y 4/2) and dark grayish brown (2.5Y 3/2) foraminifer-rich calcareous muds, with an average composition of 1%–30% foraminifers, 5%–15% quartz, 40%–60% clay, and 10%–25% detrital carbonate (dolomite-calcite). Samples from Subunit IA analyzed by XRD were all taken from light-colored layers; these have semiquantitative compositions of 50%–60% quartz, 0%–10% feldspar, approximately 30% calcite, and 5%–10% clay minerals (Fig. 6). These clay minerals are illite, chlorite, kaolinite, smectite, and mixed-layer clays (illite-smectite), in order of decreasing abundance. Bioturbation is most commonly present in the form of pyrite-impregnated burrow tubes, 2–3 mm in diameter. This bioturbation form reflects a significant supply of organic matter to the sediments, perhaps derived, at least partially, from the continental shelf. Minor lithologies in Subunit IA include a greenish gray (5GY 5/1) to dark greenish gray (5GY 4/1) marly nannofossil ooze with diffuse bioturbation and common color-banding, which occurs at the base of Subunit IA. This horizon marks the top of the most recent change in the characteristics of interglacial and interstadial sediments within Unit I.

Subunit IB. Samples 104-644A-6H-4, 68 cm, to 104-644A-10H-1, 150 cm (49.88–84.2 m sub-bottom). Subunit IB is characterized by a major change in the lithologic composition of the light layers, with an increase in siliceous and nannofossil contents. The dark layers are represented by the lithofacies types discussed in Subunit IA. One dark layer from Subunit IB was sampled for XRD analysis; this sample shows the low carbonate/clastic ratio generally characteristic of the dark layers (Fig. 6). Dark-gray (5Y 4/1) to dark grayish brown (2.5Y 3/2) and dark greenish gray (5GY 4/1) color-banded calcareous muds and minor marly nannofossil oozes are the most common lithologies within the light-colored horizons. These lithologies are shown in Figure 5, where light layers in Subunit IB generally contain more total biogenic components than light layers in Subunit IA. A similar compositional change, however, is not apparent in the XRD data for these layers (Fig. 6), because of both compositional variability of the light layers and low sampling density of light layers in Subunit IB. A minor but important (5%–10%) siliceous biogenic component, predominantly sponge spicules, is present. The loss of this siliceous component from Subunit IB to Subunit IA indicates the declining influence of open-water conditions upcore, and may reflect a reorganization of surface- and bottom-water current systems, in response to major changes in the amplitude of glacial fluctuations at this time.

Subunit IC. Samples 104-644A-10H-2, 0 cm, to 104-644A-30H-4, 26 cm (84.2–230.86 m sub-bottom). Subunit IC reflects the third shift observed in the glacial/interglacial cycles. Dark layers contain the same lithologies as in Subunit IB, with very high ratios of clastic to biogenic components (Fig. 5). Diatoms and radiolarians, as well as nannofossils, are common to abundant in the light layers, producing a range of light-layer lithologies in Subunit IC (Fig. 5). These changes indicate relatively more open-water conditions than those recorded in Subunit IB. These lithologies include muds and sandy muds (20%–30% quartz, 40%–50% clay, 5%–10% biogenic siliceous components, predominantly sponge spicules), siliceous muds (15%–20% biogenic siliceous components, mainly sponge spicules, diatoms, and radiolarians, 0%–5% nannofossils, 5%–20% quartz, and 50%–80% clay), and siliceous nannofossil muds (10%–40% nannofossils, 10%–25% biogenic siliceous components, and 40%–60% clay). The semiquantitative XRD compositions of two light layers from Subunit IC are generally similar to those of light layers from Subunit IB (Fig. 6); the major difference in composition is the presence of biogenic opal, which is not included in the XRD compositions, in Subunit IC. Dominant colors are dark gray (5Y 4/1), greenish gray (5GY 5/1), and dark greenish gray (5GY 4/1).

Unit II: Samples 104-644A-30H-4, 26 cm, to 104-644A-34H-7, 27 cm (230.86–252.8 m sub-bottom)

Age: mid- to late Pliocene.

Unit II consists of mixed biogenic siliceous and biogenic calcareous lithologies, recording a significant decrease in the importance of clastics relative to Unit I. Most important lithologies are dark greenish gray (5GY 4/1) mottled siliceous muds and muds, siliceous nannofossil oozes, and nannofossil oozes, all with common to abundant, faint pyritized burrows and scattered pyrite concretions.

The muds and siliceous muds show a compositional range of 12%–35% biogenic siliceous components, 0%–1% nannofossils, 5%–25% quartz, and 50%–80% clay, while the nannofossil oozes and siliceous nannofossil oozes contain 40%–70% nannofossils, 15%–45% biogenic siliceous components, 5%–10% quartz, and 10%–30% clay (Fig. 5). The lithologies present in Unit II at Site 644 comprise a spectrum of siliceous muds and siliceous nannofossil oozes that records the existence of open-water, moderately to highly productive surface waters. These lithologies can be correlated, in a general temporal and environmental sense, with the deposits of Unit II at both Sites 642 and

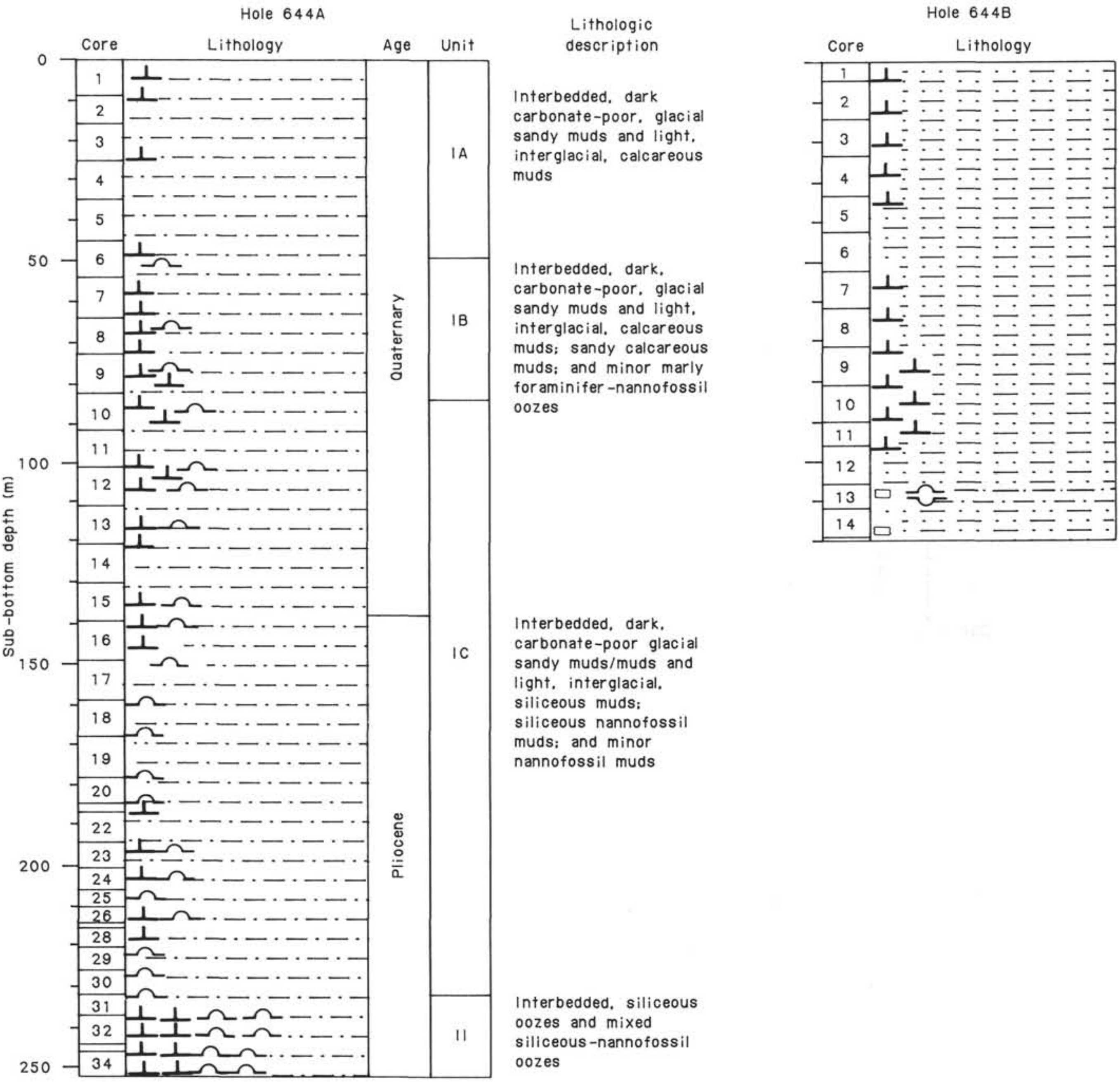

Figure 4. Graphic summaries of lithologic units at Site 644.

643 (see "Sediment Lithology," Sites 642 and 643 chapters, this volume).

Sedimentological Interpretations

Unit I, the glacial/interglacial sequence recovered at Site 644, is the thickest and most variable of the glacial/interglacial sections recovered during Leg 104. Sedimentation rates (approximately 10 cm/1000 yr) are twice as high as at Sites 642 (4.7 cm/1000 yr) and 643, promising a very high-resolution stratigraphic record at this site. The division of Unit I into three subunits of clearly different compositions corresponds to similar, but less pronounced, shifts observed in the lithologies at Sites 642 and 643. In all cases, the major change is a stepwise shift in amplitude and frequency of glacial and interglacial conditions downcore.

The most noticeable visual characteristic of Unit I at Site 644 is the presence of light and dark color-banding, similar to the alternations of light and dark layers observed in Unit I at Sites 642 and 643. The downcore distribution of dark layer coverage is summarized in Figure 7. Variations in this distribution show some correlation with the subdivisions of lithologic Unit I, and also reflect stepwise shifts in amplitude and frequency of glacial/interglacial conditions. The banding patterns at Holes 644A and 644B are similar above 60 m and below approximately 100 m. Differences between the holes in the interval from 60 to 100 m may reflect the decreased core recovery at Hole 644B. The glacial maxima (dark layers) at Site 644 are represented by thick beds that contain considerably higher amounts of ice-rafted debris than at the previous two sites. This increase probably reflects the proximity of Site 644 to a calving ice front, which

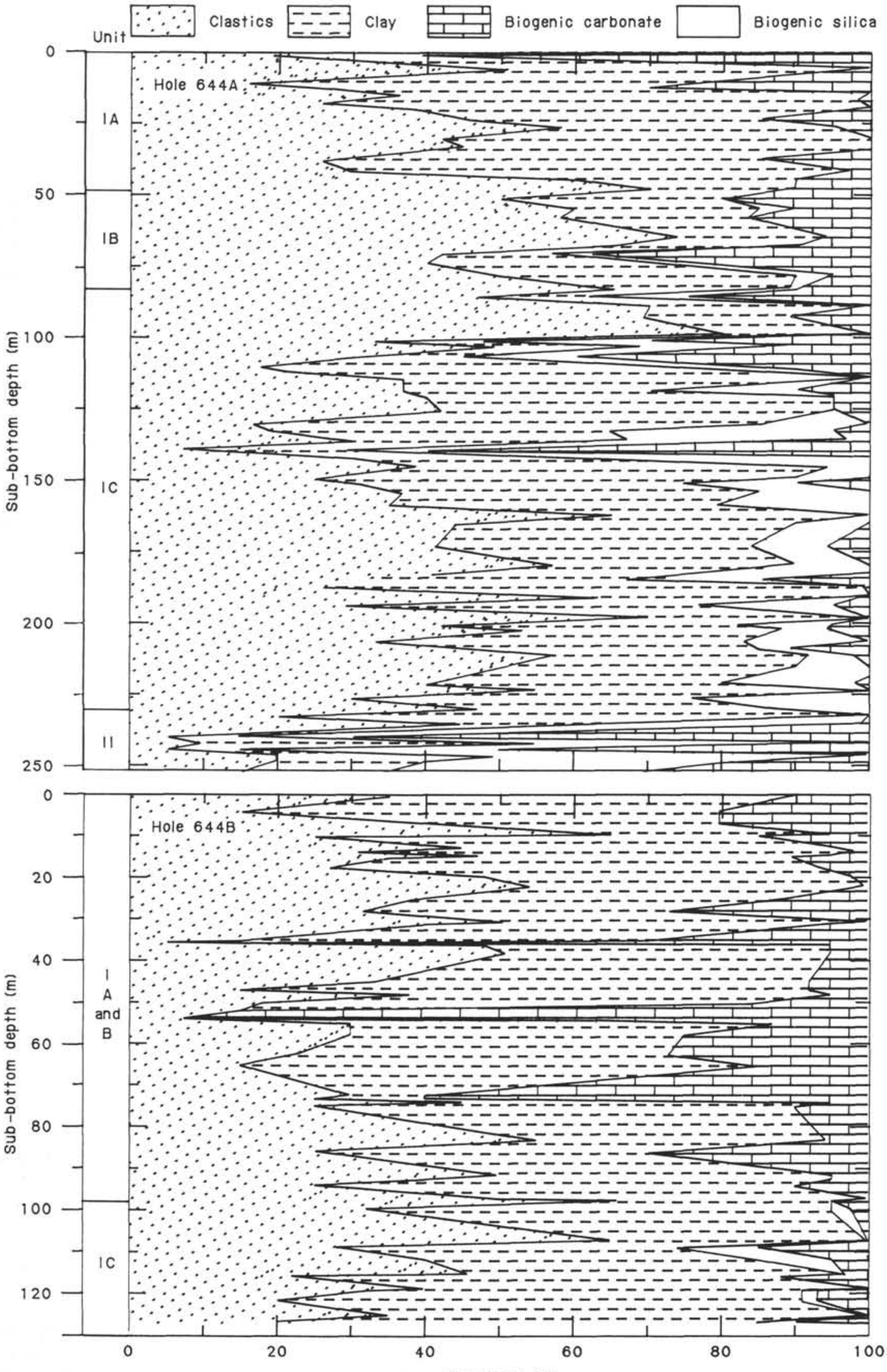

Figure 5. Summary of the composition of major lithologies at Site 644 from shipboard smear-slide data.

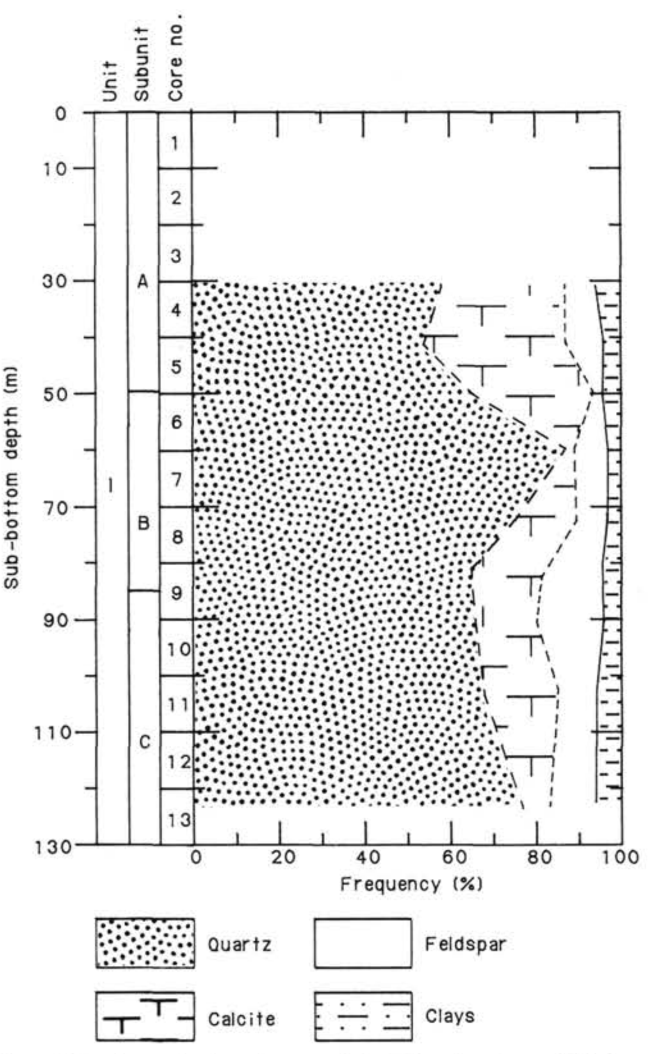

Figure 6. Semiquantitative estimates of the bulk mineralogy of lithologic Subunits IA, IB, and IC at Hole 644A, based on X-ray-diffraction peak area ratios.

was located on the continental shelf. The common occurrence of chalk fragments in the ice-rafted debris, as well as the abundance of reworked Cretaceous and early Tertiary nannofossils within the sediments, indicates that additional material was supplied by iceberg drift from southern and southeastern sources, entering from the North Sea or through the Skagerrak.

Within Unit I, variations in composition (Fig. 5) and distribution of dark layer coverage (Fig. 7) record stepwise shifts in the frequency and intensity of glacial/interglacial fluctuations. Subunit IC contains carbonate-poor glacial sandy muds and muds, interbedded with a variety of interglacial siliceous and calcareous muds; the color-banding in Subunit IC is characterized by widely spaced, weakly developed dark layers. The abundance of biogenic siliceous components in Subunit IC follows the general trend discussed for Site 643 (see "Sediment Lithology," Site 643 chapter, this volume), with very low-amplitude glacial/interglacial fluctuations indicated by both the sediment composition and the type of color-banding. Open-water conditions along the coastal portion of the Sites 643-642-644 transect were probably developed in association with repeated continuous incursions of fertile North Atlantic waters. The record of these conditions was preserved because of the generally increased rates of sedimentation at Site 644. The open-water environment at Site 644 may have contrasted with surface-water conditions dominated more by pack ice offshore (Sites 642 and 643) during the deposition of lower Subunit IC. Seasonally developed productivity plumes along the ice front may have contributed to the accumulation of biogenic silica at Site 644.

Subunit IB contains carbonate-poor, glacial sandy muds interbedded with more carbonate-rich, interglacial muds and oozes and is characterized by an upcore increase in the frequency and intensity of dark layer coverage. The lack of exact correlation between lithologic subunit boundaries and changes in dark layer coverage reflects the criteria used to define the lithologic boundaries. For example, if criteria other than the abundance or occurrence of biogenic silica had been used to define lithologic subunits, a closer correspondence between changes in dark layer coverage and lithologic unit boundaries could have been attained. Sites 642 and 643 provide examples of more obvious lithologic changes and also exhibit better correlations between lithologic subunits and dark-layer-coverage changes. Since the occurrence of biogenic silica is a crucial factor in our paleoceanographic interpretations, however, we have used it as the criteria for lithologic subdivisions at Site 644.

The presence of carbonate in Subunit IB, especially slowly accumulating, siliceous nannofossil oozes, suggests the periodic influence of less-fertile, open-water conditions than existed during the deposition of Subunit IC. The dark-layer-coverage pattern supports this interpretation, suggesting an increase in the occurrence and intensity of glacial maximum conditions through the deposition of Subunit IB, similar to patterns previously observed at Sites 642 and 643. Such an environment may have developed at Site 644 during the incursion of a weak current of temperate waters from the North Atlantic along southern Norwegian coastal areas. Corresponding shifts in carbonate abundances at Site 643 are reduced relative to Site 644, indicating that temperate conditions during this time were more common inshore than offshore. As a result, the incursions of temperate North Atlantic waters appear to have been concentrated along the coastal region (Site 644), leaving correlative colder environments farther offshore (Sites 642 and 643).

Subunit IA contains glacial sandy muds interbedded with calcareous interglacial muds (Fig. 5) and is characterized by abundant, moderately developed, dark layers (Fig. 7). The general composition of Subunit IA indicates the importance of cooler and more ice-dominated conditions, in agreement with interpretations of the youngest glacial/interglacial sediments at Sites 642 and 643. The reduced intensity of dark layer coverage also agrees with observations from Sites 642 and 643 and may reflect both productivity variations and dilution effects during this interval of maximum sedimentation rate. The more uniform nature of the youngest glacial/interglacial sediments across the Sites 643-642-644 transect suggests that ice-dominated conditions were areally extensive by the time of deposition of Subunit IA, in contrast to the onshore-offshore variations that existed during deposition of Subunits IC and IB.

In summary, the sedimentary sequence recovered at Site 644 contains an expanded record of the transition from open-water (Unit II) to ice-dominated (Subunit IA) environments within Subunits IC and IB. These deposits provide a unique opportunity to investigate a variety of transitional stages during the initiation and development of glacial/interglacial cycles in the Norwegian Sea. Such a record will complement the longer term records available from Sites 642 and 643.

Tephra Correlations with Sites 642 and 643

At Site 644, only Unit I and the uppermost part of Unit II, as defined in the Lithologic Summaries for Sites 642 and 643 ("Sedimentary Lithology" sections, this volume), were drilled.

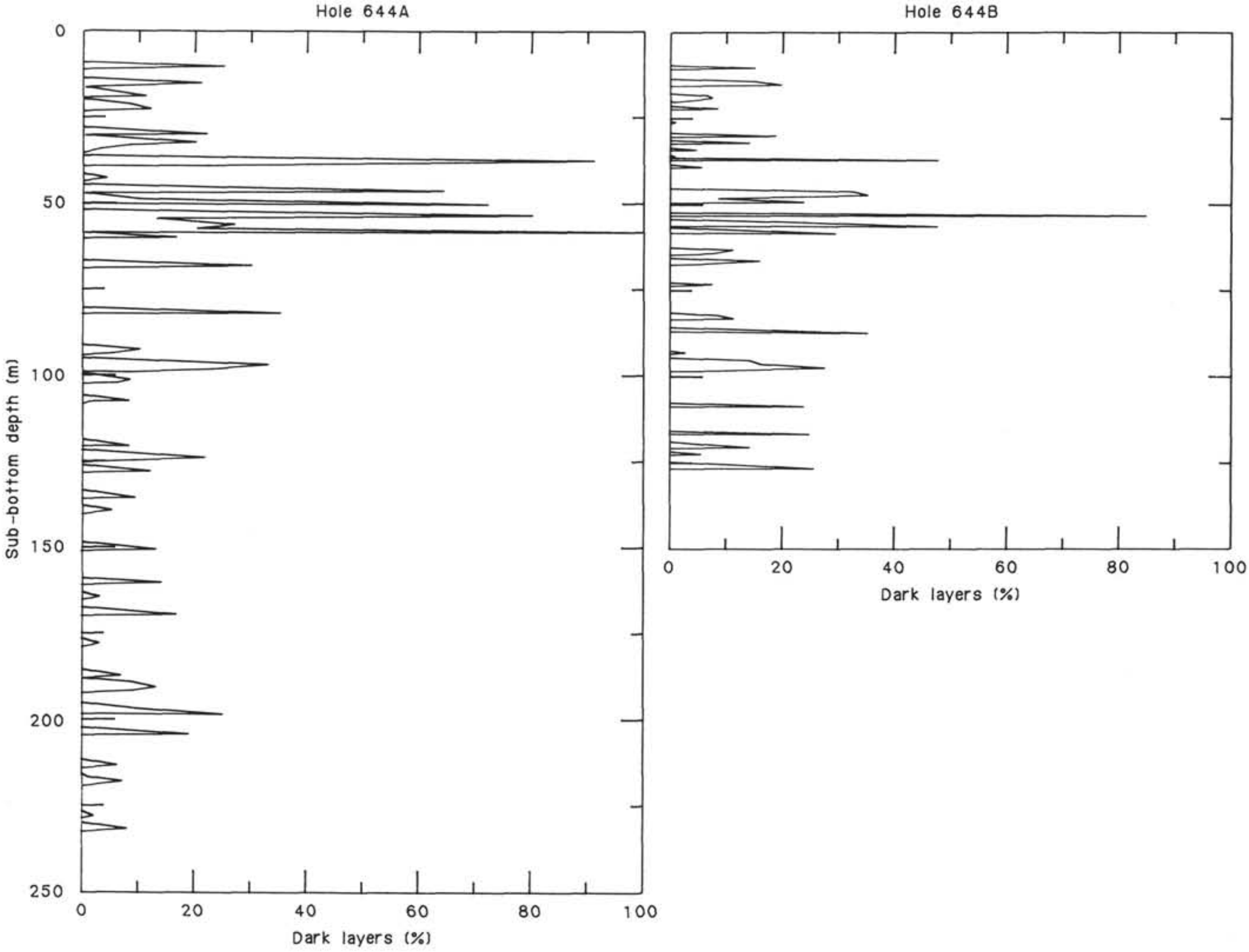

Figure 7. Percentage of core surface (per meter of core length) covered by dark layers in Unit I, plotted as a function of sub-bottom depth for Holes 644A and 644B.

Five discrete or disseminated layers of fresh ash of icelanditic to rhyolitic composition were recovered. These vary in thickness between 1 and 4 cm. Only four layers were recovered in the same interval at Sites 642 and 643. In Hole 644B, with a reduced penetration depth of about 128 m, only three ash layers occur, one of which (104-644B-05H-03, 89–91 cm) was not recovered at that interval in Hole 644A, or at Sites 642 or 643.

Based on microscope studies on smear slides, three ash layers in Hole 644A can be correlated with Sites 642 and 643. These correlations are listed next. The ages given for Site 642 ashes were calculated by using sedimentation rates given in the "Biostratigraphy" section, Site 642 chapter, this volume, and were determined on the basis of biostratigraphy. The ages for Site 644 ashes were calculated using sedimentation rates based upon the location of paleomagnetic boundaries in Hole 644A.

	Hole	Core-section	Interval (cm)	Depth (mbsf)	Age (Ma)
Ash layer 1:	642 B	—	—	—	—
	642 C	02H-4	88–98	8.78	0.205
	643 A	02H-3	72–74.5	7.52	—
	644 A	04H-1	131–135	27.01	0.237
	644 B	04H-3	32–35	—	—

	Hole	Core-section	Interval (cm)	Depth (mbsf)	Age (Ma)
Ash layer 2:	(the only Neogene to Quaternary layer drilled on ODP Leg 104, which contains brown biotite, approximately 5–7 vol %)				
	642 B	06H-1	132–133	40.22	—
	642 C	05H-3	92–94	36.82	0.856
	643 A	—	—	—	—
	644 A	11H-2	40–41	94.10	0.861
	644 B	11H-3	36–38 (?)	—	—
Ash layer 3:	642 B	07H-5	40	53.80	—
	642 C	07H-1	133–140	52.23	2.30
	643 A	—	—	—	—
	644 A	24H-3	148–150	205.48	2.20

The ages calculated are in good agreement between the two sites. In view of the excellent recovery rates at all three sites, the data indicate that, compared to the Miocene, tephra layers of airfall origin are rare in the upper Pliocene to Pleistocene section on the Vøring Plateau. As at Sites 642 and 643, no ash layer of Holocene age was recovered in either Hole 644A or Hole 644B.

BIOSTRATIGRAPHY

Diatom Biostratigraphy

Methods

A quick scan for diatoms was performed on slides prepared from the whole and sieved (>45 µm) fractions of all core-catcher samples from Hole 644A. A detailed biostratigraphic study of diatom assemblages was not possible because of a the limited time available to prepare and study samples. Species identified were primarily the larger ones, which could be quickly recognized (e.g., *Rhizosolenia barboi, R. curvirostris*, and *Nitzschia reinholdii*). We did not have enough time for consistent notation of smaller species of stratigraphic importance (e.g., *Thalassiosira nidulus*). Nevertheless, our brief survey did provide limited stratigraphic resolution, which is important for interpretation of the paleomagnetic record of the site.

Preservation and Abundance

A total 49 samples were quickly scanned to note the relative abundance of diatoms (Fig. 8). Diatoms are absent from all 11 examined intervals in the upper 83 m of Hole 644A. The first downhole occurrence of diatoms appears at approximately the Brunhes/Matuyama boundary (0.73 Ma). Below this boundary (~82 m) diatoms are consistently present, except in a few short intervals. Abundant diatoms occur at ~187 m (1.97 Ma) and at the base of the hole between 238 and 252 m (~2.83-2.65 Ma). Diatom preservation was poor to fair in samples where their abundance was noted as rare to few, and moderate in samples where abundance was noted as common to abundant.

Results

Koizumi's (1973) North Pacific diatom stratigraphy was employed in diatom biostratigraphic studies of Hole 644A. The *Denticulopsis seminae* Zone (NNPD12, 0.25-0 Ma) was not recognized, as it correlates with the barren zone in the upper 82 m. The base of this zone is defined by the last occurrence of *Rhizosolenia curvirostris* (0.25 Ma), which is found in the first sample below the barren zone (104-644A-10H-2, 84-85 cm). According to the paleomagnetic record of this site, the last-appearance datum (LAD) of *R. curvirostris* closely approximates the Matuyama/Brunhes boundary; therefore, the upper range of this species (~0.75-0.25 Ma) is not recorded in Site 644 sediments. The absence of this zone and all diatoms in this interval may be attributed to dissolution, or more likely to exclusion because of glacial conditions. The *R. curvirostris* Zone (NNPD11, 0.9-0.25 Ma) was encountered between the LAD of *Actinocyclus oculatus* in Sample 104-644A-12H, CC (111.2 m) and the LAD of *Rhizosolenia curvirostris* in Sample 104-644A-10H-2, 84-85 cm. Only the basal portion of the zone (~0.90-0.75 Ma) is represented beneath the barren interval. The LAD of *A. oculatus* in Core 104-644A-12H approximates the base of the Jaramillo Event confirming the paleomagnetic interpretation ("Paleomagnetics" section, this chapter) of the normal polarity interval in this core as the Jaramillo Event.

The interval between the base of the hole (~253 m) and the LAD of *A. oculatus* (Sample 104-644A-12H, CC) correlates with the *Denticulopsis kamtschatica* Zone (NNPD8, 3.2-2.5 Ma), *D. seminae* var. *fossilis* Zone (NNPD9, 2.5-1.7 Ma), and *A. oculatus* Zone (NNPD10, 1.7-0.9 Ma). At present these zones cannot be differentiated.

Paleoenvironment

Changes in the relative abundance of diatoms may be a good indicator of glacial-interglacial variations. This is to be expected since surface productivity is minimal during times of permanent or ephemeral sea-ice cover, unless dissolution destroys the record of productivity. The close correspondence of the relative diatom abundance curve to known trends in the late Gauss-Brunhes global oxygen-isotopic record suggests that productivity fluctuations dominate relative abundance variations of diatoms and that dissolutional influence is minimal.

Diatom productivity is highest between ~2.83 and 2.65 Ma. Abundant diatoms within this interval are interpreted to represent nonglacial conditions. Shortly after 2.65 Ma, a permanent long-term decrease in diatom productivity occurred, which followed a widespread global enrichment in ^{18}O at ~3.2 Ma (Shackleton and Opdyke, 1977). This event even more closely corresponds to a major northward expansion of Antarctic polar waters, which began at approximately 2.8 Ma and peaked between 2.58 and 2.47 Ma (Ciesielski and Weaver, 1983; Ciesielski and Grinstead, 1986). Comparison of the diatom productivity record of this site with that of the Antarctic suggests temporally equivalent major coolings of high-latitude surface waters in both hemispheres. This high-latitude cooling precedes the first formation of a major Northern Hemisphere ice sheet, which Shackleton et al. (1984) suggested may have formed at ~2.37 Ma.

Between 2.65 Ma and 0.73 Ma, numerous fluctuations are recorded in the relative abundances of diatoms. Our resolution does not allow a direct comparison with the oxygen-isotopic record for this interval. At present, eight intervals are recorded that are barren of diatoms. These intervals are interpreted to represent full glacial maxima, during which time there was little or no diatom productivity.

A single sample (104-644A-21H, CC) represents the only abundant occurrence of diatoms noted in sediments younger than 2.65 Ma. The presence of abundant diatoms and specimens of the silicoflagellate genus *Dictyocha* indicates interglacial conditions at ~1.96 Ma.

Several additional interglacial stages seem to be evident in upper Matuyama sediments between 84 and 121 m. The warmest of the episodes is inferred to be in basal Core 104-644A-12H and upper Core 104-644A-13H, where specimens of *Dictyocha* again were noted. The age of this warming event is ~0.98 Ma, which again correlates with a similar event noted in the Antarctic and sub-Antarctic (P. Ciesielski and M. Ledbetter, unpublished data). The last common occurrence of diatoms occurs in upper Core 104-644A-10H (85 m, ~0.76 Ma). Both warming events at ~0.76 and 0.98 Ma seem to correlate with a deepening of the carbonate compensation depth (CCD) and brief southward migrations of the polar front in the Antarctic region (P. Ciesielski and M. Ledbetter, unpublished data).

Diatoms are absent from 11 samples examined from Brunhes-age sediments (late Quaternary, ~0.74 to 0.08 Ma). These results indicate more prolonged and severe glacial conditions at this time.

Paleoenvironmental interpretations of the sedimentologic and micropaleontologic records of ODP Leg 104 Neogene sequences reveal a close correspondence among major paleoceanographic changes in the Norwegian Sea and the Antarctic region. Preliminary results support positive interhemisphere feedback in high-latitude climate systems. Although the timing of major paleoceanographic changes is quite similar in both these high-latitude regions, often the responses of the systems are quite different. For example, during the middle Miocene (~13 to 14 Ma) a major increase in the deposition of carbonate in the North Atlantic occurs; conversely, in the Antarctic, siliceous sedimentation begins to predominate over calcareous sedimentation. Such changes may reflect a change in the global fractionation of calcium carbonate and biogenic opal. Further detailed examination of ODP Leg 104 sediments will no doubt help elucidate the joint roles of both polar regions on the global climate-oceanographic system.

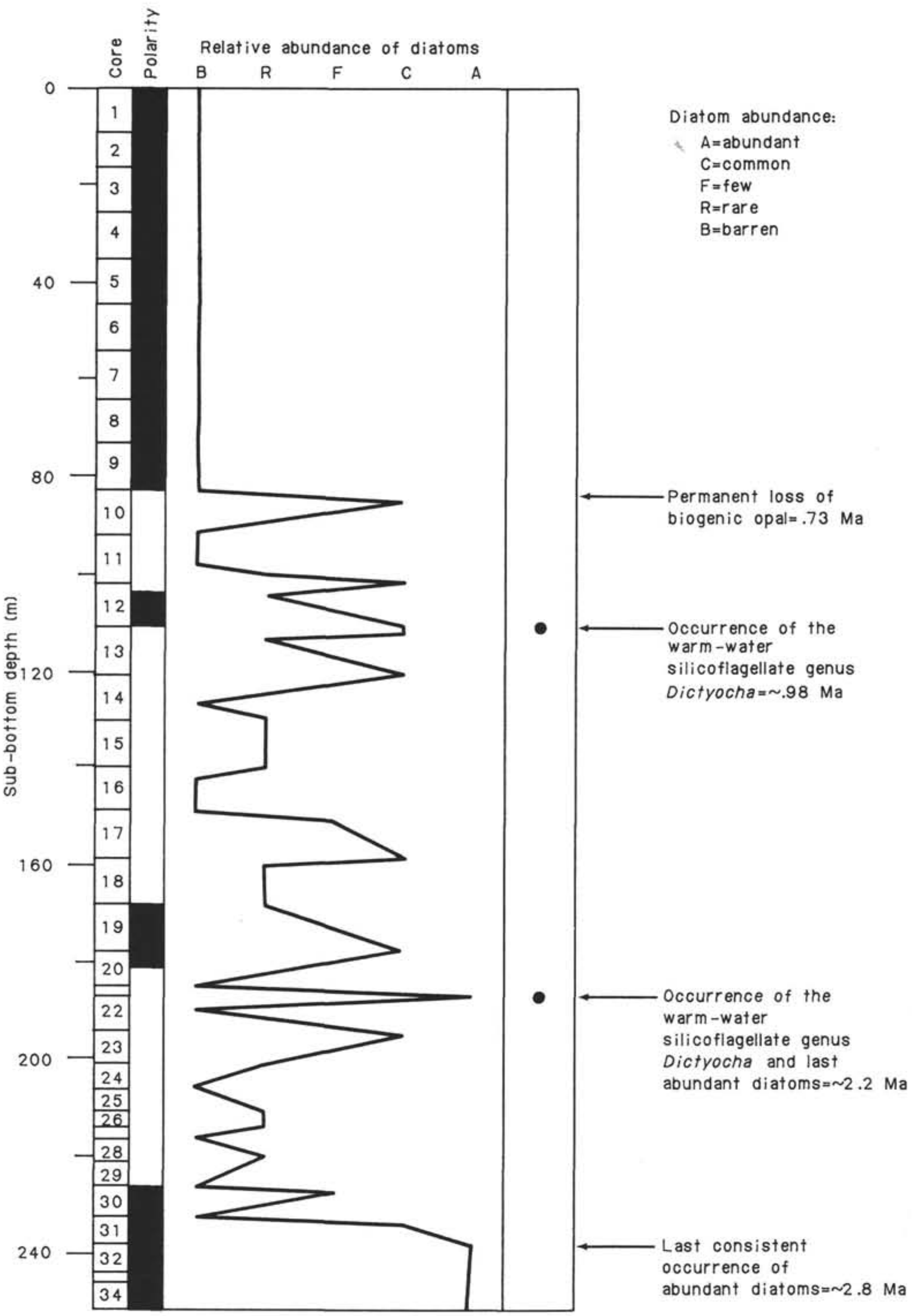

Figure 8. Relative abundance fluctuations of diatoms and occurrences of the silicoflagellate genus *Dictyocha* in Hole 644A sediments.

Silicoflagellate Biostratigraphy

Methods

A total 49 samples from Hole 644A were quickly scanned for silicoflagellates. Of these samples, 34 were core-catcher samples and 15 were from within individual cores. Slides were prepared from both the whole and sieved (>45 μm) fractions of each core-catcher sample. All other samples examined were smear-slide preparations.

Preservation and Abundance

Silicoflagellates were encountered sporadically in Cores 104-644A-1H through 104-644A-30H. Throughout this interval (~9-232 m) no more than a few specimens were found in a given sample, except in 104-644A-12H, CC, where they are abundant. Preservation in this interval is generally poor. Silicoflagellates were more frequently encountered and are well preserved in five samples examined from Cores 104-644A-31H through 104-644A-34H.

Results

The sedimentary sequence of Hole 644A can be divided into only two silicoflagellate zones. Samples 104-644A-1H, CC through 104-644A-31H-2, 50 cm, (0–239 m) is designated the *Distephanus speculum* Zone. This zone combines the *D. speculum* A Zone and the *D. speculum* B Zone of Ciesielski (1975). As defined here, the zone includes all silicoflagellate floras above the last occurrence of *D. boliviensis*.

Ciesielski (1975) correlated the last common occurrence of *D. boliviensis* to the upper Gauss paleomagnetic epoch and assigned an age of ~3.1 Ma. Ciesielski (1983) in his study of sub-Antarctic DSDP Site 514 found the last occurrence of *D. boliviensis* to appear precisely at the Gauss/Matuyama boundary (2.47 Ma). At Site 644 the last *D. boliviensis* seems to have a similar last occurrence ~14 m below a long, normal polarity interval (beginning at ~225 m), which is interpreted as the Gauss/Matuyama boundary (see "Paleomagnetics" section, this chapter). The *D. boliviensis* Zone extends from ~219 m to the base of Hole 644A at ~253 m. Species defining the base of the zone (the LAD of *Dictyocha pygmaea* and *D. pumila*) were not observed. It appears unlikely that the base of the hole should be older than the mid-Gauss epoch because higher abundances and diversities occur in the lower Gauss and Gilbert epochs.

Paleoenvironment

Three occurrences of the genus *Dictyocha* were observed in Samples 104-644A-12H, CC, 644A-13H-1, 50 cm, and 644A-21H, CC. Living *Dictyocha* spp. rarely occur in polar or subpolar surface water. In the Antarctic the genus appears restricted primarily to the north of the Antarctic Convergence in surface waters warmer than 4° to 5°C (Ciesielski, 1975). The occurrence of common to abundant diatoms in the same samples containing *Dictyocha* is inferred to indicate interglacial conditions.

Radiolarian Biostratigraphy

Site 644 recovery offers a unique opportunity to study in detail the biostratigraphy of radiolarians from the western Norwegian Sea during and after the onset of glaciation. Other localities of this age are barren of radiolarians or contain only rare scattered occurrences. Consequently, it is not possible to compare the distribution of these microfossils at Site 644 with existing reference sections, but we anticipate that Site 644 will be an important reference section in the future. The base of the section at Site 644 can be correlated with the Pliocene recovery at Site 642, however.

A discontinuous record of radiolarians is preserved in Site 644 recovery, and their frequency of occurrence ranges from rare to common (Table 3). Preservation is only moderately good: whole specimens are rare. Because only core-catcher samples have been examined, barren intervals shown in Table 3 will change as the studies progress. The section containing radiolarians can be divided into two subunits:

1. Samples 104-644A-11H, CC to 104-644A-29H, CC (101.7–226.1 mbsf): The assemblages here contain many species in common with the modern fauna, although the frequency of occurrence of individual species varies over a considerable range. The assemblages in Samples 104-644A-11H, CC, 644A-13H, CC, and 644A-22H, CC are strongly dominated by *Cycladophora davisiana*. This discovery suggests that it may be possible to correlate Site 644 units to a standard paleoceanographic climate curve.

Table 3. Stratigraphic ranges of radiolarians preserved at Site 644.

	Core no.	Depth (mbsf)	Volcanic glass	Sponge spicules	Radiolaria		*Lophospyris quadripes*	*Artostrobus lineata*	*Artostrobus seriatus*	*Corocalyptra craspedota*	*Cycladophora davisiana*	*Antarctissa whitei(?)*	*P. gracilipes*	*Echinomma leptodermum*	*Cromyechinus borealis*	*H. pachydermum*	*Stylodictya tenuispina*	*Corythospyris fiscella*	*Amphimelissa setosa(?)*	*Lithomelissa setosa*	*Lithelius spiralis*	*E. accuminatum*
					Concentration	Preservation																
Cycladophora davisiana	11	101.7			F	M		C	+		C	+	+	C				1	?			
	12	111.2			C	M								A	C			1	?			+
	13	120.7			F	M			R		C										C	
	14	130.2		F	B																	
	15	139.7			B																	
	16	149.2			B																	
	17	158.7	A	C	R	M												1			C	
	18	168.2	A	F	R	M		+								C			?		C	
	19	177.7	A	A	C	M		R	R				+					1	?			
	20	184.8	A	F	R	M															C	
	21	186.8		A	C	M		+				+							?	1		1
	22	194.1	A	A	F	M				+	C		+					1				
	23	201.1		A	F	M												1			C	
	24	206.6		F	B																	
	25	210.5		F	B																	
	26	214.3		A	B																	
	27	216.1			B																	
	28	221.1		A	F	M			+				1					1			A	
	29	226.1		A	R	M															+	
	30	232.1			B																	
Antarctissa whitei/ Lophospyris quadripes	31	238.1		A	C	M	C	+		+				R			R	+	+	+		
	32	243.7		A	C	M	1									C	R					
	33	246.0	A	A	C	M	–															
	34	252.8		A	F	M	R	+	+	1												

A = abundant, F = few, C = common, R = rare, M = moderate, B = barren, + = detected.

2. Samples 104-644A-31H, CC to 104-644A-34H, CC (238.1–252.8 mbsf): The radiolarian fauna takes on a more Tertiary aspect within this interval. *Lophospyris quadripes*, the index species for the youngest subzone (new) of the *Antarctissa whitei* Zone, is present. The top of this subzone correlates with Sample 104-642C-10H, CC (Gauss geomagnetic polarity epoch).

Paleoenvironment

Sporadic occurrences of radiolarians in the glacial marine sequences of DSDP Sites 336 and 348 were reported by Bjørklund (1976). These occurrences do not compare with the much more pervasive record at ODP Site 644. Siliceous microfossils are very rare in the glacial marine sections at Sites 642 and 643. Two possible explanations are proposed here for this disparity: improved preservation conditions or increased surface water productivity. In general, radiolarians are better preserved in sediments in which other opal particles occur to contribute dissolved silica to pore waters. For this reason, the preservation of radiolarians and other siliceous microfossils should be improved by the presence of volcanic glass in Cores 104-644A-17H through 104-644A-22H. Additionally, sponge spicules are common in many of the samples. Perhaps planktonic siliceous skeletons are better preserved at Site 644 because this site is located on a slope facies colonized by sponges.

Higher surface-water productivity is the more probable explanation for the better radiolarian preservation. Hypothetically, a narrow tongue of North Atlantic water that was compressed against the Norwegian continental margin and intermittently penetrated as far north as Site 644 between episodes of maximum glaciation (represented by the barren intervals) may have supplied the bottom waters of this locality with higher fluxes of skeletal debris than at Sites 642 and 643. The abundance of radiolarians at Site 644 appears to be inversely proportional to the concentration of clastic grains, which is consistent with this explanation.

Modern radiolarians seem to be excluded from oceanic regions of abnormally high or low salinity (greater than 38 or less than 30 ‰). Salinities in the normal open-ocean range can therefore be inferred for the Pleistocene at Site 644 on the basis of the presence of radiolarians. This paleoceanographic condition is remarkable for the continental margin of Norway during deglaciations, when increased volumes of freshwater runoff would be anticipated. The presence of radiolarians in slope sediments implies that earlier bottom-water velocities must have been much lower than those on the Norwegian continental margin today. Some of the samples examined from Site 644 show evidence of mild winnowing. Sponge spicules and heavier radiolarians are preserved, whereas small diatoms and silicoflagellates are absent.

Calcareous Nannofossil Biostratigraphy

Zone Definitions

The standard Martini (1971) nannofossil zonation was followed to some extent but because of the absence of many marker species various zones had to be combined into longer ranging ones. The nannofossil assemblages presented here are similar to those compiled in DSDP Leg 38 (Müller, 1976). See Table 4 for the zones, depths, cores, assemblages, and ages of the intervals.

Emiliania huxleyi Zone (NN21):
Bottom: FAD *E. huxleyi*
Age: late Quaternary

Gephyrocapsa oceanica Zone (NN20):
Top: FAD *E. huxleyi*
Bottom: LAD *Pseudoemiliania lacunosa*
Age: middle Quaternary

Interval with *P. lacunosa* (NN19/16):
Top: LAD *P. lacunosa*
Bottom: LAD *Reticulofenestra pseudoumbilica*
Age: middle Pliocene to middle Quaternary

Interval with *R. pseudoumbilica* (NN15/7):
Top: LAD *R. pseudoumbilica*
Bottom: LAD *Cyclocargolithus floridanus*
Age: middle Miocene to early Pliocene

Abundance, Presenation and Reworking

Results

Cores 104-644A-1H through 104-644A-3H contain an assemblage of dominantly *Gephyrocapsa*. *E. huxleyi*, the marker for NN21, could not be determined without scanning electron microscopy (SEM). This interval is thus designated as the upper to middle Pleistocene Zones NN21/20.

The marker for the upper Pliocene to lower Pleistocene Zones NN19/16, *P. lacunosa*, is first observed in Core 104-644A-6H. *P. lacunosa* is found from Cores 104-644A-6H through 104-644A-21H. This is followed by an interval barren of calcareous nannofossils to Core 104-644A-30H.

Table 4. Calcareous nannofossil biostratigraphy, Site 644.

Hole 644A interval base	Nannofossil zonation	Zonal marker	Age (Ma)	Species present
22 m 3H-4, 124 cm	*Emiliania huxleyi* (NN21)	FAD *E. huxleyi*	late Quat. (0–0.27)	*E. huxleyi, Gephyrocapsa* sp., *Coccolithus pelagicus,* small *Reticulofenestra* sp., *Coronocyclus nitescens, Cyclococcolithus leptoporus, Dictyococcites* sp., *Discolithina* sp., *Helicosphaera* sp.
51 m 6H-5, 50 cm	*Gephyrocapsa oceanica* (NN20)	LAD *P. lacunosa*	middle Quat. (0.27–0.44)	Same as NN21, but *E. huxleyi* present
Total depth	*Pseudoemiliania lacunosa* (NN19–16)	LAD *R. pseudoumbilica*	early Quat. to late Pliocene (0.44–3.2)	Same as *G. oceanica* Zone, except add *P. lacunosa*

Note: FAD = first apperance datum, LAD = last apperance datum.

Cores 104-644A-33H to 104-644A-34H (total depth) contain the same general NN19/16 assemblage. *R. pseudoumbilica* was not observed, so the total depth of the hole is late Pliocene or younger in age.

The abundance of calcareous nannofossils found at Site 644 is greater than that at Sites 642 and 643. At Site 644, the Pliocene/Pleistocene nannofossils found are usually common to abundant, while at Sites 642 and 643 they are typically few to rare. Site 644, as well as the two previous sites, contains a zone barren of nannofossils between the interval with *P. lacunosa* and the interval with *R. pseudoumbilica*. This barren interval closely approximates the Pliocene/Pleistocene boundary.

The preservation at Site 644 is also better than at the previous two sites. Moderate to good preservation is common at Site 644, compared with the poor to moderate preservation found at Sites 642 and 643.

Reworked specimens of older nannofossils are present down to the barren zone at Core 104-644A-23H. The reworking consists primarily of Cretaceous nannofossils, but Paleogene reworking was also found to a lesser extent. The reworked Cretaceous often is composed of up to 90% of the total nannofossil assemblage, while the Paleogene usually comprises less than 10%.

Paleoenvironment

As a general rule, the sediments at Site 644 contain greater abundance, preservation, and diversity than at the deeper water Sites 642 and 643, which show the influence of the relatively warmer Norwegian Current at Site 644. But on a global comparison, the abundance and diversity are still characterized by typical high-latitude, cold-water species. Site 644, as well as the other Leg 104 sites, are all missing typical low-latitude marker species, such as spheneoliths, ceratoliths, and discoasters.

Planktonic Foraminifer Biostratigraphy

Methods

Owing to time limitations only every second core-catcher sample from Hole 644A was analyzed. Yet, because of the high sedimentation rates at the site, the resolution of our study is better than that for the previous sites. The same informal zonation applied to the other sites was also used at Site 644.

Results

Nearly monospecific assemblages of *Neogloboquadrina pachyderma* sin. are present down to 82.7 mbsf (Table 5). The abundance is high despite a large content of minerogenic sand grains. The first sample with larger diversity was found at 101.7 mbsf (104-644A-11H, CC), and higher diversity sediments farther up in the section probably were not encountered because of the coarse sample spacing. *N. pachyderma* sin. is highly dominating down through 120.7 m. Beneath this level a faunal change occurs. *N. pachyderma* sin. is still present, but is much less dominant, and the more open, reticulate form of *N. pachyderma* sin. tends to be more abundant. In this lower interval, the general abundance of planktonic foraminifers is reduced, compared with the upper 120.7 m. Another faunal change is observed between Samples 104-644A-31H, CC and 104-644A-34H, CC (238.1–252.8 m). In the latter core a much richer fauna, dominated by *N. atlantica* sin., is present. *Globorotalia inflata* is found as an auxiliary species to the assemblages in Samples 104-644A-34H, CC, 644A-31H, CC, and 644A-11H, CC. The last occurrence of *N. atlantica* is in Core 104-644A-31H.

Age Interpretations

The appearance of *G. inflata* in the lowermost Sample (104-644A-34H, CC) implies that the base of the section is within N21, younger than 3.1 Ma. The last occurrence of *N. atlantica* in Sample 104-644A-31H, CC defines the boundary between zones NSPF4 and 5 at about 2.3 Ma, which is in fairly good agreement with paleomagnetic data. The first common occurrence of encrusted *N. pachyderma* sin. in Sample 104-644A-18H, CC defines the boundary to Zone NSPF6. A suggested age for this event of about 1.7 Ma agrees reasonably well with paleomagnetic data, which place the top of the Olduvai Event in Core 104-644A-18H.

Table 5. Planktonic-foraminifer core-catcher data for Hole 644A.

Core	*N. pachyderma* (sin.)	*N. pachyderma* (dex.)	*N. atlantica* (sin.)	*G. bulloides*	*G. quinqueloba*	*G. falconensis*	*G. glutinata*	*G. inflata*	*G. scitula*	*G. uvula*	Zones
1	A				R						NSPF6
3	A										
5	A										
7	A				R						
9	A	R									
11	A	R			C			R		C	
13	A	C									
15	C										
17	C	R		R		R	R				
18	C	R		R		R					
19	R	A		R	C	R	R				NSPF5
21	R			R							
23	R	F		C		R			R	R	
25	Barren										
27	Barren										
29	C	R									
31	C	C	R	R			C	R			NSPF4
34	R	R	C	C		R		R			

A = abundant, F = few, C = common, R = rare.

Paleoenvironment

Any detailed paleoenvironmental interpretation is precluded by the few samples analyzed so far. Interesting observations made from the recovered material are very encouraging, giving good prospects for postcruise paleoceanographic studies with an extremely good resolution.

As a precursor to the onset of glaciomarine sedimentation, a marked decrease in foraminiferal productivity and diversity may have occurred in the late Gauss epoch. Barren samples have been reported from the uppermost Gauss for almost all microfossil groups (this section), pointing to very low productivity during the first glacial intervals recorded at this site. Warmer periods occurred during the Matuyama epoch, as is evident from diverse planktonic foraminiferal assemblages both within the Olduvai Event and on top of the Jaramillo Event. These diverse assemblages correlate with zones of high diatom production and warm-water diatoms. As might be shown by more detailed investigations these occurrences could be related to quite extensive periods with relative warm climate within the glacial cycles. Similar evidence also appears from the sedimentological investigations of the hole. The onset of higher amplitude climatic fluctuations in the late Quaternary had a distinct response in the planktonic foraminiferal faunas, and possibly is linked with the final evolution of *N. pachyderma* sin. as a polar species. The investigations described bear some evidence for three types of climatic variability and biogenic productivity: (1) a transitional period in the late Gauss leading to the onset of large-scale glacial cycles in the Northern Hemisphere, which, at least during certain periods, reflects low productivity; (2) a period that comprises most parts of the Matuyama epoch, which experienced high-frequency, low-amplitude climatic and oceanographic changes, with two or more longer periods of higher productivity and warmer climate; and (3) a period starting at about Jaramillo time, characterized by more extensive glaciations with large climatic amplitudes intersected by periods of warm climate and high biogenic productivity.

Benthic Foraminifer Biostratigraphy

Introduction

Because of the time constraints at this site, only every other core-catcher sample was analyzed aboard ship. Thus, we cannot yet present a detailed zonation reflecting the expected climatic and oceanographic changes during the Pliocene-Pleistocene.

Results

Based on our preliminary investigation there appear to be two benthic foraminiferal subzones (Table 6, Fig. 9) at Site 644A, both of which contain *Cassidulina laevigata, Melonis zaandamae*, and *Epistominella exigua*. Subzone A1 (0–187 mbsf) is characterized by the presence of transported shelf species, including *Elphidium excavatum* and ice-rafted detritus (Table 6). In one sample of this subzone, 104-644A-11H, CC, a few specimens of *Bulimina striata* are found. Subzone A2 (187–252 mbsf) is characterized by the presence of *Cibicides "pseudoungerianus."* A barren interval in Subzone A2 is found in Samples 104-644A-25H, CC and 104-644A-27H, CC.

Most of the benthic foraminifers found at Site 644A have long ranges, and are found at present in the Norwegian Sea (Belanger and Streeter, 1980; Sejrup et al., 1981). Only one diagnostic Pliocene and late Miocene species, *B. striata* (Murray, 1984), is encountered in Sample 104-644A-11H, CC. This occurrence, however, does not agree with the biostratigraphic ages of the other microfossils (see Fig. 10) and may represent reworked material or the need to extend the range of this species.

Paleoenvironment

Site 644 was chosen to study the paleoenvironmental changes during the Pliocene-Pleistocene because the high sedimentation rate at this site gives a high-resolution record during this time interval. Benthic foraminifers indicate slightly warmer water during the deposition of the lower one-half of the core (187–252 mbsf) than at present. The higher percentage of benthic foraminifers (greater then 50%) may indicate the deflection of more saline, open, oceanic water masses off the Vøring Plateau during the late Pliocene. The barren interval encountered in Samples 104-644-25H, CC and 104-644A-27H, CC has no explanation at this time, but seems to be environmentally caused, as it affects all microfossil groups. Abundant evidence for glaciation in the form of ice-rafted detritus and transported shelf species is found in Subzone A1 (Table 6).

Palynology

Nine palynological samples were examined from Site 644 to compare the Pleistocene and late Neogene dinocyst and sporomorph assemblages of the inner basin with those found at the Vøring Plateau Site 642 and at the deep-water Site 643 on the outer slope of the plateau. Numbers of palynomorphs were high and preservation was good in all samples except 104-644A-25H, CC, which contained few, moderately to poorly preserved specimens.

Results

Table 7 lists the main dinocysts, pollen, and spores found in the samples and the tentative assignments to palynozones established from the ranges of dinocysts at Site 642 (see "Palynolo-

Table 6. Distribution (in percent of total benthic foraminifers) of the most important species of benthic foraminifers in core-catcher samples from Hole 644A.

Core	*Cassidulina laevigata*	*C. reniforme*	*C. subglobosa*	*Melonis zaandamae*	*Eponides umbonatus*	*Elphidium excavatum*	*Epistominella exigua*	*Cibicides "pseudoungerianus"*	Other species	Benthic forams (%)	Abundance	Preservation	Other fossils			Reworking	Benthic foraminifer zonations
													Siliceous fossils	Ostracodes	Other		
1	16	3	X	57	4				20	8	C	G		X	Fi	Transport from shelf	A_1
3	35	X		26	18	X			20	15	C	G					
5	2	2		X		93			3	48	C	G			Bi		
7	13	37			2	45			3	43	C	M		X	W		
9	20	40		3		27	X		10	13	F	M	Sp	X	Ec		
11	16	3	40	5			26		10	47	A	M	Sp, R		Fi, Ec		
13	41	22	6	2		1	15		13	68	A	G	R, D				
15		X		XX			XX			74	R	P					
17	31			27		8	26		8	83	A	G			W		
19	46	3		33			8		10	60	A	G	R, Sp				
21	23	10		5			52		10	98	C	G	R, Sp				
23	3		2	3			49	38	5	95	F	M	Sp, R		Fi		A_2
25											—		Sp				
27											—		(R)				
29	17	X	4	5			39	28	7	76	F	M	(Sp)				
31	16		7	18			38	14	7	95	F	M	Sp, R				
34	13		15	8			47	14	3	48	A	G	Sp, R				

Abbreviations: R = rare, F = few, C = common, A = abundant; P = poor, M = moderate, G = good; D = diatoms, R = radiolarians, Sp = sponge spicules, Ec = echinoderm remains, Bi = bivalves, W = wood fragments, Fi = fish remains, X = occurrence in sample.

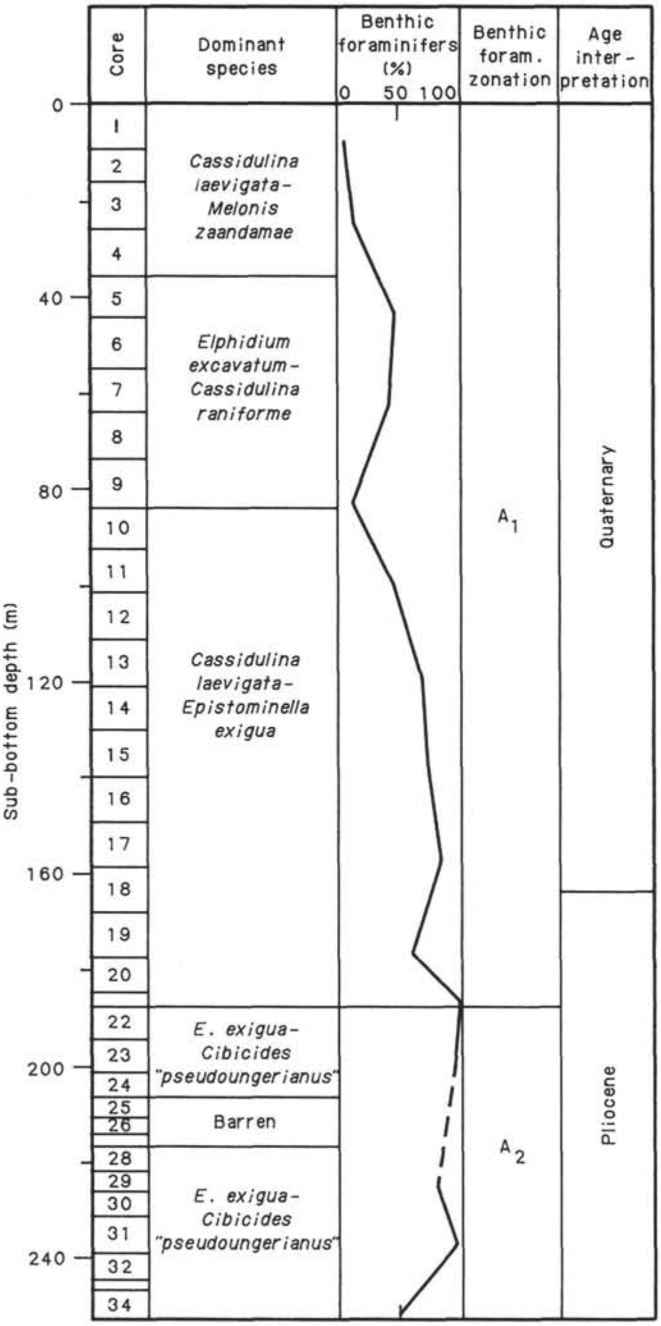

Figure 9. The benthic foraminiferal zonation in Hole 644A. The characteristic species/species group and the frequency of benthic foraminifers (in percent of total foraminifers) indicated for each core refer to the core-catcher sample. The age interpretation is based upon the magnetic measurements.

gy" in "Biostratigraphy" section, Site 642 chapter, this volume). Table 7 also includes notes on the climatic conditions indicated by the pollen assemblages.

Age and Paleoenvironment

Sample 104-644A-1H, CC (9.2 mbsf) contains an upper Pleistocene glacial stage assemblage. A larger proportion of *Bitectatodinium tepikiense* was found at this site than at the more seaward sites on the transect. The glacial stage assemblage at Site 644 is more similar to those described for the North Sea (Harland, 1977); this may reflect the greater influence of coastal water at Site 644.

Sample 104-644A-13H, CC (120.7 mbsf) contains the apparent LAD of *Achomosphaera ramulifera*, which marks the Pliocene-Pleistocene boundary at Sites 642 and 643 and in other parts of the North Atlantic. At Site 644, several *Spiniferites* species are present, in addition to the characteristic species of Zone PM2 at Site 642. In other parts of the North Atlantic, high percentages of *Spiniferites* spp. are usually associated with terrigenous or continental-shelf sediment influxes.

Samples 104-644A-15H, CC and 104-644A-17H, CC (139.7–158.7 mbsf) contain numerous *Paleostomocystis* species, as found in the lower Pliocene–upper Miocene sediments at Site 642. The presence of abundant *Paleostomocystis* is indicative of lower than normal surface-water salinity; therefore, a late glacial meltwater event is suggested for this interval. Pollen and spores indicate a warm climatic interval.

Sample 104-644A-21H, CC (186.8 mbsf) contains a low diversity of boreal oceanic species dominated by *Operculodinium centrocarpum*. *O. granulatum* n. comb. has its LAD in this sample; at Site 642, the LAD of this species occurs at the Pliocene-Pleistocene boundary.

Sample 104-644A-25H, CC (210.5 mbsf) again contains assemblages dominated by *Paleostomocystis* species, indicating a return to low-salinity surface-water conditions.

Sample 104-644A-28H, CC (221.1 mbsf) contains a boreal oceanic dinocyst assemblage dominated by *O. centrocarpum*, in which *O. crassum, Corrudinium harlandii*, and *Achomosphaera andalousiense* have their LAD. These species disappear at, or just above, the Miocene boundary at Site 642; *A. andalousiense* is a marker of the upper Miocene interval at the Andalousian stratotype. Thermophilous tree pollen indicates warm climatic conditions.

Sample 104-644A-33H, CC (246.0 mbsf) has a boreal oceanic dinocyst assemblage similar to Sample 104-644A-21H, CC. The concurrent presence of *O. granulatum, O. crassum*, and *Impagidinium patulum* marks the upper Miocene to lower Pliocene Zone PM3 at Site 642.

Sample 104-644A-34H, CC (252.8 mbsf) contains a very high diversity of species that characterize Zone PM3 at Site 642 and indicate temperate oceanic surface water. A rich, hardwood pollen flora indicates warm climatic conditions.

BIOSTRATIGRAPHIC SYNTHESIS

The section cored at Site 644 consisted of 231 m of mostly carbonate-poor, sandy muds, and 21 m of interbedded siliceous oozes (see "Sediment Lithology" section, this chapter). Ice-rafted material occurs down to 230 mbsf. The whole sequence ranges in age from late Pliocene to Recent.

Biostratigraphic Correlation

Biostratigraphic summary charts are shown in Figures 10 and 11. A detailed biostratigraphic zonation was not possible, because of time constraints. The Pliocene/Pleistocene boundary is based on the paleomagnetic stratigraphy (see "Paleomagnetics" section, this chapter), but is confirmed by several fossil groups.

Siliceous fossils are absent in the upper 85 m of the core and occur only in low numbers in most of the lower part of the section. Diatoms, silicoflagellates, and radiolarians are abundant in the lowermost 25 m of Hole 644A. Silicoflagellates give a middle Pliocene (Gauss) age for this interval. This interpretation also agrees with the planktonic foraminifer evidence; the occurrence of *Globorotalia inflata* gives a maximum age of 3.1 Ma. The base of the diatom zone NNPD11 (*Rhizosolenia curvirostris*) at 0.9 Ma coincides with the Jaramillo Event as it does

Table 7. Palynomorph assemblages in samples from Hole 644A and their inferred zonation, age, and paleoecology.

Sample and depth (mbsf)	Dinocysts	Zone and age	Pollen/ spores	Paleoclimate
-1H, CC 9.2	*Bitectatodinium tepikiense* *Brigantedinium simplex* *Multispinula minuta* *O. centrocarpum* *Votadinium calvum*	PM1a late Pleist.	*Picea* f *Cyperacea* *Sphagnum*	Glacial stage
-13H, CC 120.7	*O. centrocarpum* *Spiniferites ramosus* *S. elongatus* *B. tepikiense* *Brigantedinium* spp.	PM2 late Plio.	*Picea* c *Pinus* f *Selaginella* *Sphagnum*	Interglacial, boreal or subarctic
-15H, CC 139.7	*Palaeostomocystis* spp. *B. tepikiense* *Diconodinium inaequicornutum* *Leptodinium bacculatum* *O. crassum*	PM2 early Plio.	*Pinus* c *Picea* f *Tsuga* r *Cedrus* r *Fagus* r	Interglacial, temperate
-17H, CC 158.7	*Palaeostomocystis* spp. *Th. balcaniana* *A. umbracula* *F. filifera* *O. crassum* *L. bacculatum*	PM2/3 e/l Plio.	*Pinus* f *Cedrus* *Sphagnum*	Interglacial, temperate-boreal
-21H, CC 186.8	*O. centrocarpum* *B. tepikiense* *O. granulatum* n. comb.	PM2/3 e/l Plio.	*Pinus* *Picea* *Cedrus* *Abies* *Podocarpus*	Mixed boreal and temperate
-25H, CC 210.5	*Palaeostomocystis* sp.1 *Brigantedinium* spp.	PM2/3 e/l Plio.	*Ericales* *Rosales* *Sphagnum*	(?)Cool
-28H, CC 221.1	*Palaeostomocystis* spp. *O. crassum* *O. granulatum* *Batiacasphaera* sp. *Lingulodinium machaerophorum* *Leptodinium* spp. *A. andalousiense* *Hystrichosphaeridia obscura*	PM2/3 e/l Plio.	*Pinus* *Picea* *Cedrus* *Sphagnum* *Lycopodium* *Juglans*	Mixed boreal and temperate
-33H, CC 246.0	*O. centrocarpum* *O. granulatum* *O. crassum* *Leptodinium patulum* *Palaeostomocystis* spp.	PM3 late Mio.	*Pinus* *Picea* *Cedrus*	Boreal
-34H, CC 252.8	*L. machaerophorum* *O. centrocarpum* *A. andalousiense* *S. ramosus* *Tectatodinium simplex*	PM3 late Mio.	*Pinus* *Cedrus* *Fagus, Acer* *Quercus* *Rosaceae*	Warm, temperate

in the North Pacific. The base of the hole is within NNPD8 (*Denticulopsis kamtschatica* Zone), indicating a basal age of 3.2 to 2.5 Ma.

Radiolarians are present in three intervals of the recovery of Hole 644A: Sections 104-644A-11H-4 to 104-644A-14H-5 (95–130 mbsf), 104-644A-17H, CC to 104-644A-24H-2 (158–202 mbsf), and 104-644A-28H, CC to 104-644A-34H, CC (222–253 mbsf). The lower interval consists of sediments with common to abundant radiolarians and includes the boundary between the *Antarctissa whitei* Biozone and *Cycladophora davisiana* Biozone at 230 mbsf. The two upper intervals contain sparse radiolarian assemblages that display moderate to poor preservation. The occurrence of *C. davisiana* in these sediments undergoes marked changes in frequency of occurrence. Three subdivisions can be made, based on planktonic foraminifers. The top of zone NSPF5, with the first occurrence of encrusted *N. pachyderma* (sin), appears at the Pliocene/Pleistocene boundary.

An assemblage of benthic foraminifers, typical of Pliocene sediments at Sites 642 and 643, occurs from Sample 104-644A-17H, CC to the base of this hole. This is consistent with a Pliocene age for this section of the core.

Three intervals of nannofossils can be recognized. The boundary between Zones NN21/20 and NN 19/16 is tentative because of the spacing of the samples.

Palynomorphs from the lower 120 m of the hole show somewhat older ages than the other fossil groups and the paleomagnetic data indicate. All samples fall into Zone PM2 or PM3. Sample 104-644A-13H, CC has Pliocene-Pleistocene markers and, therefore, differs only slightly from the magnetostratigraphy. The palynomorphs of the lowermost Samples 104-644A-34H, CC and 104-644A-33H, CC give an age of ~3.4 Ma, which is only a few hundred thousand years older than indicated by paleomagnetic data, silicoflagellates, and planktonic foraminifers.

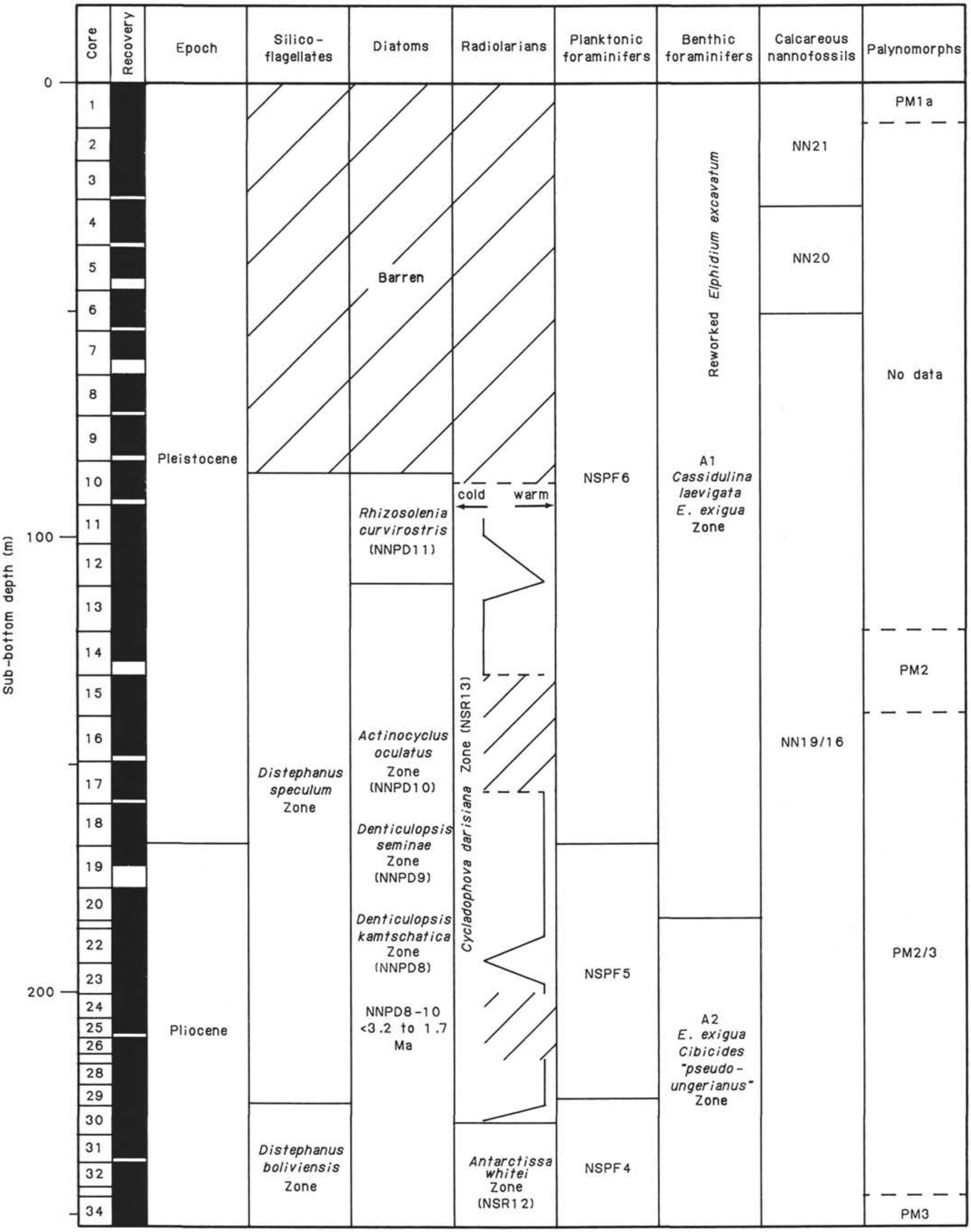

Figure 10. Summary figure of each fossil group, based on shipboard analyses of Hole 644A samples and plotted on a depth scale.

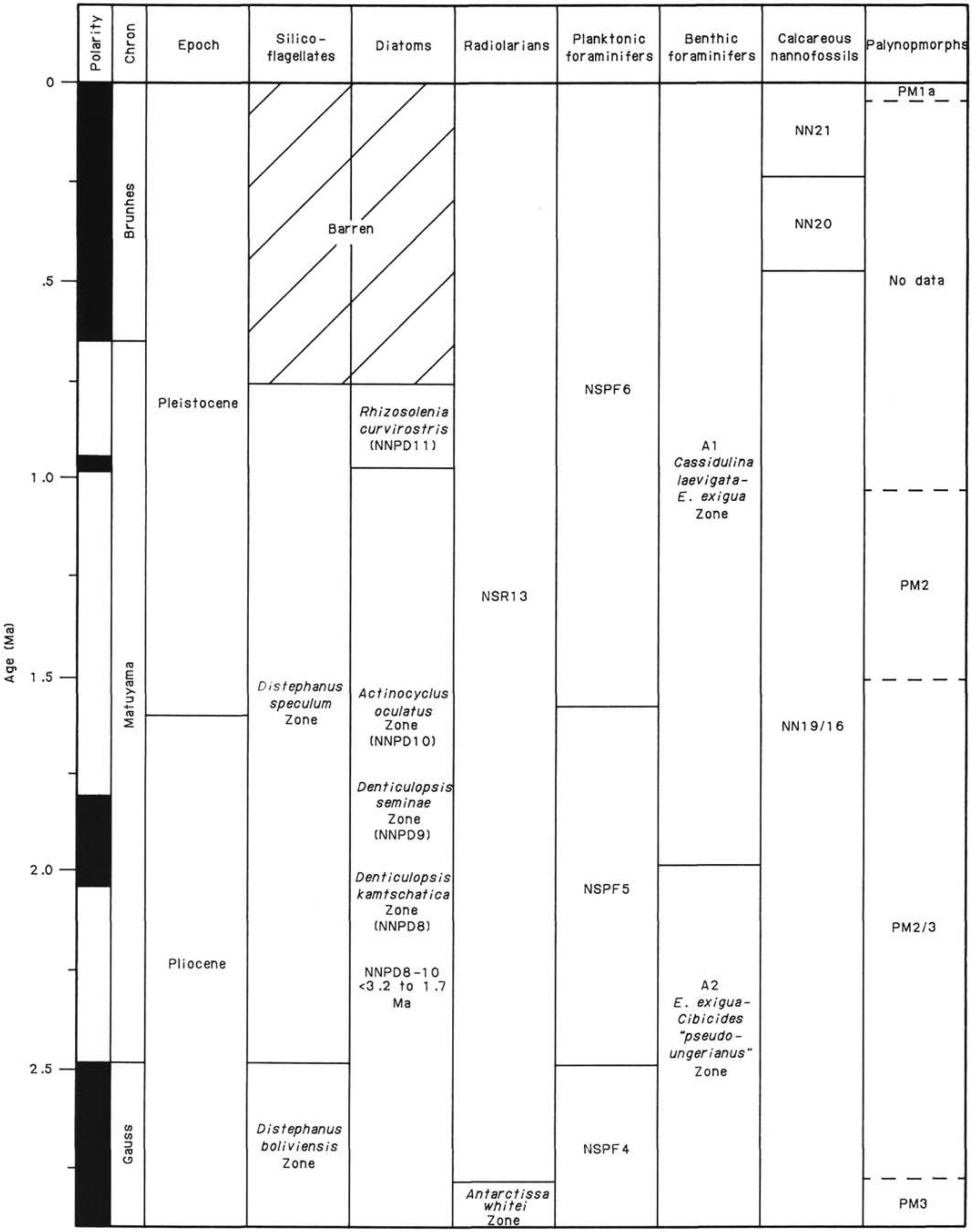

Figure 11. Paleomagnetic record of Hole 644A and biostratigraphic summary of each fossil group, plotted on an age scale.

Correlation with Sites 642 and 643

Site 644 provides an extended sequence of the middle to upper Pliocene and Quaternary deposits on the Vøring Plateau compared with the two previous sites, but the different biozones can still be recognized. An ash layer at ~94 mbsf in Hole 644A (104-644A-11H-2, 40–41 cm) can be correlated with the ash zone at 40 mbsf in Hole 642B (104-642B-6H-1, 132–133 cm) (see "Sediment Lithology" section, this chapter). This correlation indicates that average sedimentation rates have been twice as high at Site 644 for the upper Pleistocene. However, based on the paleomagnetic data the average sedimentation rate to the top of the Gauss Event at Site 644 is more than three times that observed at Site 642.

Paleoenvironment

The occurrence of ice-rafted material down to 230 mbsf indicates the minimum duration of the glacial period. Sediments from the lowermost 25 m of the hole represent temperate (nonglacial) conditions, as shown by the abundance of diatoms and silicoflagellates and the presence of warm-water-indicative planktonic foraminifers; presently, we do not know if any older glacial marine deposits can be expected below this interval. The relatively stable environment of the early Gauss was followed by a transitional time of what is interpreted as repeated climatic and oceanic oscillations. The last consistent occurrence of abundant diatoms at 2.65 Ma (236 mbsf) may indicate a major surface-water cooling that led to the glacial period in the Norwegian Sea, which may be related to a coeval northward expansion of Antarctic polar water that began at ~2.8 Ma and peaked between 2.58 and 2.47 Ma (Ciesielski and Weaver, 1983; Ciesielski and Grinstead, 1986). This subsequent cooling probably preceded the initiation of large-scale Northern Hemisphere glaciation.

Radiolarians are not preserved in the glacial marine sediments in Sites 642 and 643, where ice-rafted sedimentation commenced in middle Pliocene time. At Site 644, however, intervals of sediments as young as 0.8 Ma contain low to moderate accumulations of radiolarians. This implies that surface waters of the overlying water column at Site 644 experienced episodes of moderately high productivity and ice-free conditions for a much longer time than at the western sites.

Dominance of *C. davisiana* in Pleistocene sediments has long been regarded as an indication of cold surface-water temperatures. Assemblages containing very high frequencies of this species were observed at 98, 114–130, 194, and 230 mbsf. Consequently, proximity of the polar front to Site 644 can be inferred at 0.8, 1.0–1.2, 2.05, and 2.54 Ma.

Evidence for more temperate intervals during the glacial period is provided by warm-water-indicator species in several microfossil groups. A return to more temperate surface waters is indicated by planktonic foraminifers and radiolarians at 200 mbsf (2.1 Ma) and by both diatoms and radiolarians at 187 mbsf (1.9 Ma). Planktonic foraminifers also indicate warmer surface conditions at 179 mbsf, where diatoms occur only commonly. Palynomorphs, silicoflagellates, radiolarians, and planktonic and benthic foraminifers all indicate a warmer water interval at around 0.98 Ma at the base of the Jaramillo Event (111 mbsf). Nine samples barren of diatoms that occur from 230 to 83 mbsf can be interpreted as a series of full glacial conditions during this interval. This time of climatic fluctuations ends abruptly at around 0.76 Ma (83 mbsf) with the disappearance of siliceous microfossils.

Evidence for extensive glaciation is found in samples between 25 and 83 mbsf (equivalent to 0.1–0.76 Ma). The samples from this interval contain a large amount of terrigenous material, and transported shallow-water benthic foraminifers dominate the foraminiferal assemblage (Table 5). The transport of shelf material took place only during glacials. The upper 83 m of sediment is barren of siliceous microfossils, which may indicate full or partial ice cover. Palynomorphs and planktonic foraminifers in the upper cores also indicate glacial environments. A peculiar feature of all three sites on the Vøring Plateau is the presence of an upper Pliocene–Pleistocene barren zone in all microfossil groups. Preliminary correlations indicate that the least severe barren zone occurs at Site 644, while the barren interval spans the longest time interval at Site 643.

PALEOMAGNETICS

Coring at Hole 644A penetrated 252.8 m of sediments. Below about 100 mbsf, the nature, and especially the relative high gas content, of the sediments, repeatedly caused severe problems in retrieving a reasonably complete and undisturbed sedimentary sequence. The disturbance was particularly noticeable in the lower part of Hole 644A; therefore, quality and quantity of the recovered core was not always adequate for detailed magnetostratigraphic analyses.

Thirty-four cores from Hole 644A were measured for their natural remanent magnetization properties using the pass-through cryogenic magnetometer aboard ship. Despite the difficulties mentioned, the data obtained by shore-based paleomagnetic analyses of 415 discrete samples using detailed alternating field (AF) demagnetization techniques (Table 8) enabled us to establish a very complete, preliminary upper Cenozoic magnetostratigraphy (Fig. 12). In general, and in contrast to results of the other sites drilled during Leg 104, the paleomagnetic record shows a remarkable agreement with paleontologic findings.

The magnetostratigraphy of Hole 644A is summarized in Figure 13 and Table 9. All ages given in this report refer to the polarity time scale of Berggren et al. (1985) if not otherwise indicated. Major geomagnetic boundaries identified were the Brunhes/Matuyama (0.73 Ma/Ma) and the Matuyama/Gauss (2.47 Ma/Ma) transitions at around 82 and 225 mbsf, respectively. The Brunhes/Matuyama boundary apparently falls in between Cores 104-644A-9H and 104-644A-10H. Core 104-644A-9H did not have a full recovery. The missing material (about 2 m) limits our precision in defining the position of the boundary. Owing to the high sedimentation rate during the Brunhes period (about 112 m/m.y.), four short events of reversed polarity may be recognized in this youngest geomagnetic epoch. At present, however, each of these events is documented only by a single data point. Although all four reversals are clearly indicated by stable negative inclinations in core sections showing no immediate evidence of disturbance, an accidental misorientation during sampling cannot be excluded. Additional paleomagnetic work on the critical intervals, combined with isotope data, will provide needed data for interpretation of the still rather controversial Brunhes event stratigraphy.

In the Matuyama epoch, the Jaramillo Event (0.91 to 0.98 Ma) extends between 103.81 and 111.22 mbsf. The top of the Olduvai Event (1.66 m.y.) occurs at 166.31 mbsf, and its base is at 180.81 mbsf. This latter horizon should closely mark the Pleistocene/Pliocene boundary. At around 196 mbsf, a short normal polarity event is recorded between the Olduvai and the Matuyama/Gauss boundary. Assuming a constant sedimentation rate of 75 m/m.y. in this interval yields an interpolated age of 2.08 Ma. Therefore, this event could represent one of the Reunion events (McDougall and Watkins, 1973).

The base of the hole at 252.8 mbsf is situated in the youngest part of the normal Gauss period. The sediment column at Hole 644A accumulated at an average rate of 91 m/m.y. This rate decreases downhole almost continuously from 112 m/m.y. during the Brunhes epoch, to 75 m/m.y. in the early part of the Matuyama epoch (Table 9). Extrapolation indicates an age of about 2.84 Ma at the base of the hole.

Table 8. Paleomagnetic properties of Hole 644A sediments.

Sample interval (cm)	Sub-bottom depth (m)	J (NRM)[a] (Gauss)	NRM[a]		AF stable		Pol.	MDF (Oe)
			I	D	I	D		
*1-1, 35-37	0.36	3.08 E-5	+65.7	155.2	+67.3	154.1		273
*1-1, 85-87	0.86	1.29 E-5	+75.8	116.8	+64.6	112.6		201
*1-1, 135-137	1.36	9.09 E-6	+75.9	210.8	+74.6	214.9		243
*1-2, 35-37	1.86	1.41 E-5	+19.8	185.7	+70.3	185.2		276
*1-2, 85-87	2.36	6.25 E-6	+44.0	128.9	+63.6	127.7		288
*1-2, 135-137	2.86	1.41 E-5	−43.0	156.6	−41.8	160.8		273
*1-3, 35-37	3.36	4.52 E-6	+6.1	189.5	+7.5	187.6		244
*1-3, 85-87	3.86	1.80 E-6	−32.3	182.2	−62.2	152.7		352
*1-3, 135-137	4.36	6.02 E-6	+5.4	217.8	+5.2	228.1		282
*1-4, 35-37	4.86	5.80 E-6	+43.3	253.4	+32.5	262.1		278
*1-4, 85-87	5.36	3.72 E-6	−2.3	186.1	+7.6	198.9		299
*1-4, 135-137	5.86	7.32 E-6	−12.0	347.9	+36.5	184.1		309
*1-5, 35-37	6.36	2.51 E-5	+17.2	257.5	+15.9	258.9		263
*1-5, 85-87	6.86	2.44 E-5	+19.8	224.9	+15.3	226.3		271
*1-5, 135-137	7.36	1.58 E-5	−9.3	209.7	−12.8	209.4		287
*1-6, 35-37	7.86	2.54 E-5	+51.7	261.2	+53.4	263.1		252
*1-6, 85-87	8.36	2.14 E-5	+25.2	271.0	+16.3	276.9		233
*1-6, 135-137	8.86	1.22 E-5	−17.4	227.8	−21.1	234.4		251
*2-1, 35-37	9.56	9.56 E-6	+47.2	247.4	+49.2	235.2		245
*2-1, 85-87	10.06	3.26 E-6	+27.8	87.8	+29.7	165.8		386
2-1, 135-137	10.56	1.16 E-5	+55.7	205.5	+65.9	224.1	N	279
2-2, 35-37	11.06	1.92 E-5	+43.5	225.3	+46.5	220.8	N	312
2-2, 85-87	11.56	5.45 E-6	+69.5	167.4	+84.0	223.1	N	339
2-2, 135-137	12.06	1.28 E-5	+74.3	200.1	+74.4	225.0	N	295
*2-3, 35-37	12.56	3.16 E-6	+32.7	152.1	+31.4	167.6		172
2-3, 85-87	13.06	2.54 E-5	+71.2	131.4	+70.4	135.0	N	253
2-3, 135-137	13.56	6.29 E-6	+51.6	233.2	+69.0	191.3	N	232
2-4, 35-37	14.06	5.48 E-5	+68.9	140.4	+72.3	135.4	N	345
2-4, 85-87	14.56	7.53 E-5	+50.8	237.8	+63.3	174.5	N	158
2-4, 135-137	15.06	3.33 E-5	+68.9	157.7	−65.7	334.7		316
2-5, 35-37	15.56	1.97 E-5	+68.0	126.4	+67.4	131.6	N	297
*3-1, 35-37	16.56	4.23 E-5	+64.6	141.0	+67.8	143.0		305
*3-1, 85-87	17.06	1.73 E-5	+68.2	117.3	+70.0	112.6		258
*3-1, 135-137	17.56	1.22 E-5	+71.3	110.1	+68.7	124.0		219
*3-2, 35-37	18.06	5.83 E-6	+72.6	102.9	+72.7	126.9		251
3-2, 85-87	18.56	8.03 E-6	+54.0	169.5	+65.9	136.4	N	184
3-2, 135-137	19.06	7.44 E-6	+61.2	175.8	+60.2	183.2	N	174
3-3, 33-35	19.54	3.52 E-5	+67.2	132.9	+69.3	130.6	N	298
3-3, 85-87	20.06	3.99 E-5	+73.6	155.2	+77.8	145.1	N	281
3-4, 35-37	21.06	6.03 E-5	+65.2	168.1	+69.7	167.3	N	300
3-4, 85-87	21.56	1.99 E-5	+75.8	162.1	+76.8	171.8	N	268
3-4, 135-137	22.06	1.33 E-5	+56.9	185.6	+60.1	197.1	N	189
3-5, 35-37	22.56	4.55 E-5	+72.9	165.8	+73.5	172.2	N	264
3-5, 85-87	23.06	1.03 E-5	+14.2	203.5	−39.1	163.8		46
3-5, 135-137	23.56	3.46 E-5	+67.1	221.2	+65.6	228.1	N	263
3-6, 35-37	24.06	1.34 E-5	+77.4	177.9	+82.2	186.4	N	244
4-1, 18-20	25.89	2.05 E-5	+64.0	122.5	+65.5	115.7	N	238
4-1, 85-87	26.56	2.40 E-5	+84.7	25.0	+79.8	356.6	N	250
4-1, 135-137	27.06	4.73 E-5	+80.9	33.7	+80.0	34.1	N	243
4-2, 35-37	27.56	1.69 E-6	−67.3	111.9	−81.1	118.4		>600
4-2, 85-87	28.06	2.68 E-5	+85.0	57.0	+86.4	3.3	N	210
4-2, 135-137	28.56	6.13 E-5	+75.0	325.9	+73.1	326.4	N	285
4-3, 35-37	29.06	5.89 E-5	+86.3	340.4	+82.7	344.9	N	224
4-3, 80-82	29.51	3.67 E-5	+82.4	357.4	+78.7	347.7	N	268
4-3, 135-137	30.06	7.23 E-6	+84.5	51.9	+84.4	5.2	N	137
4-4, 35-37	30.56	2.01 E-5	+83.9	21.0	+81.7	16.5	N	277
4-4, 85-87	31.06	5.63 E-6	+79.6	3.5	+76.6	353.8	N	312
4-4, 135-137	31.56	3.22 E-5	+79.2	255.3	+78.6	260.6	N	345
4-5, 35-37	32.06	3.88 E-5	+77.6	260.0	+78.2	265.3	N	361
4-5, 85-87	32.56	4.47 E-6	+61.7	214.8	+78.3	184.0	N	144
4-5, 135-137	33.06	1.01 E-5	+87.2	219.4	+87.0	283.6	N	247
4-6, 35-37	33.56	4.36 E-5	+78.5	335.8	+75.1	332.6	N	251
4-6, 85-87	34.06	4.70 E-5	+80.6	20.8	+80.3	6.5	N	267
5-1, 34-36	35.55	1.98 E-4	+78.5	68.6	+71.6	82.0	N	399
5-1, 84-86	36.05	2.46 E-5	+84.7	311.6	+81.4	320.5	N	225
*5-1, 134-136	36.55	1.50 E-6	+60.5	274.7	+62.1	258.6		133
5-2, 35-37	37.06	1.27 E-6	+78.5	288.2	−55.8	231.9		46
5-2, 85-87	37.56	4.00 E-5	+79.5	290.3	+78.5	297.4	N	412
5-2, 128-130	37.99	3.75 E-5	+76.2	330.8	+76.3	328.5	N	317
5-3, 35-37	38.56	3.03 E-5	+75.0	305.0	+75.0	312.5	N	402
5-3, 85-87	39.06	5.87 E-5	+78.3	352.8	+77.2	353.0	N	456
5-3, 128-130	39.49	3.28 E-5	+83.0	341.7	+81.8	329.6	N	349
5-4, 35-37	40.06	9.48 E-6	+81.4	276.8	+78.2	300.9	N	418
5-4, 85-87	40.56	2.24 E-5	+78.2	18.7	+76.4	12.1	N	268
5-4, 139-131	41.00	1.68 E-5	+77.6	25.5	+76.4	14.4	N	321
5-5, 35-37	41.56	5.31 E-5	+84.8	311.2	+83.3	307.3	N	392

Table 8 (continued).

Sample interval (cm)	Sub-bottom depth (m)	J (NRM)[a] (Gauss)	NRM[a]		AF stable		Pol.	MDF (Oe)
			I	D	I	D		
5-5, 85-87	42.06	1.08 E-5	+82.8	333.9	+76.9	315.4	N	405
5-5, 135-137	42.56	3.25 E-6	+67.3	57.4	+68.4	74.7	N	53
6-1, 35-37	45.06	2.75 E-5	+80.6	163.3	+84.1	174.2	N	329
6-1, 85-87	45.56	2.27 E-6	+40.9	119.6	+71.9	59.3	N	205
6-1, 135-137	46.06	3.53 E-5	+76.0	98.4	+76.4	93.3	N	487
6-2, 35-37	46.56	3.74 E-6	+57.3	112.8	+65.9	110.4	N	125
6-2, 85-87	47.06	7.78 E-6	+71.5	106.5	+70.0	107.6	N	226
6-2, 135-137	47.56	7.35 E-6	+73.9	111.7	+77.0	99.2	N	258
6-3, 35-37	48.06	3.17 E-5	+83.2	103.6	+83.8	98.6	N	251
6-3, 85-87	48.56	6.16 E-5	+74.3	90.0	+73.9	89.5	N	250
6-3, 135-137	49.06	2.28 E-5	+69.2	113.0	+72.3	99.4	N	220
6-4, 35-37	49.56	7.32 E-5	+85.2	99.2	+85.7	74.6	N	262
6-4, 85-87	50.06	3.06 E-5	+81.5	128.5	+82.5	133.1	N	314
6-4, 105-107	50.26	8.61 E-6	+83.1	130.1	+85.0	127.4	N	207
6-5, 35-37	51.06	4.68 E-5	+82.0	182.3	+82.6	193.3	N	228
6-5, 85-87	51.56	4.65 E-5	+77.7	86.3	+76.5	86.2	N	230
6-5, 135-137	52.06	2.48 E-5	+82.2	123.8	+83.7	111.7	N	208
6-6, 35-37	52.56	6.62 E-7	+67.5	106.1	+62.0	76.4	N	175
6-6, 85-87	53.06	1.55 E-5	+53.7	104.0	+62.8	101.4	N	149
*7-1, 18-20	54.39	8.02 E-7	+49.2	99.6	+47.1	104.0		196
7-1, 71-73	54.92	3.57 E-5	+82.5	235.4	+83.2	206.0	N	243
7-1, 120-122	55.41	2.03 E-5	+76.6	234.1	+76.7	246.1	N	218
7-2, 27-29	55.98	8.62 E-6	+69.3	222.4	+68.7	224.5	N	249
7-2, 49-51	56.20	1.41 E-6	+85.8	314.6	+68.1	299.1	N	76
7-2, 70-72	56.41	1.50 E-6	+60.5	131.3	+65.1	160.2	N	71
7-2, 107-109	56.78	7.01 E-7	+83.2	49.6	+73.2	59.5	N	140
7-3, 13-15	57.34	2.12 E-5	+68.8	240.1	+74.6	227.0	N	374
7-3, 47-49	57.68	1.57 E-5	+75.1	217.6	+75.7	226.5	N	309
7-3, 72-74	57.93	2.46 E-5	+77.7	203.4	+80.5	219.1	N	452
7-3, 105-107	58.26	1.40 E-5	+79.7	189.0	+79.3	199.9	N	363
7-4, 12-14	58.83	5.37 E-6	+70.7	222.1	+71.9	216.1	N	298
7-4, 47-49	59.18	6.97 E-6	+80.4	174.3	+83.0	191.3	N	325
7-4, 82-84	59.53	5.88 E-5	+74.1	265.7	+74.9	293.0	N	416
*8-1, 33-35	64.04	1.52 E-5	+44.2	80.6	−35.8	37.8		336
*8-1, 69-71	64.40	1.67 E-5	+81.3	123.0	+81.6	168.4		219
*8-1, 109-111	64.80	2.82 E-5	+80.3	233.8	+78.2	232.5		234
8-2, 34-36	65.55	1.77 E-5	+84.5	45.7	+83.0	23.0	N	158
8-2, 85-87	66.06	1.37 E-4	+85.1	1.3	+76.2	316.2	N	76
8-2, 134-136	66.55	1.51 E-5	+58.7	282.4	+78.9	288.9	N	309
8-3, 34-36	67.05	2.64 E-5	+78.9	103.3	+79.3	94.7	N	270
8-3, 84-86	67.55	7.57 E-6	+76.1	142.2	+80.1	143.1	N	327
8-3, 135-137	68.06	1.11 E-5	+72.9	111.9	+75.2	114.2	N	279
8-4, 19-21	68.40	4.79 E-5	+36.8	271.4	+71.3	284.4	N	74
8-5, 19-21	69.90	2.12 E-5	+85.3	21.3	+82.5	190.2	N	263
8-5, 83-85	70.54	2.22 E-5	+57.9	213.8	+70.2	256.3	N	364
8-5, 134-136	71.05	1.28 E-5	+70.1	235.1	+75.2	269.9	N	291
8-6, 19-21	71.40	1.34 E-5	+58.2	155.5	+54.9	153.8	N	91
8-6, 60-62	71.81	7.60 E-6	+73.5	10.1	+72.0	11.1	N	176
8-7, 13-15	72.84	4.86 E-5	+71.8	98.3	+73.3	98.6	N	237
9-1, 35-37	73.56	2.48 E-5	+85.1	169.2	+85.8	181.3	N	227
9-1, 85-87	74.06	1.25 E-5	+89.1	130.4	+85.8	290.0	N	127
9-1, 135-137	74.56	4.76 E-6	+84.0	291.1	+74.5	305.7	N	147
9-2, 35-37	75.06	2.98 E-6	+84.2	111.8	+81.5	52.1	N	99
9-2, 85-87	75.56	4.05 E-6	+70.2	152.3	+80.9	188.2	N	174
9-2, 135-137	76.06	2.37 E-5	+73.8	246.1	+72.6	253.3	N	197
9-3, 35-37	76.56	1.23 E-5	+84.2	290.0	+78.9	297.4	N	184
9-3, 85-87	77.06	2.84 E-5	+76.5	253.4	+75.3	255.8	N	185
9-3, 135-137	77.56	8.61 E-6	+88.2	167.7	+86.4	289.3	N	201
9-4, 35-37	78.06	3.68 E-5	+73.9	191.7	+76.0	195.8	N	243
9-4, 85-87	78.56	5.39 E-5	+81.1	197.8	+80.6	204.9	N	253
9-4, 103-105	78.74	5.15 E-5	+85.9	254.3	+84.0	273.5	N	243
9-5, 35-37	79.56	1.19 E-5	+37.4	173.9	+54.8	192.6	N	167
9-5, 85-87	80.06	3.11 E-6	+87.7	153.8	+83.2	280.8	N	415
9-5, 135-137	80.56	1.36 E-6	+75.6	158.0	+82.0	160.3	N	188
10-3, 35-37	86.06	8.34 E-6	−78.2	53.0	−78.5	8.7	R	270
10-3, 85-87	86.56	2.20 E-5	−74.8	93.0	−81.5	47.1	R	268
10-3, 135-137	87.06	2.48 E-5	−73.5	62.4	−72.6	38.1	R	260
10-4, 35-37	87.56	3.75 E-6	−40.8	91.0	−60.2	66.1	R	361
10-4, 85-87	88.06	3.59 E-6	−71.7	333.0	−65.3	328.7	R	218
10-4, 135-137	88.56	2.95 E-6	−62.1	22.9	−56.2	38.7	R	234
10-5, 35-37	89.06	4.77 E-5	−40.7	183.0	−71.6	190.2	R	570
10-5, 85-87	89.56	4.60 E-6	−70.4	64.0	−71.9	2.6	R	512
10-5, 135-137	90.06	7.25 E-6	+62.7	116.1	−58.2	38.0	R	579
11-1, 34-36	92.55	2.26 E-5	−64.9	204.8	−67.7	206.9	R	30
11-1, 85-87	93.06	1.28 E-6	+85.6	31.5	−45.3	37.2	R	32
11-1, 135-137	93.56	9.36 E-6	−56.8	101.4	−74.8	90.1	R	324

Table 8 (continued).

Sample interval (cm)	Sub-bottom depth (m)	J (NRM)[a] (Gauss)	NRM[a]		AF stable		Pol.	MDF (Oe)
			I	D	I	D		
11-2, 34-36	94.05	1.53 E-5	-69.6	155.9	-76.5	162.2	R	298
11-2, 85-87	94.56	3.43 E-5	--79.1	201.7	-80.2	217.6	R	281
11-2, 135-137	95.06	3.79 E-6	-33.8	167.6	-66.6	181.3	R	246
11-3, 34-36	95.55	9.72 E-8	-74.8	241.4	-80.5	69.2	R	>500
11-3, 85-87	96.06	2.37 E-7	-10.1	338.1	-55.9	210.7	R	>500
11-3, 135-137	96.56	1.54 E-6	-85.4	209.3	-87.2	206.6	R	570
11-4, 34-36	97.05	3.18 E-6	+59.0	263.9	-53.4	250.8	R	547
11-4, 85-87	97.56	1.91 E-5	-80.6	181.1	-82.6	210.3	R	500
11-4, 135-137	98.06	1.27 E-5	-86.6	106.7	-87.5	123.7	R	439
11-5, 34-36	98.55	1.04 E-6	-8.0	239.3	-62.2	242.0	R	>1000
11-5, 85-87	99.06	1.79 E-5	-16.1	267.3	-76.2	131.6	R	200
11-5, 135-137	99.56	5.11 E-6	-54.9	180.3	-75.6	222.3	R	453
11-6, 34-36	100.05	1.05 E-5	-54.9	170.7	-68.8	180.2	R	285
11-6, 85-87	100.56	6.31 E-6	-77.8	156.2	-82.7	201.9	R	299
11-6, 135-137	101.06	2.12 E-6	+66.1	190.9	-74.8	128.0	R	28
11-7, 18-20	101.39	1.58 E-6	+66.4	112.8	-62.4	346.9	R	35
12-1, 35-37	102.06	1.05 E-5	-10.9	111.7	-70.6	35.1	R	215
12-1, 84-86	102.55	5.65 E-6	-30.4	72.3	-54.5	54.2	R	237
12-1, 135-137	103.06	6.21 E-6	-66.2	83.0	-73.8	59.8	R	236
12-2, 35-37	103.56	2.08 E-5	-67.0	99.8	-71.2	88.8	R	273
12-2, 85-87	104.06	6.56 E-6	+63.2	141.8	+63.2	135.5	N	128
12-2, 135-137	104.56	1.13 E-5	+82.2	134.5	+84.9	139.3	N	200
12-3, 35-37	105.06	3.58 E-5	+51.4	203.0	+76.1	176.3	N	130
12-3, 85-87	105.56	1.84 E-5	+72.4	220.9	+72.5	234.7	N	205
12-3, 135-137	106.06	1.81 E-5	+63.9	241.5	+62.8	247.8	N	201
12-4, 34-36	106.55	9.65 E-6	+74.7	170.4	+81.6	188.0	N	166
12-4, 84-86	107.05	8.78 E-6	+70.8	142.8	+78.9	135.5	N	171
12-4, 134-136	107.55	1.13 E-5	+76.4	195.6	+76.6	215.2	N	152
12-5, 35-37	108.06	2.28 E-5	+80.4	154.6	+85.5	146.2	N	198
12-5, 85-87	108.56	2.06 E-5	+54.6	200.7	+56.4	207.3	N	196
12-5, 135-137	109.06	4.15 E-6	+78.0	159.2	+82.7	172.9	N	220
12-6, 35-37	109.56	5.86 E-6	+77.7	185.4	+81.4	206.7	N	199
12-6, 85-87	110.06	2.24 E-6	+89.1	89.6	+82.2	298.8	N	195
12-6, 135-137	110.56	2.33 E-7	+46.0	130.4	+52.7	131.4	N	132
12-7, 27-29	110.98	1.78 E-7	+20.1	124.4	-52.3	137.7	R	140
*13-1, 58-60	111.79	1.83 E-7	-14.8	114.0	-79.3	161.1		>500
*13-1, 85-87	112.06	9.86 E-7	+32.8	83.1	-67.6	82.2		182
*13-1, 135-137	112.56	3.44 E-6	+8.7	132.7	-34.4	113.9		179
*13-2, 36-38	113.07	1.77 E-6	+66.4	130.6	-49.8	118.1		60
*13-2, 85-87	113.56	1.74 E-6	-43.0	359.3	-44.9	327.9		370
*13-2, 135-137	114.06	1.00 E-6	-22.0	89.8	-37.9	45.0		281
*13-3, 45-47	114.66	1.31 E-5	-39.0	79.8	-51.1	77.3		275
*13-4, 25-27	115.96	1.25 E-5	+53.0	112.6	+54.3	120.9		213
*13-4, 79-81	116.50	4.73 E-6	-79.2	138.4	-81.4	127.5		227
*13-4, 125-127	116.96	3.11 E-7	-46.8	132.5	-71.9	266.6		98
*13-5, 37-39	117.58	7.71 E-6	+23.0	142.7	-49.3	129.5		46
*13-5, 77-79	117.98	3.14 E-6	+76.8	127.8	-72.6	359.1		160
*13-6, 18-20	118.89	8.73 E-6	-64.3	118.7	-72.0	161.8		49
*13-6, 77-79	119.48	2.94 E-6	+38.9	281.2	-82.8	346.4		32
*13-7, 33-35	120.54	9.19 E-7	+74.7	30.7	-62.9	35.9		75
*13-7, 84-86	121.05	6.07 E-6	+43.5	132.4	-8.4	138.5		38
*13-7, 133-135	121.54	370 E-7	+62.8	69.0	-0.7	65.1		50
14-2, 85-87	123.06	6.00 E-5	-4.7	124.4	-63.3	112.1	R	49
14-2, 135-137	123.56	5.93 E-6	-83.8	158.4	-75.3	262.7	R	399
14-3, 35-37	124.06	5.86 E-6	+41.9	119.1	-15.8	32.8	R	176
14-3, 85-87	124.56	4.48 E-5	-58.5	77.9	-62.5	74.2	R	270
14-4, 35-37	125.56	9.92 E-6	-58.7	116.0	-70.6	79.5	R	247
14-4, 85-87	126.06	6.46 E-7	-43.5	335.1	-46.7	10.4	R	39
14-5, 35-37	127.06	3.52 E-6	-61.7	100.6	-64.1	101.9	R	457
14-5, 85-87	127.56	4.50 E-6	-46.0	23.2	-62.9	40.7	R	237
14-5, 135-137	128.06	2.39 E-6	+9.7	104.8	-69.2	77.3	R	346
*15-1, 35-37	130.56	3.00 E-6	-61.1	132.5	-63.7	123.7		26
15-1, 85-87	131.06	3.69 E-6	+43.6	297.9	-77.1	259.0	R	30
15-1, 135-137	131.56	6.70 E-7	+68.1	244.3	-73.3	249.2	R	442
15-2, 35-37	132.06	1.26 E-7	-12.1	161.8	-83.5	230.6	R	>500
15-2, 85-87	132.56	1.04 E-5	+66.0	111.3	-81.0	241.0	R	37
15-2, 135-137	133.06	9.11 E-8	-23.6	35.0	-77.6	12.2	R	>500
15-3, 85-87	134.06	1.35 E-7	+67.6	0.3	-72.6	288.2	R	80
15-3, 135-137	134.56	3.35 E-7	+49.8	346.8	-59.4	346.4	R	354
15-4, 35-37	135.06	4.27 E-7	-60.6	308.5	-71.2	291.9	R	32
15-4, 85-87	135.56	5.91 E-7	-43.2	57.2	-68.8	19.1	R	654
15-5, 35-37	136.56	3.08 E-7	-4.5	131.1	-61.6	141.5	R	27
15-5, 85-87	137.06	1.42 E-7	-13.5	81.5	-71.1	118.7	R	>350
15-5, 135-137	137.56	1.42 E-6	+27.5	73.3	-53.4	36.8	R	28
15-6, 35-37	138.06	6.65 E-7	+63.0	72.1	-36.1	26.5	R	61
15-7, 35-37	139.56	5.20 E-6	+33.6	132.6	-62.6	56.3	R	26

Table 8 (continued).

Sample interval (cm)	Sub-bottom depth (m)	J (NRM)[a] (Gauss)	NRM[a]		AF stable		Pol.	MDF (Oe)
			I	D	I	D		
16-1, 85–87	140.56	4.01 E-7	+74.9	95.6	−31.7	92.5	R	22
16-1, 135–137	141.06	1.34 E-6	+76.8	128.2	−69.2	64.0	R	27
16-2, 35–37	141.56	1.76 E-6	+68.0	117.7	−25.9	40.5	R	42
16-2, 85–87	142.06	3.00 E-6	+81.9	15.7	−72.1	296.1	R	23
16-2, 135–137	142.56	5.72 E-7	+41.6	85.1	−81.7	31.3	R	697
16-3, 35–37	143.06	4.01 E-7	+24.8	73.9	−70.4	55.7	R	494
16-3, 85–87	143.56	1.07 E-6	+40.3	357.5	−18.5	336.4	R	28
16-3, 135–137	144.06	1.21 E-6	+15.5	27.8	−48.9	18.3	R	27
16-4, 35–37	144.56	2.74 E-7	+62.3	105.9	−36.7	39.9	R	29
16-4, 85–87	145.06	1.88 E-7	+75.0	91.8	−58.3	271.8	R	20
16-4, 135–137	145.56	2.40 E-7	+43.6	88.1	−66.1	21.0	R	355
16-5, 35–37	146.06	2.40 E-7	−1.5	115.2	−57.6	357.6	R	>500
16-5, 85–87	146.56	2.08 E-7	+63.7	84.3	−57.1	80.2	R	39
16-5, 135–137	147.06	1.99 E-7	+61.3	348.3	−64.8	332.5	R	45
16-6, 35–37	147.56	9.60 E-7	+77.2	143.4	−70.4	355.7	R	31
*17-1, 35–37	149.56	2.33 E-7	+13.7	11.2	−49.5	59.8		291
17-1, 135–137	150.56	2.44 E-7	−23.9	120.2	−60.1	104.2	R	266
17-2, 31–33	151.02	7.79 E-8	+2.3	72.2	−79.6	175.7	R	131
*17-2, 56–58	151.27	1.57 E-7	+30.5	82.7	+5.9	147.4		51
17-3, 35–37	152.56	1.82 E-7	−14.6	95.8	−48.5	74.4	R	381
17-3, 56–58	152.77	1.83 E-7	−32.6	79.1	−62.4	54.1	R	298
17-4, 37–39	154.08	1.29 E-7	+45.2	148.2	−73.2	34.9	R	38
17-4, 95–97	154.66	1.86 E-7	−33.3	121.4	−69.8	126.7	R	53
17-4, 133–135	155.04	2.32 E-7	−19.5	115.1	−58.7	90.1	R	104
17-5, 35–37	155.56	1.43 E-7	−17.3	57.0	−67.2	78.5	R	>300
17-5, 117–119	156.38	2.30 E-7	−32.1	90.4	−72.6	297.1	R	103
17-6, 49–51	157.20	2.01 E-7	+15.7	157.2	−63.3	176.2	R	660
17-6, 85–87	157.56	4.91 E-7	+60.6	202.4	−70.6	115.2	R	606
17-7, 23–25	158.44	2.49 E-7	−12.3	87.0	−53.4	48.5	R	891
18-1, 35–37	159.06	1.57 E-7	−31.7	101.1	−84.8	28.0	R	>400
18-1, 95–97	159.66	9.20 E-8	−4.6	108.4	−18.9	149.7	R	100
18-1, 135–137	160.06	1.88 E-7	+27.9	125.3	−71.2	114.8	R	48
18-2, 35–37	160.56	4.53 E-7	−16.3	109.9	−59.2	107.8	R	540
18-2, 95–97	161.16	1.25 E-6	+5.9	143.4	−62.2	124.9	R	351
18-2, 135–137	161.56	3.09 E-7	+8.7	136.4	−74.0	123.1	R	429
18-3, 35–37	162.06	7.06 E-7	−12.4	173.7	−68.6	131.4	R	205
18-3, 95–97	162.66	2.56 E-7	−58.1	107.3	−69.6	105.0	R	>620
18-3, 135–137	163.06	6.85 E-7	+58.2	198.1	−62.8	107.7	R	103
18-4, 35–37	163.56	6.84 E-7	+33.1	134.2	−74.8	113.7	R	255
18-4, 95–97	164.16	2.73 E-7	+31.2	147.9	−43.3	142.6	R	431
18-5, 35–37	165.06	1.46 E-7	−35.0	87.4	−68.5	71.3	R	>500
18-5, 95–97	165.66	7.02 E-8	−64.3	71.7	−75.7	2.7	R	>500
18-5, 135–137	166.06	8.26 E-8	+53.7	60.4	−69.1	72.6	R	41
18-6, 35–37	166.56	1.77 E-7	+65.6	28.9	−66.3	205.0	R	79
18-6, 93–95	167.14	2.47 E-7	+51.5	351.3	+55.9	339.8	N	200
18-7, 35–37	168.06	5.26 E-7	+75.9	155.4	+76.1	171.3	N	43
*19-3, 9–11	171.30	2.18 E-7	+27.0	118.2	+39.8	105.9		296
19-4, 35–37	173.06	1.03 E-6	+66.5	156.0	+75.6	164.7	N	346
19-4, 85–87	173.56	3.27 E-7	+49.6	151.1	+66.9	132.1	N	303
19-4, 130–132	174.01	2.94 E-7	+42.0	142.5	+65.8	136.0	N	258
19-5, 35–37	174.56	1.43 E-7	+51.7	150.2	+64.2	173.8	N	384
19-5, 85–87	175.06	1.89 E-7	+43.4	116.3	+64.0	130.6	N	443
19-5, 135–137	175.56	1.74 E-7	+63.5	45.0	+68.3	11.9	N	230
20-1, 35–37	178.06	6.47 E-7	+84.1	333.7	+75.3	337.8	N	238
20-1, 85–87	178.56	1.36 E-6	+81.5	68.5	+73.2	297.1	N	64
20-1,1 135–137	179.06	4.83 E-7	+75.9	31.1	+69.6	314.4	N	297
20-2, 35-37	179.56	1.23 E-6	+80.1	202.5	+76.8	237.7	N	277
20-2, 85–87	180.06	2.27 E-7	+68.5	96.7	+75.8	77.5	N	151
20-2, 135–137	180.56	4.66 E-7	+72.2	121.0	+73.3	141.2	N	110
20-3, 35–37	181.06	2.57 E-7	−14.4	88.8	−76.0	89.4	R	>750
20-3, 85–87	181.56	2.42 E-7	+19.3	83.7	−42.0	65.0	R	367
20-3, 135–137	182.06	3.48 E-7	−57.7	9.0	−67.0	22.1	R	669
20-4, 35–37	182.56	1.79 E-7	+71.2	288.7	−64.3	17.5	R	82
20-4, 85–87	183.06	1.75 E-7	+15.0	68.8	−58.9	85.8	R	678
20-5, 34–36	184.05	7.48 E-7	−55.6	49.9	−68.8	31.5	R	>750
20-5, 84–86	184.55	2.55 E-7	−21.5	72.6	−59.7	54.7	R	>750
*21-1, 35–37	185.16	1.28 E-7	+43.8	17.2	−34.3	332.9		132
21-1, 85–87	185.66	6.55 E-8	+72.0	50.9	−69.0	287.4	R	46
*21-1, 135–137	186.16	1.77 E-7	+26.8	121.0	−2.9	138.3		76
21-2, 8–10	186.39	9.62 E-7	−50.4	334.5	−64.0	187.5	R	42
22-1, 35–37	187.16	1.79 E-7	−26.2	71.6	−62.5	135.6	R	692
22-1, 81–83	187.62	1.01 E-7	+11.3	32.9	−60.5	108.7	R	>500
22-1, 117–119	187.98	1.10 E-7	−36.4	121.4	−64.6	134.0	R	135
22-2, 32–34	188.63	2.79 E-7	+6.0	56.0	−67.4	35.0	R	389
22-2, 82–84	189.13	1.13 E-6	−63.1	36.7	−67.7	9.6	R	>750
22-3, 35–37	190.16	6.68 E-6	−36.2	86.9	−61.5	161.7	R	507

Table 8 (continued).

Sample interval (cm)	Sub-bottom depth (m)	J (NRM)[a] (Gauss)	NRM[a]		AF stable		Pol.	MDF (Oe)
			I	D	I	D		
22-3, 82–84	190.63	9.00 E-8	+23.1	53.9	−84.7	107.7	R	>400
22-3, 135–137	191.16	3.59 E-6	+83.2	67.7	−63.6	278.5	R	59
22-4, 35–37	191.66	1.46 E-7	−50.3	155.5	−73.9	63.8	R	>400
22-4, 82–84	192.13	1.41 E-7	+11.4	82.8	−67.2	40.4	R	185
22-5, 35–37	193.16	7.15 E-8	−37.2	116.7	−58.6	146.8	R	>150
22-5, 82–84	193.63	4.41 E-7	−56.0	55.2	−69.8	43.5	R	498
*23-1, 41–43	194.52	1.54 E-7	+66.7	90.9	+60.5	74.2		93
23-2, 35–37	195.96	3.16 E-7	+51.5	61.0	+45.7	44.5	N	427
23-2, 85–87	196.46	1.33 E-7	+26.7	51.6	−9.1	54.2		84
23-2, 135–137	196.96	3.78 E-7	−31.8	112.5	−50.0	108.3	R	>500
23-3, 35–37	197.46	5.90 E-7	−72.0	21.0	−74.3	0.5	R	>500
23-3, 85–87	197.96	3.51 E-7	−60.7	14.0	−67.6	341.5	R	>500
23-3,1 35–137	198.46	3.48 E-6	−64.0	12.2	−65.0	359.9	R	>500
23-4, 35–37	198.96	2.35 E-7	+11.2	136.2	−78.4	43.1	R	>500
23-4, 83–85	199.44	7.13 E-8	−44.5	88.7	−70.5	273.7	R	>400
23-4, 132–134	199.93	7.57 E-8	−29.0	53.4	−64.1	0.4	R	>300
23-5, 35–37	200.46	3.31 E-8	−58.5	0.3	−75.7	343.7	R	>500
23-5, 85–87	200.96	2.22 E-7	−23.3	111.8	−61.7	197.1	R	33
23-5, 135–137	201.46	3.51 E-8	−47.4	16.8	−69.3	346.6	R	>500
24-1, 85–87	201.96	1.42 E-7	+54.0	68.6	−49.9	43.9	R	157
24-1, 135–137	202.46	1.22 E-7	+48.3	22.4	−66.0	30.9	R	368
24-2, 35–37	202.96	8.25 E-7	−70.2	122.9	−76.1	119.7	R	>500
24-2, 85–87	203.46	2.14 E-6	−69.4	41.8	−70.9	36.0	R	>500
24-3, 35–37	204.46	1.74 E-7	+48.6	45.4	−73.3	93.6	R	49
24-3, 85–87	204.96	1.12 E-7	+1.6	73.1	−68.1	62.5	R	>500
24-3, 135–137	205.46	1.68 E-7	+53.2	22.8	−57.1	51.2	R	445
24-4, 35–37	205.96	3.61 E-7	+28.5	56.3	−74.3	27.7	R	>500
*25-1, 30–32	206.31	1.65 E-7	+8.8	322.1	−58.0	341.9		>500
25-1, 85–87	206.86	9.22 E-8	−3.3	51.3	−68.1	58.6	R	>400
25-1, 135–137	207.36	1.09 E-7	−41.6	37.3	−67.8	24.7	R	>400
25-2, 30–32	207.81	1.74 E-7	+15.9	68.1	−73.1	34.1	R	>500
25-2, 85–87	208.36	1.97 E-7	−6.4	48.4	−68.2	64.5	R	482
25-3, 30–32	209.31	1.26 E-7	−1.9	44.2	−39.4	46.0	R	>200
26-1, 35–37	210.86	1.10 E-7	+10.8	52.9	−57.3	133.2	R	>300
26-1, 85–87	211.36	1.10 E-7	+42.0	46.9	−63.6	127.4	R	>400
26-1, 135–137	211.86	1.56 E-7	−14.6	123.8	−68.6	131.6	R	>500
26-2, 35–37	212.36	6.62 E-7	−68.9	126.1	−77.0	125.5	R	>500
26-2, 85–87	212.86	1.12 E-6	−62.3	169.9	−65.6	173.5	R	>300
26-2, 135–137	213.36	8.89 E-7	−49.0	111.4	−62.4	112.6	R	480
26-3, 35–37	213.86	6.04 E-8	+5.8	62.9	−55.0	118.5	R	>150
27-1, 85–87	215.16	1.99 E-7	−56.1	64.8	−67.3	18.0	R	409
27-1, 115–117	215.46	4.29 E-7	−84.0	60.8	−85.2	6.1	R	548
*28-1, 35–37	216.46	1.66 E-7	−40.1	68.7	−64.1	24.9		382
28-1, 85–87	216.96	1.60 E-6	−64.5	46.8	−69.3	35.2	R	487
28-1, 135–137	217.46	2.06 E-6	−64.3	100.5	−72.7	33.5	R	270
28-2, 35–37	217.96	3.36 E-6	−69.6	48.6	−73.5	38.4	R	548
28-2, 85–87	218.46	3.63 E-6	−68.8	34.6	−72.3	24.4	R	>500
28-2, 135–137	218.96	2.36 E-6	−71.3	54.6	−63.7	8.6	R	495
28-3, 35–37	219.46	1.89 E-7	+65.1	72.1	−17.7	37.6	R	47
28-3, 85–87	219.96	1.38 E-7	+36.9	52.3	−70.2	27.2	R	79
28-4, 35–37	220.96	2.06 E-7	+21.1	79.9	−54.3	61.8	R	78
29-1, 35–37	221.46	2.53 E-7	+14.5	96.4	−52.5	119.0	R	76
29-1, 85–87	221.96	1.17 E-7	+36.5	81.7	−62.2	65.2	R	41
29-1, 135–137	222.46	7.42 E-8	+60.2	14.8	−14.5	254.9	R	43
29-2, 35–37	222.96	1.12 E-7	−26.5	23.3	−61.7	1.5	R	143
29-2, 85–87	223.46	1.44 E-7	+51.0	37.7	−60.9	5.5	R	126
29-3, 35–37	224.46	6.57 E-7	−1.6	117.0	−56.3	123.7	R	262
29-3, 85–87	224.96	4.13 E-7	−12.4	112.0	−65.9	166.3	R	246
29-3, 135–137	225.46	1.38 E-7	+70.1	56.2	+79.0	257.3	N	175
30-1, 35–37	226.46	3.10 E-7	+75.5	89.1	+64.5	76.0	N	66
30-1, 85–87	226.96	9.83 E-7	+72.8	201.8	+71.3	222.3	N	459
30-1, 135–137	227.46	5.34 E-7	+68.0	99.6	+57.3	119.0	N	262
30-2, 35–37	227.96	3.95 E-7	+55.8	99.8	+64.5	127.3	N	132
30-2, 85–87	228.46	2.75 E-7	+80.0	40.1	+67.1	9.7	N	63
30-2, 135–137	228.96	4.29 E-7	+68.6	116.6	+62.4	95.4	N	93
30-3, 35–37	229.46	4.34 E-7	+66.0	49.8	+79.4	31.1	N	118
30-3, 85–87	229.96	4.69 E-7	+78.7	146.0	+70.2	176.2	N	84
30-3, 135–137	230.46	1.56 E-6	+73.8	212.6	+72.3	221.4	N	442
30-4, 35–37	230.96	1.08 E-6	+75.9	151.5	+81.1	176.1	N	423
30-4, 85–87	231.46	1.18 E-6	+80.9	140.0	+83.8	150.0	N	370
30-4, 135–137	231.96	2.55 E-6	+87.5	193.4	+85.1	254.1	N	446
31-1, 35–37	232.46	1.16 E-6	−74.9	6.4	−79.6	318.0		>750
31-1, 85–87	232.96	4.98 E-6	+75.5	136.9	+76.8	137.2	N	472
31-1, 135–137	233.46	7.89 E-6	+75.5	158.0	+75.4	159.1	N	459
31-2, 35–37	233.96	9.95 E-7	+63.6	43.0	+68.1	40.0	N	431
31-2, 85–87	234.46	3.18 E-7	+68.8	118.5	+66.0	125.5	N	64

Table 8 (continued).

Sample interval (cm)	Sub-bottom depth (m)	J (NRM)[a] (Gauss)	NRM[a]		AF stable		Pol.	MDF (Oe)
			I	D	I	D		
31-2, 135-137	234.96	2.99 E-7	+71.3	123.4	+70.7	94.5	N	97
31-3, 35-37	235.46	4.07 E-7	+58.5	89.5	+71.2	359.4	N	126
31-3, 85-87	235.96	6.47 E-7	+66.4	99.5	+66.2	94.3	N	132
31-4, 35-37	236.96	6.27 E-7	+77.7	100.5	+77.7	93.9	N	182
31-4, 85-87	237.46	7.00 E-7	+72.5	122.9	+73.0	129.5	N	134
*32-1, 35-37	238.46	4.10 E-7	+23.0	93.5	+26.9	79.1	N	147
32-1, 85-87	238.96	7.24 E-7	+35.3	126.9	+48.2	111.6	N	121
32-2, 35-37	239.96	4.70 E-7	+61.5	123.6	+62.5	121.8	N	127
32-2, 85-87	240.46	3.19 E-7	+60.2	85.4	+61.2	79.9	N	127
32-2, 135-137	240.96	5.12 E-7	+81.1	122.2	+80.8	77.7	N	137
32-3, 35-37	241.46	8.87 E-7	+57.0	112.8	+58.9	105.0	N	106
32-3, 85-87	241.96	6.40 E-7	+74.6	12.0	+65.8	324.9	N	123
32-3, 135-137	242.46	9.31 E-7	+72.5	107.0	+76.2	102.8	N	150
32-4, 35-37	242.96	5.50 E-7	+65.7	122.4	+64.1	131.0	N	127
32-4, 85-87	243.46	3.34 E-7	+60.7	132.0	+64.8	134.1	N	176
32-4, 135-137	243.96	3.70 E-7	+54.4	100.4	+54.9	101.9	N	175
33-1, 135-137	245.06	3.09 E-7	+71.4	82.6	+74.3	45.7	N	185
33-2, 35-37	245.56	3.01 E-7	+72.3	53.9	+72.1	48.9	N	156
34-1, 35-37	246.36	8.18 E-7	+69.8	77.6	+70.8	58.2	N	191
34-1, 85-87	246.86	5.44 E-7	+55.5	63.9	+57.1	57.6	N	84
34-1, 135-137	247.36	4.78 E-7	+54.3	93.9	+59.8	94.9	N	143
34-2, 35-37	247.86	6.42 E-7	+52.8	104.5	+66.0	88.6	N	137
34-2, 85-87	248.36	7.01 E-7	+43.3	62.7	+56.9	31.8	N	249
34-2, 135-137	248.86	2.27 E-6	+67.8	126.2	+70.0	122.3	N	183
34-3, 23-25	249.24	9.60 E-7	+61.5	313.0	+69.7	338.3	N	198
34-4, 35-37	250.86	2.88 E-6	+77.4	19.3	+78.2	18.5	N	469
34-4, 85-87	251.36	3.14 E-6	+67.1	49.0	+67.6	46.6	N	479
34-4, 135-137	251.86	8.33 E-7	+58.1	51.9	+55.1	49.9	N	385
34-5, 35-37	252.36	6.63 E-7	+62.8	40.0	+61.8	39.3	N	195
34-5, 85-87	252.86	4.61 E-7	+70.1	40.4	+68.6	32.8	N	234
34-5, 135-137	253.36	3.17 E-7	+59.0	78.6	+66.2	75.8	N	148
34-6, 35-37	253.86	4.32 E-7	+65.3	72.6	+63.4	71.0	N	176
34-6, 85-87	254.36	5.85 E-7	+64.2	48.4	+59.2	46.0	N	156
34-6, 135-137	254.86	5.02 E-7	+77.9	61.9	+70.8	4.0	N	133
34-6, 135-137	254.86	5.02 E-7	+77.9	61.9	+70.8	4.0	N	133

[a] Abbreviations: J = intensity, I = inclination, D = declination of natural remanent magnetization (NRM) and stable remanence after AF demagnetization, Pol = polarity, N = normal, R = reversed, MDF = median destructive field.

Asterisks denote disturbed core intervals.

The sediment cores recovered from Hole 644B were also measured with the cryogenic magnetometer aboard ship. However, data from shore-based studies are not yet available for this report.

GEOCHEMISTRY

Organic

Based on previous studies of DSDP Leg 38 (Morris, 1976), we predicted that sediments at Site 644 should contain significant quantities of biogenic gas, but expected no petroleum-related compounds unless sediments of Miocene age were drilled. The following statements concerning the safety aspects of the proposed location were prepared to obtain a license from the Norwegian Petroleum Directorate to drill this site.

1. The Ocean Drilling Program (ODP) Leg 104 requests permission to drill by hydraulic piston core (HPC) the proposed site VOR-5 in the Vøring Basin to a total sub-bottom depth of 250 m, instead of to 50 m as previously permitted. Earlier scientific studies in this region show that no significant safety hazards are to be anticipated when drilling this 250-m interval.

2. Drilling in the Vøring Basin by the *Glomar Challenger* (DSDP Leg 38) encountered no significant safety problems at three sites within about 60 nmi of the proposed site VOR-5. At DSDP Sites 339 (108 m total depth) and 340 (104.5 m total depth) no hydrocarbon gas or oil was detected.

3. Possible petroleum-related compounds were encountered, however, at DSDP Site 341 (456 m total depth), but only at depths greater than 400 m in Miocene sediment. Cores taken at depths between 408.5 and 456 m had a petroliferous odor, but no gas or liquid petroleum was detected or recovered from this site. The sediments of these Miocene age cores cannot be the source of significant oil accumulations at this time. The proposed drilling at VOR-5 to 250 m would not reach Miocene sediments (anticipated depth at VOR-5 of 430 m) and, therefore, would not be expected to encounter possible petroleum-related substances.

4. Hydrocarbon gas was found in the upper 250 m of sediment at DSDP Site 341, starting at about 50 m sub-bottom. This gas was dominantly methane (99.9+%) accompanied by traces of ethane. This chemical composition is typical of gases found in all shallow marine sediments, is the result of biogenic activity and is *not* related to petroleum. Furthermore, the carbon isotopic signature of this methane confirms the biogenic source of this gas.

5. Drilling by hydraulic piston core (HPC) to refusal or to 250 m, whichever is less, as proposed at VOR-5, is not considered hazardous because a high-pressure hydrocarbon accumulation would be most unlikely at such shallow depths in such relatively unconsolidated sediments.

6. Therefore, the evidence collected previously, especially from DSDP Site 341, indicates that Site VOR-5 can be drilled safely to 250 m. We anticipate that biogenic gas will be found

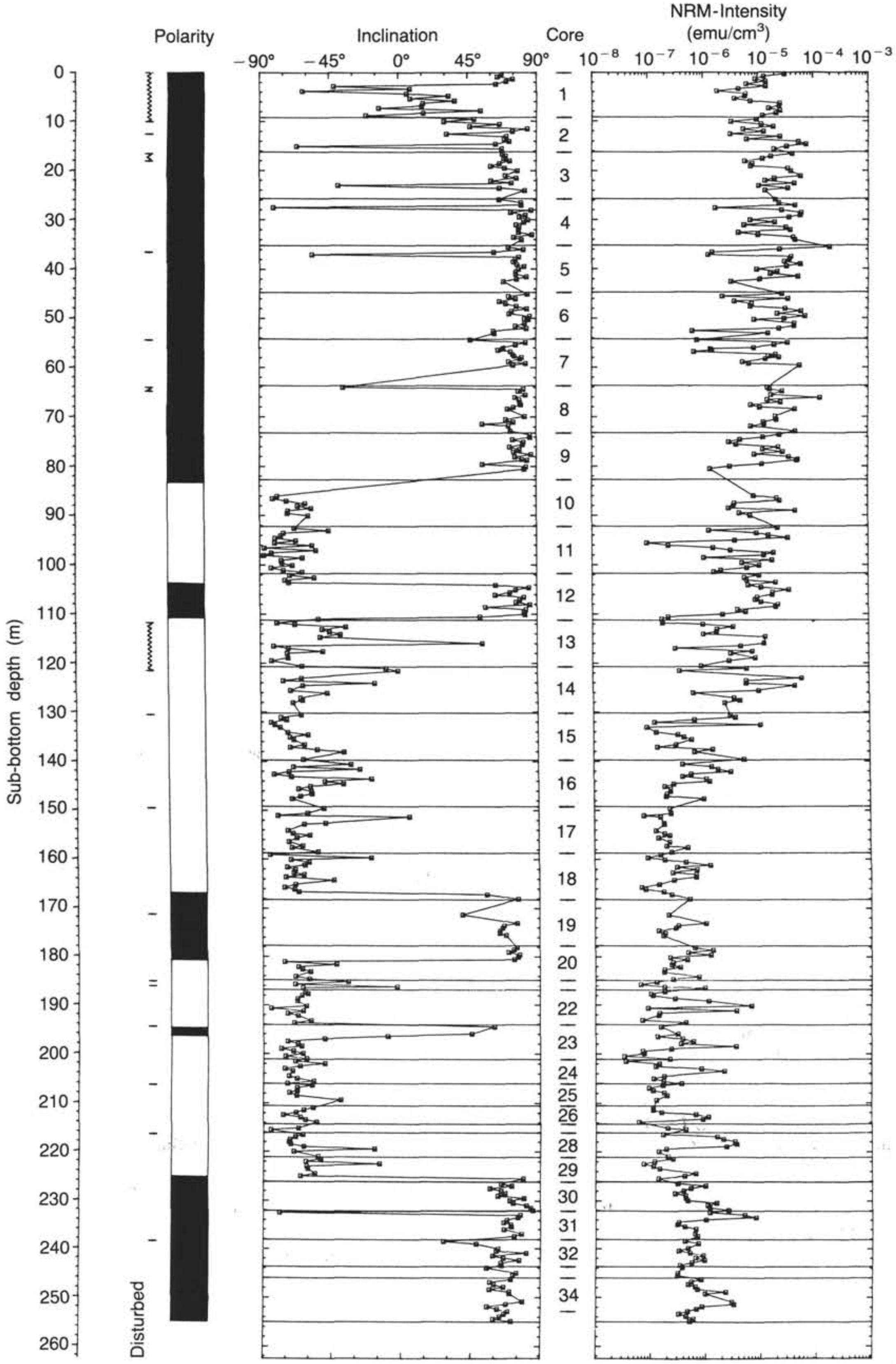

Figure 12. Stratigraphic sequence of Hole 644A showing the variations in inclination of the characteristic remanent magnetization and in NRM intensity. Horizontal lines indicate core boundaries. The paleomagnetic polarity log is based on stable inclinations, black being normal and white being reversed polarity. Disturbed intervals are indicated next to the polarity columns.

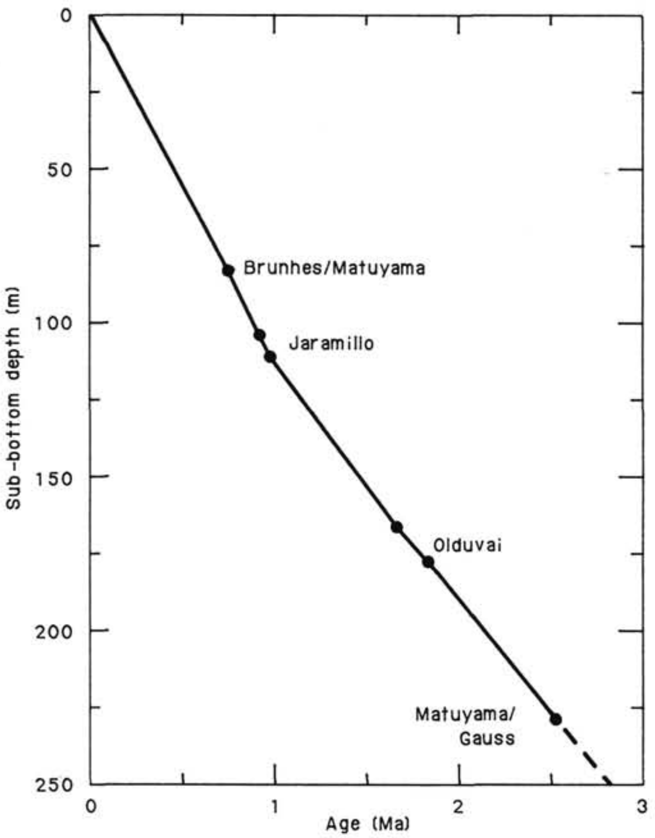

Figure 13. Apparent sediment accumulation at Site 644, derived from the correlation of the downhole pattern in remanent magnetization polarity with the geomagnetic polarity time scale of Berggren et al. (1985).

but that no petroleum-related compounds will be encountered. We will, of course, closely monitor the hydrocarbon chemistry during the proposed drilling and will cease drilling if there is any indication of petroleum-related substances.

Our predictions were correct, and indeed significant quantities of biogenic gas were found at this site starting at a sub-bottom depth below about 22 m. No petroleum-related compounds were identified, however, although very low concentrations of hydrocarbon gases related to early, thermal diagenetic processes were seen toward the bottom of the hole (250 m).

Because gassy sediments at Site 644 were expected, and the hydrocarbon chemistry was to be closely monitored, the sampling strategy was altered to collect sediments for gas analyses every other core instead of every third core, as at Sites 642 and 643. Sampling for interstitial-water chemistry and, consequently, for organic and inorganic carbon measurements was also changed. These samples were taken every other core through Core 104-644A-7H, at which point the samples were collected every third core.

Hydrocarbon Gases

In contrast to the results for Sites 642 and 643, where the maximum concentration of methane was 23 ppm, the headspace-derived gas at Site 644 had a maximum of 51% methane at 77.6 m sub-bottom (Table 10). Samples at sub-bottom depths of 5.9 and 22.1 m contained 23 and 820 ppm of methane, respectively, but deeper samples all had more than 1% methane. A depth profile of methane concentrations shows two maxima at 78 and 235 m, with a low of 1% at 200 m (Fig. 14).

Significant gas-expansion cracks occurred in cores from 73.2 to 158.7 m sub-bottom. The gas in these cracks was collected by Vacutainer, and the amount of methane in the gas mixtures was measured by gas chromatography. Our results showed that methane composed between 45% and 89% of the gas mixture. The balance of the gas was probably air.

The rapid increase in concentrations of methane below a sub-bottom depth of about 22 m follows a rapid decrease in the amount of sulfate in the pore waters (Fig. 14). At 200 mbsf, where methane values reached a minimum, sulfate concentrations increased from 0 to 4 mmol and then decreased again with depth as methane concentrations increased. The general inverse correlation of methane and sulfate concentrations shows that the occurrence of methane is tied to the absence of sulfate. Thus, this site demonstrates the classic profile of a zone of sulfate reduction overlying a zone of methane production (Claypool and Kaplan, 1974). The methane-sulfate relationship indicates that the environment at Site 644 is reducing and that the methane is a product of microbial reduction of CO_2 ultimately derived from organic matter.

In addition to methane, higher-molecular-weight hydrocarbon gases were also present. Ethane appeared first with depth, followed by propane, *n*-butane, and finally *n*-pentane. Figure 15 shows a gas chromatogram of the hydrocarbon gases extracted from sediments recovered at 125 m sub-bottom; for comparison, a chromatogram of a standard gas mixture is included. Overall, a general increase in concentrations of the higher-molecular-weight hydrocarbon gases occurs with depth. Methane/ethane ratios (Table 10) decreased irregularly with depth as shown in Figure 14. These high ratios, reflecting the hydrocarbon composition of the gas at Site 644, indicate that the methane is dominantly biological in origin.

Table 9. Magnetostratigraphic summary for Hole 644A.

Epoch	Event	Boundary Core-Sect.-Int. (cm)	Depth (mbsf)	Age (Ma)	Apparent sedimentation rate (m/m.y.)
Brunhes					112
		9-CC-14/top core 10	81.77	0.73	
Matuyama					122
	Jaramillo, top —	12-2-36/12-2-86	103.81	0.91	
					106
	Jaramillo, base —	12-7-28/12-CC-22	111.22	0.98	
					81
	Olduvai, top —	18-5-136/18-6-36	166.31	1.66	
					66
	Olduvai, base	20-2-136/20-3-36	180.81	1.88	
Matuyama					75
		29-3-86/29-3-136	225.21	2.47	
Gauss					

Table 10. Organic geochemistry at Site 644.

Core	Section	Depth (mbsf)	Methane (%)	Ethane (ppm)	C_1/C_2	Org C (%)	Inorg C (%)
1	4	5.9	0.01			0.37	1.32
3	4	22.1	0.08			0.64	0.72
5	3	39.6	3.40	7.9	4,250	0.68	1.60
7	2	57.1	39.80	9.3	42,800	0.96	1.56
9	3	77.6	51.30	14.3	35,900		
10	4	88.6				0.46	1.68
11	5	99.6	16.50	*6.0	27,500		
14	3	125.1	38.40	15.4	24,950	0.77	2.11
15	4	136.1	23.60	12.5	18,960		
16	4	145.6				0.81	0.67
17	2	152.1	13.30	8.2	16,300		
20	4	183.6	7.20	12.2	5,950	0.64	0.22
22	4	192.7	2.30	8.3	2,810		
23	4	200.0	1.00	5.4	1,800		
25	2	208.9	23.40	11.5	20,400	0.82	0.62
28	2	219.0	31.70	11.8	26,880		
29	2	224.0	14.30	9.6	14,970	0.73	0.47
31	2	235.0	41.40	19.7	21,050		
34	4	251.9	27.40	16.7	16,420	0.69	0.47

*Original value of 29.7 ppm resulted from integration error.

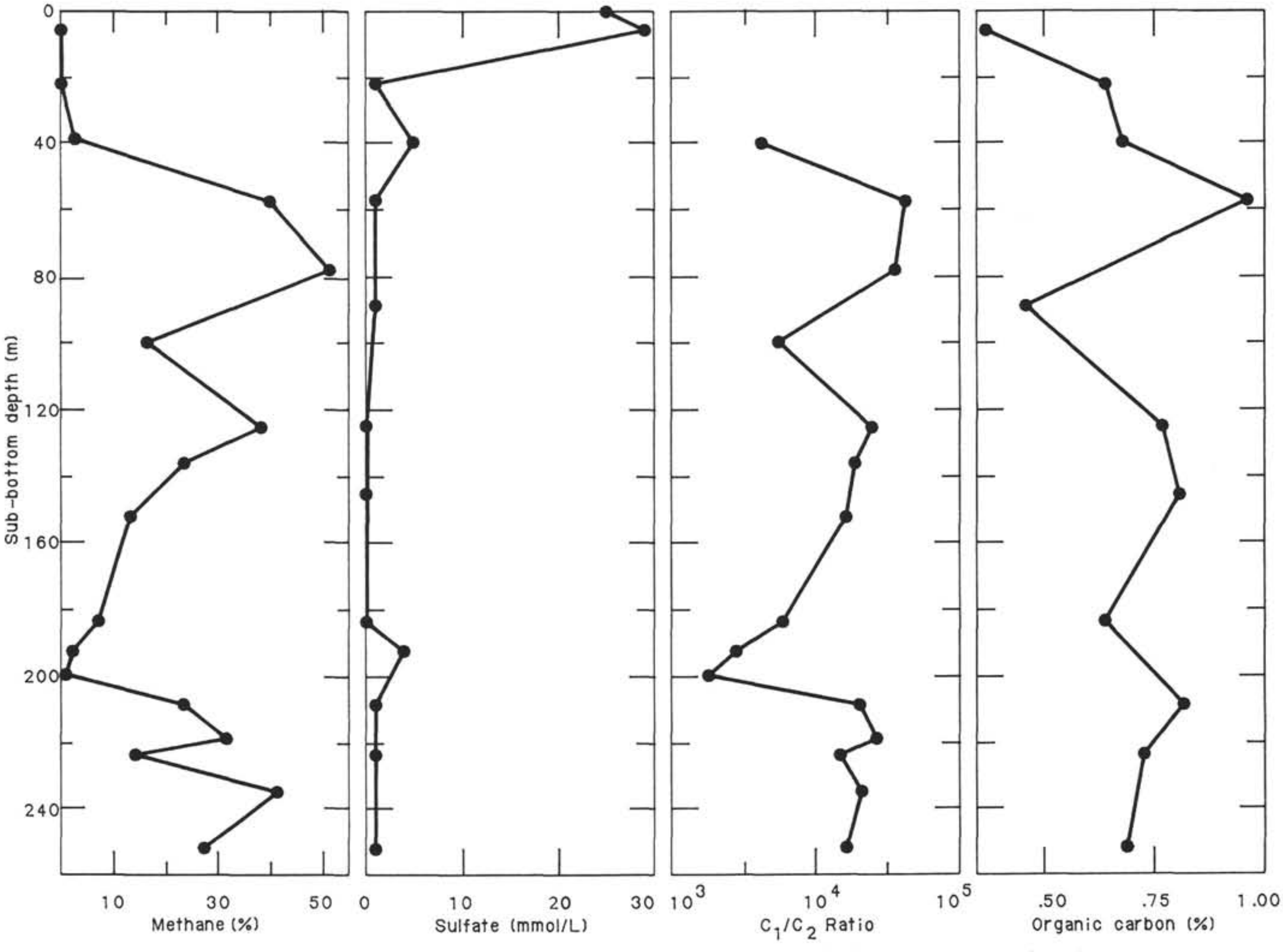

Figure 14. Profiles (with depth) at Site 644. Graphs show methane, sulfate, methane/ethane (C_1/C_2) ratio, and organic carbon.

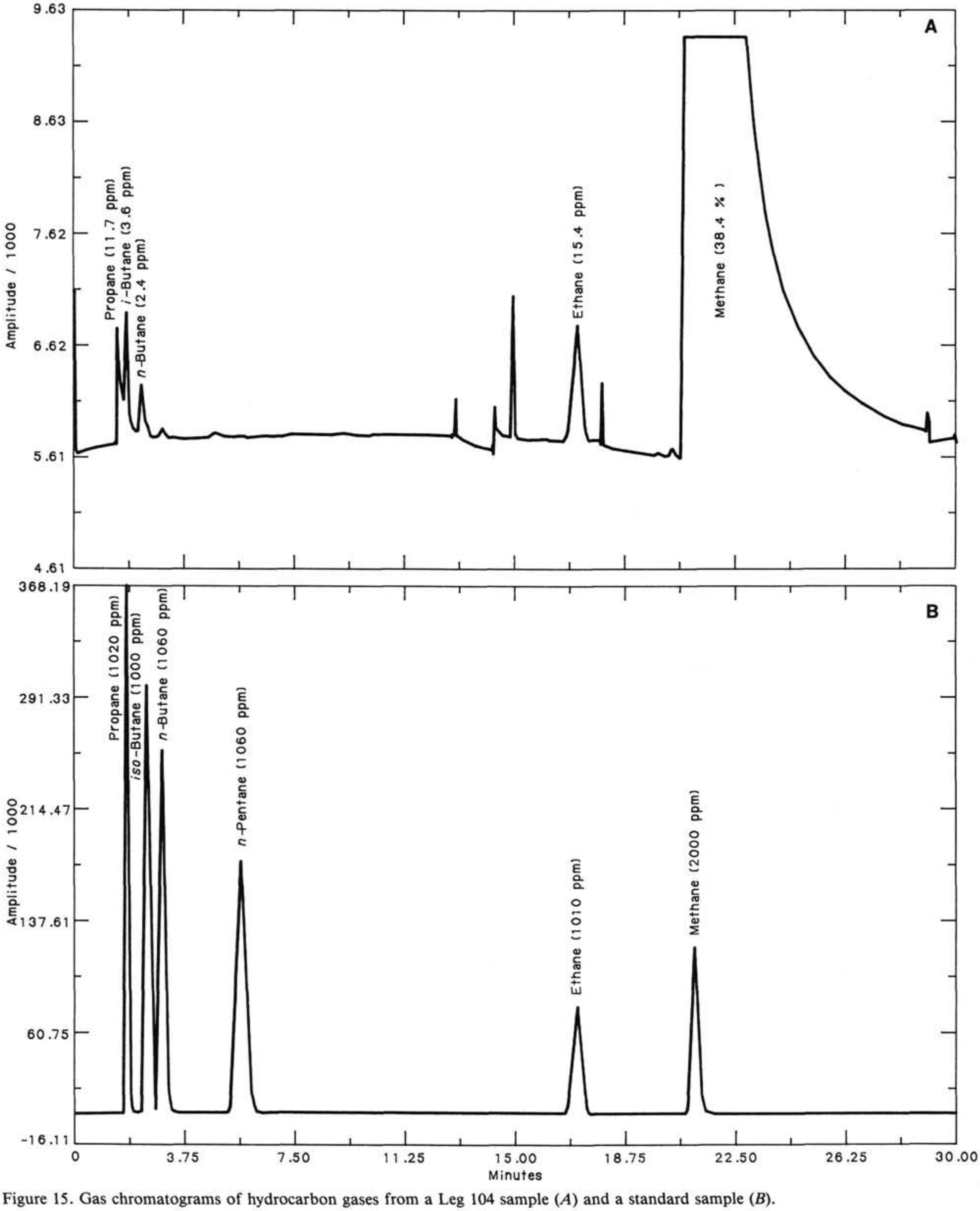

Figure 15. Gas chromatograms of hydrocarbon gases from a Leg 104 sample (*A*) and a standard sample (*B*).

Carbon and Organic Matter

The amount of organic carbon measured in samples from this site (Table 10) was less than 1% (averaging 0.7%). A profile of organic carbon concentrations with depth is shown in Figure 14; no obvious correlation with depth between organic carbon and methane exists. These sediments have less organic carbon than the sediments at Site 642, yet methane is significantly more abundant at Site 644. The difference in concentrations of methane at the two sites must ultimately be linked to the fact that the sediments at Site 644 are reducing, whereas at Site 642 the sediments are probably oxidizing, thus inhibiting methanogenesis.

Carbonate carbon at Site 644 is variable (Table 10), with amounts not exceeding 2.1%.

Organic matter in sediments at Site 644 was analyzed by Rock-Eval pyrolysis (Table 11). In general, the measured parameters suggest that the organic matter is immature and highly oxygenated. T_{max} values are usually low (average 428°C), whereas oxygen indices (OI) are all greater than 250 (mg CO_2/g organic C). Hydrogen indices (HI) are all very low and less than 171 (mg hydrocarbons/g organic C). These indices, if correctly interpreted, suggest that this organic matter is dominantly terrestrial in origin and very immature.

Inorganic

The programs for monitoring interstitial water and inorganic and organic carbon were slightly altered at Site 644, compared with the programs for the two previous sites. The sampling scheme entailed a sample collected every other core from Core 104-644A-1H (5.9 m) to Core 644A-7H (54 m), then every third core until the hole was terminated (250 m). This closely spaced sampling scheme was used to obtain more information to aid in interpreting the hydrocarbon gas chemistry. Twelve sediment samples were analyzed for pore-water chemistry.

The results of the interstitial-water analysis are presented in Table 12. Concentrations of sulfate, calcium, magnesium, and alkalinity vs. depth are depicted in Figure 16. Sulfate is depleted in the upper 50 m. This depletion of sulfate corresponds with the onset of methanogenesis, as discussed previously. This type of sulfate profile is typical of hemipelagic sedimentary environments with high deposition rates and abundant organic carbon (Gieskes, 1981). The sulfate profile at Site 644 contrasts with that at the two previous sites, where sulfate only decreases slightly with depth. Alkalinity increases with depth in the top 25 m of sediment. Below this depth alkalinity generally decreases, but only slightly. At about 210 mbsf the alkalinity trend changes and values increase to the bottom of the hole. A maximum value of 21.1 meq/L in the upper section of the hole at this site occurs at 22.1 mbsf. This maximum value is within the zone of intense sulfate reduction where CO_2 is released simultaneously with the production of sulfide and, in these sulfate-depleted waters, reacts with calcium to form various carbonates (Mechalas, 1974). That this process is active is supported by the observation that calcium carbonate is most abundant at this site in sediments shallower than 125 mbsf. The alkalinity values obtained here are also much higher than at the previous two sites. Calcium ion concentrations show two high values at 22.1 and 57.1 mbsf in an otherwise uneventful profile. The magnesium profile is similar to profiles from the previous two sites; a regular decrease occurs with depth below about 57.1 mbsf. Salinity decreases with depth from 35.5 parts per thousand (ppt) at 5.9 mbsf to 31.8 ppt at 251.9 mbsf, reflecting the loss of magnesium, sulfate, and chloride ions. The general decrease in the chloride ion with depth suggests that it is being bound to the clays with burial (Gieskes, 1981) or that the methane at this site is present as gas hydrate (Harrison et al., 1982).

Table 11. Rock-Eval data from Site 644.

Core	Sec.	Depth (mbsf)	T_{max}	S_1	S_2	S_3	TOC	HI	OI
1	4	5.9	384	0.39	0.63	2.44	0.38	165	642
3	4	22.1	472	0.38	0.87	2.67	0.56	155	476
5	3	39.6	427	0.09	0.66	2.89	0.72	91	401
7	2	57.1	418	0.13	0.88	3.55	1.05	83	338
10	4	88.6	444	0.06	0.35	2.10	0.42	83	500
14	3	125.0	406	0.25	1.12	5.66	1.08	103	524
16	4	145.6	390	0.44	1.15	2.38	0.13		
20	4	183.6	425	0.34	0.98	1.57	0.61	160	257
25	2	208.9	394	0.31	0.84	2.96	0.49	171	604
29	2	224.0	450	0.23	0.88	3.63	0.67	131	541
34	4	251.9	494	0.38	1.04	2.59	0.71	146	364

Abbreviations: S_1 (mg HC/g rock) = volatile hydrocarbons, S_2 (mg HC/g rock) = kerogen-derived hydrocarbons, S_3 (mg CO_2/g rock) = organic CO_2 from kerogen, TOC = total organic carbon, HI (100 S_2/C_{org}) = Hydrogen Index, OI (100 S_3/C_{org}) = Oxygen Index, T_{max} = temperature (°C) of maximum hydrocarbon generation from kerogen.

PHYSICAL PROPERTIES

Introduction

Drilling at Site 644 penetrated approximately 250 m of sediments. Physical properties measured at the site were index properties, thermal conductivity, and undrained shear strength. Compressional-wave velocity could not be measured because of the gassy nature of the sediments (see "Geochemistry" section, this chapter).

As at previous sites of Leg 104, the character and distribution of physical-properties profiles are closely associated with sediment type. Changes in the physical-properties profiles correlate closely with lithologic unit boundaries and also correlate between sites. A summary of physical-properties data for Site 644 is tabulated in Table 13.

Index Properties

Index-properties profiles (bulk density, porosity, and water content) are plotted relative to sub-bottom depth, along with thermal conductivity, in Figure 17. The vertical distribution of these properties shows the expected relationships with each other. Bulk density is inversely correlated with porosity and water content (Hamilton, 1974). The overall trends with depth also are those expected and reflect the effects of burial diagenesis: bulk

Table 12. Interstitial water data from Site 644.

Core	Sect.	Depth (mbsf)	pH	Alkalinity (meq/L)	Salinity (ppt)	Chlorinity (mmol/L)	Sulfate (mmol/L)	Calcium (mmol/L)	Magnesium (mmol/L)
Seawater		0	7.83	2.51	34.1	556	25	12	54
1	4	5.9	7.80	9.24	35.5	560	29	9	46
3	4	22.1	8.15	21.14	33.8	561	1	49	50
5	3	39.6	8.16	19.05	32.4	554	5	8	50
7	2	57.1	8.00	16.87	31.8	554	1	84	53
10	4	88.6	8.13	16.70	31.9	553	1	7	35
14	3	125.0		18.76	32.0	552	0	7	30
16	4	145.6		18.70	31.9	550	0	6	30
20	4	183.6	7.90	17.17	32.0	553	0	8	24
22	4	192.7	8.21	16.77	31.0	556	4	18	23
25	2	208.9	8.12	15.93	31.0	547	1	9	20
29	2	224.0	8.18	18.56	32.0	530	1	6	22
34	4	251.9	7.99	25.32	31.8	538	1	12	18

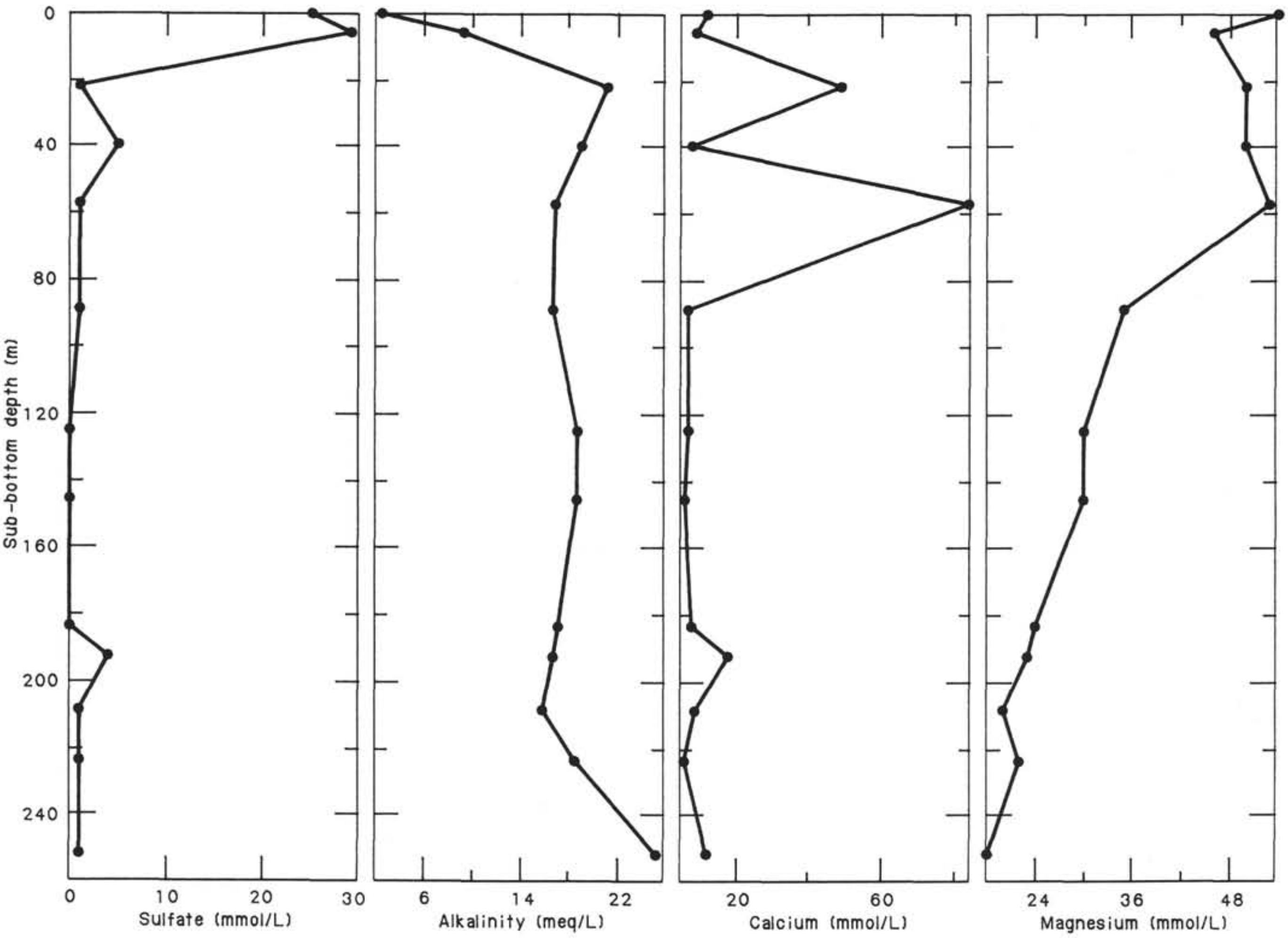

Figure 16. Sulfate, alkalinity, calcium, and magnesium profiles with depth at Site 644.

density tends to increase with depth while porosity and water content generally decrease with depth.

The trend of some portions of the index-properties profiles is an exception to the overall trend in that these properties show reverse gradients. These intervals generally correlate with sediment type, which can be more important than diagenesis for determining the distribution of physical properties (Bennett and Nelson, 1983).

Lithologic Subunits IA and IB consist of interbedded, carbonate-poor glacial muds and interglacial calcareous mud (see "Sedimentary Lithology" section, this chapter). The clastic content tends to increase downward in these subunits, while carbonate and clay content decrease. This change is reflected in trends of increasing bulk density and decreasing porosity and water content (Fig. 17). The decrease in porosity and water content probably results from decreasing clay content, rather than any decreases in the amount of carbonate present.

Average values for the index properties of Subunit IA are bulk density, 1.73 g/cm^3; porosity, 58.8%; and water content, 55.4%. Average values of these properties for Subunit IB are 1.84 g/cm^3, 56.5%, and 43.5%, respectively.

Subunit IC consists of interbedded calcareous mud, sandy mud, and siliceous nannofossil muds. The general composition trend in this subunit is toward an increasing amount of biogenic silica and decreasing carbonate down core. The clastic and clay contents vary widely, but are of relatively constant proportion.

The changes in index properties associated with these lithologic changes are a reversal of the trend in bulk density. This anomalous trend of decreasing bulk density with depth was also observed at Sites 642 and 643 and correlates at each site with an increase in biogenic silica.

Porosity and water content values vary widely over Subunit IC, reflecting variations in composition; however, the average value of these properties does not vary much with depth (Fig. 17). The lack of gradient probably reflects the relatively constant proportions of clastics and clays in the interval and suggests that little, if any, of this porosity is associated with the siliceous fossils. Average values for bulk density, porosity, and water content for Subunit IC are 1.78 g/cm^3, 58.0%, and 49.7%, respectively.

The contact between Units I and II is fairly abrupt on index-property profiles and is marked by a sudden shift to sharply decreasing bulk density and increasing porosity and water content. These changes probably reflect the relatively sudden increases in percent of carbonate and biogenic silica at this boundary.

Undrained Shear Strength

The undrained shear-strength profile for Site 644 is plotted in Figure 18. The trend is one of linear increase in average value with depth but with increasing variability. Some of this variability may be caused by disturbance from hydraulic piston coring

Table 13. Summary of physical properties data for sediments from Site 644.

Core/Sec*	Sub-bottom depth (m)	Bulk density (g/cm^3)	Porosity (%)	Water content (%)	Shear strength (kPa)	Thermal conductivity (10^{-3} cal × $°C^{-1}$ × cm^{-1} × s^{-1})
1-2B	2.10	1.62	68.8	69	39.55	
1-2	2.10	1.75	59.3	51		3.000
1-4	5.10	1.65	65.7	65	4.27	2.521
2-2B	6.70	1.54	58.7	80	9.04	
1-6	8.10	1.59	68.9	75	4.47	
2-2	11.30	1.56	70.4	82	6.31	2.535
2-4	14.30	1.68	62.4	59	14.33	3.014
2-4	14.70	1.99	43.8	29	23.96	3.130
3-2	18.40	1.75	59.4	51	14.69	3.130
3-4	21.40	1.71	42.0	33	22.60	2.704
3-6	22.50	1.77	60.2	52	19.21	3.036
4-2B	24.19	1.73	61.0	51	10.74	
4-2	27.80	1.60	66.1	70	37.06	2.698
4-4	30.80	1.76	60.2	52	30.28	3.026
4-5	32.75	1.95	46.8	32	30.74	2.672
5-2B	33.69	1.67	61.1	68	21.47	
4-6	33.80	1.68	63.0	60	40.12	3.052
5-2	37.30	1.75	58.6	50	29.61	3.528
5-4	40.95	1.79	57.4	47	38.76	3.528
6-18	43.19	1.78	48.9	52	26.56	
6-2	45.29	1.95	45.5	31	23.73	3.240
6-4	48.29	1.73	64.6	59	46.33	3.100
6-6	51.29	1.76	60.0	52	30.51	2.580
7-18	52.69	1.98	57.1	33	38.42	
7-2	55.75	2.00	43.3	27	74.58	3.920
7-4	58.75	1.72	60.0	53	45.20	2.480
8-3B	62.19	1.97	56.4	32	30.51	
8-2	65.79	1.95	50.2	35	36.73	3.230
8-4	68.79	1.88	55.5	42	41.81	2.780
9-1B	71.69	1.78	54.4	47	37.29	
8-6	71.79	1.73	62.1	56	45.20	2.900
9-2	75.29	1.85	54.0	41	64.98	3.090
9-6	80.74	1.64	63.5	63	116.39	3.050
10-1B	81.19	1.87	61.9	41	38.42	
10-2	84.79	1.70	63.9	60	71.19	2.640
10-4	87.80	1.97	46.2	31	76.84	3.910
11-3B	90.69	1.77	64.2	54	114.13	
10-6	90.80	1.97	48.7	33	61.02	3.590
11-2	94.60				71.76	1.710
11-4	97.60	1.82	56.4	45	77.97	2.850
11-6	100.60	1.71	61.5	56	96.62	2.720
12-2	103.80	1.74	61.6	55	98.31	2.650
13-3B	106.29	1.69	62.0	60	142.15	
12-4	106.80	1.69	61.7	57	126.56	2.770
12-6	109.80	1.69	62.2	58	87.01	2.610
13-2	113.30	1.74	62.1	55	36.50	2.800
15-3B	119.79	1.67	62.0	58		
13-7	121.00	1.69	62.2	58	41.58	2.810
14-3	124.30	2.04	39.3	24	50.85	2.450
14-5	127.30	1.83	57.0	45	76.84	2.730
15-2	132.30	1.70	52.3	44	118.65	2.880
15-4	135.30	1.75	61.2	54	141.70	3.190
15-6	138.30	1.86	52.8	40	70.96	3.190
16-2	141.80	1.69	61.0	56	145.54	2.840
16-4	144.80	1.67	52.2	59	164.64	2.710
16-6	147.80	1.75	59.0	51	72.09	2.830
17-3	152.70	1.72	62.3	57	84.98	2.602
17-4	154.60	1.69	60.9	56	93.79	
17-5	155.60	1.77	60.1	52	98.65	
18-2	160.80	1.97	45.2	30	125.43	3.318
18-4	163.80	1.74	60.8	54	152.55	2.738
18-6	166.80	1.72	62.7	57		2.704
19-3	172.00	1.71	61.0	56	140.68	2.888
19-4	173.30	1.75	58.4	50	201.25	
20-2	179.80	1.90	61.0	56	159.90	2.779
20-4	182.80	1.71	61.0	56	216.96	2.717
21-1	185.50	1.68	62.1	59	110.00	
22-3	190.40	1.78	60.6	52	104.52	3.083
22-3	190.65	2.00	47.9	32		
22-5	191.90	1.78	60.1	51	209.05	
23-3	197.70	1.87	50.8	37	185.32	3.083
23-5	199.70	1.80	55.6	45	205.66	2.823
24-2	203.20	1.79	57.1	47	202.84	2.778
24-4	206.00	1.79	59.1	49	133.45	2.768
25-2	208.10	1.75	56.6	48	215.83	2.702
25-3	209.60	1.77	59.5	51	226.00	2.675
26-2	212.29	1.79	55.8	49	226.00	2.922
27-1	214.89	1.79	49.4	45	82.49	2.770
28-2	218.19	1.88	57.3	36	282.50	3.218
28-4	220.89	1.80	59.3	47	176.28	2.796
29-2	222.60	1.81	59.6	49	226.00	2.817
29-4	225.60	1.77	64.0	51	90.40	2.690
30-2	228.19	1.70	65.0	60	226.00	2.668
30-4	231.19	1.72	65.5	60	226.00	2.683
31-2	234.19	1.67	66.3	64	157.07	2.582
31-3	237.19	1.64	63.7	68	226.00	2.582
32-4	241.11	1.62	68.4	69	226.00	2.473
34-2	244.11	1.54	62.1	78		2.303
34-4	247.11	1.67	66.8	59	226.00	2.563
32-3	259.60	1.61	66.8	65	153.12	2.531

* B following section number denoites sample from Hole 644B.

or the presence of biogenic methane. The overall trend is typical of marine sediments and reflects burial diagenesis.

The abrupt change in shear-strength gradient observed at Sites 642 and 643 at about 70 mbsf does not occur at Site 644. The variability in values measured does begin to increase significantly at about this point, which also marks the first occurrence of significant amounts of biogenic silica in the section. The percent of biogenic silica at this depth, however, is much less than at previous sites and also increases more gradually than at the other sites. This gradual increase of silica content may explain the absence of an abrupt decrease in gradient. The sudden decrease in shear-strength gradient at Sites 642 and 643 is associated with sharp increases in the amount of biogenic silica. Sediments with higher proportions of biogenic silica have a reduced shear strength relative to clays and carbonate (Bryant et al., 1981).

Sudden, sharp reductions in undrained shear strength occur at about 100 and 150 mbsf. The former occurrence correlates approximately with the contact between Subunits IB and IC, which is associated with a change from increasing clastic and clay content downcore to a decreasing trend in these constituents. The 150-mbsf shift correlates with a reverse to increasing clastic and clay with depth.

Thermal Conductivity and Thermal Gradient

The thermal conductivity profile at Site 644 (Fig. 17) shows an expected, positive correlation with bulk density and a negative correlation with porosity and water content. The decrease with depth to about 50 mbsf is not as evident as at Sites 642 and 643, although the range of values is comparable.

A geothermal gradient of approximately 6.5° to 6.9°C/100 m was measured in the sediment sequence at Site 644 using a temperature recorder developed by Woods Hole Oceanographic Institution. Using a thermal conductivity coefficient of 2.2×10^{-3} cal × $°C^{-1}$ × cm^{-1} × s^{-1} and downhole temperature readings obtained during drilling at the site, the heat flow (preliminary) for this site was computed as 61 mW/m^2.

Summary

In general, the physical-properties profiles at Site 644 show the same relationships and general trends as at previous sites. The major differences occur in the greater range of values for all physical properties measured, which results in less well-defined trends. For the portion of the section that the three sites have in common (approximately the upper 250 mbsf), Site 644 sediments are notably more dense and, consequently, have less porosity and lower water content and higher thermal conductivity relative to the previous sites. This is probably a consequence of relatively greater clastic content at Site 644.

SEISMIC CORRELATION

Site 644 is located in the central Vøring Basin (Fig. 2), in an area of flat-lying undisturbed Cenozoic sediments. The seismic record there (Fig. 19) shows a series of well-defined horizons in the upper part of the section. Of these, three horizons have been identified as base-Pliocene (*O*), base Miocene (*A*), and mid-Oligocene (*A'*), respectively (Skogseid, 1983; see Chapter 1, this volume). Above the base Pliocene a distinct regionally continuous marker occurs at 1.79 s, with a more diffuse reflector at 1.95 s.

The lithologic units defined by the drilled sediments were converted to reflection time, assuming a velocity of 1.6 km/s. Figure 19 shows that the reflector at 1.95 s corresponds to the base of the glacial sequence at the transition between Units I and II. At this level, there is a typical decrease in sediment bulk density (Fig. 17, "Physical Properties" section, this chapter) that most likely creates the reflector.

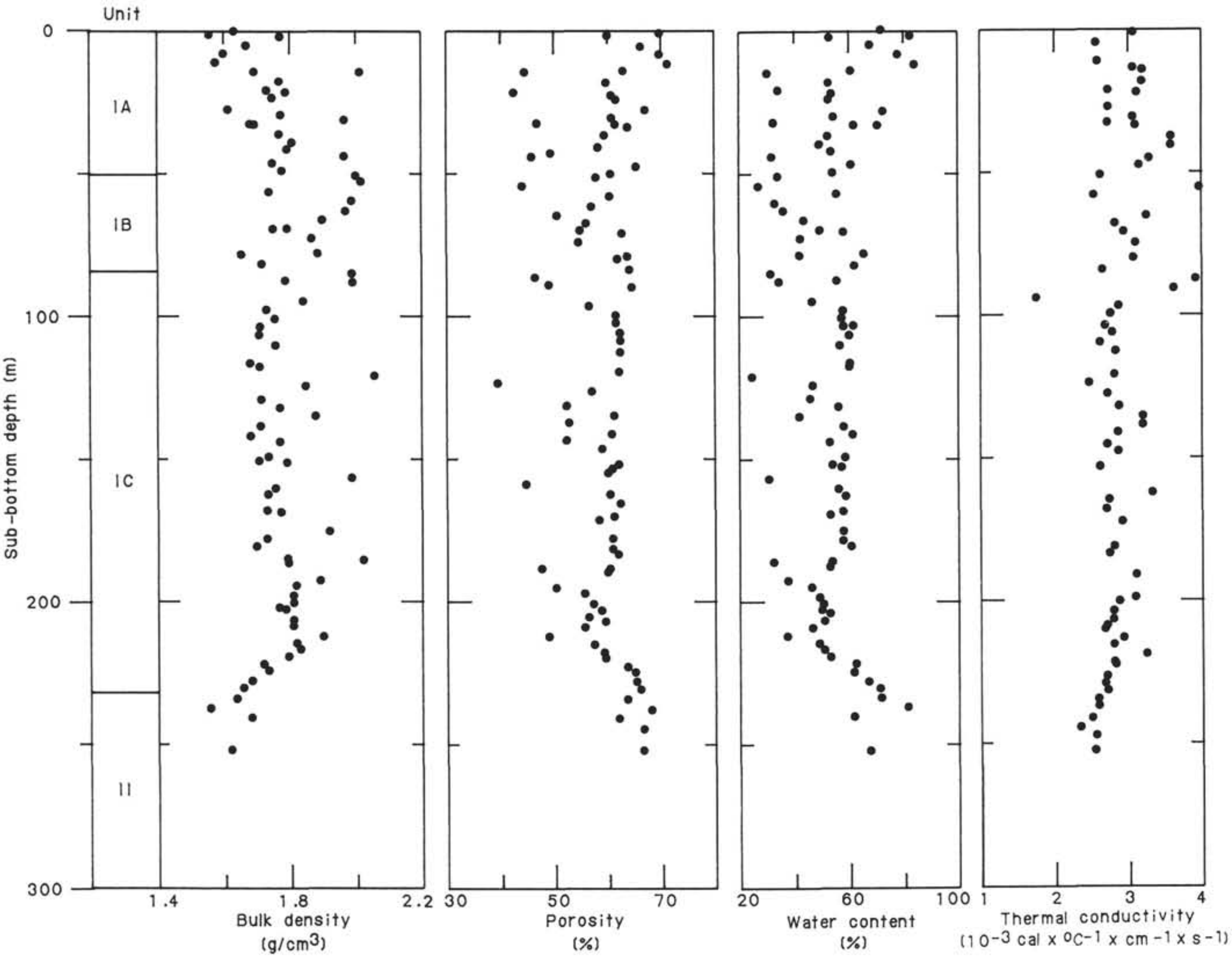

Figure 17. Index properties (bulk density, porosity, and water content) and thermal conductivity profiles for Site 644.

The upper reflector at 1.79 s corresponds to the uppermost part of Subunit IC at a depth of about 115 mbsf. This reflector may be associated with the major concentrations of ethane gas at this level, an inference that is supported by the negative polarity of the reflected signal.

REFERENCES

Belanger, P. E., and Streeter, S. S., 1980. Distribution and ecology of benthic foraminifera in the Norwegian-Greenland Sea. *Mar. Micropaleontol.*, 5:401-428.

Bennett, R. H., and Nelson, T. A., 1983. Seafloor characteristics and dynamics affecting geotechnical properties at shelf break. *SEPM Spec. Publ.*, 33:333-555.

Berggren, W. A., Kent, D. V., and Flynn, J. J., 1985. Paleogene geochronology and chronostratigraphy. *In* Snelling, N. J. (Ed.), *Geochronology and the Geological Record*: Geol. Soc. London, Spec. Paper, 141-195.

Bjørklund, K. R., 1976. Radiolaria from the Norwegian Sea, Leg 38 of the Deep Sea Drilling Project. *In* Talwani, M., Udintsev, G., et al., *Init. Repts. DSDP*, 38: Washington (U.S. Govt. Printing Office), 1101-1168.

Bryant, W. R., Bennett, R. H., and Katherman, C. E., 1981. Shear strength, consolidation, porosity and permeability of oceanic sediments. *In* Emiliani, C. (Ed.), *The Sea*: *The Oceanic Lithosphere*, Vol. 7: 1555-1616.

Ciesielski, P. F., 1975. Biostratigraphy and paleoecology of Neogene and Oligocene silicoflagellates from cores recovered during Antarctic Leg 28, Deep Sea Drilling Project. *In* Hayes, D. E., Frakes, L. A., et al., *Init. Repts. DSDP*, 28: Washington (U.S. Govt. Printing Office), 625-692.

________, 1983. The Neogene and Quaternary diatom biostratigraphy of subantarctic sediments, Deep Sea Drilling Project Leg 71. *In* Ludwig, W. J., Krasheninnikov, V. A., et al., *Init. Repts. DSDP*, 71, Pt. 2: Washington (U.S. Govt. Printing Office), 635-665.

Ciesielski, P. F., and Grinstead, G., 1986. Pliocene variations in the position of the Antarctic Convergence in the Southwest Atlantic. *Paleoceanography*, 1:197-232.

Ciesielski, P. F., and Weaver, F. M., 1983. Neogene and Quaternary paleoenvironmental history of Deep Sea Drilling Project Leg 71 sediments, Southwest Atlantic Ocean. *In* Ludwig, W. J., Krasheninnikov, V. A., et al., *Init. Repts. DSDP*, 71: Washington (U.S. Govt. Printing Office), 461-477.

Claypool, G. E., and Kaplan, I. R., 1974. The origin and distribution of methane in marine sediments. *In* Kaplan, I. R. (Ed.), *Natural Gases in Marine Sediments*: New York (Plenum), 94-129.

Gieskes, J. M., 1981. Deep Sea Drilling interstitial water studies. Implications for chemical alteration of the oceanic crust Layers I and II. *In The Deep Sea Drilling Project: A Decade of Research*. SEPM Spec. Publ., 32:149-167.

Hamilton, E. L., 1974. Prediction of deep sea sediment properties: State of the art. *In* Inderbitzen, A. L., (Ed.), *Deep Sea Sediments, Physical and Mechanical Properties*: New York (Plenum Press), 1-43.

Harland, R., 1977. Recent and Late Quaternary (Flandrian and Devensian) dinoflagellate cysts from marine continental shelf sediments around the British Isles. *Paleontographica* Abt. B 164:87-126.

Harrison, W. E., Hesse, R., and Gieskes, J. M., 1982. Relationship between sedimentary facies and interstitial water chemistry of slope, trench and Cocos Plate sites from the Middle America Trench transect, active margin off Guatemala, Deep Sea Drilling Project Leg 67. *In* Aubouin, J., von Huene, R., et al., *Init. Repts. DSDP*, 67: Washington (U.S. Govt. Printing Office), 603-615.

Koizumi, I., 1973. The late Cenozoic diatoms of Sites 183-193, Leg 19 Deep Sea Drilling Project. *In* Creager, J. S., Scholl, D. W., et al., *Init. Repts. DSDP*, 19: Washington (U.S. Govt. Printing Office), 805-855.

McDougall, I., and Watkins, N. D., 1973. Age and duration of the Reunion geomagnetic polarity event. *Earth Planet. Sci. Lett.*, 19:443-452.

Martini, E., 1971. Standard Tertiary and Quaternary calcareous nannoplankton zonation. *In* Farinacc, A. (Ed.), *Proc. Second Plankt. Conf.*, Rome, 1970, Vol. 2: 739-785.

Mechalas, B. J., 1974. Pathways and environmental requirements for biogenic gas production in the ocean. *In* Kaplan, I. R. (Ed.), *Natural Gases in Marine Sediments: Mar. Science*, 3:11-26.

Morris, D. A., 1976. Organic diagenesis of Miocene sediments from Site 341, Vøring Plateau, Norway. *In* Talwani, M., Udintsev, G., et al., *Init. Repts. DSDP*, 38: Washington (U.S. Govt. Printing Office), 809-814.

Müller, D., 1976. Tertiary and Quaternary calcareous nannoplankton in the Norwegian-Greenland Sea, DSDP Leg 38. *In* Talwani, M., Udintsev, G., et al., *Init. Repts. DSDP*, 38: Washington (U.S. Govt. Printing Office), 823-841.

Murray, J. W., 1984. Paleogene and Neogene benthic foraminifers from Rockall Plateau. *In* Roberts, D. G., Schnitker, D., et al., *Init. Repts. DSDP*, 81: Washington (U.S. Govt. Printing Office), 503-539.

Sejrup, H. P., Fjaeran, T., Hald, M., Beck, L., Hagen, J., Miljeteig, I., Morvik, I., and Norvik, O., 1981. Benthonic foraminifera in surface samples from the Norwegian continental margin between 62° and 65°N. *J. Foram. Res.*, 11:277-295.

Shackleton, N. J., Backman, J., et al., 1984. Oxygen isotopic calibration of the onset of ice-rafting and the history of glaciation in the North Atlantic region. *Nature*, 307:620-623.

Shackleton, N. J., and Opdyke, N. D., 1977. Oxygen isotopic and paleomagnetic evidence for early northern hemisphere glaciation. *Nature*, 270:216-219.

Skogseid, J., 1983. A marine geophysical study of profiles between the Vøring Plateau margin and the Jan Mayen Ridge [Cand. Sci. Thesis]. University of Oslo, Oslo.

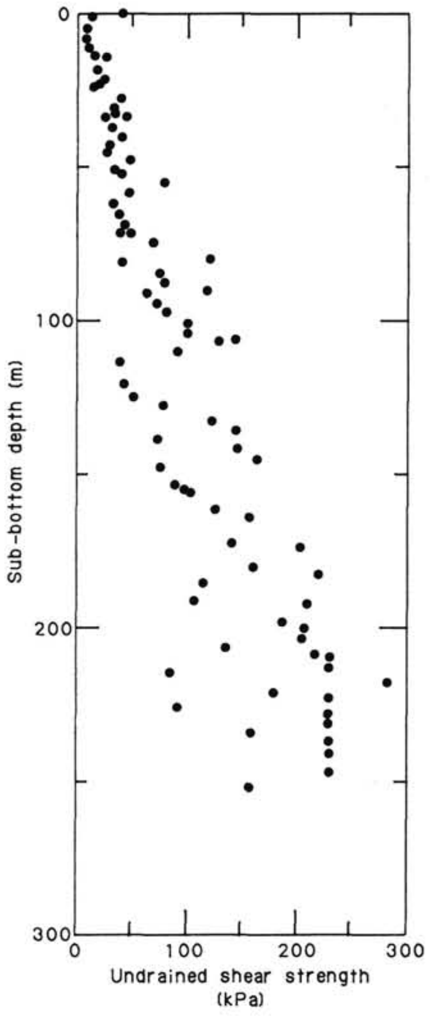

Figure 18. Undrained-shear-strength profile for Site 644.

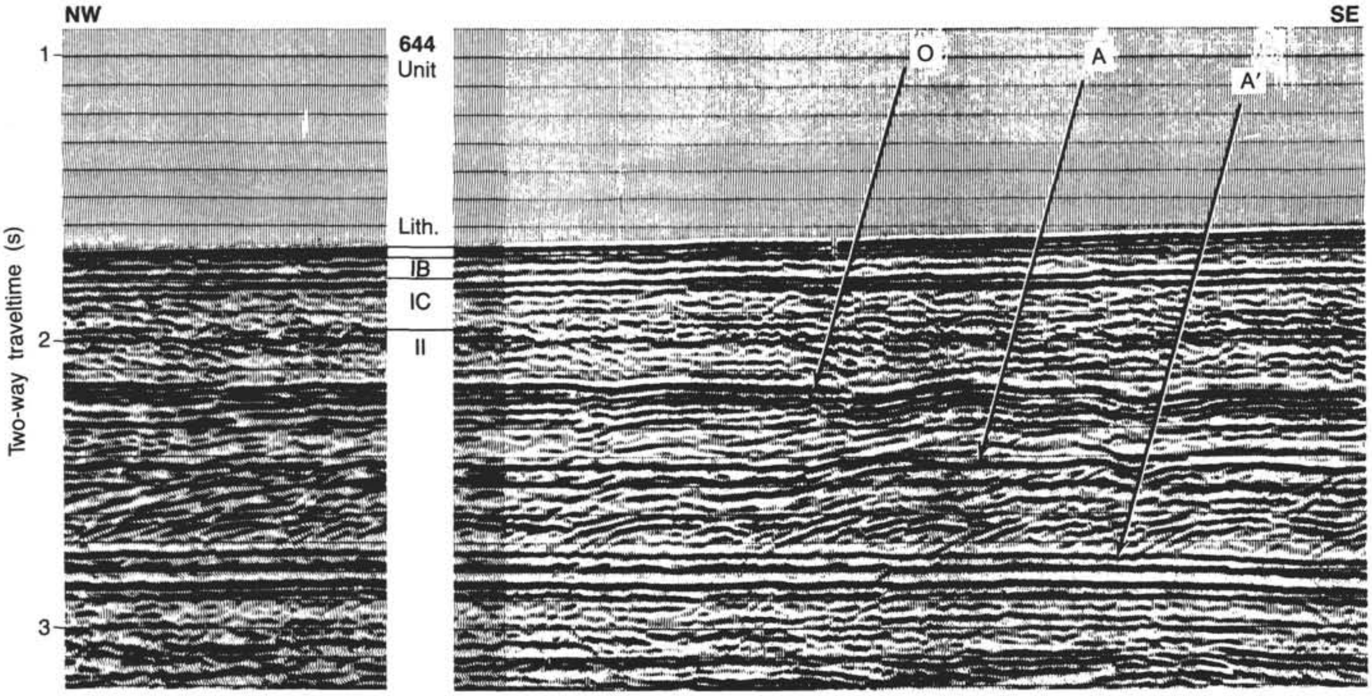

Figure 19. Seismic time-section across Site 644, line NH-1. Lithologic section from "Sediment Lithology" section, this chapter. Seismic interpretation is from Skogseid (1983).

SITE 644 HOLE A CORE 1H CORED INTERVAL 1226.3-1235.5 mbsl; 0.0-9.2 mbsf

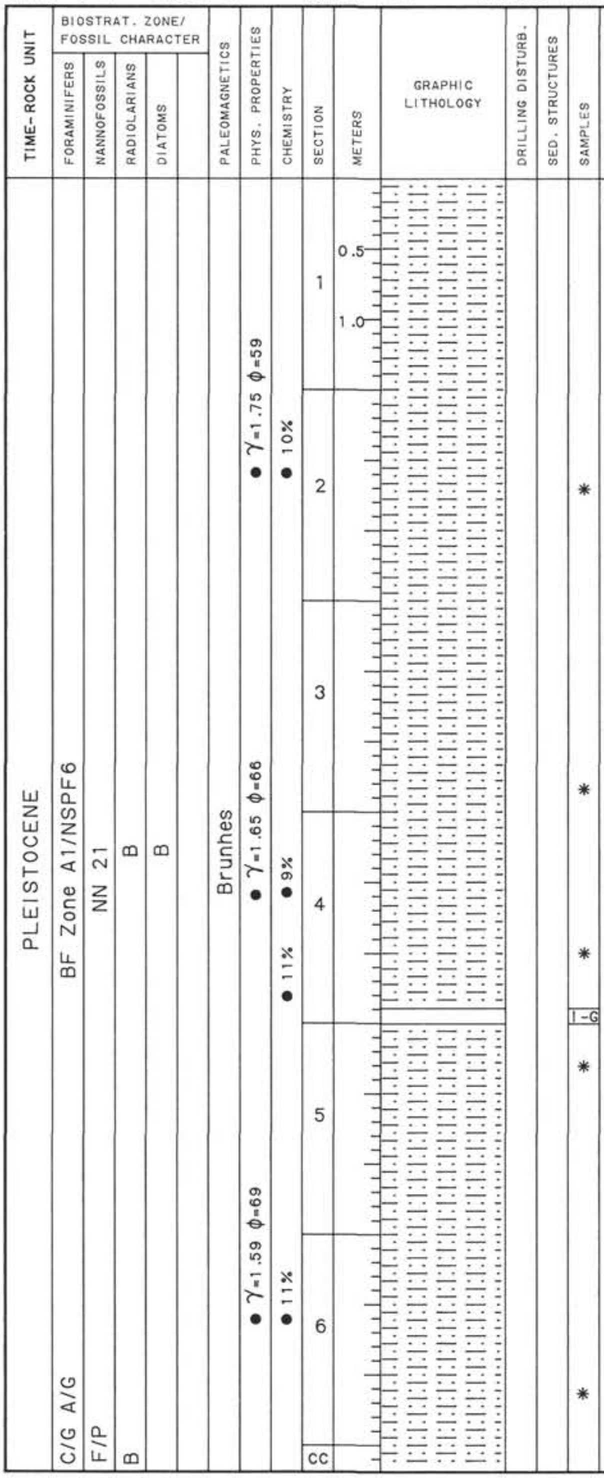

LITHOLOGIC DESCRIPTION

GLACIAL AND INTERGLACIAL MUDS AND SANDY MUDS

Entire core is undisturbed.

Major lithologies:
a. Calcareous mud and sandy calcareous mud, olive gray (5Y 4/2), mottled and bioturbated, with a few scattered dropstones. Section 1 to Section 2.
b. Silty mud, olive gray (5Y 4/2) to dark gray (5Y 4/1), mottled and bioturbated, with a few scattered dropstones. Section 3 to CC.

Minor lithology: Sandy nannofossil mud, brownish gray (2.5Y 4/2). Section 1, 0–15 cm.

SMEAR SLIDE SUMMARY (%):

	2, 80 D	3, 137 D	4, 100 M	5, 30 D	6, 15 M
TEXTURE:					
Sand	10	10	20	2	88
Silt	30	15	20	33	—
Clay	60	75	60	65	12
COMPOSITION:					
Quartz	20	25	35	10	85
Feldspar	3	—	5	—	—
Clay	60	72	63	64	12
Calcite/dolomite	15	10	—	25	—
Accessory minerals	1	1	2	1	2
Foraminifers	1	—	—	—	—

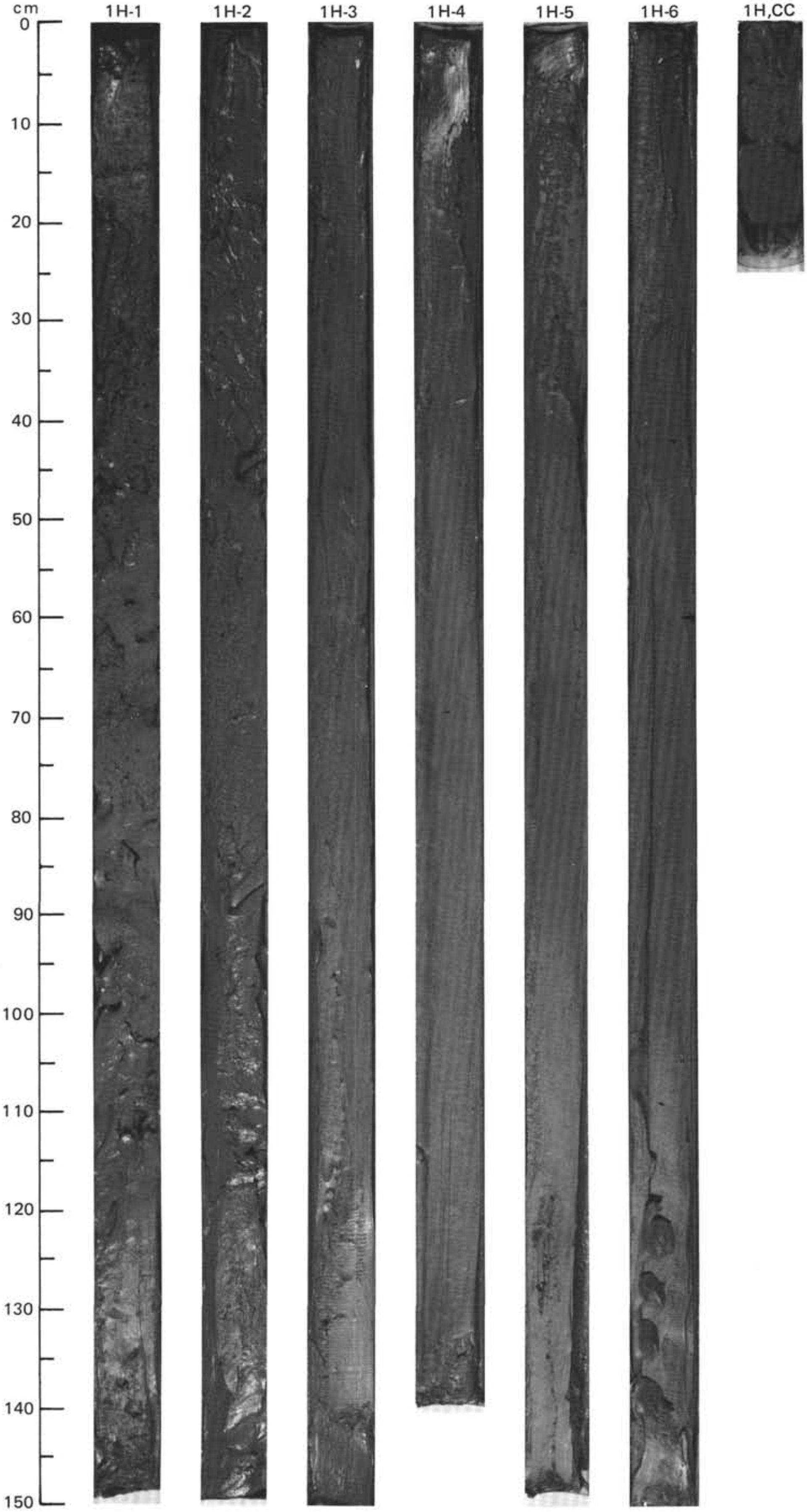
cm
0
10
20
30
40
50
60
70
80
90
100
110
120
130
140
150
1H-1
1H-2
1H-3
1H-4
1H-5
1H-6
1H,CC

SITE 644 HOLE A CORE 2H CORED INTERVAL 1235.2-1242.5 mbsl; 9.2-16.2 mbsf

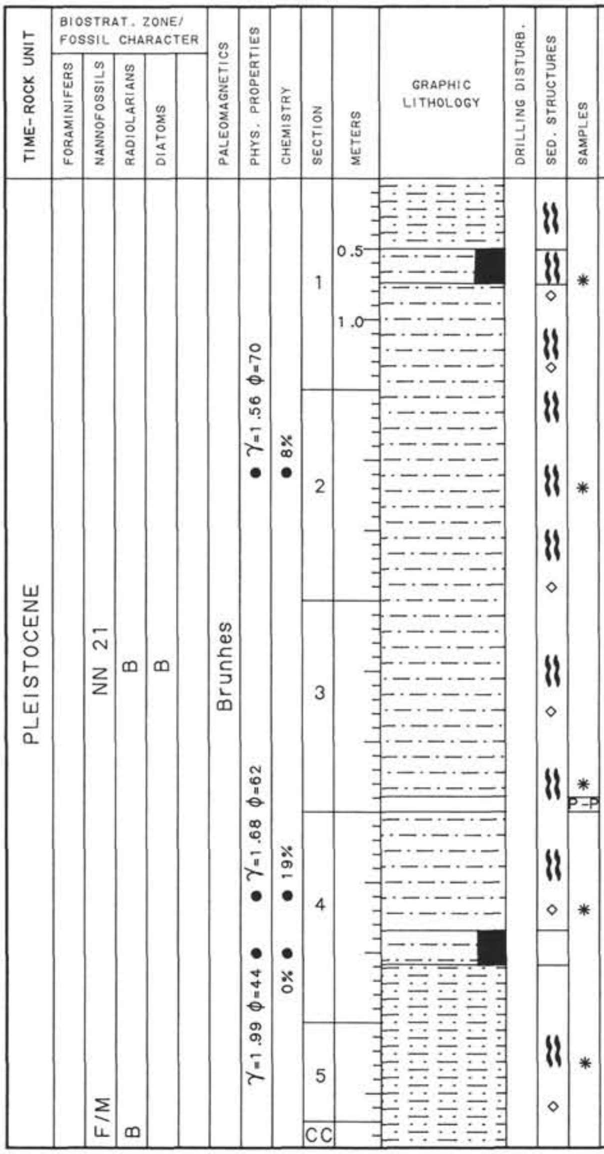

LITHOLOGIC DESCRIPTION

GLACIAL MUDS AND SANDY MUDS

Entire core is undisturbed.

Major lithology: Sandy calcareous mud, olive gray (5Y 4/2) to dark grayish brown (2.5Y 3/2), extensively bioturbated with pyrite-impregnated burrow tubes 2–3 mm in diameter. Contains a few scattered dropstones and minor greenish gray color banding. Section 1, 0–50 cm; Section 1, 75 cm, to Section 4, 86 cm; Section 5, 0–70 cm; CC, 0–20 cm.

Minor lithologies:
a. Sandy mud, grading from basal very dark gray (5Y 3/1) mud upward into dark olive gray (5Y 3/2) laminated sandy mud with abundant dropstones and Fe/Mn impregnations. The top of the sequence is bioturbated. Section 1, 50–75 cm.
b. Sandy mud, very dark gray (5Y 3/2), with scattered dropstones. Section 4, 86–108 cm.

Dropstones at Section 3, 75 cm; Section 4, 13 and 86 cm; Section 5, 5 and 67 cm.

SMEAR SLIDE SUMMARY (%):

	1, 74 M	2, 70 D	3, 132 D	4, 70 D	5, 20 D
TEXTURE:					
Sand	1	15	5	5	5
Silt	20	30	32	35	30
Clay	79	55	63	60	65
COMPOSITION:					
Quartz	1	20	15	10	20
Feldspar	—	2	1	1	5
Clay	74	55	63	58	49
Calcite/dolomite	20	20	20	30	25
Accessory minerals	—	2	1	—	1
Foraminifers	—	—	1	—	—
Nannofossils	5	1	—	—	—

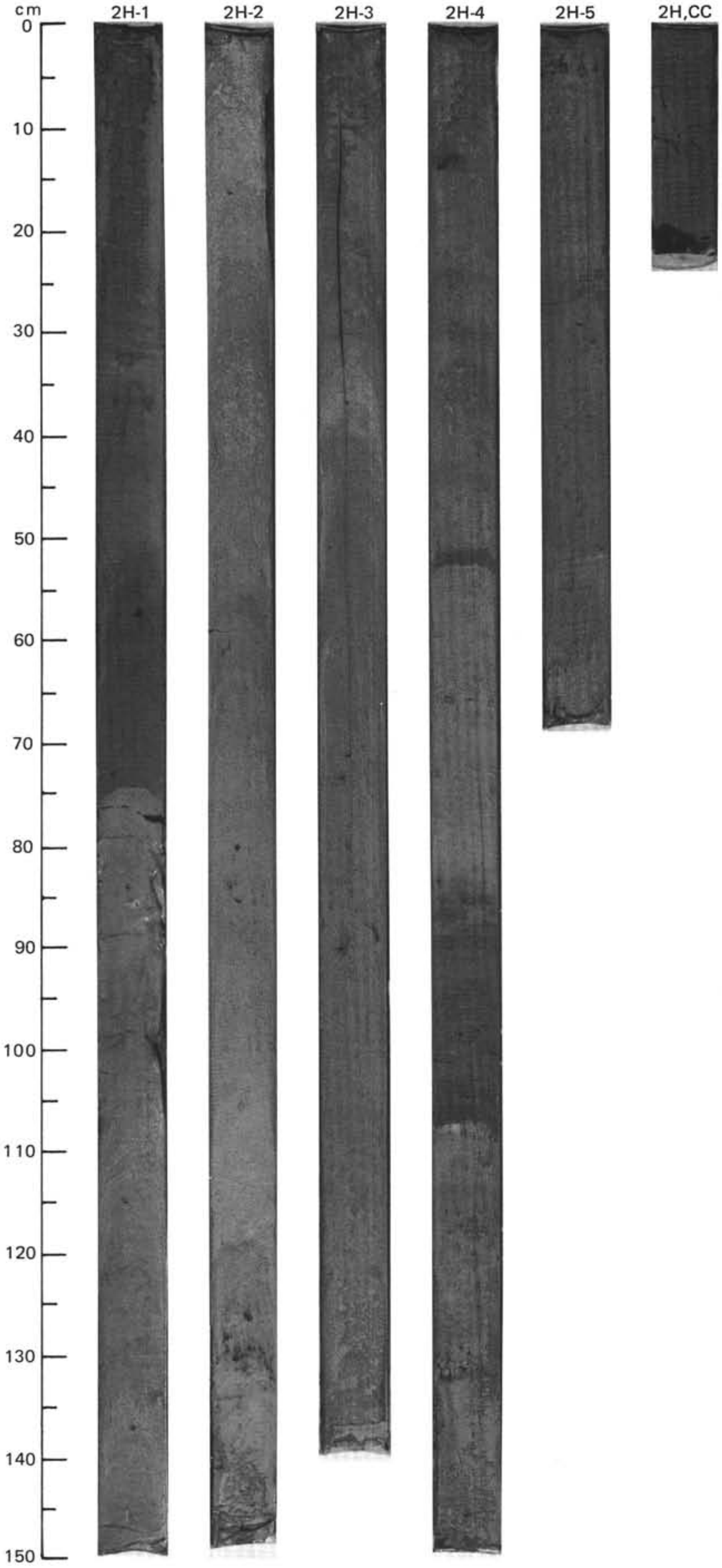
cm
0
10
20
30
40
50
60
70
80
90
100
110
120
130
140
150
2H-1
2H-2
2H-3
2H-4
2H-5
2H,CC

SITE 644 HOLE A CORE 3H CORED INTERVAL 1242.5-1252.0 mbsl; 16.2-25.7 mbsf

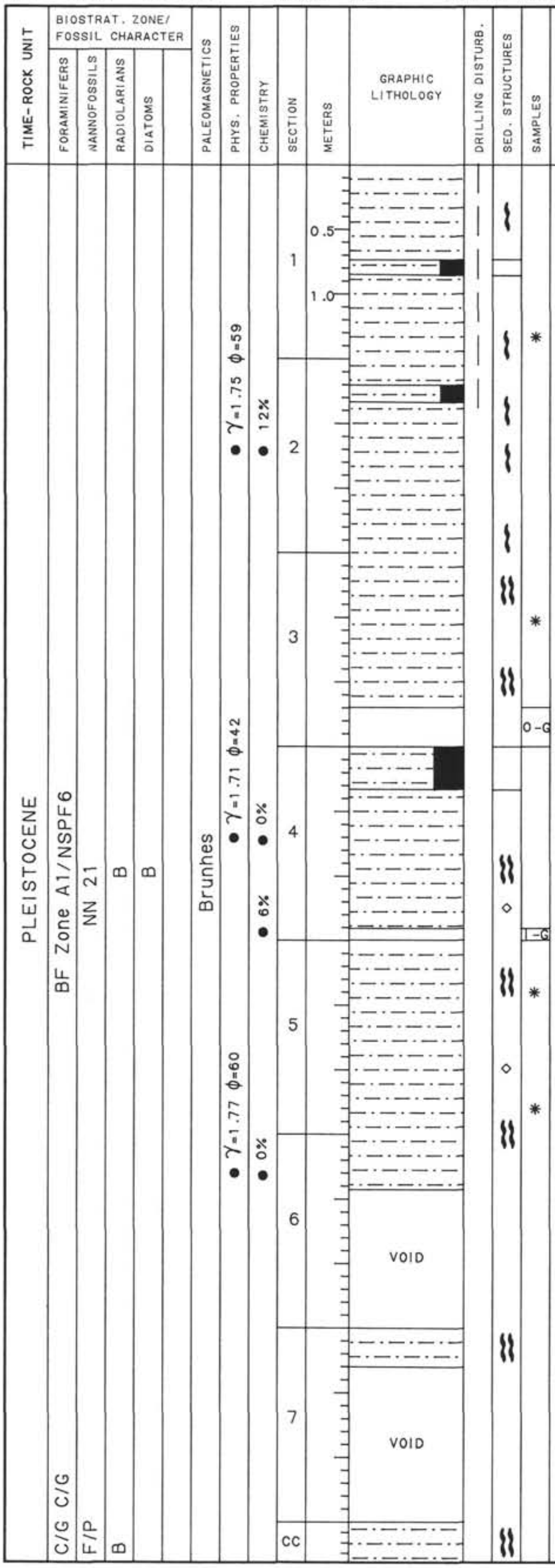

LITHOLOGIC DESCRIPTION

GLACIAL AND INTERGLACIAL MUDS AND SANDY MUDS

Section 1 to Section 2, 35 cm, is slightly disturbed. Remainder of the core is undisturbed.

Major lithology: Mud and sandy calcareous mud, dark grayish brown (2.5Y 3/2), and extensively bioturbated (abundant pyrite-impregnated burrow tubes approximately 2–3 mm in diameter). Commonly contains indistinct greenish gray color banding and a few scattered dropstones. Section 1, 0–77 cm; Section 1, 81 cm, to Section 2, 20 cm; Section 2, 32 cm, to Section 4, 22 cm; Section 4, 32 cm, to CC.

Minor lithology: Sandy mud, very dark gray (5Y 3/1) with scattered dropstones. Section 1, 77–81 cm; Section 2, 20–32 cm; Section 4, 22–32 cm.

Dropstones at Section 4, 125 cm; Section 5, 112 cm.

SMEAR SLIDE SUMMARY (%):

	1, 137 D	3, 50 D	5, 40 M	5, 133 D
TEXTURE:				
Sand	10	10	30	20
Silt	15	25	10	35
Clay	75	65	60	45
COMPOSITION:				
Quartz	15	5	20	25
Feldspar	—	—	1	—
Clay	72	63	58	39
Calcite/dolomite	10	30	—	20
Accessory minerals	1	—	1	1
Pyrite	—	—	20	—
Foraminifers	2	1	—	10
Nannofossils	—	1	—	5

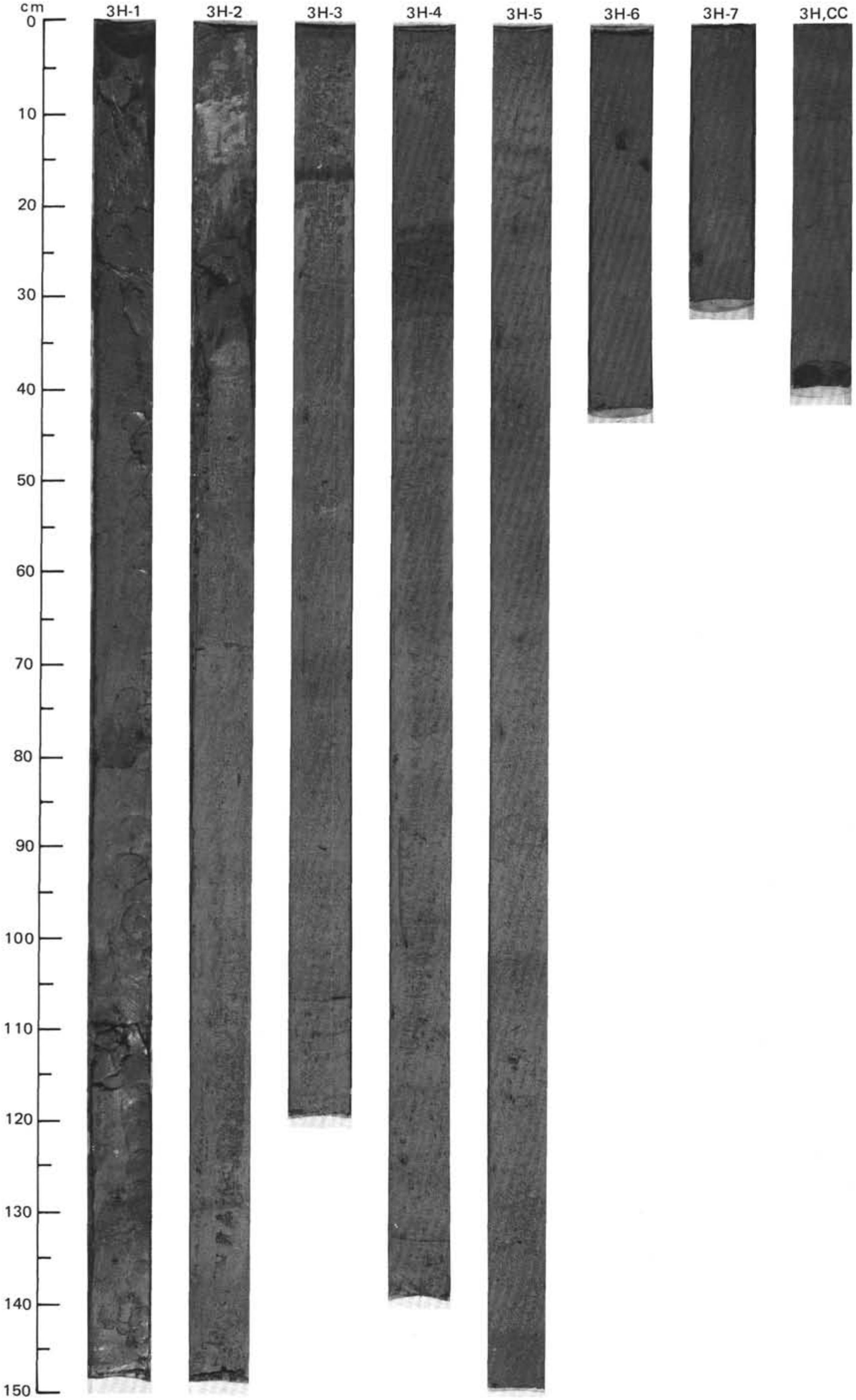
cm
0
10
20
30
40
50
60
70
80
90
100
110
120
130
140
150
3H-1
3H-2
3H-3
3H-4
3H-5
3H-6
3H-7
3H,CC

SITE 644 HOLE A CORE 4H CORED INTERVAL 1252.0-1261.5 mbsl; 25.7-35.2 mbsf

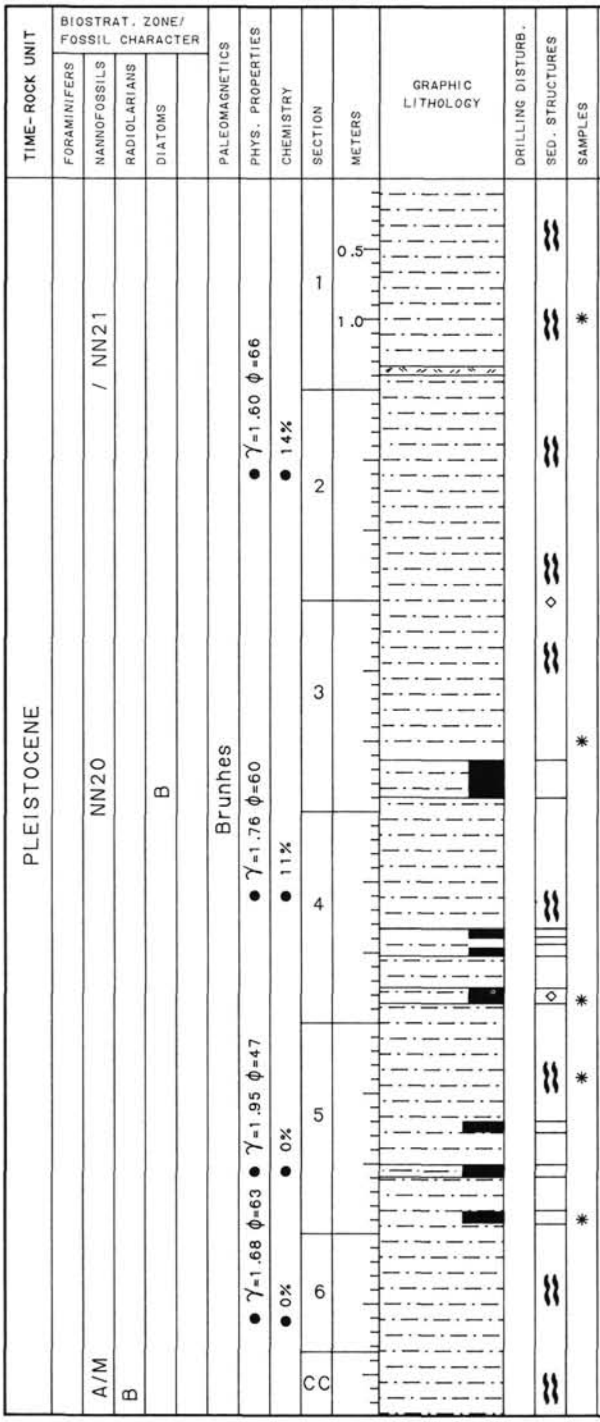

LITHOLOGIC DESCRIPTION

GLACIAL/INTERGLACIAL MUDS AND SANDY MUDS

Entire core is undisturbed.

Major lithology: Sandy mud and mud, dark gray (5Y 4/1), strongly bioturbated with pyritized burrow tubes, and containing diffuse greenish color bands. Section 1 to Section 3, 114 cm (Section 3, 20–36 and 36–44 cm, have intense pyrite impregnation); Section 3, 129 cm, to Section 4, 85 cm; Section 4, 87–95 and 102–124 cm; Section 4, 135 cm, to Section 5, 72 cm; Section 4, 74–101 and 107–135 cm; Section 5, 138 cm, to Section 6, 85 cm; CC.

Minor lithologies:
a. Sandy mud, dark olive gray (5Y 3/2), bioturbated. Section 3, 97 cm.
b. Sandy mud, very dark gray (5Y 3/1), with abundant dropstones. Section 3, 114–129 cm; Section 4, 85–87, 95–102, and 124–135 cm; Section 5, 72–74, 101–107, and 135–138 cm.
c. Volcanic ash, very dark gray (5Y 3/1), inversely graded, with a very sharp base and a gradational top. Section 1, 131–135 cm.

Large (~ 2 cm), angular granitic dropstones at Section 2, 142 cm; Section 4, 129 cm.

SMEAR SLIDE SUMMARY (%):

	1, 90 D	3, 97 M	4, 129 M	5, 39 D	5, 135 M
TEXTURE:					
Sand	25	25	20	5	94
Silt	30	25	24	40	—
Clay	45	50	56	55	6
COMPOSITION:					
Quartz	30	40	35	25	90
Feldspar	—	5	5	—	2
Mica	2	—	2	—	1
Clay	37	50	56	55	6
Volcanic glass	—	—	—	2	—
Calcite/dolomite	25	3	—	15	—
Accessory minerals	1	1	2	1	1
Glauconite	—	1	—	2	—
Foraminifers	—	—	—	Tr	—
Nannofossils	5	—	—	Tr	—

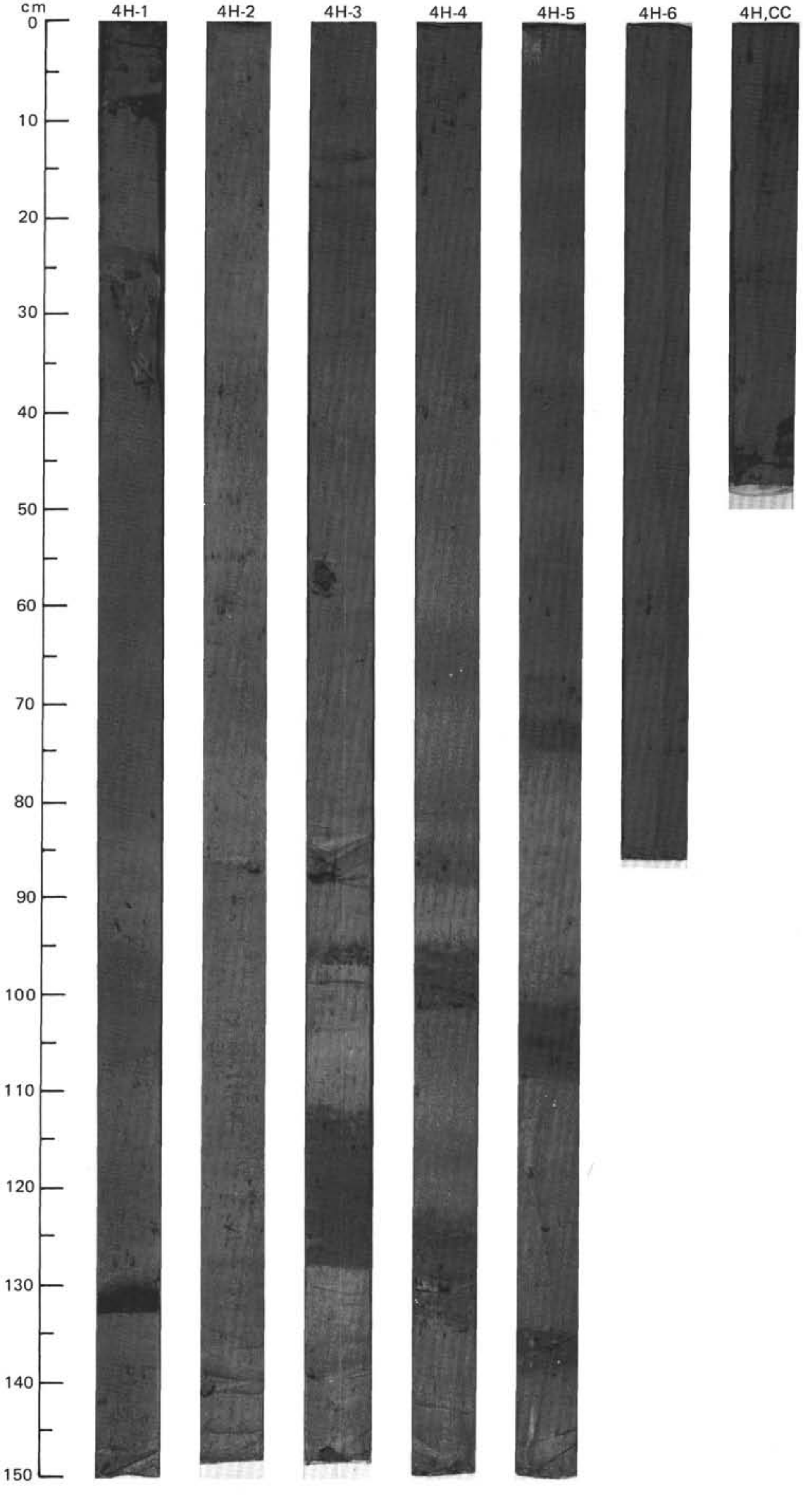
cm
0
10
20
30
40
50
60
70
80
90
100
110
120
130
140
150
4H-1
4H-2
4H-3
4H-4
4H-5
4H-6
4H,CC

SITE 644 HOLE A CORE 5H CORED INTERVAL 1261.5-1271.0 mbsl; 35.2-44.7 mbsf

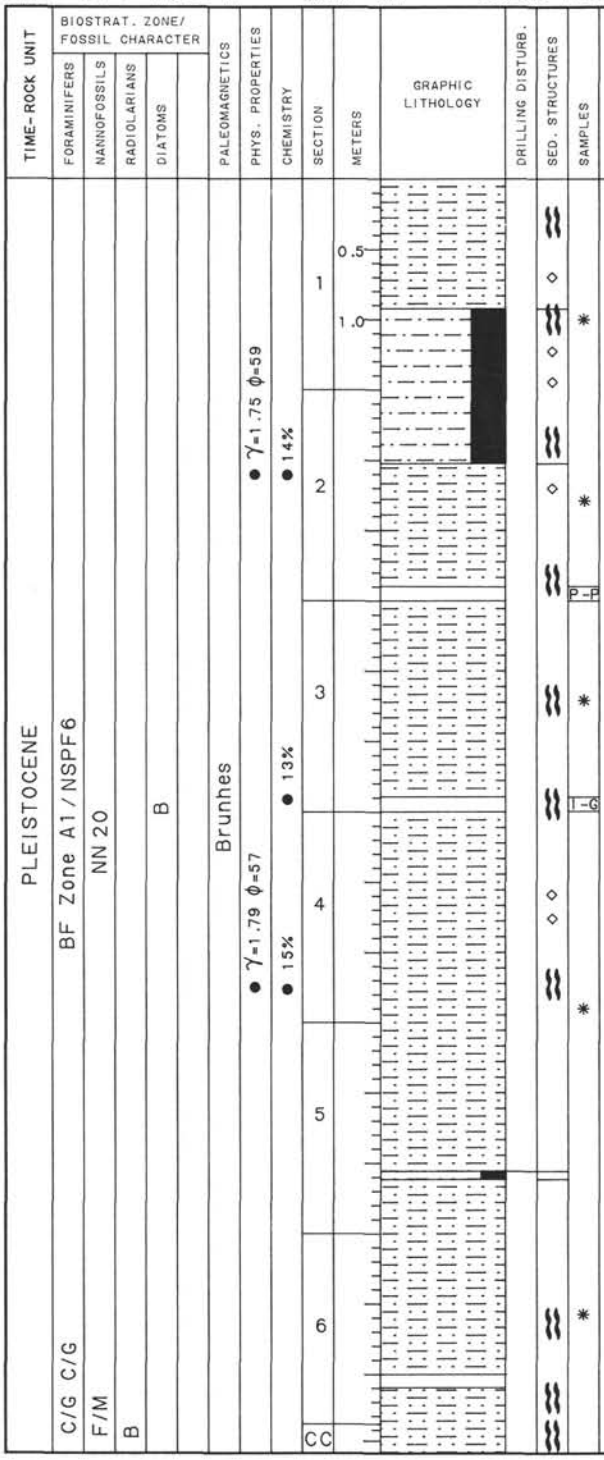

LITHOLOGIC DESCRIPTION

GLACIAL AND INTERGLACIAL MUDS AND SANDY MUDS

Entire core is undisturbed.

Major lithology: Mud, calcareous mud, and minor amounts of sandy mud, dark brownish gray (2.5Y 3/2) to dark gray (5Y 4/1), extensively bioturbated with pyritized burrows. Section 1, 0–89 cm; Section 2, 52–133 cm; Section 2, 135 cm, to Section 5, 106 cm; Section 5, 110 cm, to CC.

Minor lithologies:
a. Sandy mud, very dark gray (5Y 3/1), with scattered dropstones. Section 1, 89 cm, to Section 2, 52 cm; Section 5, 106–110 cm.
b. Sand, greenish gray (5GY 5/2), with a sharp base and a gradational top. Section 22, 133–135 cm.

Large dropstones at Section 1, 74, 188–122 cm (well-rounded, coarse conglomeratic sandstone), and 144–150 cm (large, angular basalt pebble); Section 2, 72 cm; Section 4, 54 and 67 cm.

SMEAR SLIDE SUMMARY (%):

	1, 39 M	2, 84 D	3, 68 D	4, 136 M	5, 60 D
TEXTURE:					
Sand	20	1	2	50	1
Silt	40	25	32	40	29
Clay	40	74	66	10	70
COMPOSITION:					
Quartz	40	5	15	70	5
Feldspar	5	—	2	10	—
Mica	—	—	—	5	3
Clay	40	59	66	10	68
Calcite/dolomite	—	20	14	—	20
Accessory minerals	5	1	2	5	2
Glauconite	10	—	—	—	—
Foraminifers	—	—	Tr	—	—
Nannofossils	—	15	—	—	2

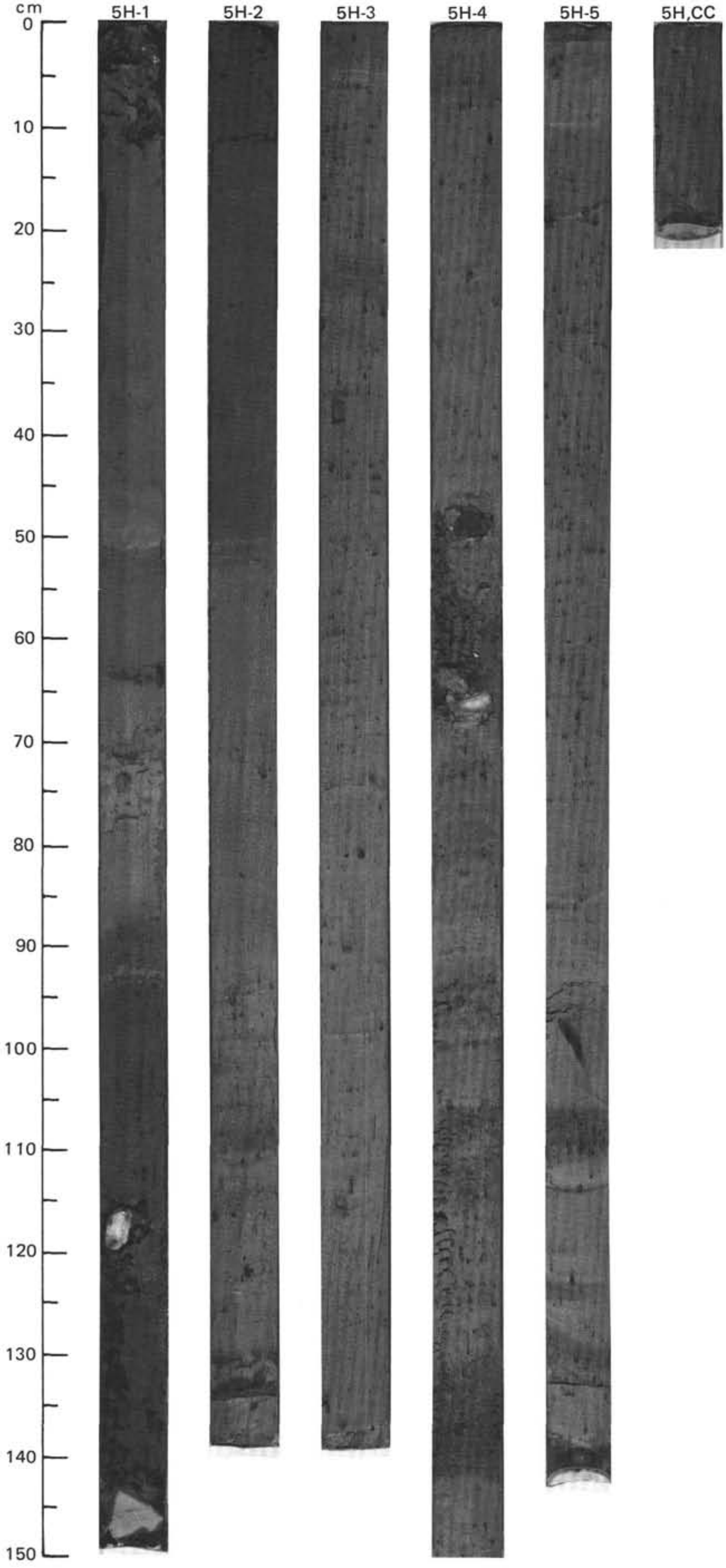
cm
0
10
20
30
40
50
60
70
80
90
100
110
120
130
140
150
5H-1
5H-2
5H-3
5H-4
5H-5
5H,CC

SITE 644 HOLE A CORE 6H CORED INTERVAL 1271.0-1280.5 mbsl; 44.7-54.2 mbsf

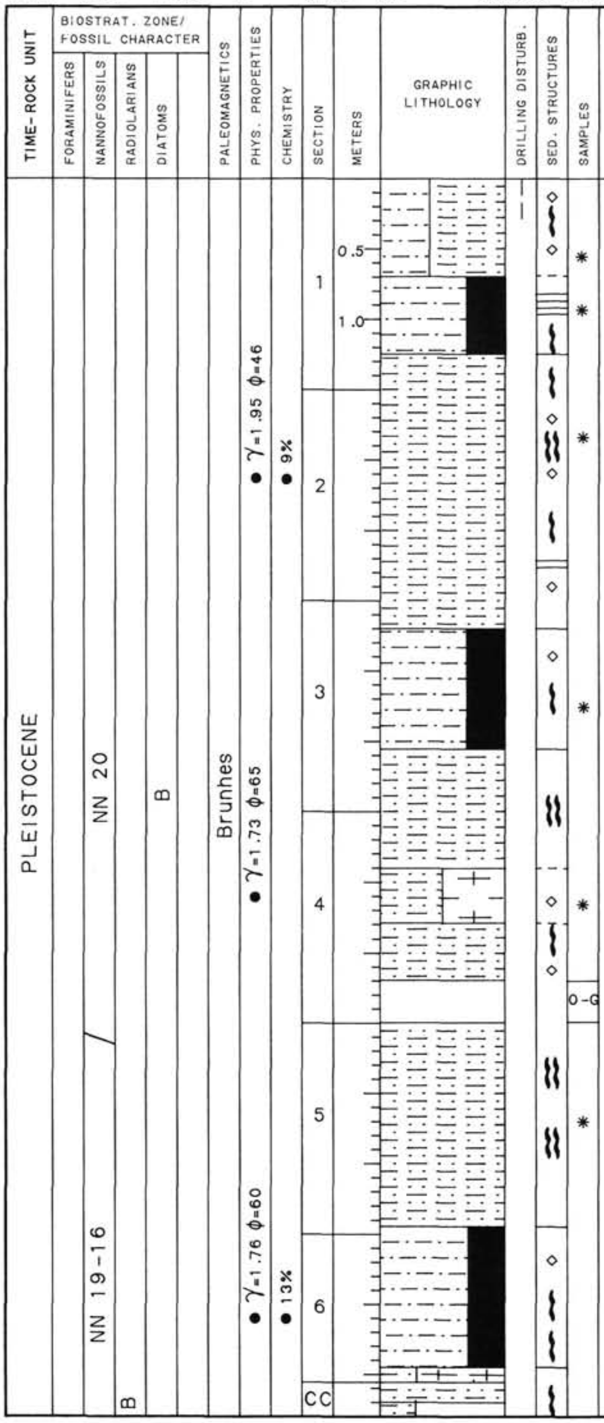

LITHOLOGIC DESCRIPTION

CALCAREOUS MUD AND SANDY MUD

Entire core is undisturbed.

Major lithologies:
a. Calcareous mud, dark gray (5Y 4/1) to gray (5Y 5/1) and olive gray (5Y 4/2). Small pyritized burrows common, and minor small dropstones throughout.
b. *Sandy mud, very dark gray (5Y 3/1), bioturbated, with scattered large dropstones.*

Minor lithology: Marly foraminiferal nannofossil ooze, greenish gray (5GY 5/1) to dark greenish gray (5GY 4/1), with diffuse color banding common. Section 1, 39–82 cm; Section 6, 98–107 cm; CC, 16–27 cm.

SMEAR SLIDE SUMMARY (%):

	1, 58 D	1, 97 D	2, 33 D	3, 80 D	4, 68 M	5, 72 D	CC, 21 M
TEXTURE:							
Sand	15	70	10	55	30	5	—
Silt	55	5	50	15	20	35	—
Clay	30	25	40	30	50	60	—
COMPOSITION:							
Quartz	30	60	20	30	15	35	12
Clay	30	25	40	20	20	30	20
Calcite/dolomite	30	5	28	25	20	25	—
Accessory minerals	—	10	1	10	—	—	—
Pyrite	—	—	—	5	—	—	—
Foraminifers	—	—	1	—	15	—	10
Nannofossils	10	—	10	10	30	20	55
Sponge spicules	—	—	—	—	—	—	3

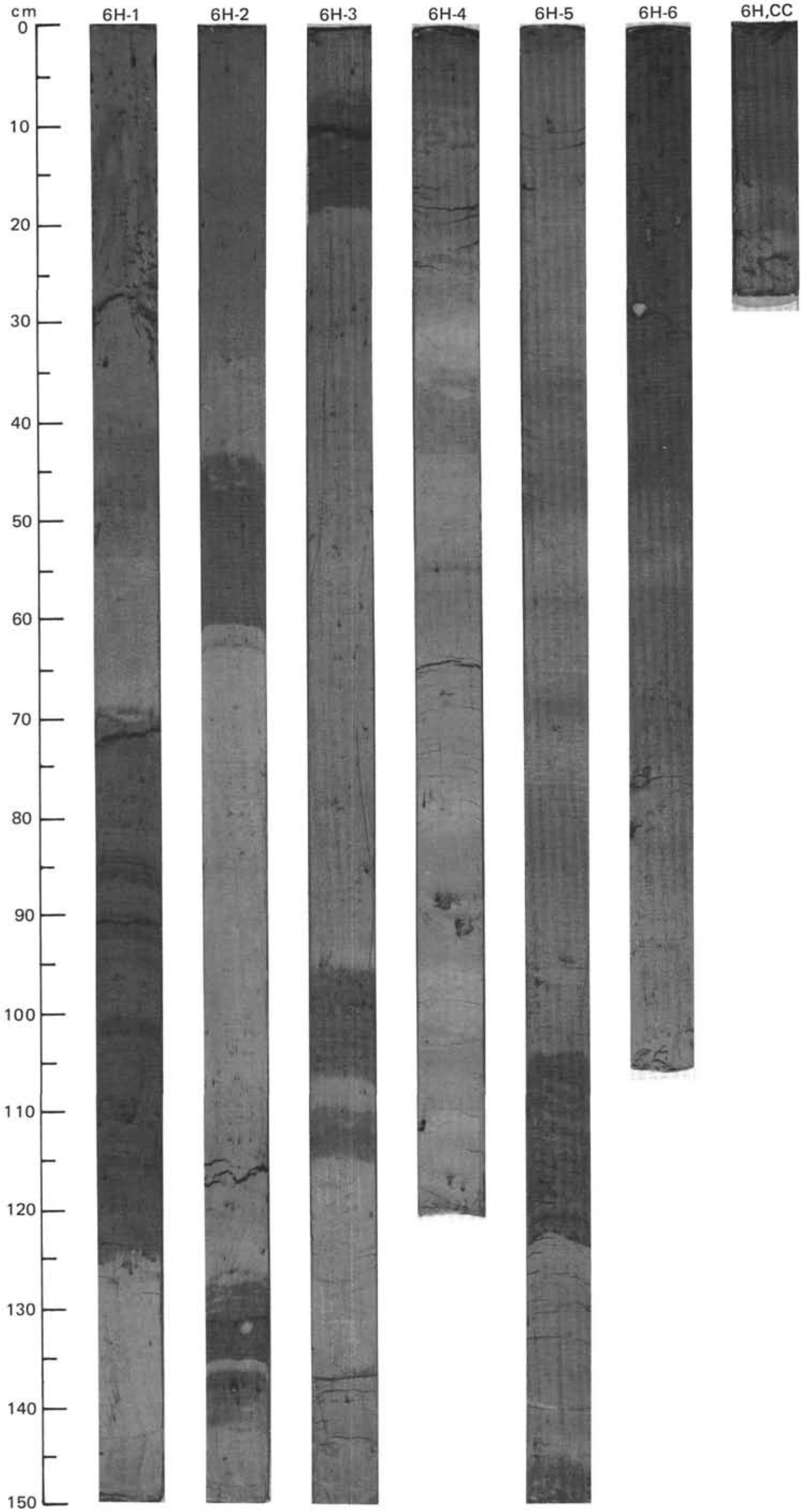
cm
0
10
20
30
40
50
60
70
80
90
100
110
120
130
140
150
6H-1
6H-2
6H-3
6H-4
6H-5
6H-6
6H,CC

SITE 644 HOLE A CORE 7H CORED INTERVAL 1280.5-1290.0 mbsl; 54.2-63.7 mbsf

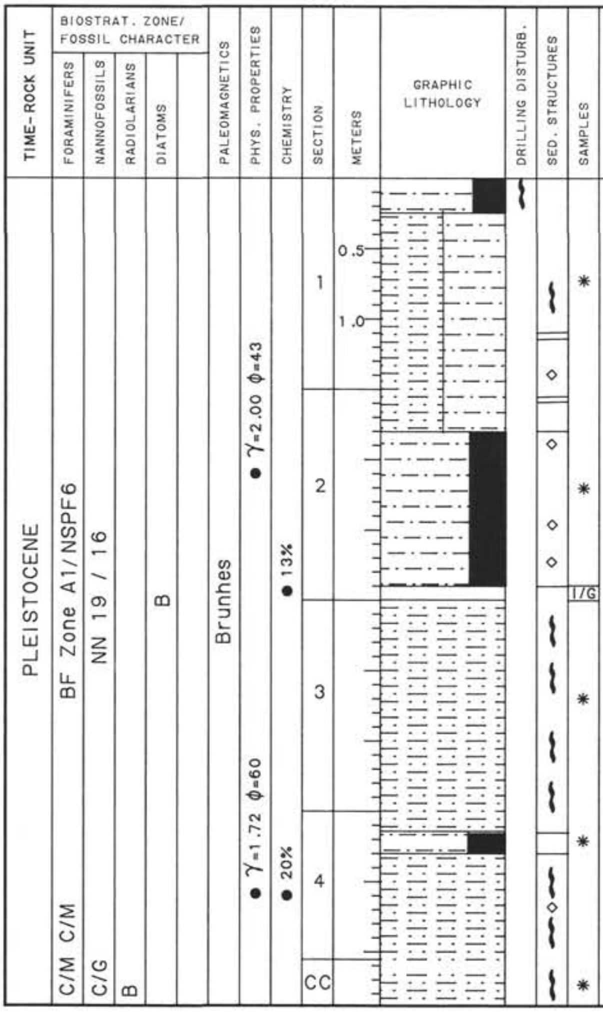

LITHOLOGIC DESCRIPTION

CALCAREOUS MUD AND SANDY MUD

Entire core is undisturbed.

Major lithologies:
a. Calcareous mud, dark gray (5Y 5/1) to very dark grayish brown (2.5Y 4/2), with abundant mottling and faint color banding. Small pyritized burrows common, small dropstones present in trace to minor amounts.
b. Sandy mud, very dark gray (5Y 3/1), with dropstones common to abundant throughout.

SMEAR SLIDE SUMMARY (%):

	1, 73 D	2, 70 D	3, 68 D	4, 24 D	CC, 27 D
TEXTURE:					
Sand	30	30	10	40	10
Silt	40	30	50	30	55
Clay	30	40	40	30	35
COMPOSITION:					
Quartz	20	50	20	60	10
Feldspar	—	5	—	—	—
Clay	25	40	25	20	19
Calcite/dolomite	40	5	25	10	55
Accessory minerals	—	—	3	4	—
Foraminifers	5	—	2	1	1
Nannofossils	5	—	15	5	15
Sponge spicules	5	—	—	—	—

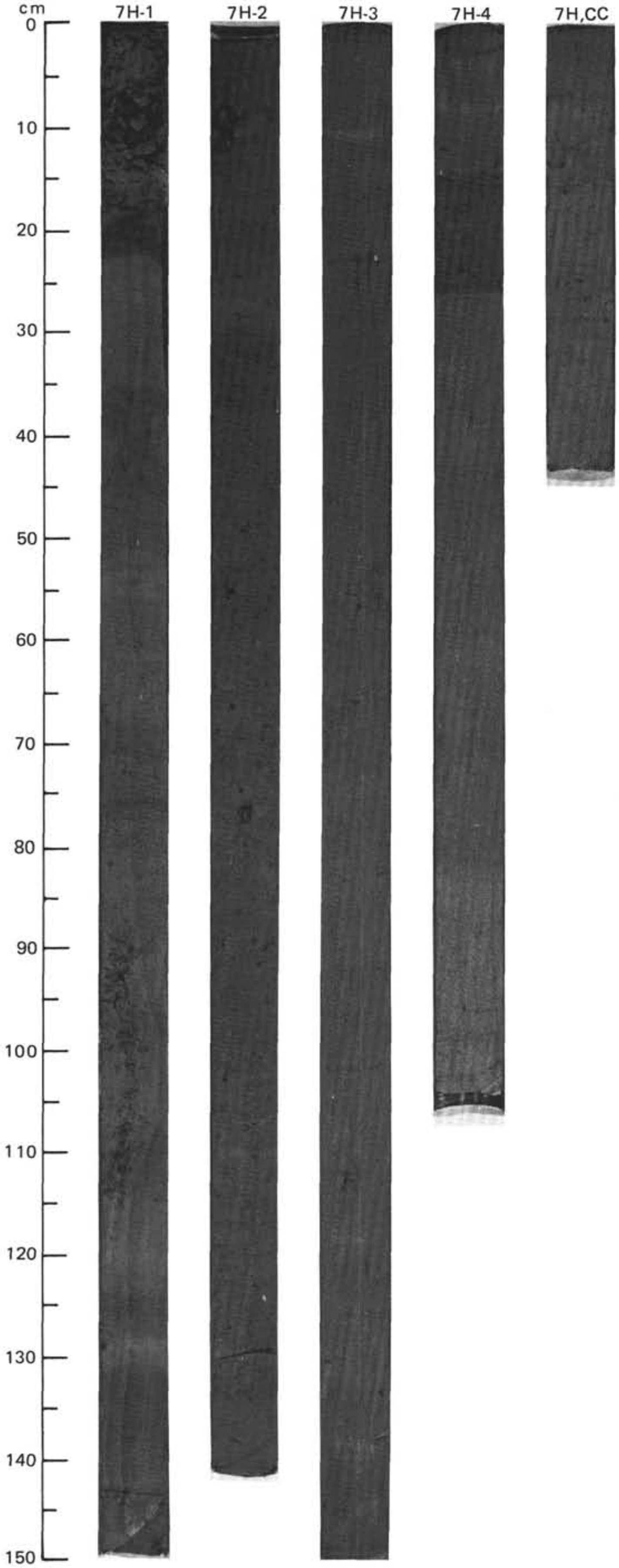
cm
0
10
20
30
40
50
60
70
80
90
100
110
120
130
140
150
7H-1
7H-2
7H-3
7H-4
7H,CC

SITE 644 HOLE A CORE 8H CORED INTERVAL 1290.0-1299.5 mbsl; 63.7-73.2 mbsf

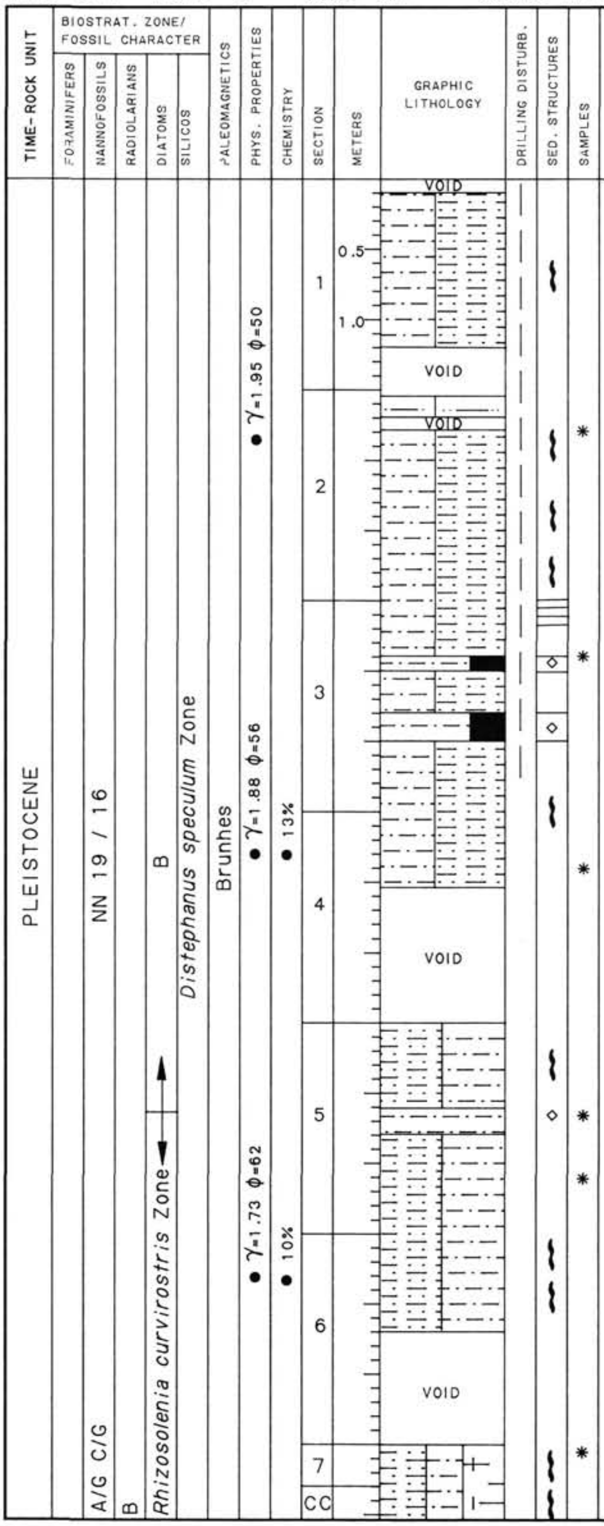

LITHOLOGIC DESCRIPTION

CALCAREOUS MUD

Entire core is slightly to moderately disturbed.

Major lithology: Calcareous mud, dark gray (5Y 4/1) to dark grayish brown (2.5Y 4/2), with faint color banding. Pyritized burrows minor to common throughout.

Minor lithologies:
a. Sandy mud, very dark gray (5Y 3/1), with abundant dropstones throughout.
b. Marly foraminiferal nannofossil ooze, dark greenish gray (5GY 4/1), with minor diffuse color banding.

SMEAR SLIDE SUMMARY (%):

	2, 33 D	3, 42 M	4, 38 D	5, 69 M	5, 110 D	7, 10 M
TEXTURE:						
Sand	20	45	20	35	15	20
Silt	50	20	45	35	55	50
Clay	30	35	35	30	30	50
COMPOSITION:						
Quartz	30	60	35	70	25	25
Clay	20	30	25	30	30	15
Calcite/dolomite	40	5	30	—	35	15
Accessory minerals	1	—	—	—	—	2
Pyrite	2	—	—	—	—	—
Foraminifers	1	—	—	—	—	3
Nannofossils	5	5	10	—	10	35
Sponge spicules	1	—	—	—	—	5

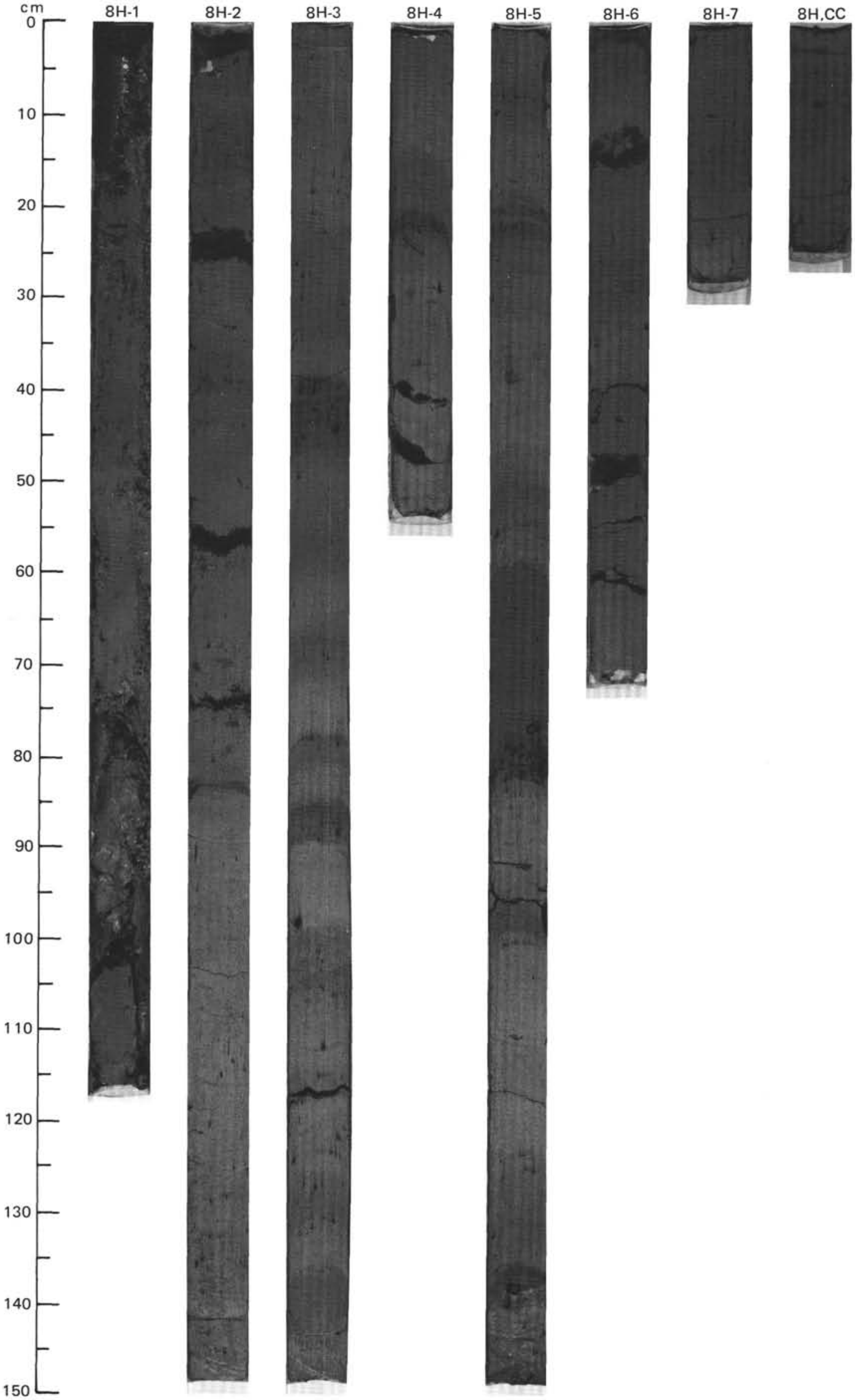
cm
0
10
20
30
40
50
60
70
80
90
100
110
120
130
140
150
8H-1
8H-2
8H-3
8H-4
8H-5
8H-6
8H-7
8H,CC

SITE 644 HOLE A CORE 9H CORED INTERVAL 1299.5-1309.0 mbsl; 73.2-82.7 mbsf

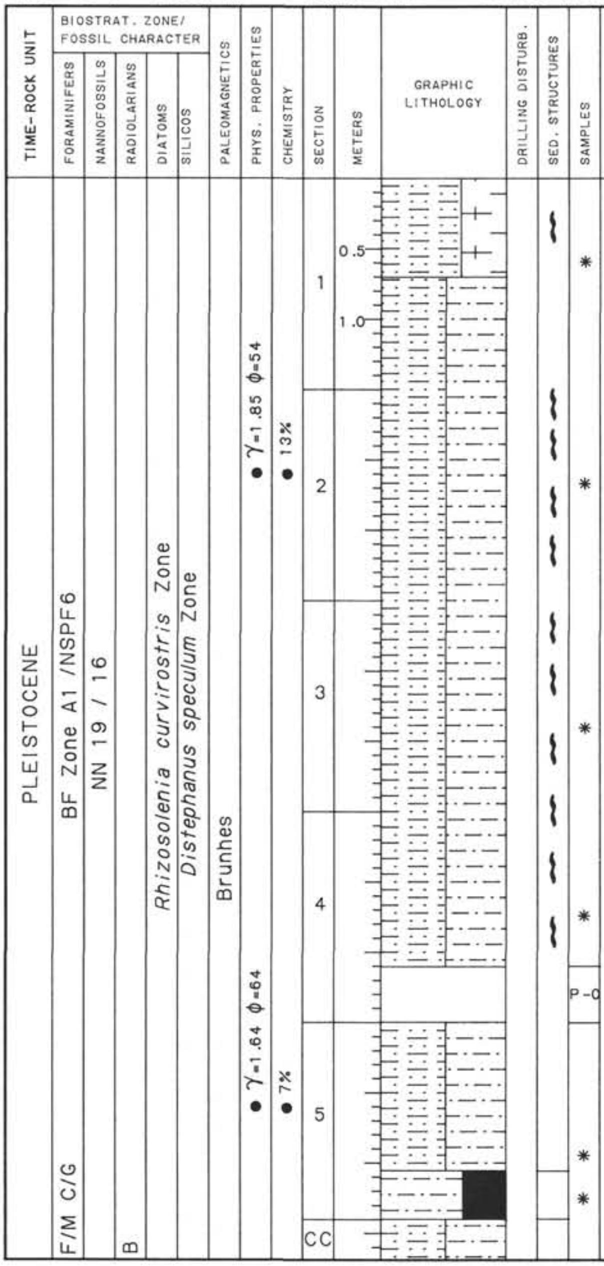

LITHOLOGIC DESCRIPTION

CALCAREOUS MUD

Entire core is undisturbed.

Major lithology: *Calcareous mud*, dark greenish gray (5GY 4/1), with minor color banding, minor bioturbation, and common pyritized burrows.

Minor lithologies:
a. Sandy mud, dark gray (5Y 4/1) to very dark gray (5Y 3/1), with pyritized burrows and minor mudstone dropstones.
b. Marly foraminiferal nannofossil ooze, dark greenish gray (5GY 4/1), with faint color banding in green.

SMEAR SLIDE SUMMARY (%):

	1, 69 M	2, 69 D	3, 84 D	4, 86 D	5, 90 D	5, 125 M
TEXTURE:						
Sand	20	5	15	35	35	10
Silt	30	55	40	25	35	60
Clay	50	40	65	40	30	30
COMPOSITION:						
Quartz	20	20	15	30	30	65
Mica	—	—	—	—	—	2
Clay	30	20	30	40	30	30
Calcite/dolomite	15	40	30	20	30	—
Accessory minerals	5	—	—	—	2	2
Pyrite	—	—	—	—	2	1
Foraminifers	10	—	2	—	1	—
Nannofossils	15	20	15	5	5	—
Sponge spicules	5	—	8	5	—	—

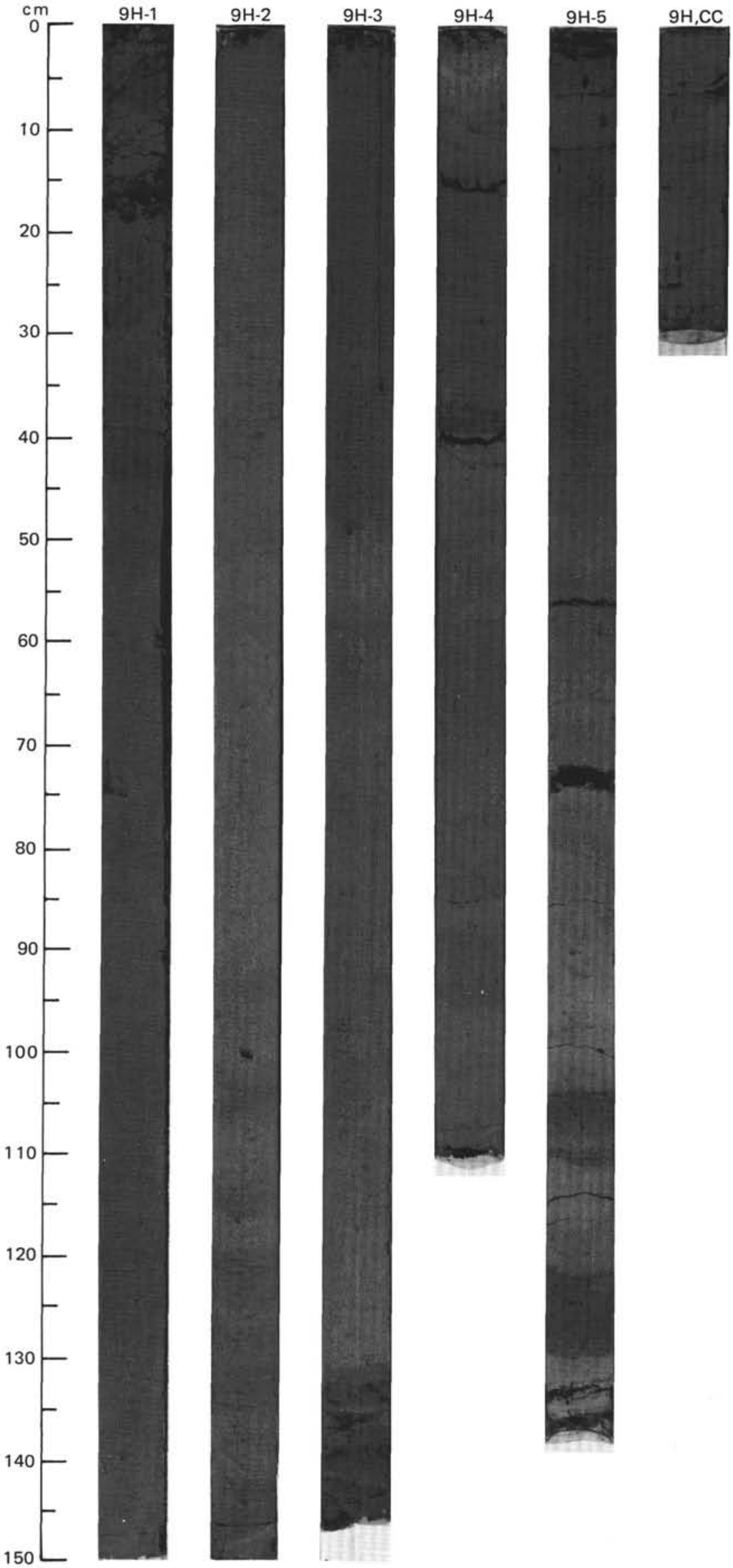
cm
0
10
20
30
40
50
60
70
80
90
100
110
120
130
140
150
9H-1
9H-2
9H-3
9H-4
9H-5
9H,CC

SITE 644 HOLE A CORE 10H CORED INTERVAL 1309.0-1318.5 mbsl; 82.7-92.2 mbsf

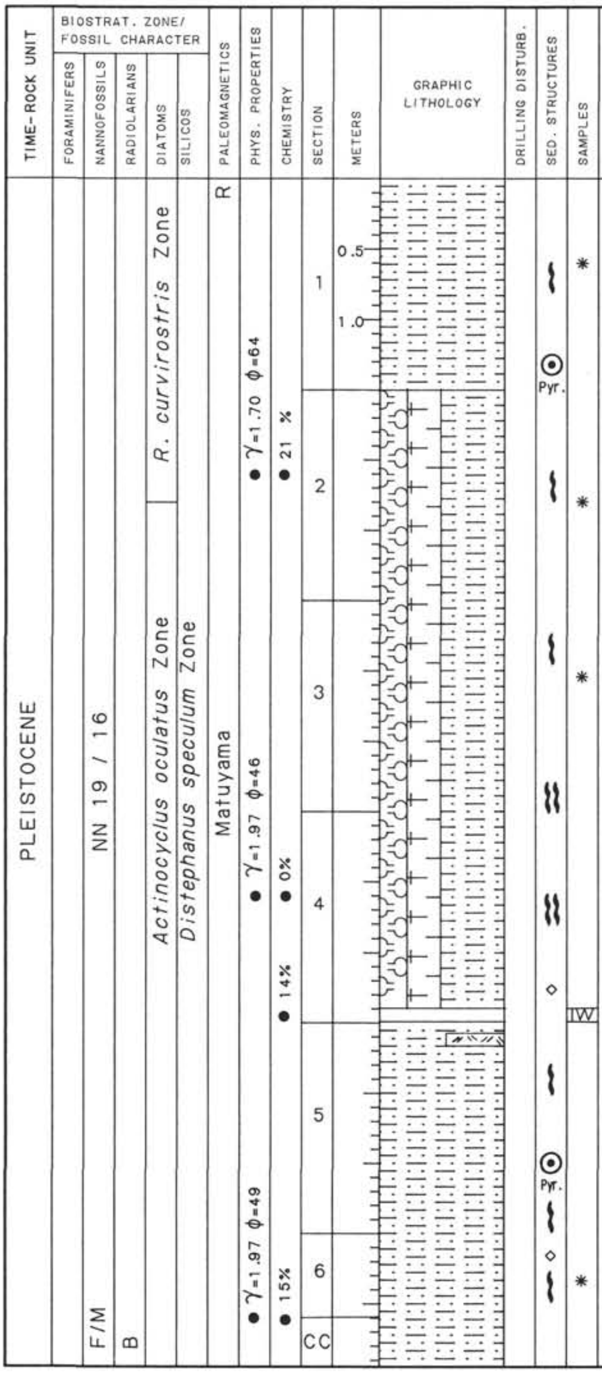

LITHOLOGIC DESCRIPTION

CALCAREOUS MUD AND SILICEOUS NANNNOFOSSIL MUD

Entire core is undisturbed.

Major lithologies:
a. Calcareous mud, dark gray (5Y 4/1), with common faint mottling to faint color banding. Pyritized burrows common.
b. Siliceous nannofossil mud, dark greenish gray (5GY 4/1), with minor to common diffuse color banding.

Minor lithology: Volcanic ash, disseminated, at Section 5, 110–111 cm.

SMEAR SLIDE SUMMARY (%):

	1, 63 D	2, 82 D	3, 59 D	6, 36 D
TEXTURE:				
Sand	5	10	20	10
Silt	55	40	40	40
Clay	40	50	40	50
COMPOSITION:				
Quartz	40	10	15	25
Clay	25	20	15	40
Volcanic glass	—	2	3	—
Calcite/dolomite	25	10	25	30
Accessory minerals	—	—	2	—
Pyrite	—	—	1	2
Foraminifers	2	10	5	—
Nannofossils	8	30	20	5
Diatoms	—	7	3	—
Sponge spicules	—	10	10	—

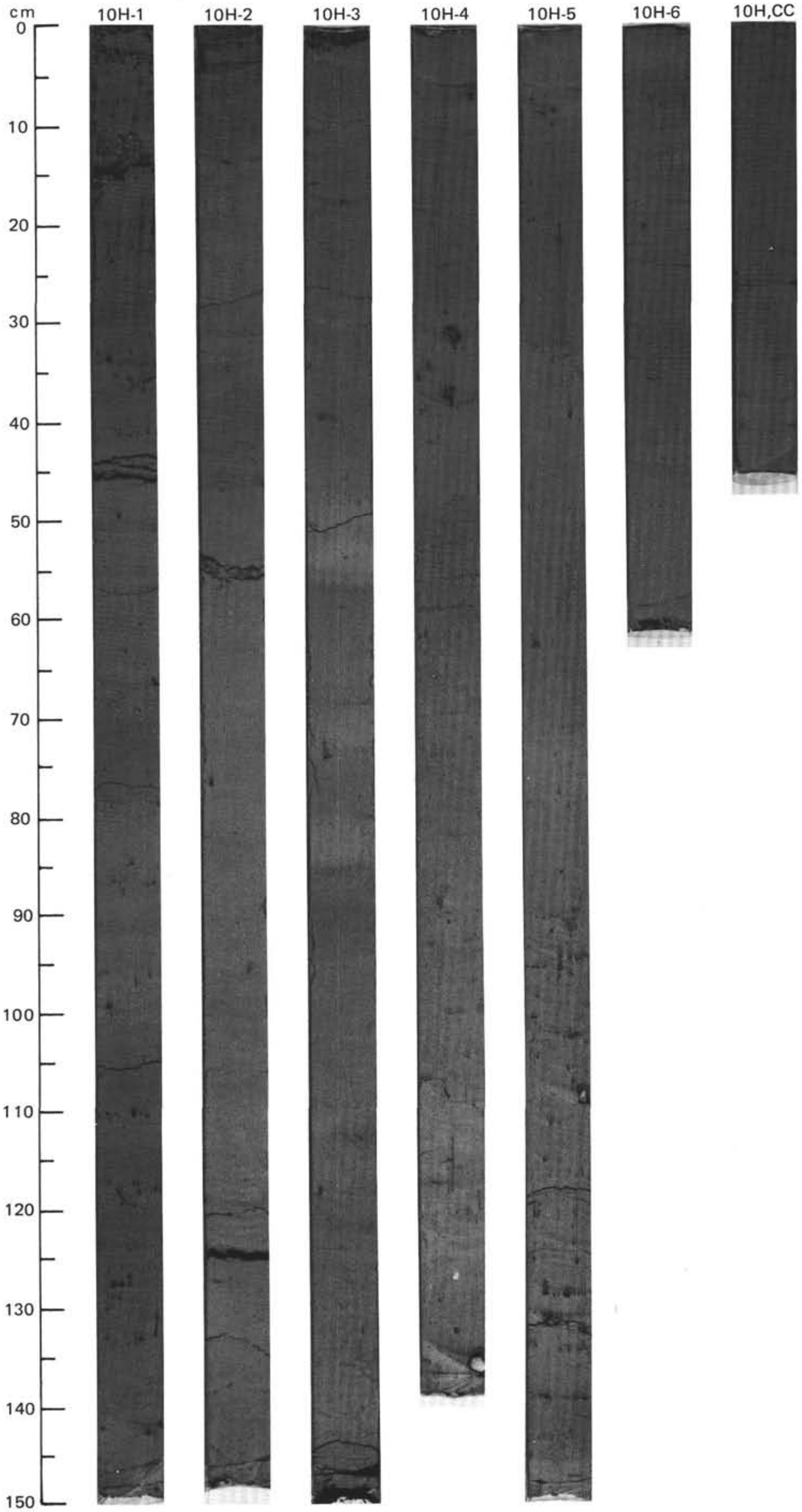
cm
0
10
20
30
40
50
60
70
80
90
100
110
120
130
140
150
10H-1
10H-2
10H-3
10H-4
10H-5
10H-6
10H,CC

SITE 644 HOLE A CORE 11H CORED INTERVAL 1318.5-1328.0 mbsl; 92.2-101.7 mbsf

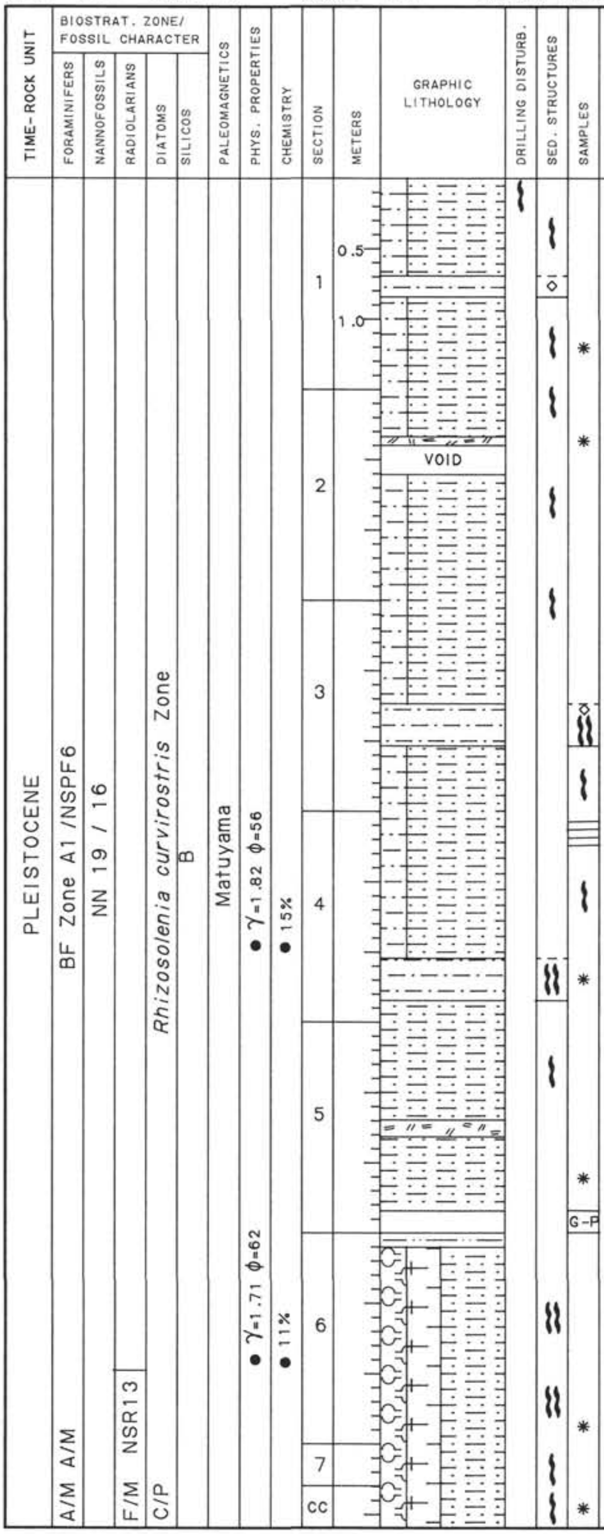

LITHOLOGIC DESCRIPTION

CALCAREOUS MUDS AND SILICEOUS NANNNOFOSSIL MUDS

Entire core is undisturbed.

Major lithologies:

a. Calcareous mud, dark gray (5Y 4/1) to dark greenish gray (5GY 4/1), with common faint mottles. Contains scattered pyrite concretions and pyritized burrows.

b. Siliceous nannofossil mud, dark greenish gray (5GY 4/1), moderately to heavily bioturbated.

Minor lithologies:

a. Sandy mud, very dark gray (5Y 3/1), with common small sand pockets and minor dropstones.

b. Volcanic ash layers: Section 2, 41–42 cm, and Section 5, 78–80 cm.

SMEAR SLIDE SUMMARY (%):

	1, 122 D	2, 41 M	4, 122 D	5, 110 M	6, 142 D	CC, 20 D
TEXTURE:						
Sand	20	80	40	5	20	30
Silt	50	20	40	65	60	60
Clay	30	—	20	30	40	30
COMPOSITION:						
Quartz	50	—	68	40	20	30
Feldspar	1	—	2	1	1	—
Mica	—	—	1	1	—	—
Clay	20	—	20	30	15	20
Volcanic glass	—	75	—	—	12	3
Calcite/dolomite	15	—	5	15	10	10
Accessory minerals	1	—	3	2	1	—
Pyrite	1	25	1	1	—	—
Foraminifers	—	—	—	1	10	1
Nannofossils	—	—	—	3	20	15
Diatoms	—	—	—	3	5	10
Radiolarians	—	—	—	—	2	1
Sponge spicules	—	—	—	3	15	10

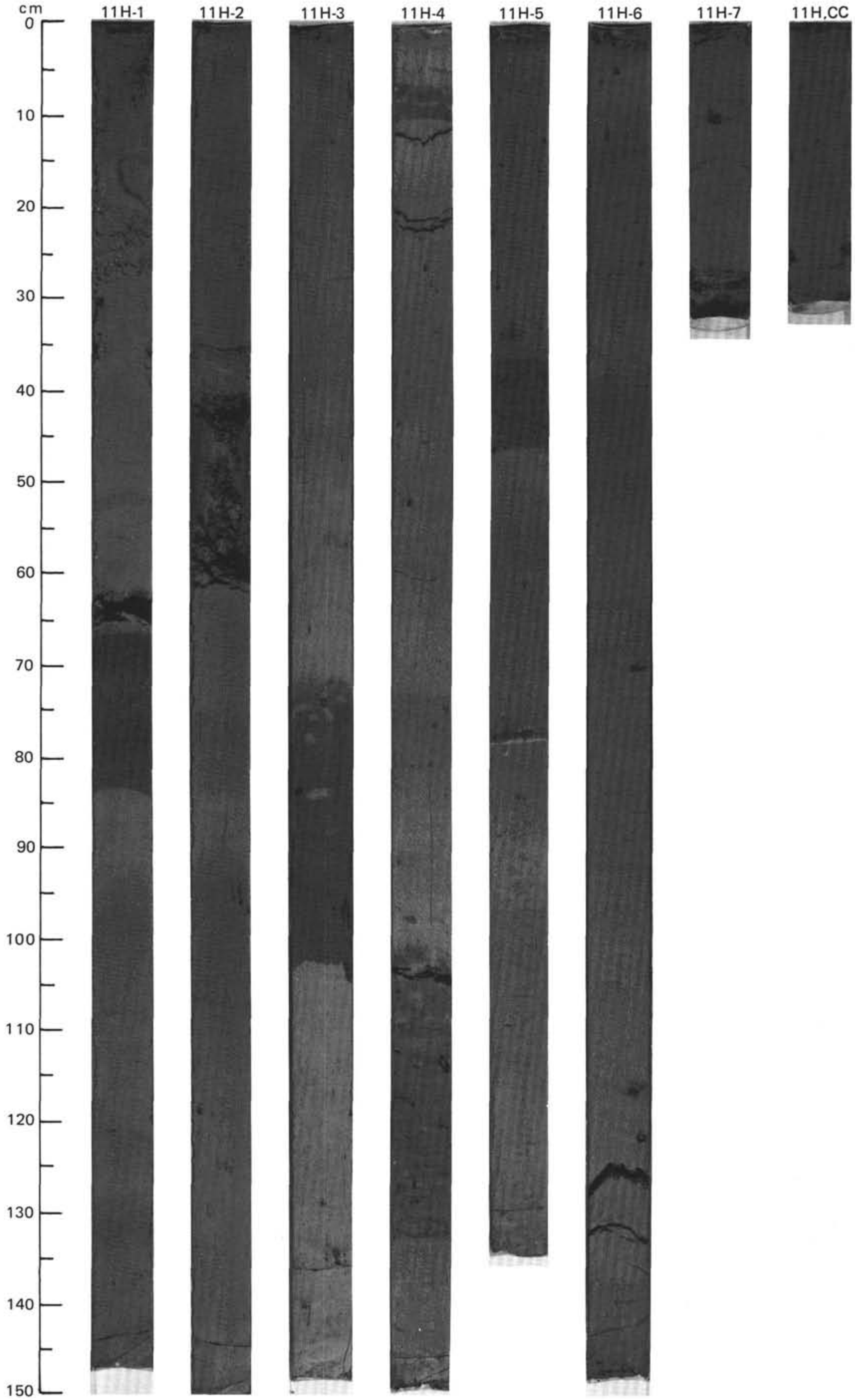
cm
0
10
20
30
40
50
60
70
80
90
100
110
120
130
140
150
11H-1
11H-2
11H-3
11H-4
11H-5
11H-6
11H-7
11H,CC

SITE 644 HOLE A CORE 12H CORED INTERVAL 1328.0-1337.5 mbsl; 101.7-111.2 mbsf

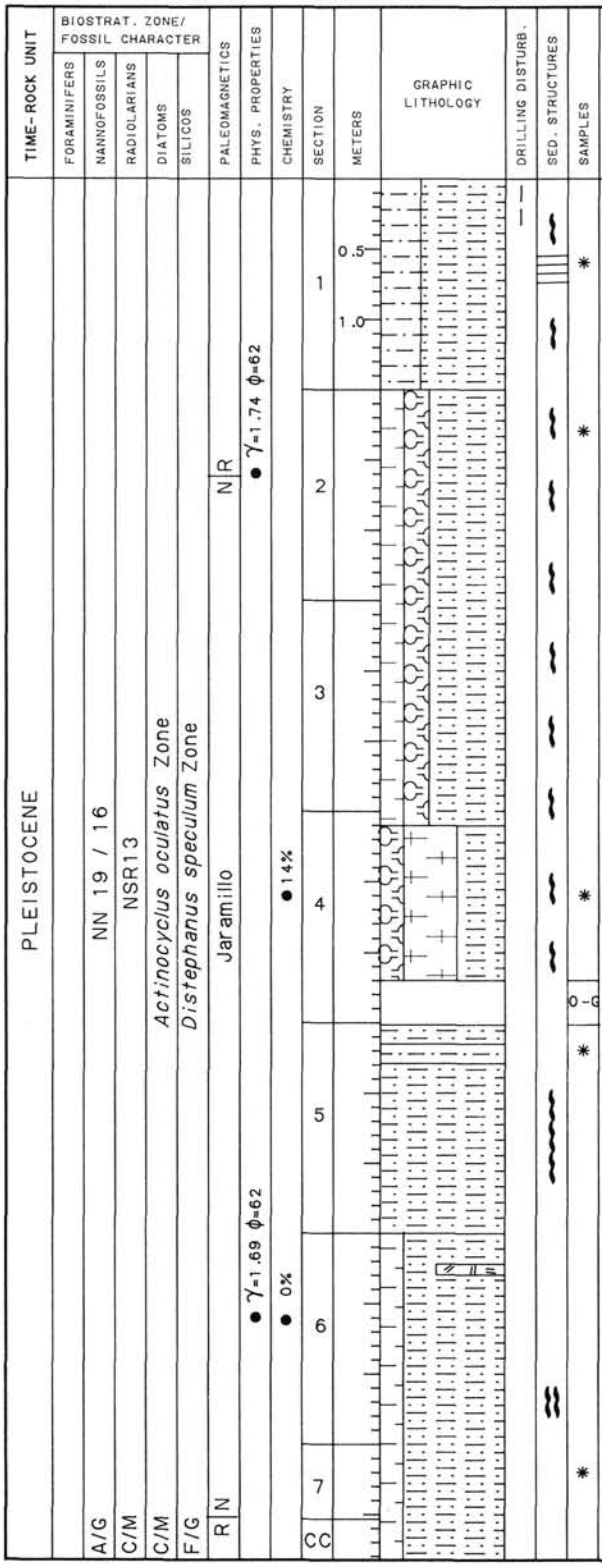

LITHOLOGIC DESCRIPTION

CALCAREOUS MUD AND MARLY NANNOFOSSIL-SILICEOUS OOZE

Entire core is undisturbed.

Major lithologies:
a. Calcareous mud, dark greenish gray (5GY 4/1), with minor faint color banding. Pyritized burrows common.
b. Marly nannofossil-siliceous ooze, dark greenish gray (5GY 4/1) and uniform in appearance.

Minor lithologies:
a. Siliceous nannofossil ooze, dark greenish gray (5GY 4/1). Section 4, 0–120 cm.
b. Foraminiferal mud, dark gray (5Y 4/1). Section 6.
c. Sandy mud, very dark gray (5Y 3/1), with common mudstone dropstones. Section 1, 22–36 cm; Section 5, 12–31 cm.
d. Volcanic ash, disseminated. Section 6, 28–30 cm.

SMEAR SLIDE SUMMARY (%):

	1, 70 D	2, 35 D	4, 70 M	5, 20 M	6, 119 M
TEXTURE:					
Sand	35	30	5	20	1
Silt	35	40	45	45	49
Clay	30	30	50	35	50
COMPOSITION:					
Quartz	35	35	10	50	10
Feldspar	—	—	—	10	—
Clay	10	20	15	33	45
Volcanic glass	3	—	—	—	
Calcite/dolomite	15	10	10	—	5
Accessory minerals	2	—	—	2	—
Pyrite	3	1	—	—	—
Glauconite	—	—	—	5	—
Foraminifers	3	—	10	—	20
Nannofossils	8	—	40	—	5
Diatoms	14	—	5	—	10
Sponge spicules	10	—	10	—	5

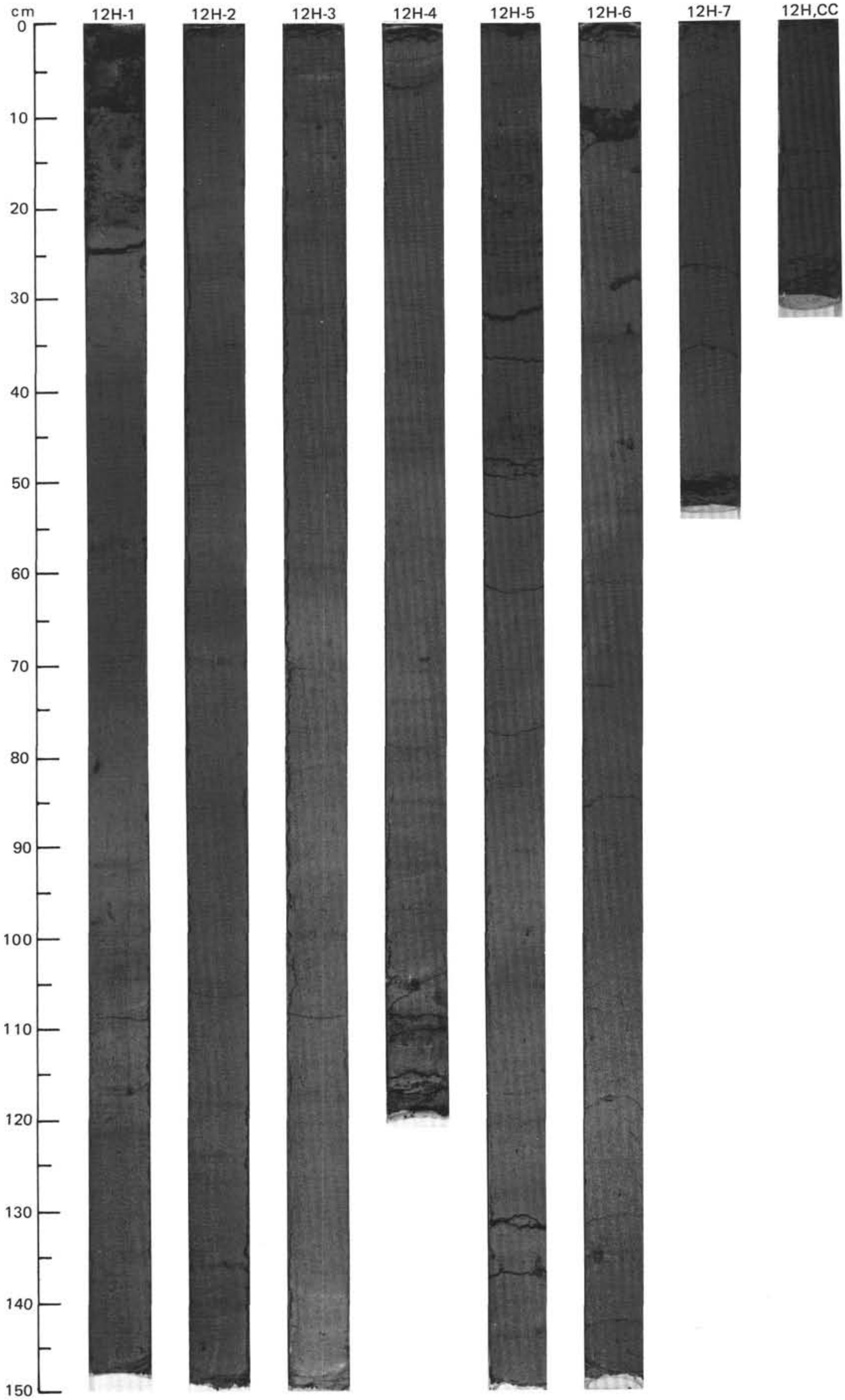
cm
0
10
20
30
40
50
60
70
80
90
100
110
120
130
140
150
12H-1
12H-2
12H-3
12H-4
12H-5
12H-6
12H-7
12H,CC

SITE 644 HOLE A CORE 13H CORED INTERVAL 1337.5-1347.0 mbsl; 111.2-120.7 mbsf

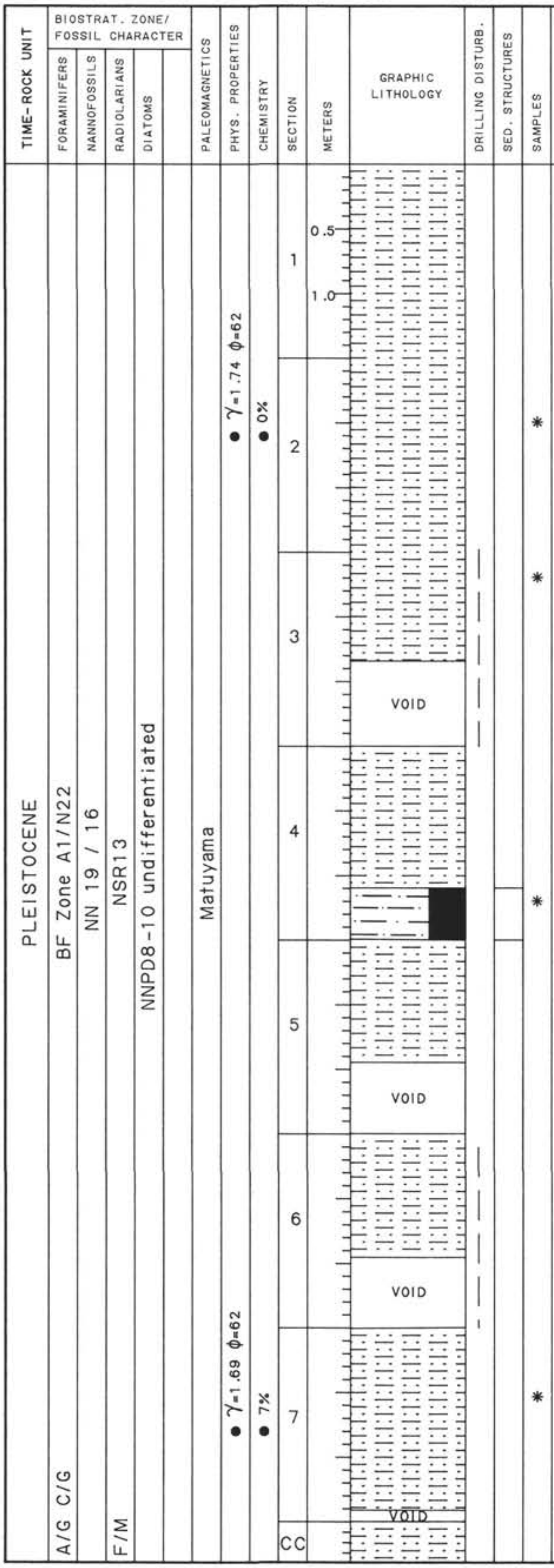

LITHOLOGIC DESCRIPTION

SILICEOUS MUD AND GLACIAL SANDY MUD

Sections 3 and 6 are moderately disturbed. Remainder of the core is undisturbed.

Major lithologies:
a. Siliceous mud, dark greenish gray (5GY 4/1), and mottled with pyritized burrows. Section 1.
b. Mud, dark gray (5Y 4/1) to dark greenish gray (5GY 4/1), mottled with dark gray and black. Section 22 to Section 3, 4 cm; Section 3, 5 cm, to Section 4, 110 cm; Section 5 to CC.

Minor lithology: Sandy mud, very dark gray (5Y 3/1), with scattered dropstones. Section 3, 4–5 cm; Section 4, 110–150 cm.

SMEAR SLIDE SUMMARY (%):

	2, 56 D	3, 29 D	4, 127 M	7, 80 D
TEXTURE:				
Sand	2	5	5	5
Silt	38	32	24	50
Clay	60	63	71	45
COMPOSITION:				
Quartz	10	30	15	15
Mica	—	—	1	—
Clay	60	63	71	43
Volcanic glass	5	—	—	5
Calcite/dolomite	10	5	10	20
Accessory minerals	—	2	2	—
Pyrite	10	—	—	—
Glauconite	—	—	1	—
Foraminifers	—	—	—	2
Diatoms	Tr	—	—	5
Sponge spicules	5	—	—	10

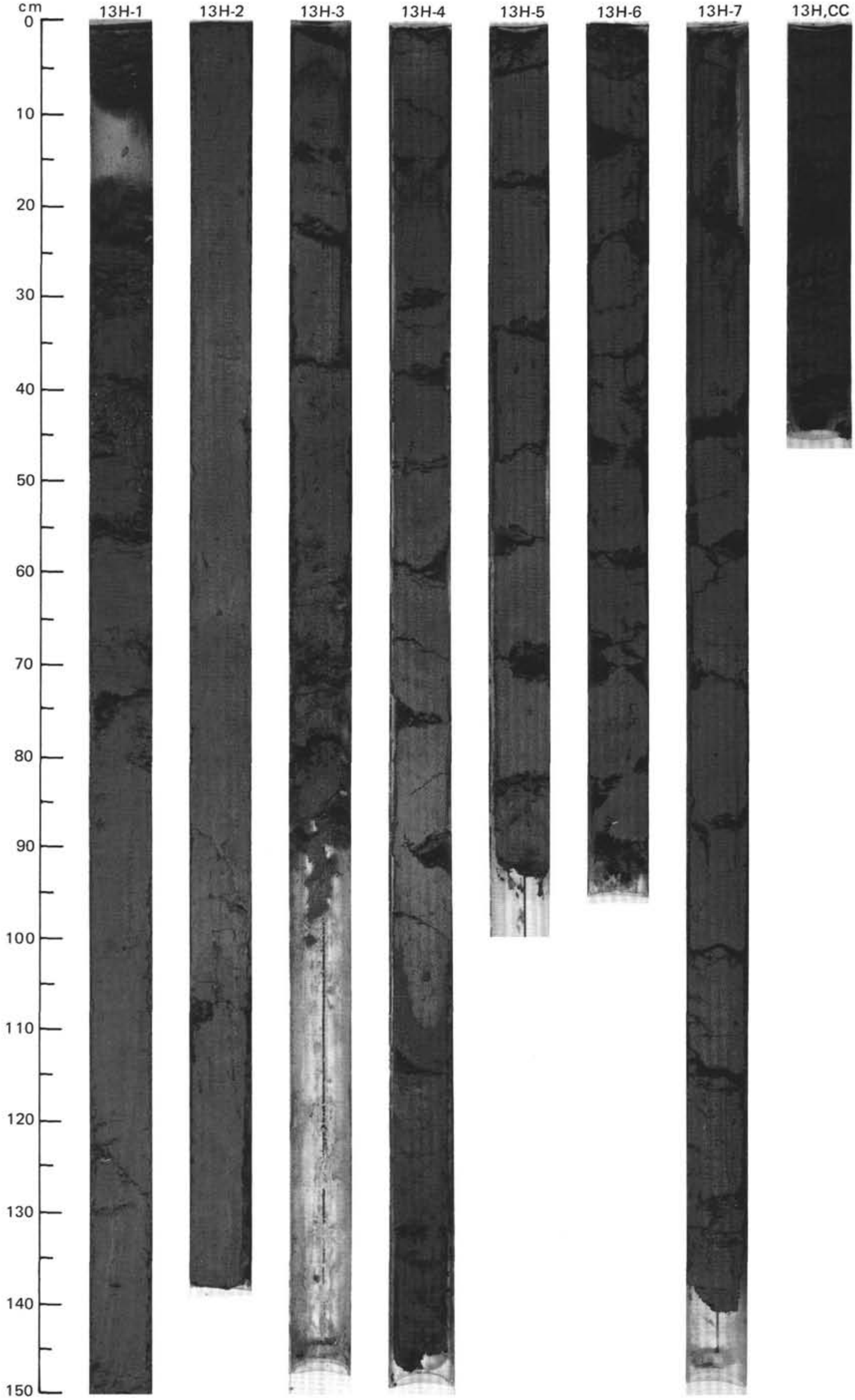
cm
0
10
20
30
40
50
60
70
80
90
100
110
120
130
140
150
13H-1
13H-2
13H-3
13H-4
13H-5
13H-6
13H-7
13H,CC

SITE 644 HOLE A CORE 14H CORED INTERVAL 1347.0-1356.5 mbsl; 120.7-130.2 mbsf

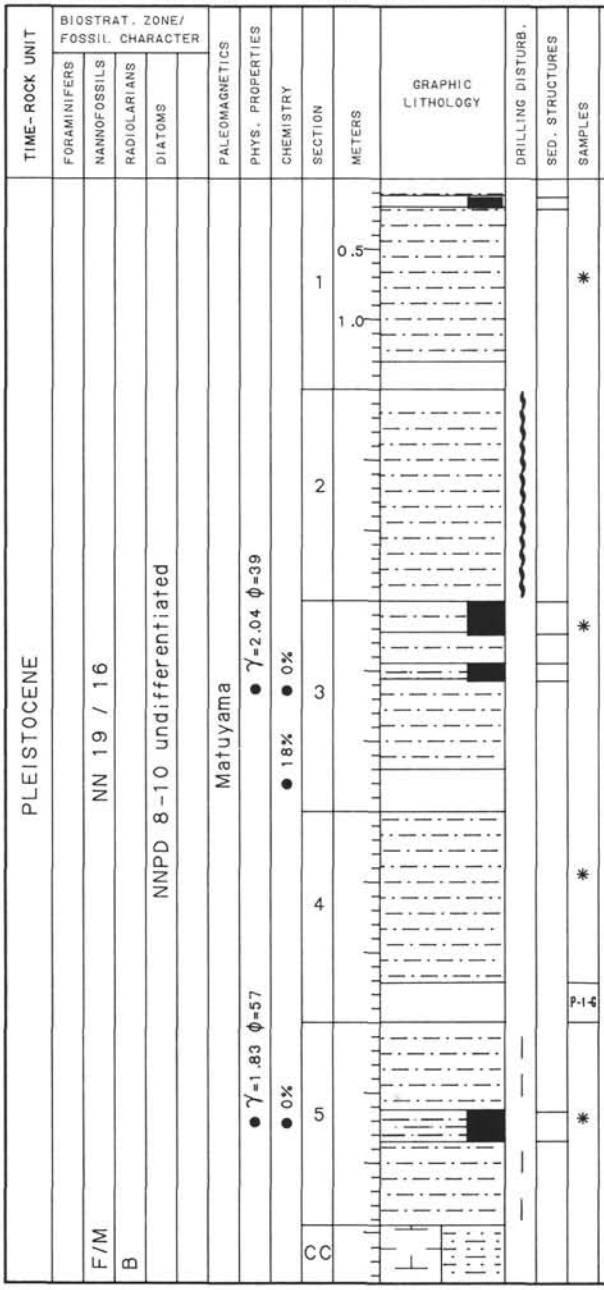

LITHOLOGIC DESCRIPTION

SILICEOUS MUDS AND GLACIAL SANDY MUDS

Section 2, 20–80 cm, is highly disturbed. Section 5 is moderately disturbed. Remainder of the core is undisturbed.

Major lithology: Sandy mud, dark greenish gray (5GY 4/1) to dark gray (5Y 4/1), with diffuse color bands in green and brown. Pyritized burrows are locally abundant. Section 1, 0–11 cm; Section 1, 19 cm, to Section 2; Section 3, 22–44 cm; Section 3, 53 cm, to Section 5, 66 cm; Section 5, 73–77 and 82–143 cm.

Minor lithology: Sandy mud, very dark gray (5Y 3/1), with scattered dropstones. Section 1, 11–19 cm; Section 3, 0–22 cm; Section 3, 44–53 cm; Section 5, 66–73 and 77–82 cm.

SMEAR SLIDE SUMMARY (%):

	1, 70 D	3, 16 M	4, 40 D	5, 69 M
TEXTURE:				
Sand	15	25	15	30
Silt	30	45	32	40
Clay	55	30	53	30
COMPOSITION:				
Quartz	30	60	30	50
Feldspar	—	10	—	10
Clay	55	29	53	30
Volcanic glass	2	1	5	—
Calcite/dolomite	5	5	5	5
Accessory minerals	2	5	2	5
Glauconite	1	—	—	—
Sponge spicules	5	—	—	—

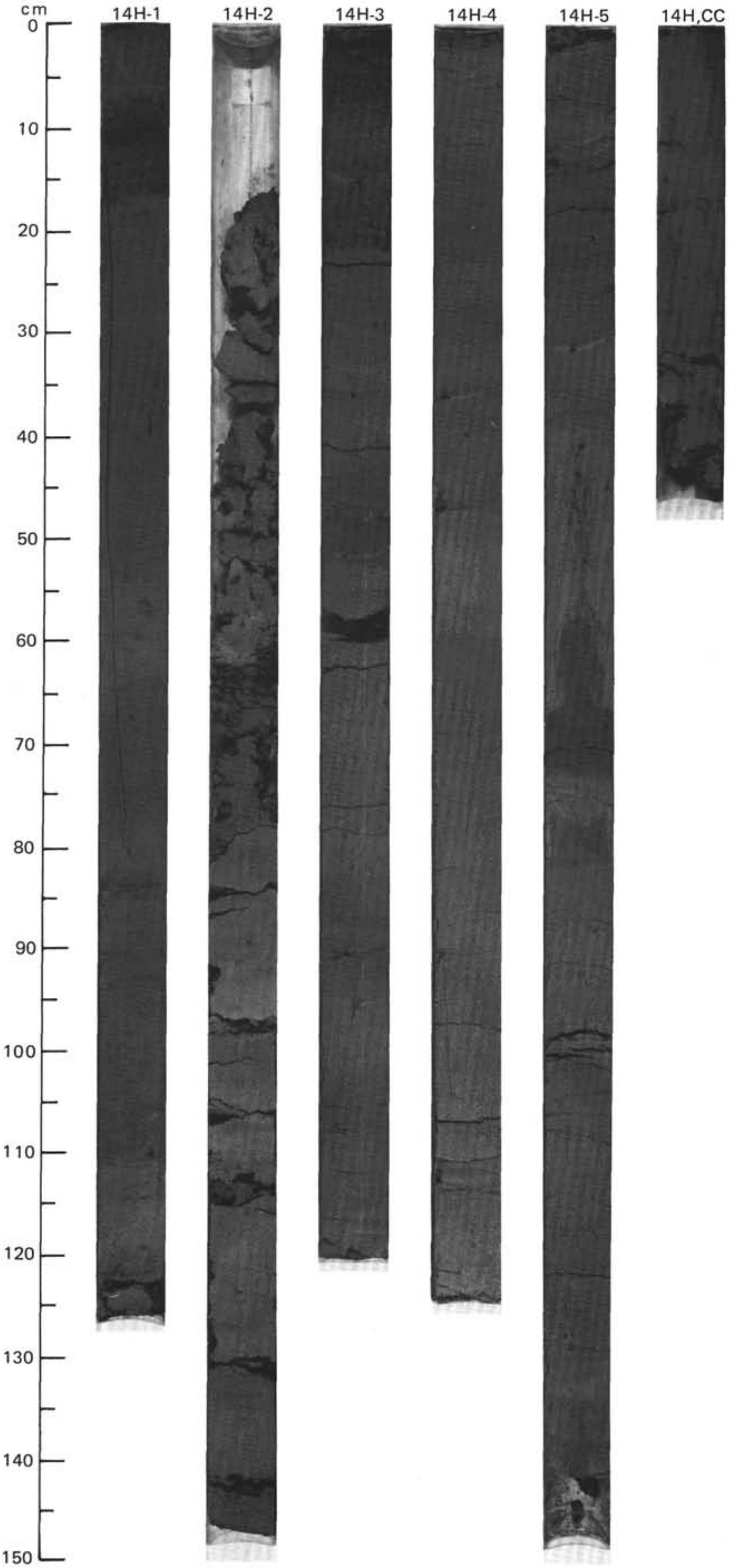
cm
0
10
20
30
40
50
60
70
80
90
100
110
120
130
140
150
14H-1
14H-2
14H-3
14H-4
14H-5
14H,CC

SITE 644 HOLE A CORE 15H CORED INTERVAL 1356.5-1366.0 mbsl; 130.2-139.7 mbsf

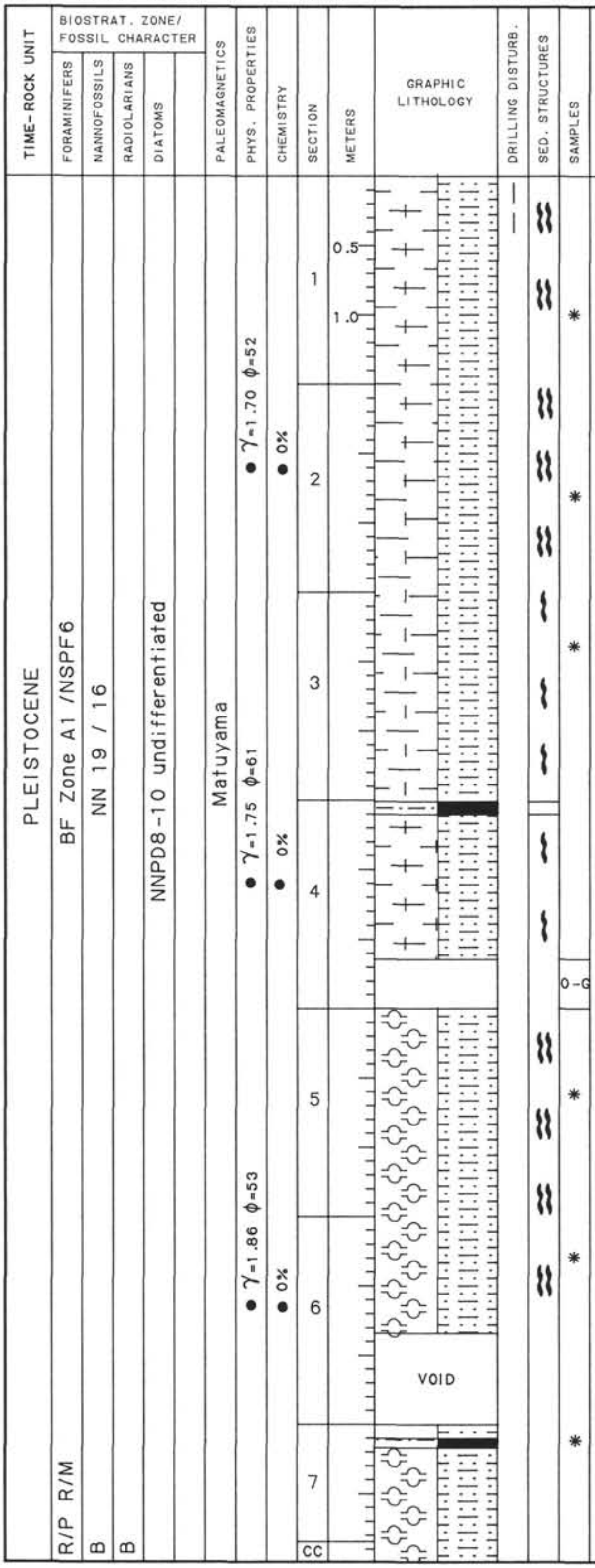

LITHOLOGIC DESCRIPTION

SILICEOUS MUD AND GLACIAL SANDY MUD

Section 1, 0–40 cm, is modertely disturbed. Remainder of the core is undisturbed.

Major lithology: Siliceous mud, dark greenish gray (5GY 4/1) to dark gray (5Y 4/1), extensively mottled and bioturbated, with pyritized burrows common. Section 1 to Section 3; Section 4, 9 cm, to Section 7, 10 cm; Section 7, 15 cm, to CC.

Minor lithology: Sandy mud, very dark gray (5Y 3/1), with numerous scattered dropstones. Section 4, 0–9 cm; Section 7, 10–15 cm.

SMEAR SLIDE SUMMARY (%):

	1, 100 D	2, 81 D	3, 43 D	5, 60 D	6, 30 D	7, 13 M
TEXTURE:						
Sand	5	5	5	10	5	25
Silt	27	33	44	50	64	33
Clay	68	62	51	40	31	42
COMPOSITION:						
Quartz	15	25	15	20	15	50
Feldspar	—	—	2	—	—	5
Clay	68	62	46	37	26	42
Volcanic glass	1	5	1	—	1	—
Calcite/dolomite	—	—	—	10	20	1
Accessory minerals	1	1	1	—	—	2
Foraminifers	—	—	Tr	—	2	—
Nannofossils	—	—	5	3	5	—
Diatoms	5	2	10	10	5	—
Sponge spicules	10	5	20	20	25	—

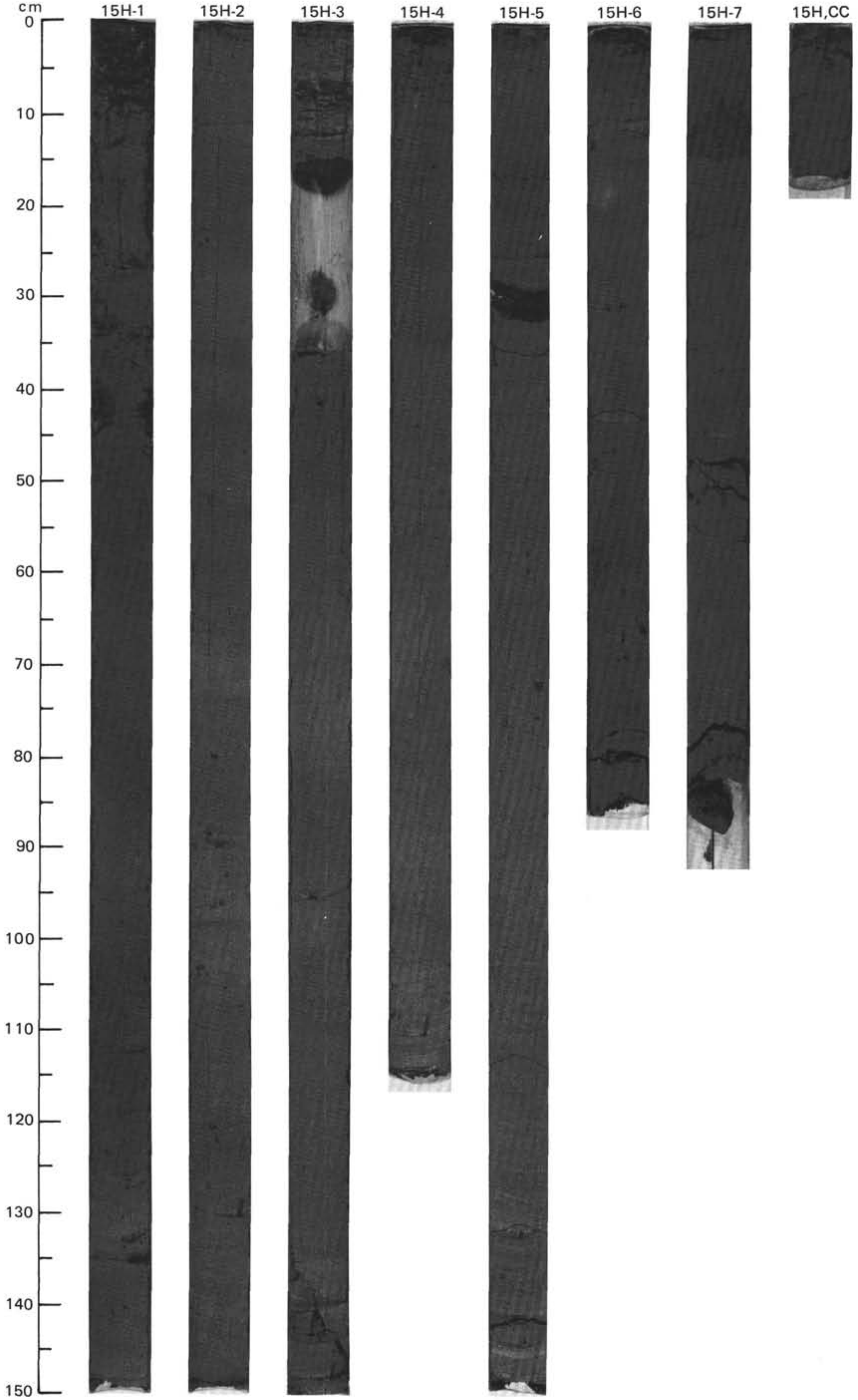
cm
0
10
20
30
40
50
60
70
80
90
100
110
120
130
140
150
15H-1
15H-2
15H-3
15H-4
15H-5
15H-6
15H-7
15H,CC

SITE 644 HOLE A CORE 16H CORED INTERVAL 1366.0-1375.5 mbsl; 139.7-149.2 mbsf

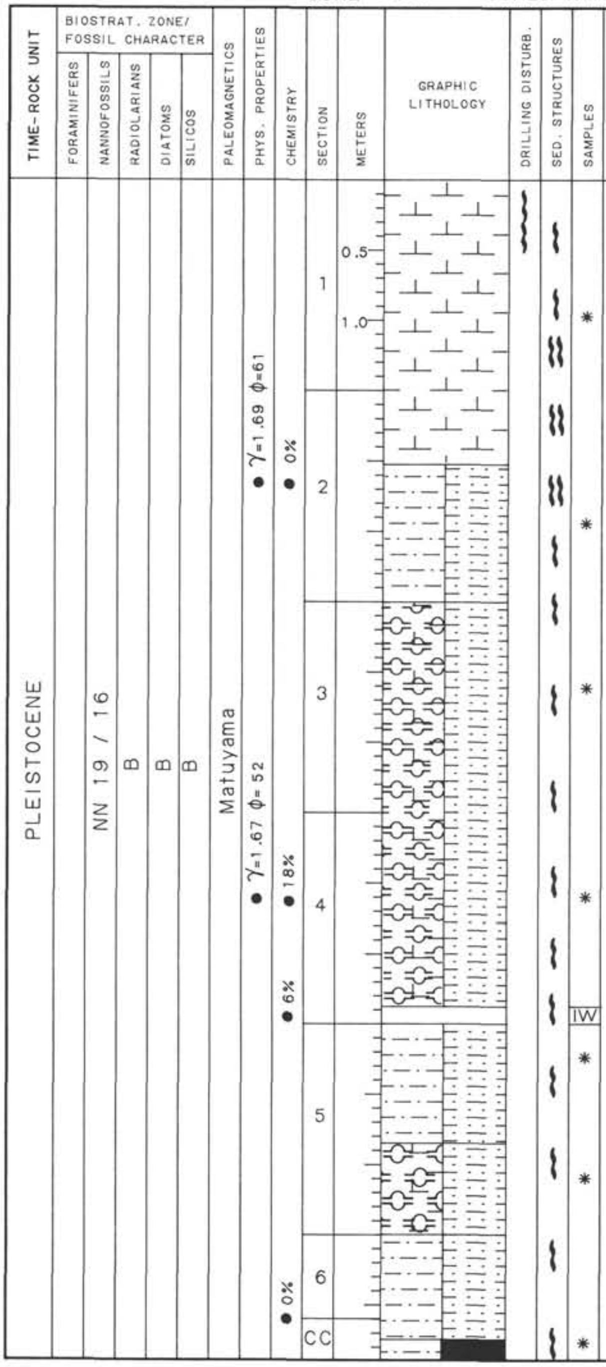

LITHOLOGIC DESCRIPTION

SILICEOUS NANNOFOSSIL MUD AND GLACIAL SANDY MUD

Section 1, 0–56 cm, is highly disturbed. Remainder of the core is undisturbed.

Major lithologies:
a. Siliceous nannofossil and siliceous mud, greenish gray (5GY 5/1) to dark greenish gray (5GY 4/1), moderately bioturbated, with pyritized burrows common.
b. Sandy mud to mud, dark greenish gray (5GY 4/1), moderately bioturbated and mottled. Section 2, 56–150 cm.

Minor lithologies:
a. Nannofossil ooze, greenish gray (5GY 5/1), mottled and moderately bioturbated. Section 1 to Section 2, 56 cm.
b. Sandy mud, very dark gray (5Y 3/1), with scattered dropstones. CC, 17–30 cm.

SMEAR SLIDE SUMMARY (%):

	1, 91 D	2, 89 D	3, 68 D	4, 63 D	5, 83 D	5, 116 D	CC, 16 M
TEXTURE:							
Sand	—	15	5	5	10	3	20
Silt	18	37	40	31	44	42	45
Clay	82	48	55	64	56	55	35
COMPOSITION:							
Quartz	2	30	20	20	30	15	50
Feldspar	—	3	3	5	5	—	10
Clay	22	48	55	54	56	35	35
Calcite/dolomite	5	15	5	—	—	15	—
Accessory minerals	—	2	2	1	3	—	5
Foraminifers	Tr	—	—	Tr	—	—	—
Nannofossils	60	—	—	10	—	20	—
Diatoms	5	—	5	5	1	5	—
Sponge spicules	5	—	10	15	5	10	—

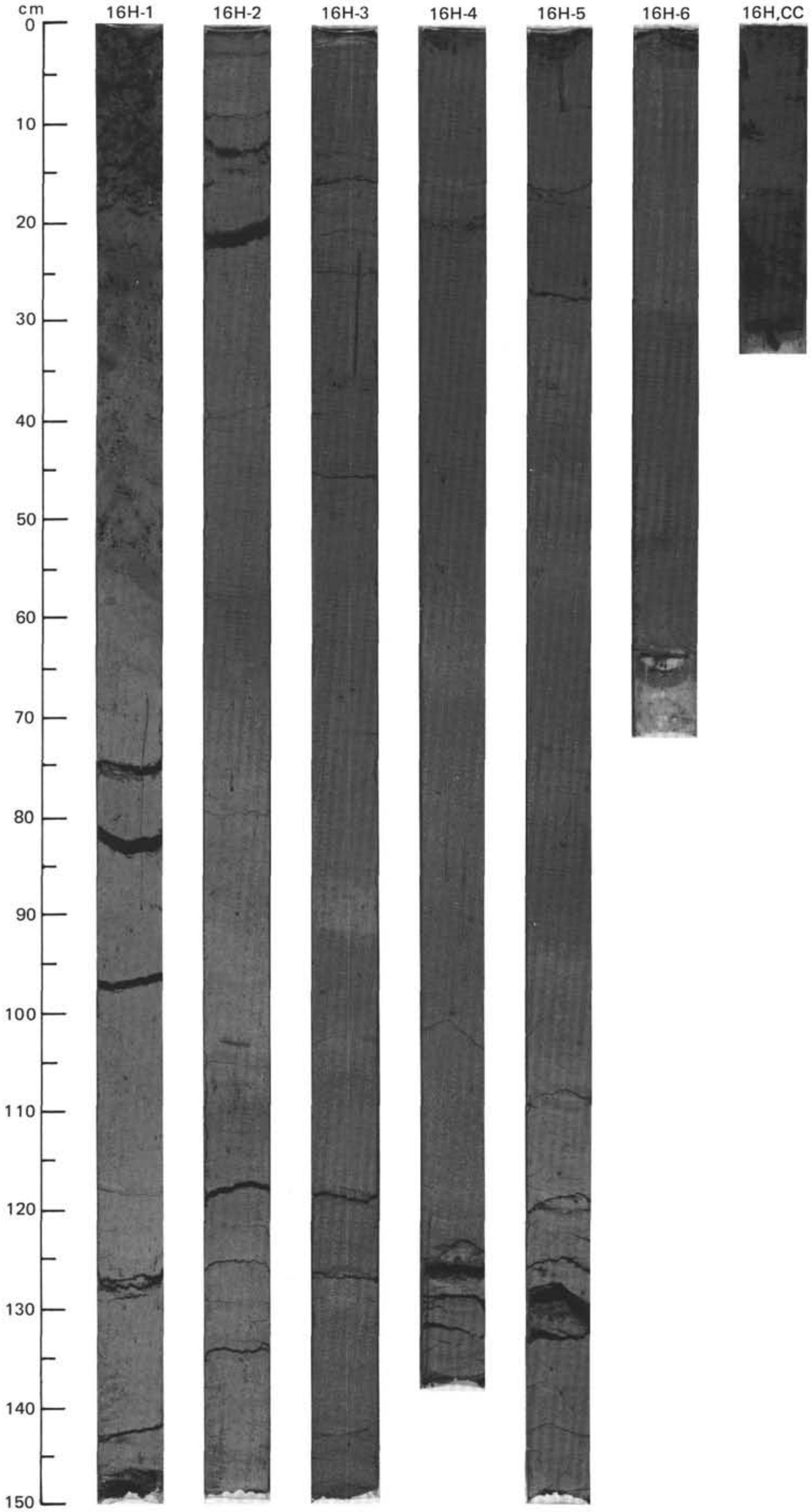
cm
0
10
20
30
40
50
60
70
80
90
100
110
120
130
140
150
16H-1
16H-2
16H-3
16H-4
16H-5
16H-6
16H,CC

SITE 644 HOLE A CORE 17H CORED INTERVAL 1375.5-1385.0 mbsl; 149.2-158.7 mbsf

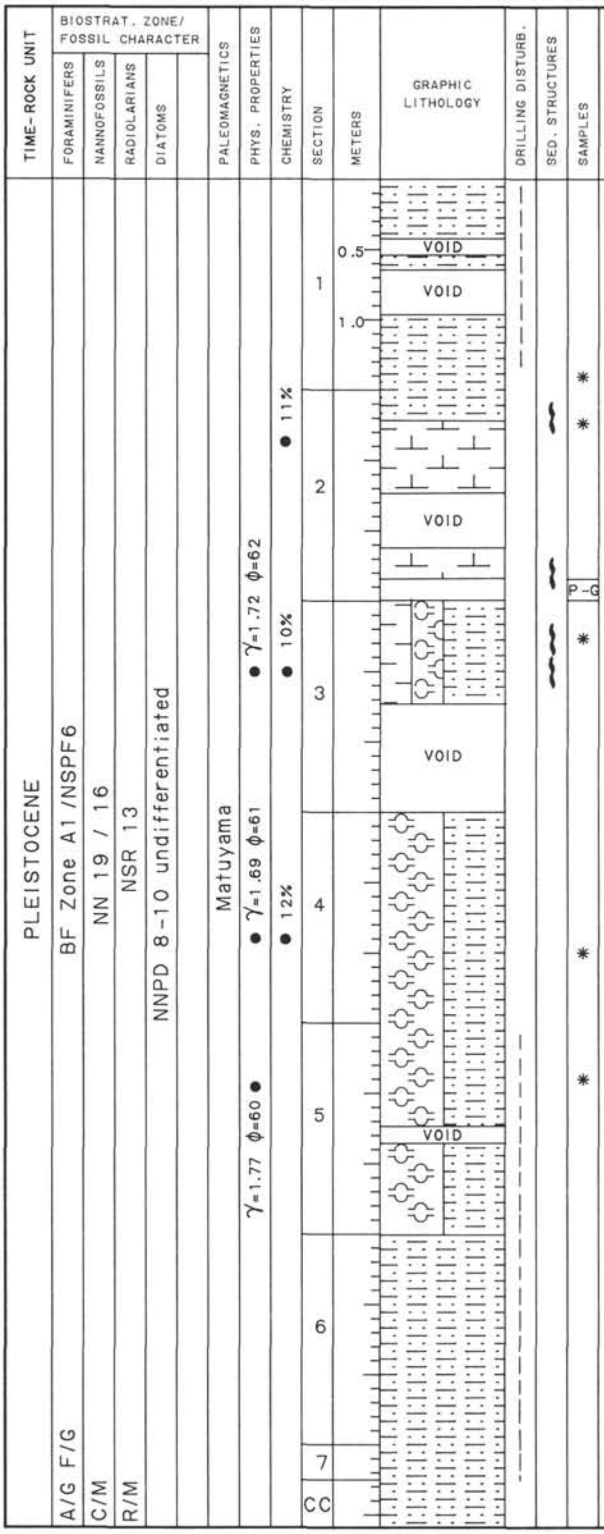

LITHOLOGIC DESCRIPTION

SILICEOUS MUD AND SILICEOUS NANNOFOSSIL MUD

Sections 1, 6, and 7 are moderately disturbed. Remainder of the core is undisturbed.

Major lithologies:
a. Siliceous mud and siliceous nannofossil mud, dark greenish gray (5GY 4/1), moderately mottled and bioturbated. Section 3 to Section 5.
b. Silty mud and mud, dark greenish gray (5GY 4/1), moderately mottled and bioturbated. Section 1 to Section 2, 20 cm; Section 6 to CC.

Minor lithology: Nannofossil ooze, greenish gray (5GY 5/1), moderately mottled. Secton 2, 20–150 cm.

SMEAR SLIDE SUMMARY (%):

	1, 138 D	2, 25 D	3, 23 D	4, 94 D	5, 39 D	6, 87 D
TEXTURE:						
Sand	5	—	5	5	5	1
Silt	30	16	21	32	47	29
Clay	65	84	64	63	48	70
COMPOSITION:						
Quartz	20	3	15	10	20	20
Feldspar	—	—	—	—	—	1
Clay	65	24	44	58	48	70
Volcanic glass	2	—	1	—	5	5
Calcite/dolomite	2	—	15	10	10	1
Accessory minerals	1	—	—	1	2	—
Foraminifers	—	1	—	1	—	—
Nannofossils	—	60	20	5	—	—
Diatoms	—	2	—	5	—	—
Sponge spicules	10	10	15	20	15	3

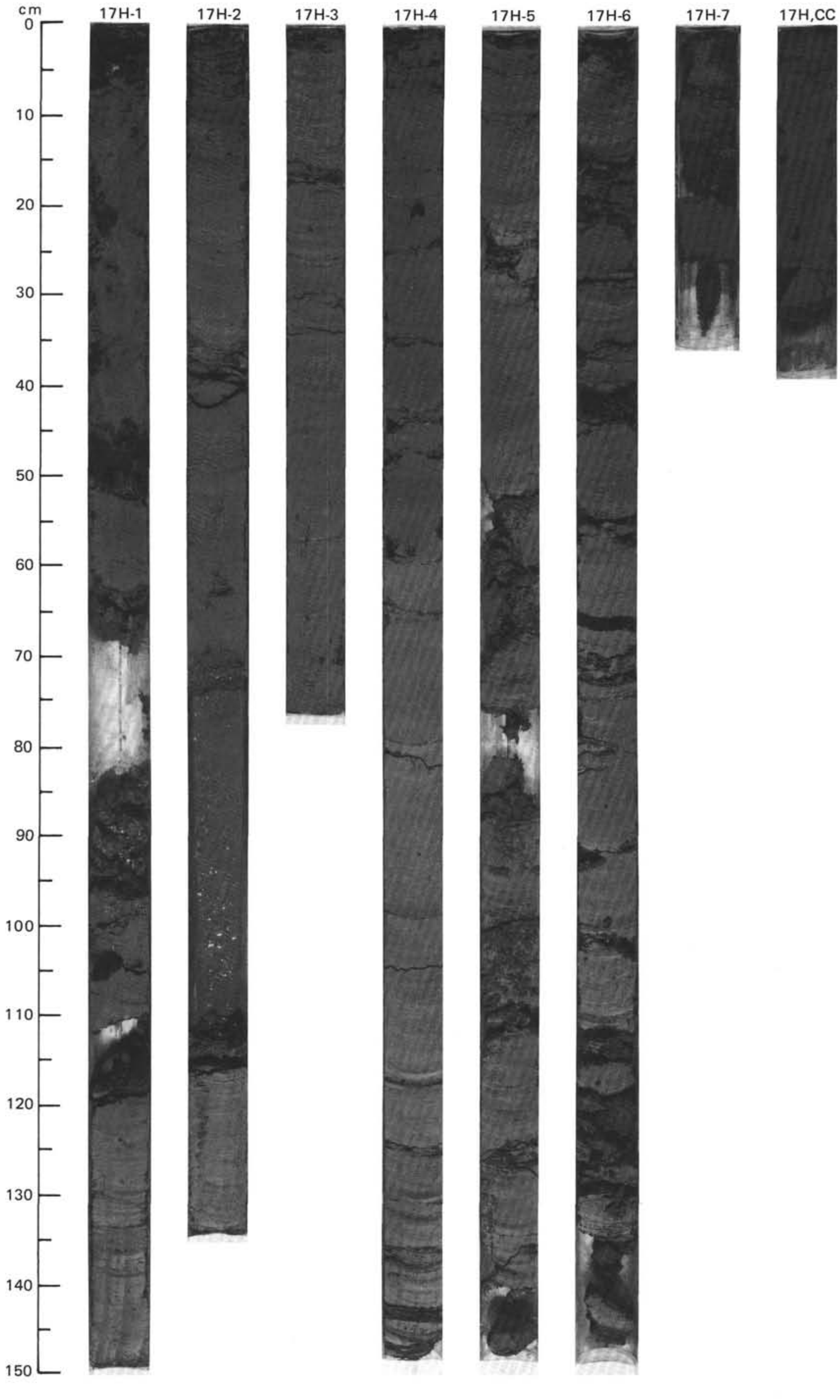
cm
0
10
20
30
40
50
60
70
80
90
100
110
120
130
140
150
17H-1
17H-2
17H-3
17H-4
17H-5
17H-6
17H-7
17H,CC

SITE 644 HOLE A CORE 18H CORED INTERVAL 1385.0-1394.5 mbsl; 158.7-168.2 mbsf

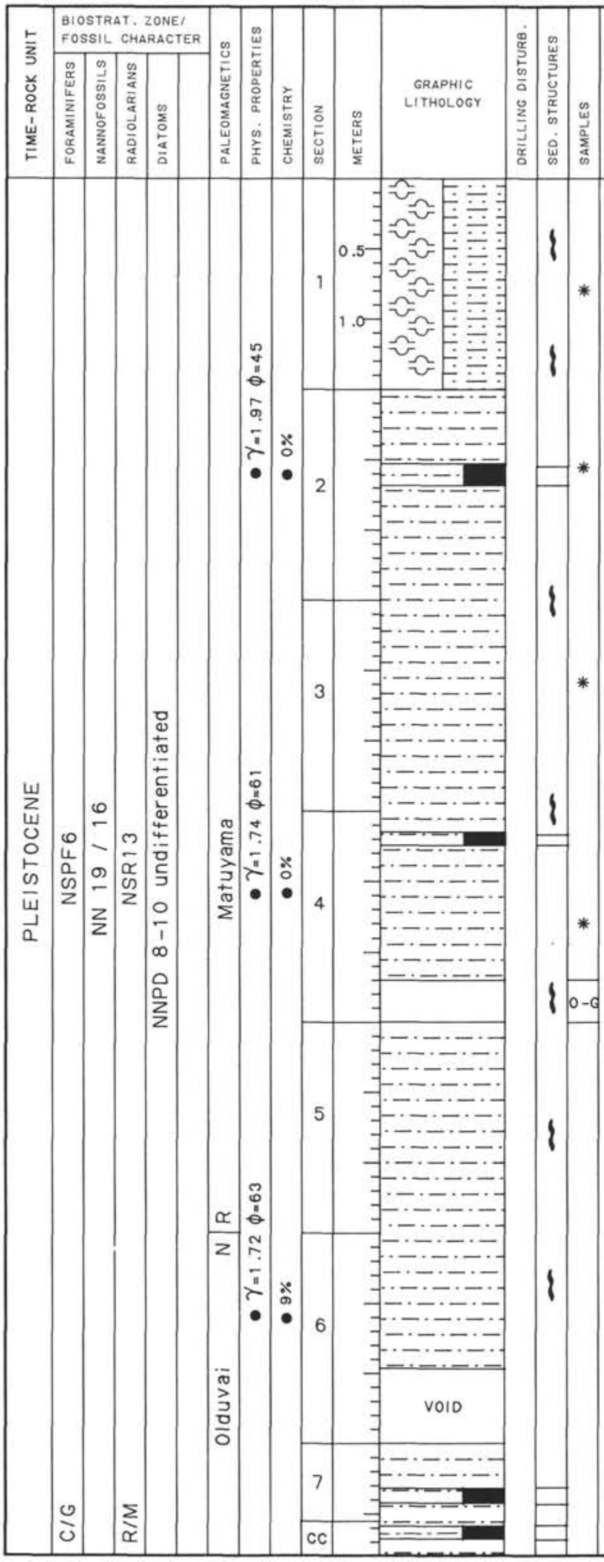

LITHOLOGIC DESCRIPTION

SILICEOUS MUD AND GLACIAL SANDY MUD

Entire core is undisturbed.

Major lithologies:
a. Siliceous mud, dark greenish gray (5GY 4/1), mottled and bioturbated. Section 1.
b. Sandy mud and mud, dark greenish gray (5GY 4/1), mottled and bioturbated, with diffuse color banding in brown and green. Section 2, 0–53 cm; Section 2, 67 cm, to Section 4, 8 cm; Section 4, 11 cm, to Section 7, 35 cm; Section 7, 42 cm, to CC, 5 cm; CC, 15–24 cm.

Minor lithology: Sandy mud, very dark gray (5Y 3/1), with scattered large dropstones. Section 22, 53–67 cm; Section 4, 8–11 cm; Section 7, 35–42 cm; CC, 5–15 cm.

SMEAR SLIDE SUMMARY (%):

	1, 79 D	2, 60 M	3, 60 D	4, 73 D
TEXTURE:				
Sand	5	20	10	10
Silt	51	38	30	33
Clay	44	42	60	57
COMPOSITION:				
Quartz	25	50	30	30
Feldspar	3	5	5	5
Clay	44	42	62	57
Volcanic glass	5	—	—	—
Calcite/dolomite	2	1	—	—
Accessory minerals	—	—	3	2
Glauconite	—	2	—	—
Diatoms	5	—	—	1
Radiolarians	1	—	—	—
Sponge spicules	15	—	—	5

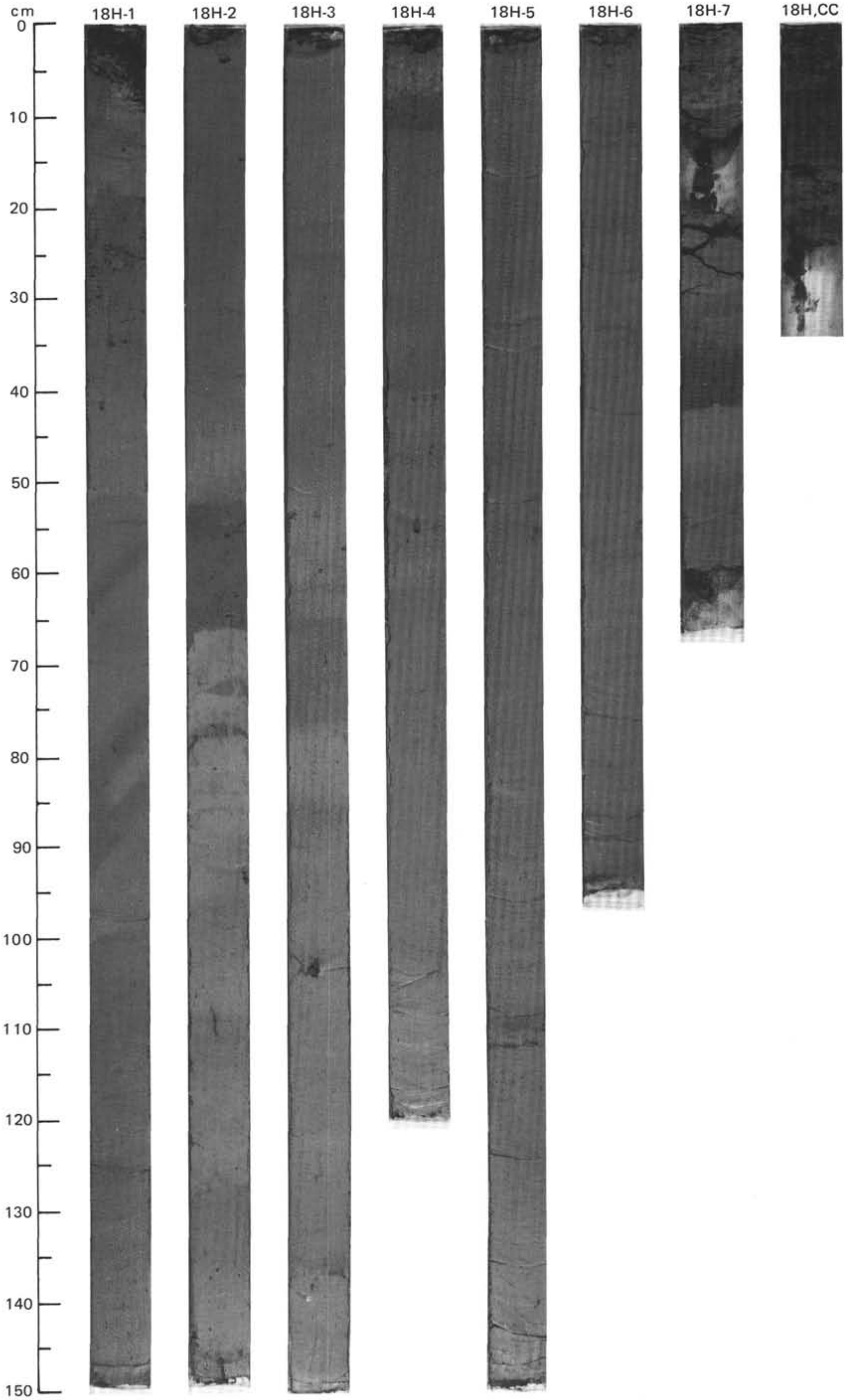
cm
0
10
20
30
40
50
60
70
80
90
100
110
120
130
140
150
18H-1
18H-2
18H-3
18H-4
18H-5
18H-6
18H-7
18H,CC

SITE 644 HOLE A CORE 19H CORED INTERVAL 1394.5-1404.5 mbsl; 168.2-177.7 mbsf

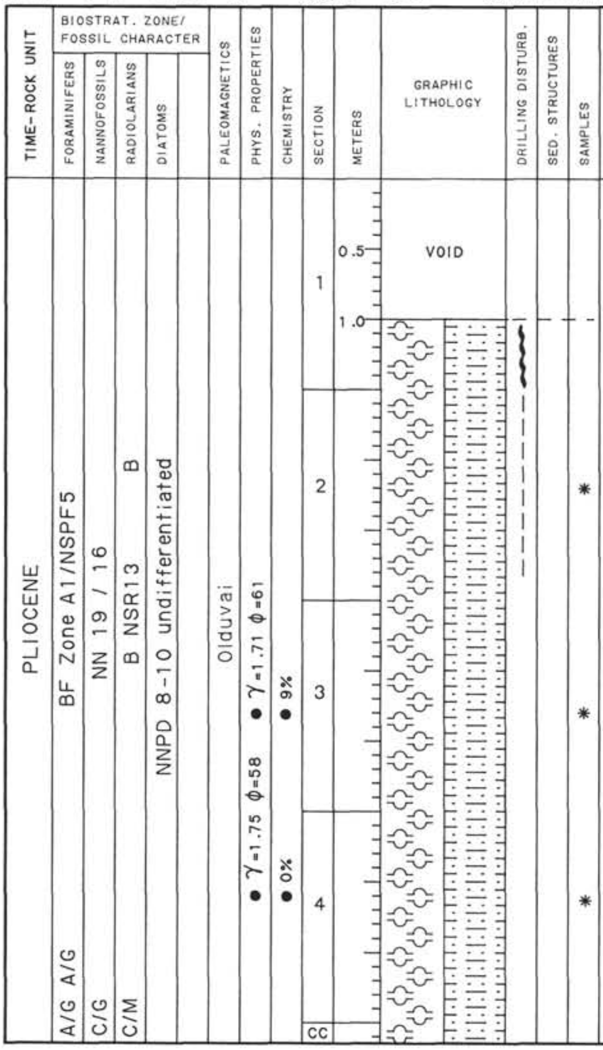

LITHOLOGIC DESCRIPTION

NANNOFOSSIL-SILICEOUS MUD

Section 1, 0–100 cm, is a void. Section 1, 100 cm, to Section 3, 30 cm, is highly disturbed. Remainder of the core is undisturbed.

Major lithologies:
a. Mud, dark greenish gray (5GY 4/1), mottled. Section 2.
b. Nannofossil-siliceous mud, dark greenish gray (5GY 4/1), slightly mottled. Section 3 to CC.

SMEAR SLIDE SUMMARY (%):

	2, 63 D	3, 80 D	4, 63 D
TEXTURE:			
Sand	1	5	7
Silt	21	35	45
Clay	78	60	48
COMPOSITION:			
Quartz	10	20	30
Feldspar	2	—	3
Clay	78	55	43
Volcanic glass	5	—	2
Calcite/dolomite	2	5	5
Accessory minerals	1	—	1
Glauconite	—	5	—
Foraminifers	—	—	1
Nannofossils	—	5	5
Diatoms	—	5	—
Sponge spicules	—	5	7

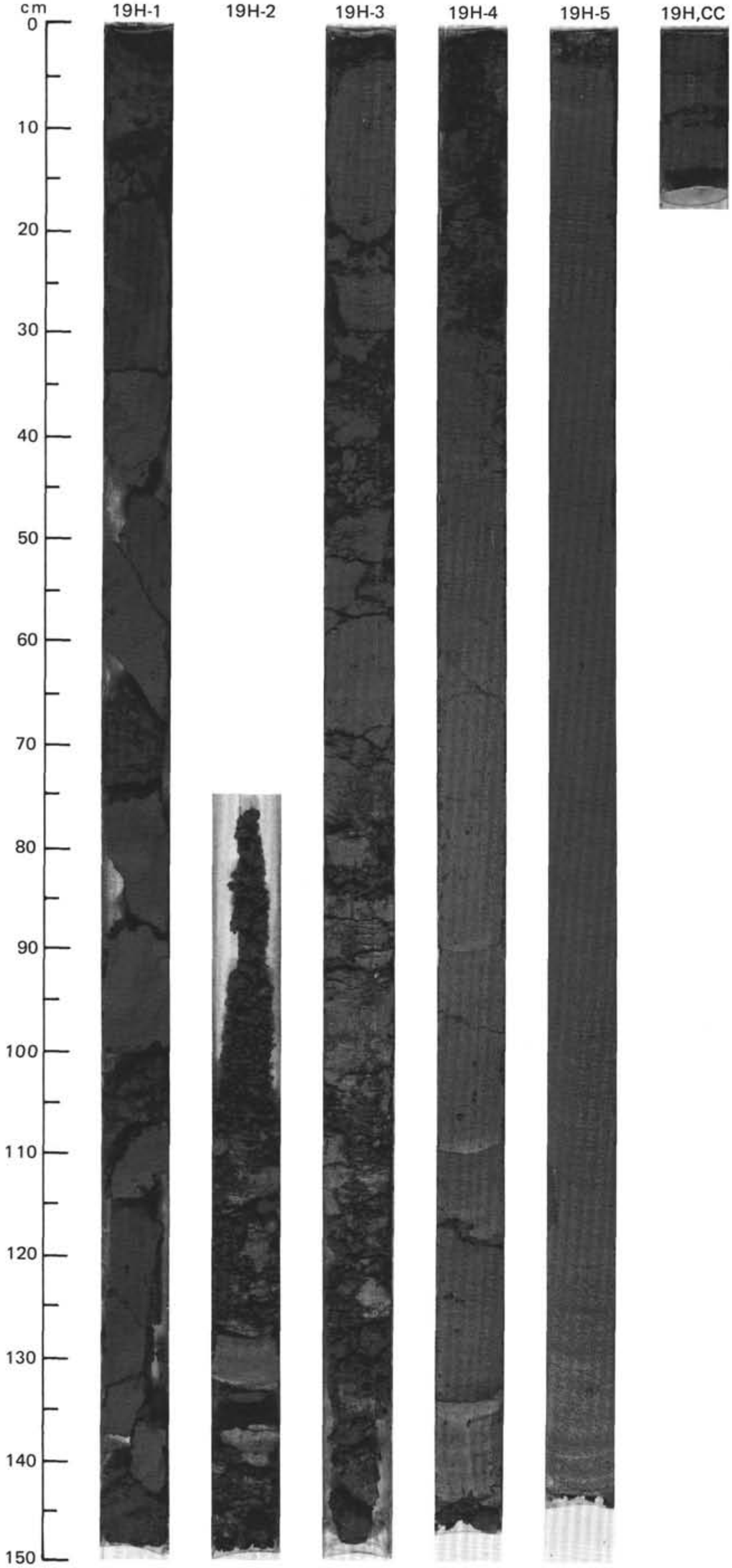
cm
0
10
20
30
40
50
60
70
80
90
100
110
120
130
140
150
19H-1
19H-2
19H-3
19H-4
19H-5
19H,CC

SITE 644 HOLE A CORE 20H CORED INTERVAL 1404.0-1411.1 mbsl; 177.7-184.8 mbsf

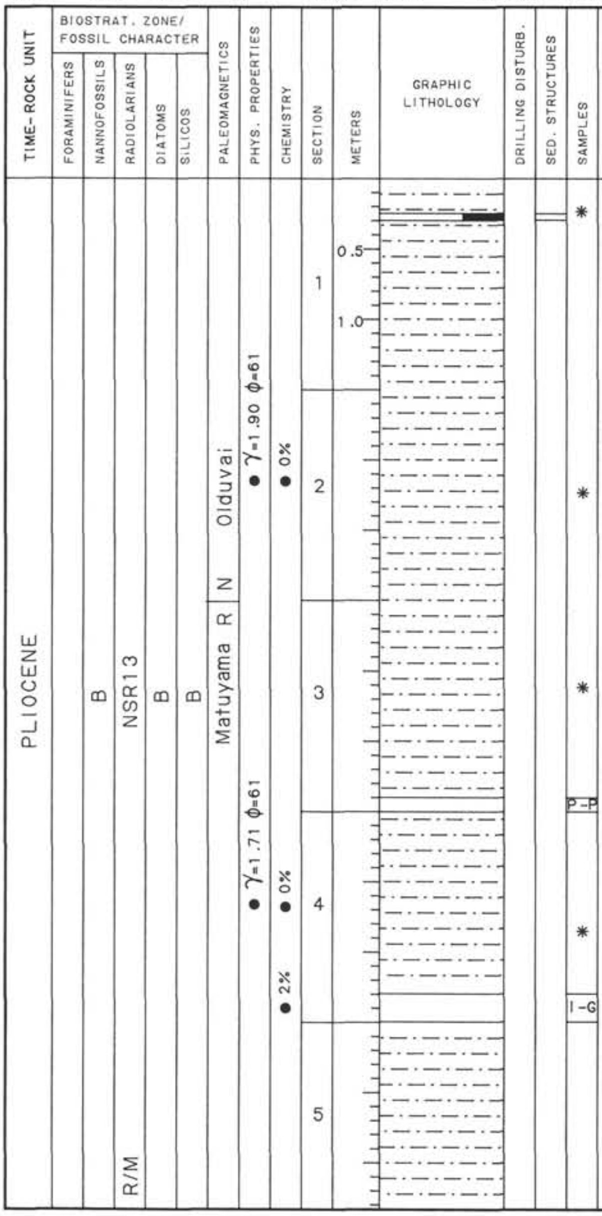

LITHOLOGIC DESCRIPTION

GLACIAL SANDY MUD

Entire core is undisturbed.

Major lithology: Sandy mud, dark greenish gray (5GY 4/1), mottled and bioturbated. Section 1, 0–27 cm; Section 1, 30 cm, to CC.

Minor lithology: Sandy mud, very dark gray (5Y 3/1), with scattered dropstones. Section 1, 27–30 cm.

SMEAR SLIDE SUMMARY (%):

	1, 28 M	2, 71 D	3, 54 D	4, 83 D
TEXTURE:				
Sand	20	5	20	15
Silt	37	62	53	46
Clay	43	33	27	39
COMPOSITION:				
Quartz	40	40	30	30
Feldspar	5	5	10	2
Clay	43	33	27	39
Volcanic glass	2	—	3	2
Calcite/dolomite	5	10	5	5
Accessory minerals	5	—	3	2
Pyrite	—	—	20	—
Diatoms	—	5	—	5
Radiolarians	—	—	—	5
Sponge spicules	—	5	2	10

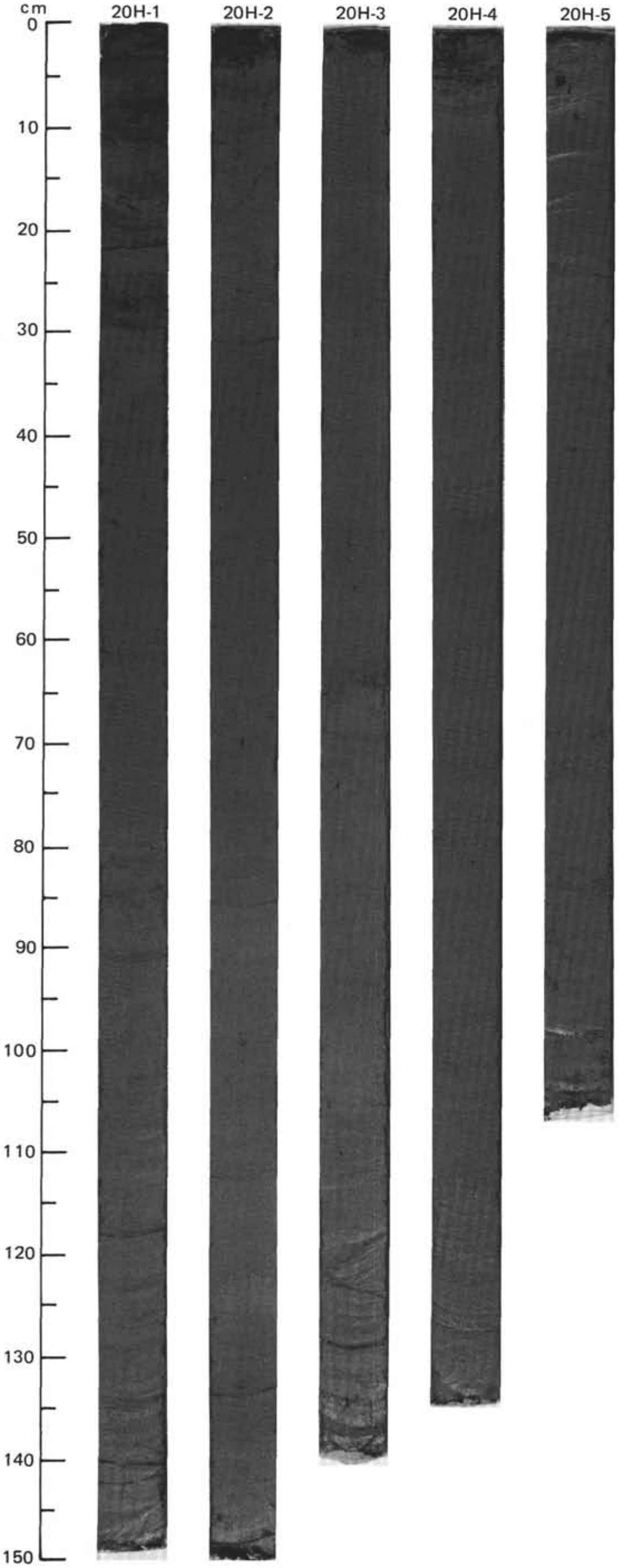
cm
0
10
20
30
40
50
60
70
80
90
100
110
120
130
140
150
20H-1
20H-2
20H-3
20H-4
20H-5

SITE 644 HOLE A CORE 21H CORED INTERVAL 1411.1-1413.1 mbsl;184.8-186.8 mbsf

TIME-ROCK UNIT	BIOSTRAT. ZONE/ FOSSIL CHARACTER: FORAMINIFERS	NANNOFOSSILS	RADIOLARIANS	DIATOMS	SILICOS	PALEOMAGNETICS	PHYS. PROPERTIES	CHEMISTRY	SECTION	METERS	SAMPLES
PLIOCENE	BF Zone A1/NSPF5 F/M	? C/G F/P	NSR13 C/M	NNPD 8-10 undifferentiated A/M	*Distephanus speculum* Zone F/M	Matuyama	γ=1.68 φ=62	● 0%	1 2 CC	0.5 1.0	* *

GRAPHIC LITHOLOGY · DRILLING DISTURB. · SED. STRUCTURES

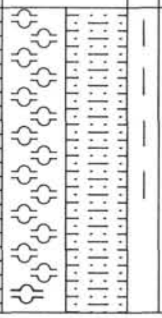

LITHOLOGIC DESCRIPTION

SILICEOUS MUD

Section 1 is moderately disturbed. The remainder of the core is undisturbed.

Major lithology: Siliceous mud, dark greenish gray (5GY 4/1) and mottled.

SMEAR SLIDE SUMMARY (%):

	1, 8 D	2, 8 D
TEXTURE:		
Sand	10	7
Silt	29	47
Clay	61	46
COMPOSITION:		
Quartz	15	30
Feldspar	—	5
Clay	51	46
Volcanic glass	1	2
Calcite/dolomite	—	1
Accessory minerals	—	1
Foraminifers	5	—
Nannofossils	10	—
Diatoms	3	5
Radiolarians	5	—
Sponge spicules	10	10

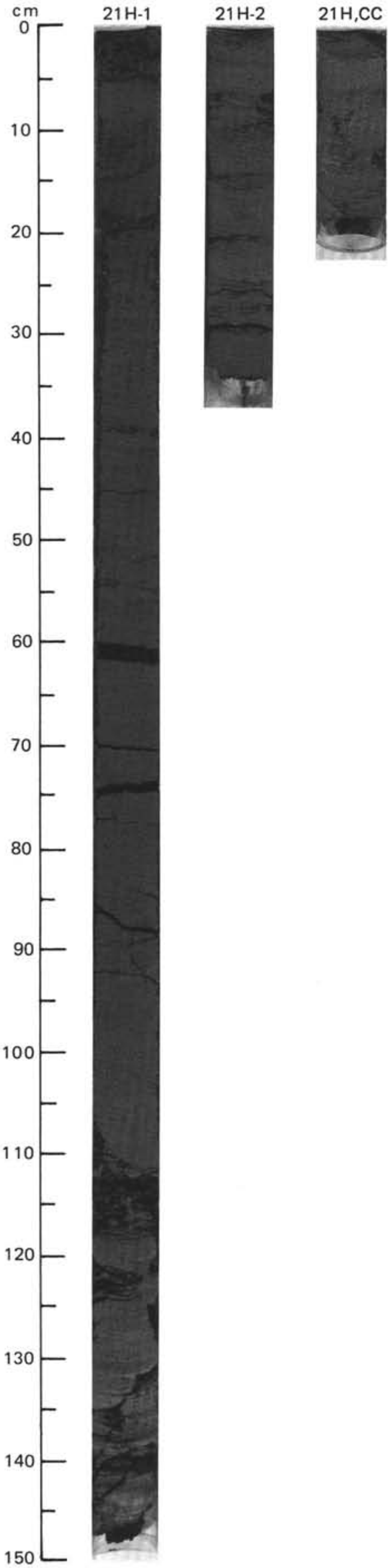
cm
0
10
20
30
40
50
60
70
80
90
100
110
120
130
140
150
21H-1
21H-2
21H,CC

SITE 644 HOLE A CORE 22H CORED INTERVAL 1413.1-1420.4 mbsl; 186.8-194.1 mbsf

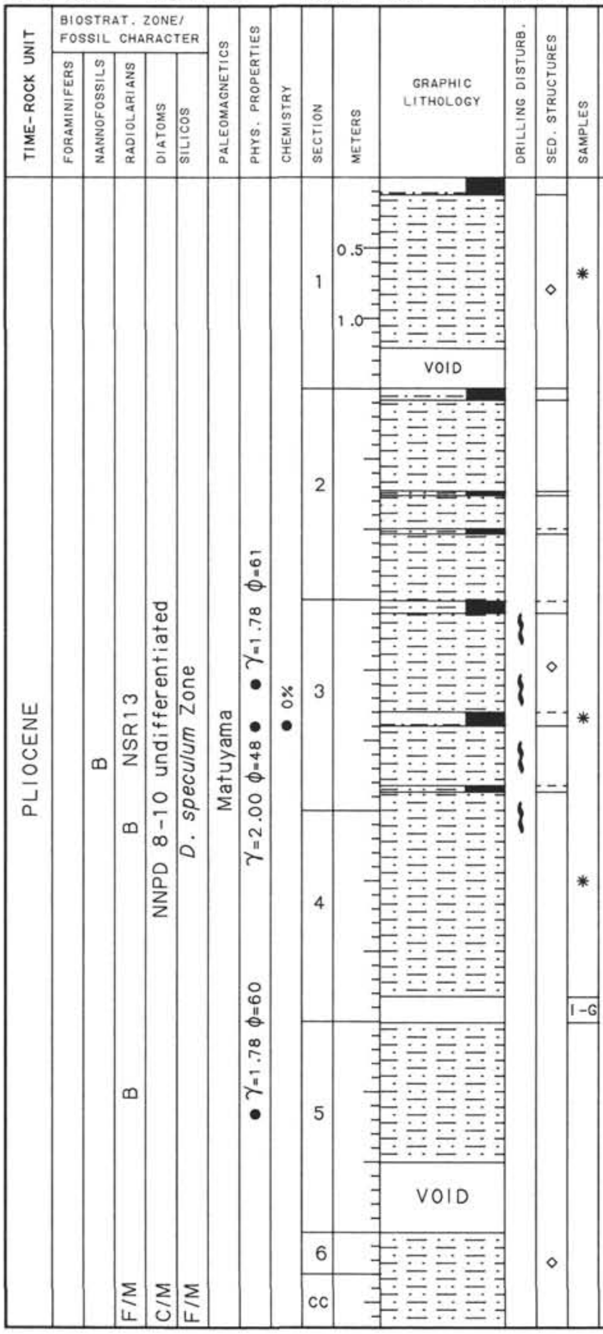

LITHOLOGIC DESCRIPTION

MUD AND SANDY MUD

Section 3 is moderately to highly disturbed. The remainder of the core is undisturbed.

Major lithologies:
a. Mud and sandy mud, dark greenish gray (5GY 4/1), with minor to common mottles and pyritized burrows, scattered dropstones. Section 1, 0–5 and 12–124 cm; Section 2, 8–76 and 77–101 cm; Section 3, 10–83 and 89–133 cm; Section 3, 136 cm, to CC.
b. Sandy mud, very dark gray (5Y 3/1), with common to abundant dropstones. Section 1, 5–12 cm; Section 2, 0–8, 76–77, and 101–104 cm; Section 3, 0–10, 83–89, and 133–136 cm.

Large dropstones at Section 1, 80 cm; Section 3, 49–51 cm; Section 6, 25–28 cm.

SMEAR SLIDE SUMMARY (%):

	1, 70 D	8, 84 M	4, 47 D
TEXTURE:			
Sand	7	10	20
Silt	20	40	43
Clay	73	50	37
COMPOSITION:			
Quartz	20	30	50
Feldspar	—	5	10
Clay	73	50	37
Calcite/dolomite	5	—	—
Accessory minerals	—	—	3
Glauconite	1	—	—
Pyrite	—	15	—
Sponge spicules	1	—	—

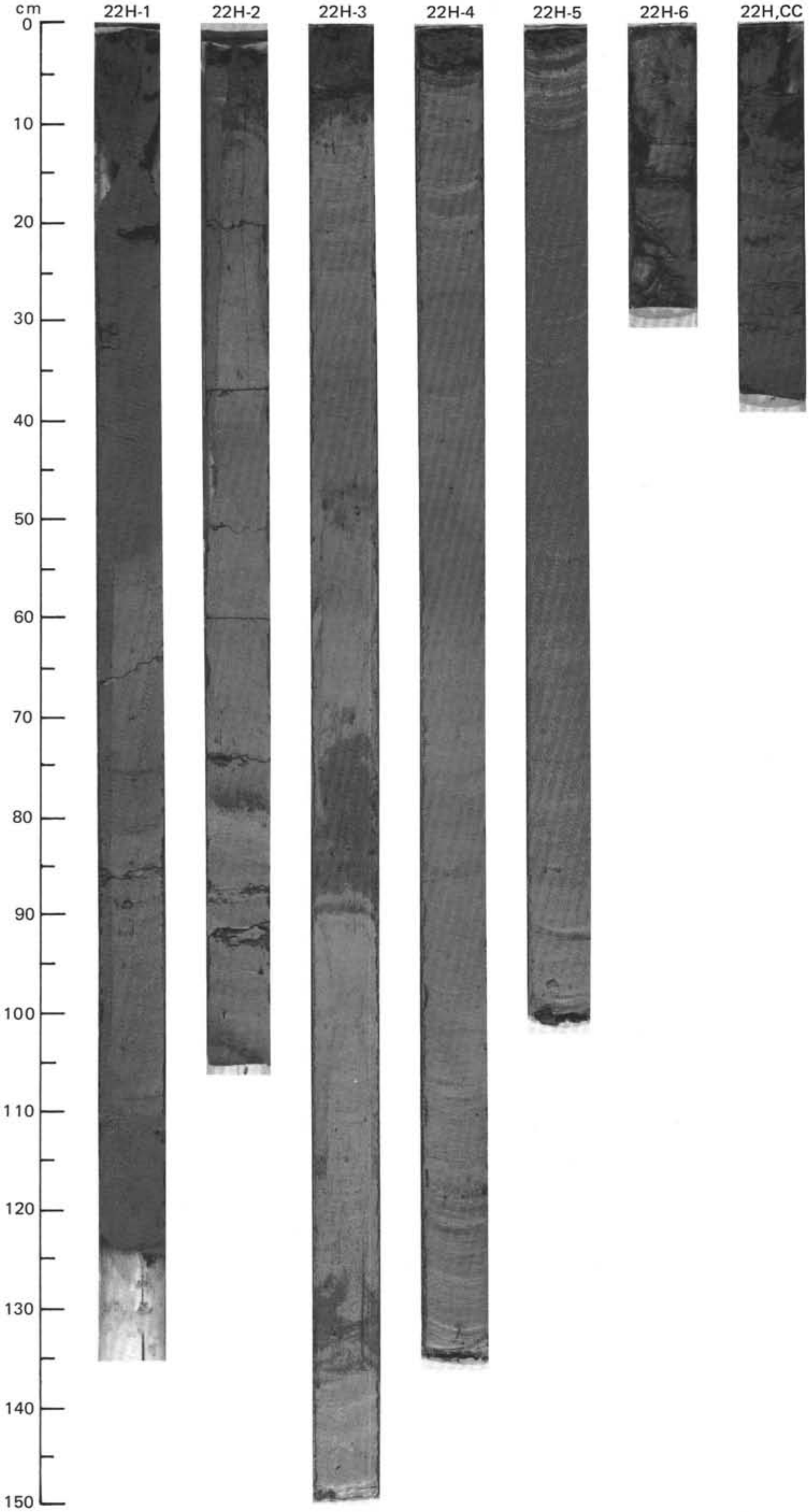
cm
0
10
20
30
40
50
60
70
80
90
100
110
120
130
140
150
22H-1
22H-2
22H-3
22H-4
22H-5
22H-6
22H,CC

SITE 644 HOLE A CORE 23H CORED INTERVAL 1420.4-1427.4 mbsl; 194.1-201.1 mbsf

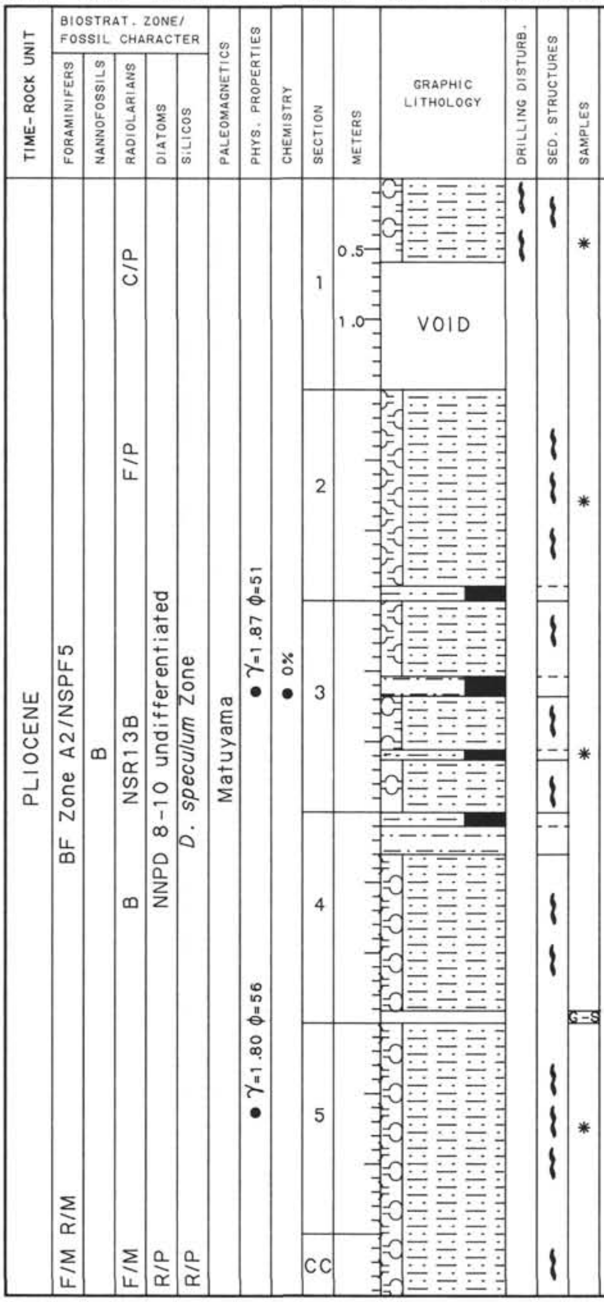

LITHOLOGIC DESCRIPTION

SILICEOUS/NANNOFOSSIL-SILICEOUS MUD AND SANDY MUD

Section 1 is moderately to highly disturbed. Remainder of the core is undisturbed.

Major lithologies:
a. Siliceous mud and nannofossil siliceous mud, dark greenish gray (5GY 4/1), with minor to abundant pyritized burrows and rare to common cm-scale mottling.
b. Sandy mud, very dark gray (5Y 3/1), with minor to common dropstones.

SMEAR SLIDE SUMMARY (%):

	1, 46 D	2, 76 D	3, 108 D	5, 75 D
TEXTURE:				
Sand	7	5	40	5
Silt	42	33	30	55
Clay	51	62	30	40
COMPOSITION:				
Quartz	15	25	65	30
Feldspar	2	5	2	—
Mica	—	—	1	—
Clay	48	62	30	40
Volcanic glass	1	1	—	—
Calcite/dolomite	10	—	—	10
Accessory minerals	1	2	5	1
Glauconite	—	—	1	—
Pyrite	—	—	—	1
Nannofossils	5	—	—	5
Diatoms	5	2	—	2
Radiolarians	3	—	—	1
Sponge spicules	10	3	1	10

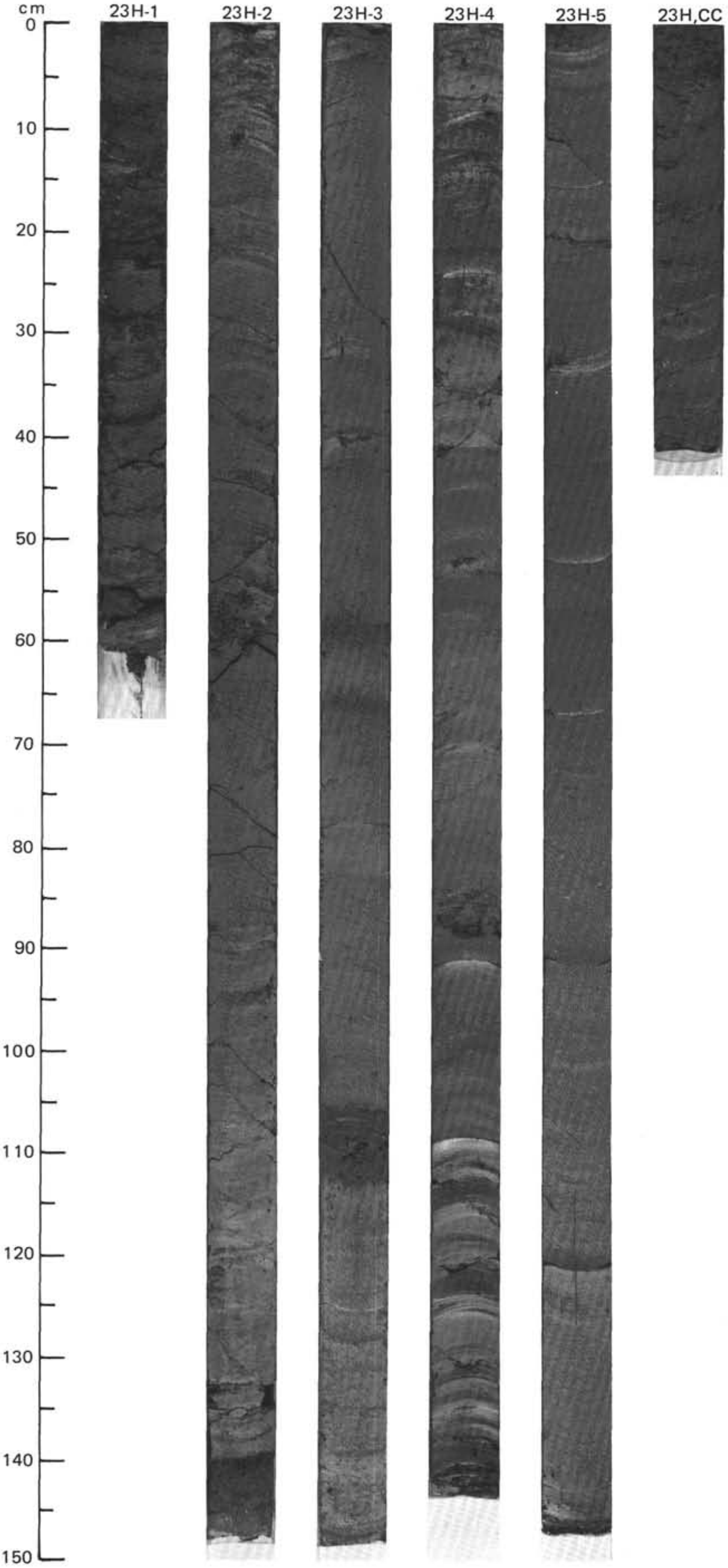
cm
0
10
20
30
40
50
60
70
80
90
100
110
120
130
140
150
23H-1
23H-2
23H-3
23H-4
23H-5
23H,CC

SITE 644 HOLE A CORE 24H CORED INTERVAL 1427.4-1432.3 mbsl; 201.1-206 mbsf

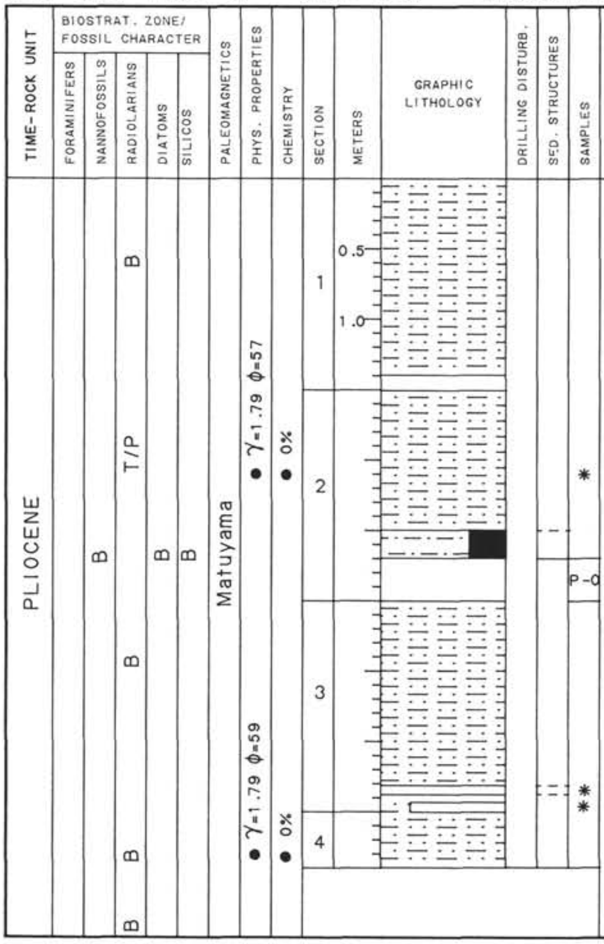

LITHOLOGIC DESCRIPTION

MUD AND SANDY MUD

Section 1, 0–60 cm, is slightly disturbed. Remainder of the core is undisturbed.

Major lithologies:
a. Mud, dark greenish gray (5GY 4/1), with common pyritized burrows and mottling. Section 1 to Section 22, 101 cm; Section 3 to Section 4.
b. Sandy mud, very dark gray (5Y 3/1), with dropstones and sandy patches common. Section 1, 101–120 cm.

Minor lithologies:
a. Nannofossil ooze, olive gray (5Y 4/2) and bioturbated. Section 3, 133–137 cm.
b. Volcanic ash, slightly disseminated and dark greenish gray (5GY 4/1). Section 3, 148–150 cm.

SMEAR SLIDE SUMMARY (%):

	2, 60 D	3, 135 M	3, 149 M
TEXTURE:			
Sand	5	—	60
Silt	50	4	30
Clay	45	96	10
COMPOSITION:			
Quartz	40	—	—
Mica	1	—	—
Clay	35	20	12
Volcanic glass	—	—	85
Calcite/dolomite	10	—	—
Accessory minerals	1	—	1
Pyrite	1	1	—
Foraminifers	1	—	—
Nannofossils	5	77	—
Diatoms	1	—	1
Sponge spicules	5	2	1

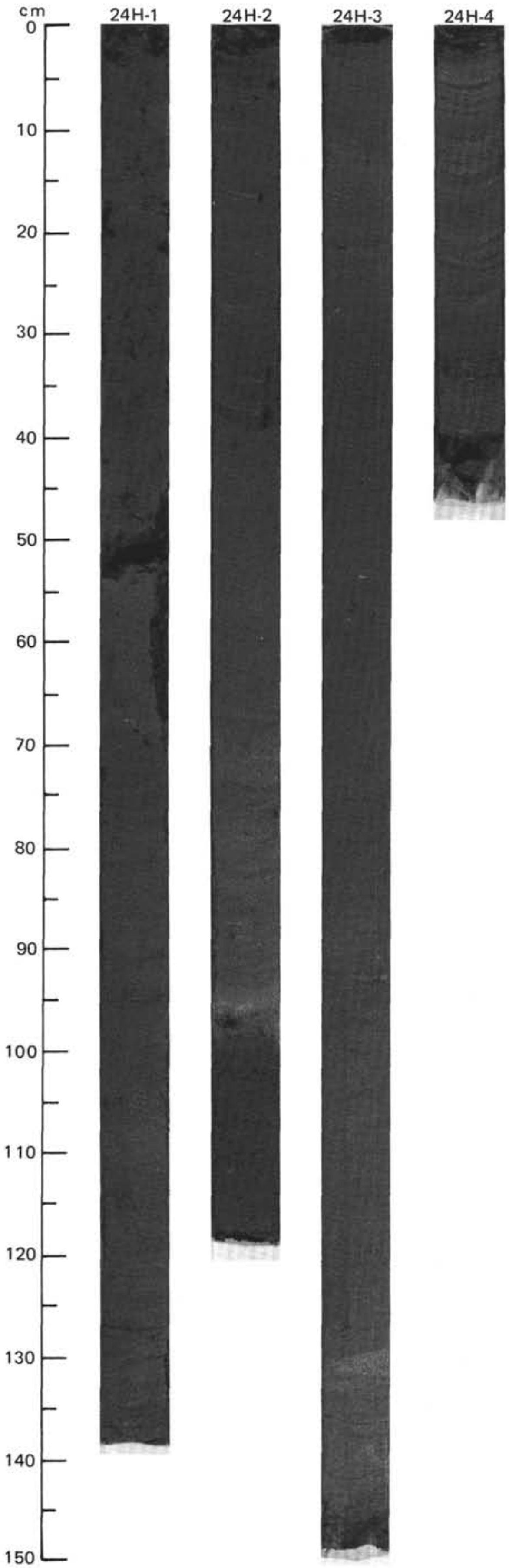
cm
0
10
20
30
40
50
60
70
80
90
100
110
120
130
140
150
24H-1
24H-2
24H-3
24H-4

SITE 644 HOLE A CORE 25H CORED INTERVAL 1432.3-1436.8 mbsl; 206-210.5 mbsf

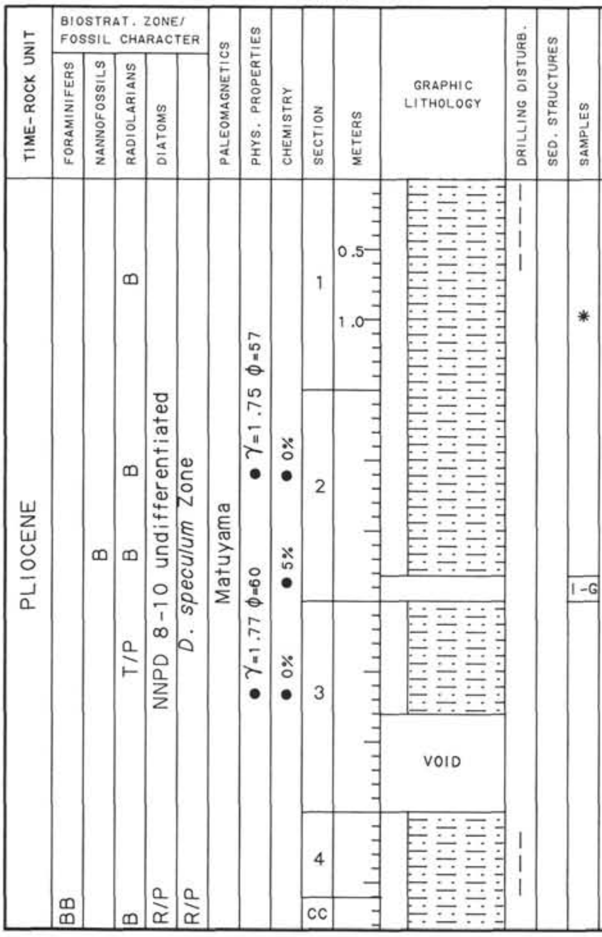

LITHOLOGIC DESCRIPTION

MUD AND SILICEOUS MUD

Section 1, 0–66 cm, and Section 4, 17–60 cm, are moderately disturbed. Remainder of the core is undisturbed.

Major lithology: Mud and siliceous mud, dark greenish gray (5GY 4/1), with common to abundant pyritized burrows.

SMEAR SLIDE SUMMARY (%):

	1, 100 D	3, 50 D
TEXTURE:		
Sand	5	—
Silt	45	55
Clay	50	45
COMPOSITION:		
Quartz	30	40
Clay	50	40
Volcanic glass	3	—
Calcite/dolomite	—	5
Nannofossils	—	3
Diatoms	1	2
Radiolarians	1	—
Sponge spicules	15	10

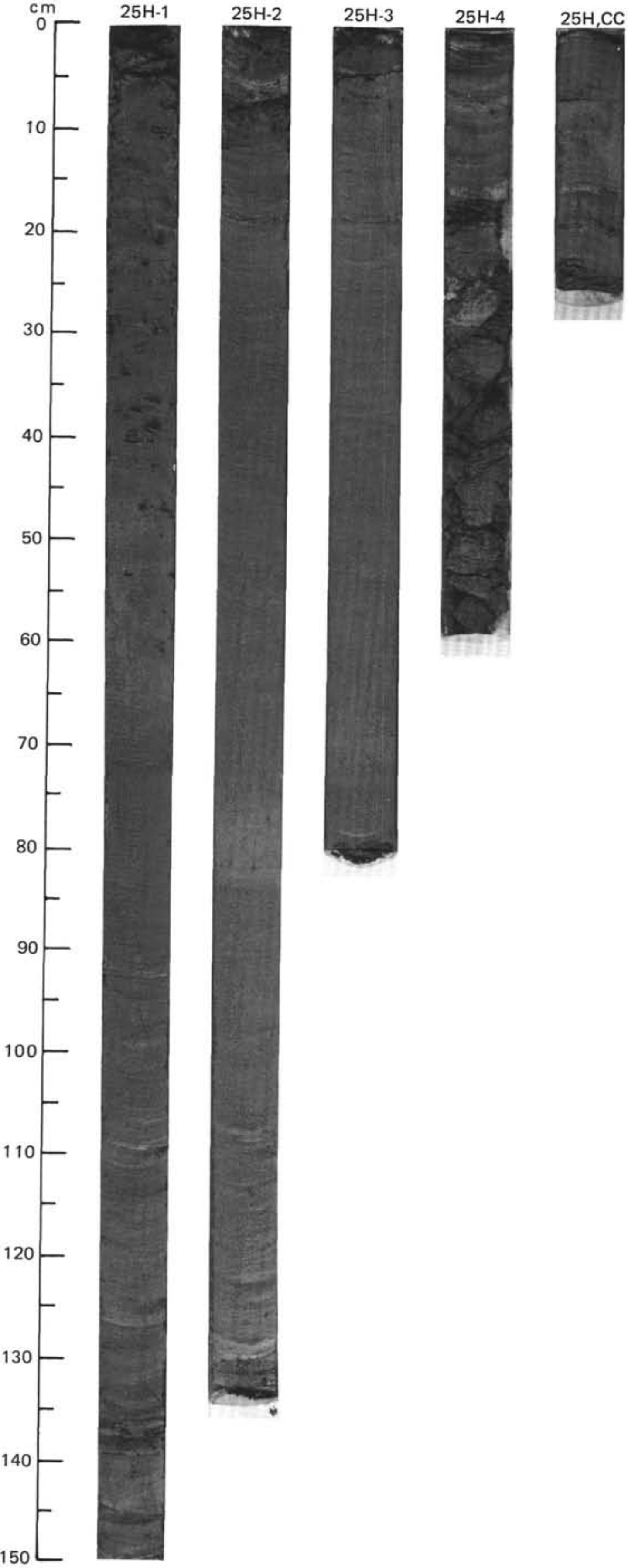
cm
0
10
20
30
40
50
60
70
80
90
100
110
120
130
140
150
25H-1
25H-2
25H-3
25H-4
25H,CC

SITE 644 HOLE A CORE 26H CORED INTERVAL 1436.8-1440.6 mbsl; 210.5-214.3 mbsf

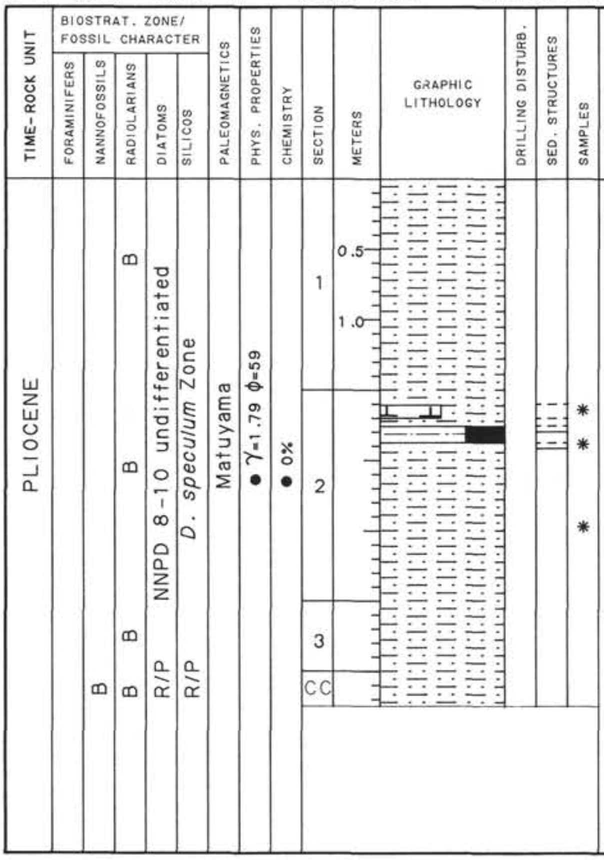

LITHOLOGIC DESCRIPTION

MUD

Entire core is undisturbed.

Major lithology: Mud, dark greenish gray (5GY 4/1), with pyritized burrows common, minor mottling and faint color banding.

Minor lithologies:
a. Sandy mud, very dark gray (5Y 3/1), with minor small dropstones. Section 2, 27–29 and 38–42 cm.
b. Nannofossil mud, olive gray (5Y 4/2), moderately mottled. Section 2, 12–20 cm.

SMEAR SLIDE SUMMARY (%):

	2, 15 M	2, 40 M	2, 90 D
TEXTURE:			
Sand	1	25	10
Silt	34	40	50
Clay	65	35	40
COMPOSITION:			
Quartz	—	60	50
Feldspar	—	1	—
Clay	15	35	35
Calcite/dolomite	30	—	5
Accessory minerals	—	3	2
Pyrite	—	1	—
Foraminifers	3	—	1
Nannofossils	50	—	1
Diatoms	—	—	1
Sponge spicules	2	—	5

SITE 644 HOLE A CORE 27H CORED INTERVAL 1440.6-1442.4 mbsl; 214.3-216.1 mbsf

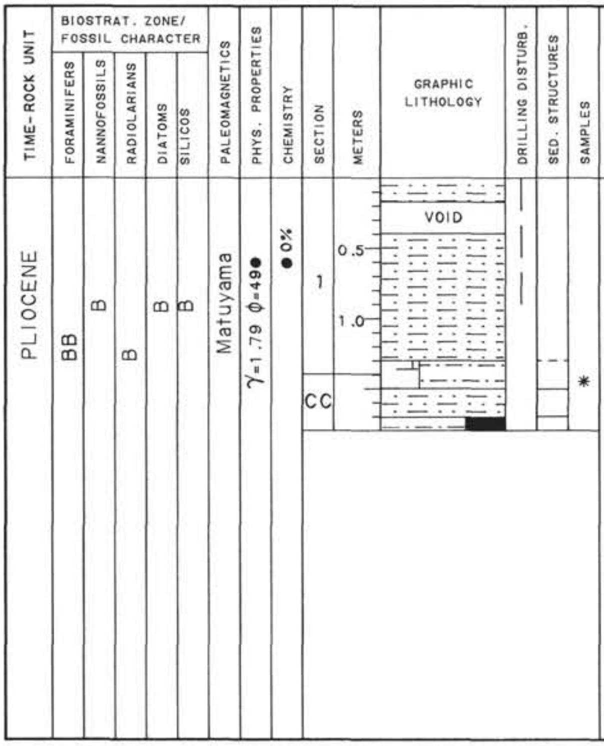

LITHOLOGIC DESCRIPTION

MUD AND SANDY MUD AND SANDY NANNOFOSSIL MUD

Section 1, 0–69 cm, is moderately disturbed. Remainder of the core is undisturbed.

Major lithologies:
a. Mud, dark greenish gray (5GY 4/1), with pyritized burrows common, and scattered pyrite concretions. Section 1, 0–18 and 40–131 cm; CC, 8–34 cm.
b. Sandy mud and sandy nannofossil mud, very dark gray (5Y 3/1). Section 1, 131 cm, to CC, 8 cm; CC, 34–38 cm.

SMEAR SLIDE SUMMARY (%):

	CC, 6 M
TEXTURE:	
Sand	30
Silt	10
Clay	60
COMPOSITION:	
Quartz	30
Clay	35
Calcite/dolomite	10
Nannofossils	25

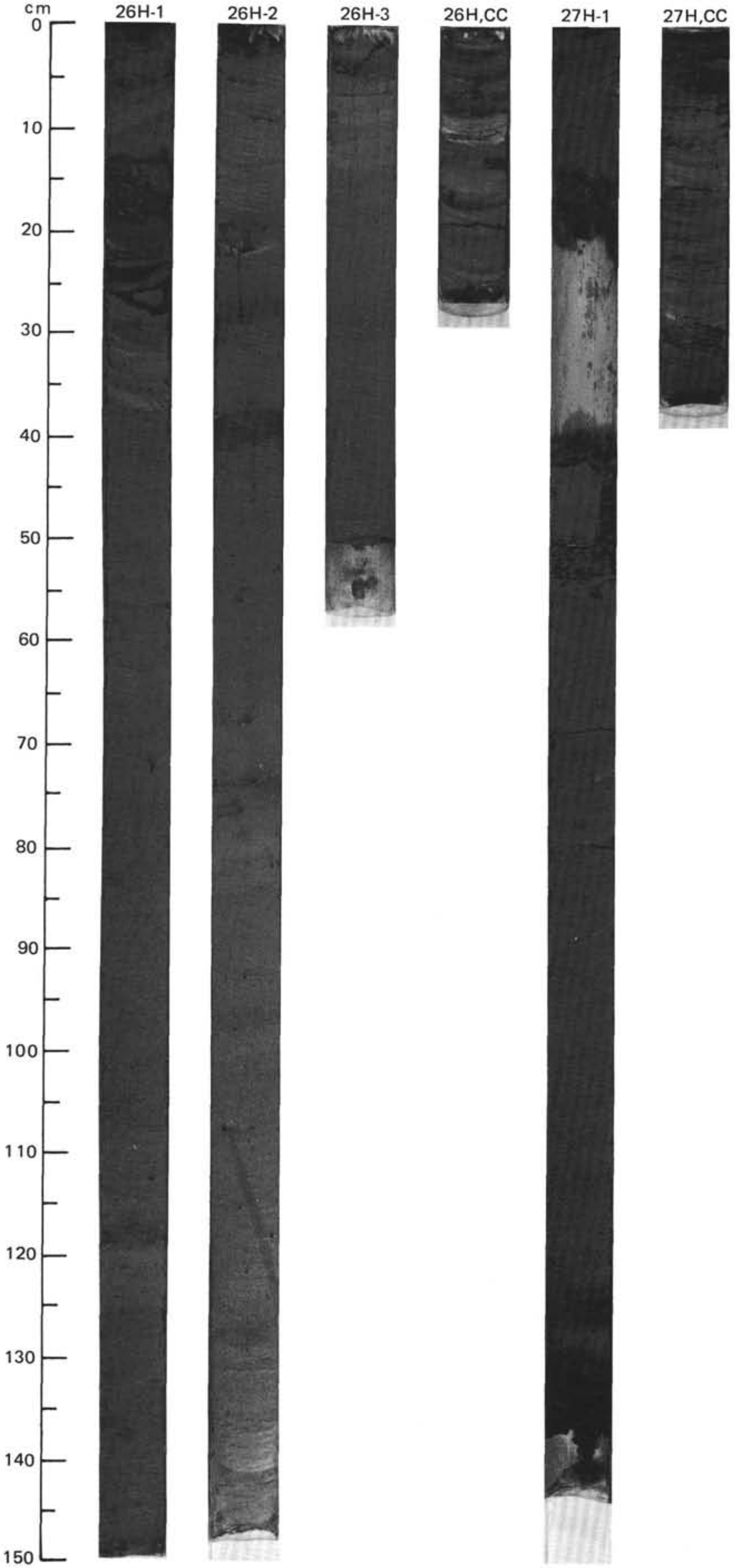
cm
0
10
20
30
40
50
60
70
80
90
100
110
120
130
140
150
26H-1
26H-2
26H-3
26H,CC
27H-1
27H,CC

SITE 644 HOLE A CORE 28H CORED INTERVAL 1442.4-1447.4 mbsl; 216.1-221.1 mbsf

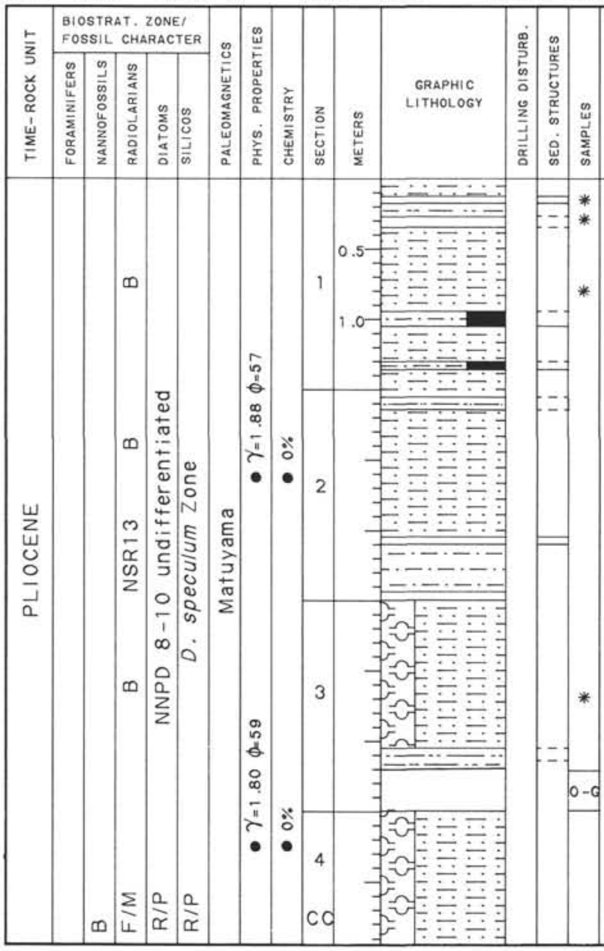

LITHOLOGIC DESCRIPTION

MUD AND SILICEOUS MUD

Entire core is undisturbed.

Major lithology: Mud and siliceous mud, dark greenish gray (5GY 4/1), with mottling, pyritized burrows, and pyrite concretions minor to common in abundance.

Minor lithologies:
a. Sandy mud, very dark gray (5Y 3/1), with minor dropstones. Section 1, 15–16, 96–102, and 132–133 cm.
b. Nannofossil mud, greenish gray (5GY 5/1), intensely bioturbated and mottled. Section 1, 29–34 cm; Section 2, 8–14 cm; Section 3, 107–112 cm.
c. Sandy limestone, "drilling biscuit" containing 15%–20% well-rounded, fine to medium sand-sized clastic grains in a micritic matrix. Section 2, 106–110 cm.

SMEAR SLIDE SUMMARY (%):

	1, 16 M	1, 32 M	1, 80 D	3, 70 D
TEXTURE:				
Sand	15	—	10	10
Silt	35	10	40	50
Clay	50	90	50	40
COMPOSITION:				
Quartz	25	10	25	35
Feldspar	—	—	1	—
Mica	—	—	1	—
Clay	40	50	45	40
Volcanic glass	—	—	—	3
Calcite/dolomite	25	—	15	3
Accessory minerals	—	—	1	1
Pyrite	—	—	1	1
Foraminifers	—	—	1	—
Nannofossils	10	40	5	—
Diatoms	—	—	—	1
Radiolarians	—	—	—	1
Sponge spicules	—	—	5	15

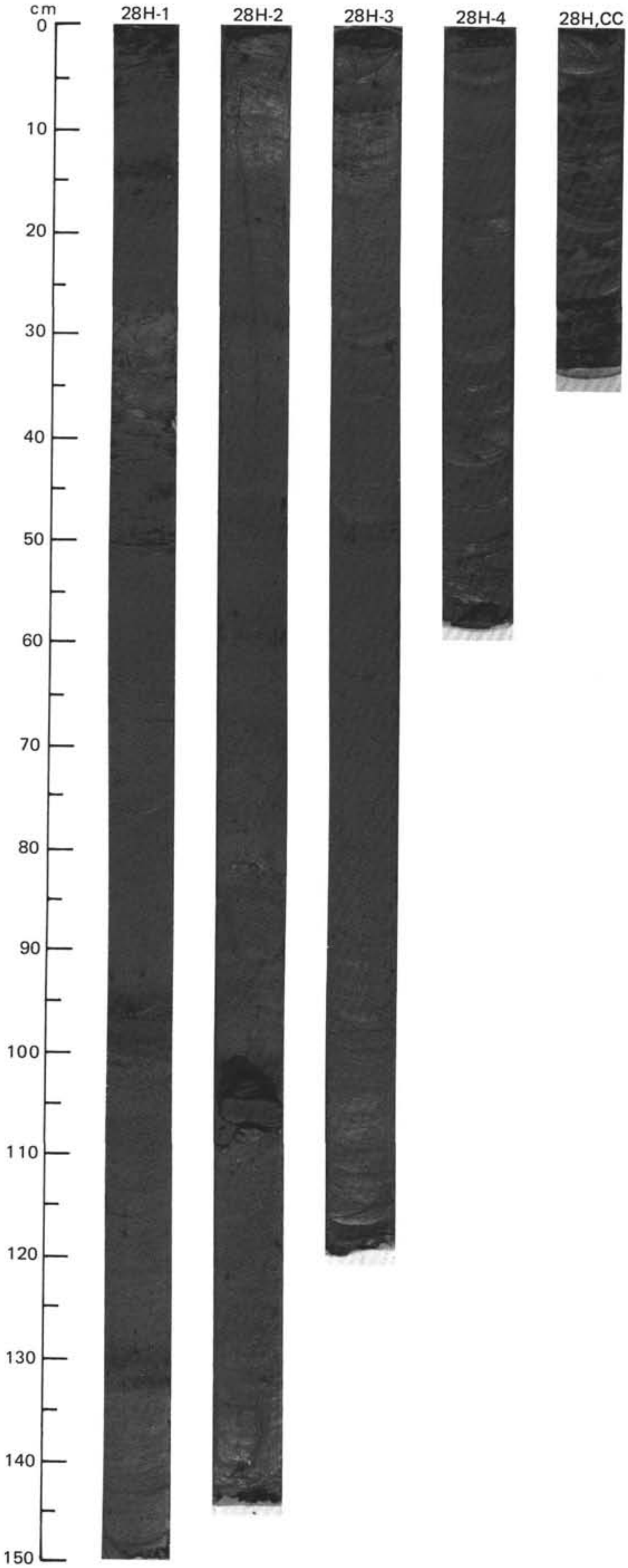
cm
0
10
20
30
40
50
60
70
80
90
100
110
120
130
140
150
28H-1
28H-2
28H-3
28H-4
28H,CC

SITE 644 HOLE A CORE 29H CORED INTERVAL 1447.4-1452.4 mbsl; 221.1-226.1 mbsf

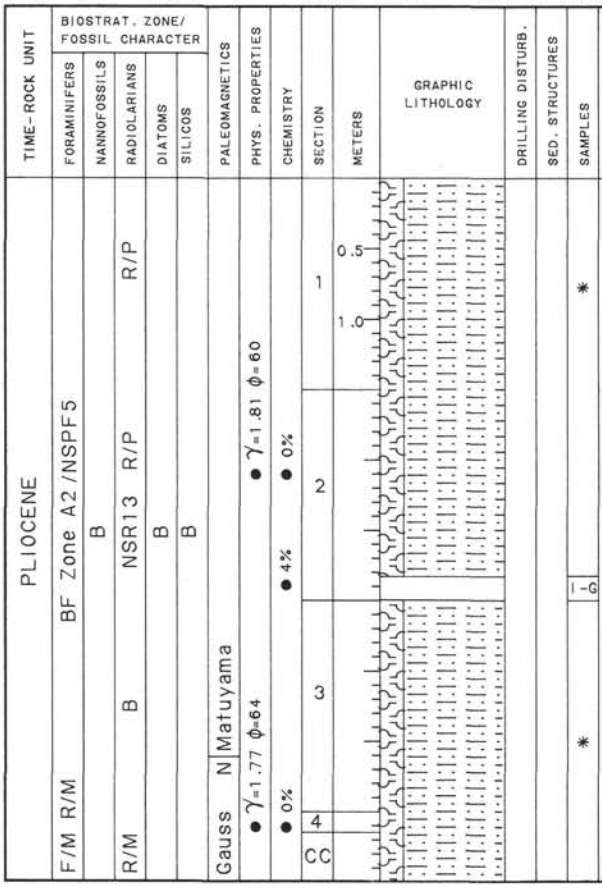

LITHOLOGIC DESCRIPTION

MUD AND SILICEOUS MUD

Entire core is undisturbed.

Major lithology: Mud and siliceous mud, dark greenish gray (5GY 4/1), with minor to common mottling and pyritized burrows.

SMEAR SLIDE SUMMARY (%):

	1, 76 D	3, 100 D
TEXTURE:		
Sand	10	5
Silt	40	50
Clay	50	45
COMPOSITION:		
Quartz	30	40
Feldspar	1	—
Mica	1	—
Clay	40	45
Volcanic glass	3	—
Calcite/dolomite	3	5
Accessory minerals	1	—
Pyrite	1	—
Nannofossils	2	—
Diatoms	2	—
Radiolarians	1	—
Sponge spicules	15	10

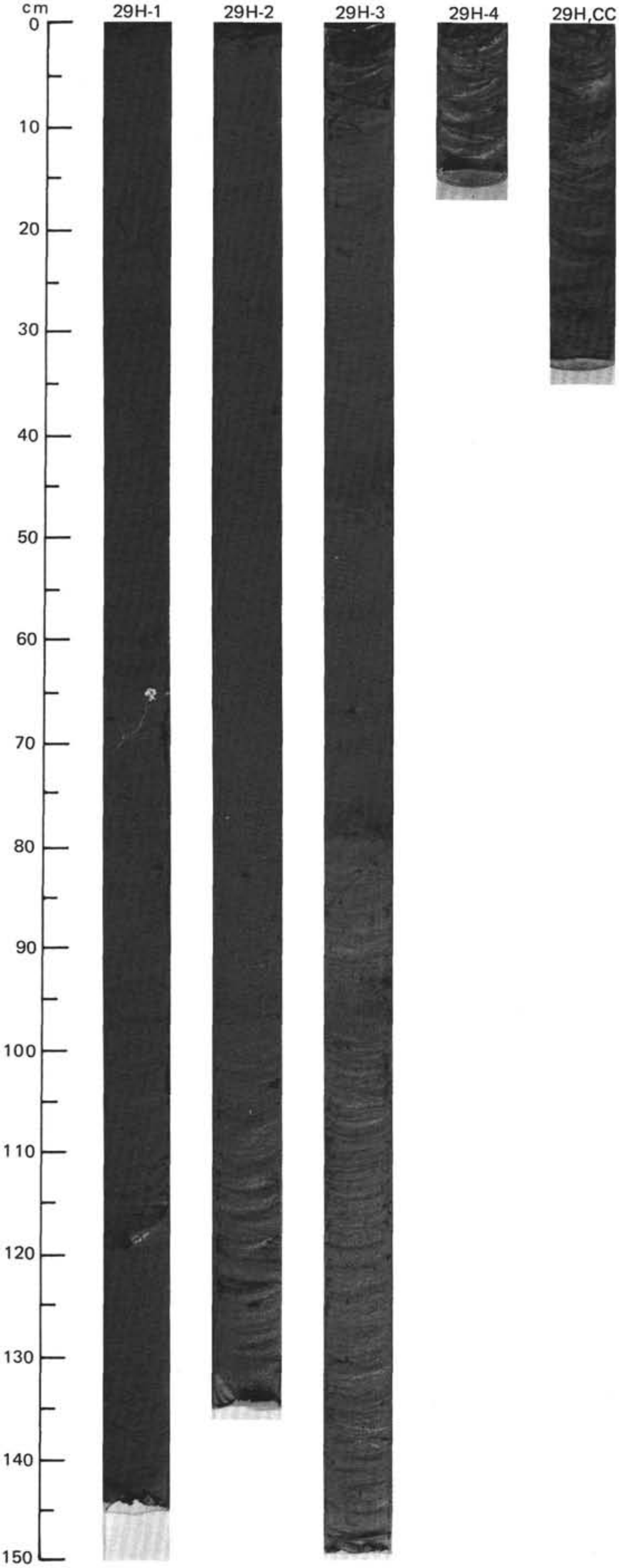
cm
0
10
20
30
40
50
60
70
80
90
100
110
120
130
140
150
29H-1
29H-2
29H-3
29H-4
29H,CC

SITE 644 HOLE A CORE 30H CORED INTERVAL 1452.4-1458.4 mbsl; 226.1-232.1 mbsf

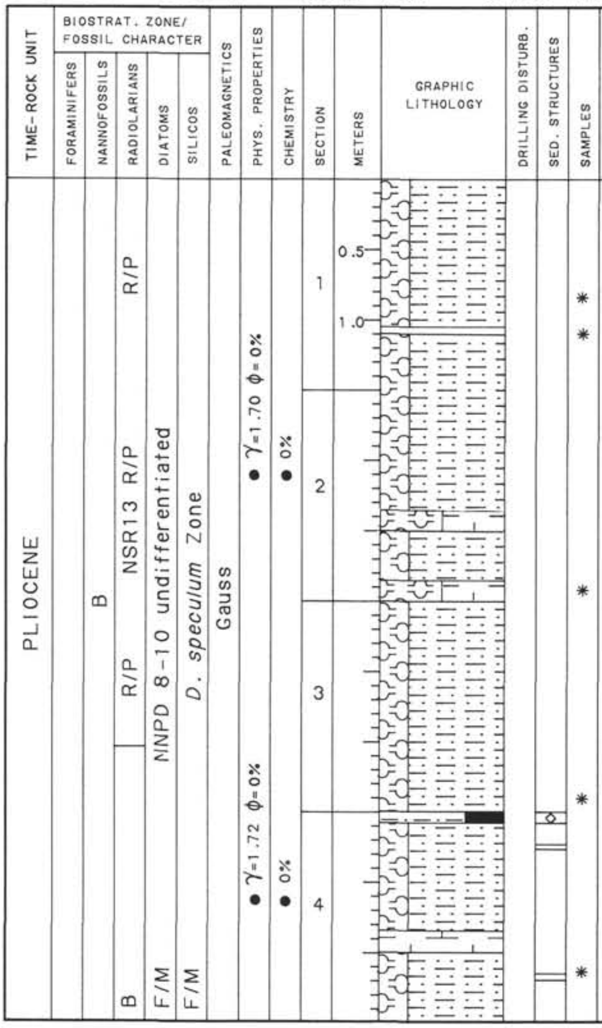

LITHOLOGIC DESCRIPTION

MUD AND SILICEOUS MUD

Entire core is undisturbed.

Major lithology: Mud and siliceous mud, dark greenish gray (5GY 4/1), with common to abundant pyritized burrows, and scattered pyrite concretions.

Minor lithologies:
a. Sandy mud, very dark gray (5Y 3/1), with a pebble-sized dropstone at Section 4, 2 cm. Section 1, 108–110 cm; Section 4, 0–6 and 24–26 cm.
b. Nannofossil ooze, greenish gray (5GY 5/1) to olive gray (5Y 4/2). Moderately to heavily bioturbated and mottled. Section 2, 86–98 cm; Section 4, 86–98 and 114–119 cm.

SMEAR SLIDE SUMMARY (%):

	1, 80 D	1, 111 M	2, 92 M	3, 140 D	4, 114 M
TEXTURE:					
Sand	5	60	5	5	—
Silt	45	10	45	55	—
Clay	50	30	50	40	100
COMPOSITION:					
Quartz	35	60	15	40	—
Clay	45	30	10	40	10
Volcanic glass	5	—	—	2	—
Calcite/dolomite	—	—	—	5	—
Accessory minerals	—	7	—	—	—
Glauconite	—	3	—	—	—
Nannofossils	1	—	40	1	90
Diatoms	3	—	10	1	—
Radiolarians	1	—	—	1	—
Sponge spicules	20	—	25	10	—

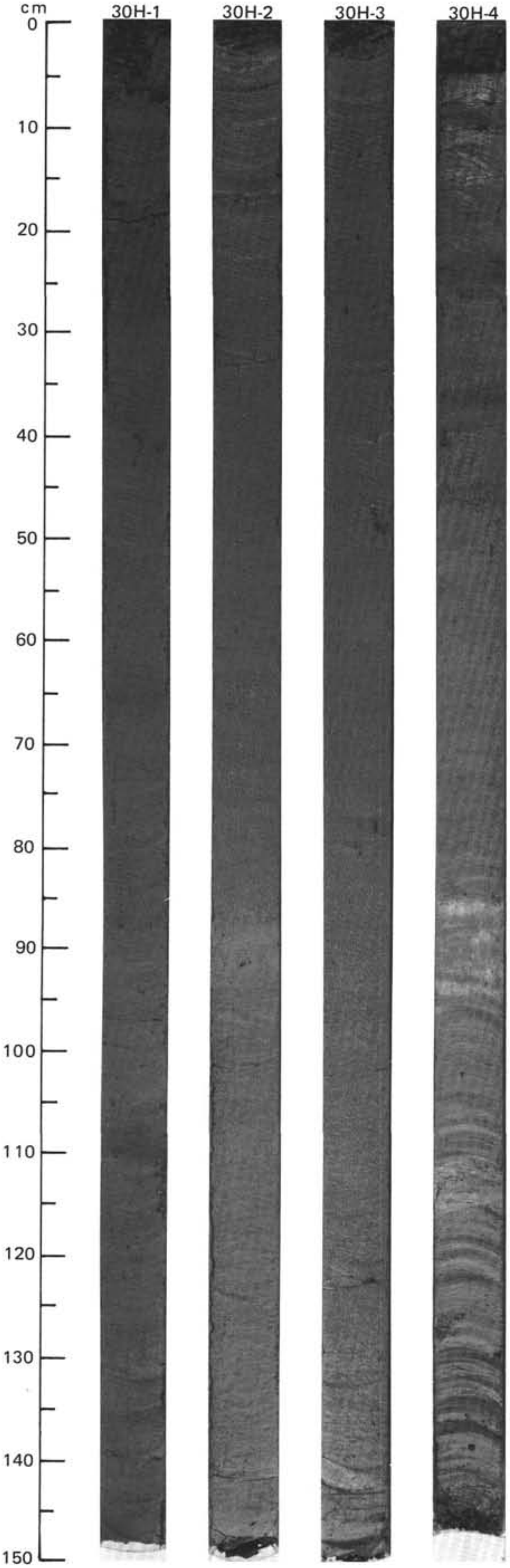
cm
0
10
20
30
40
50
60
70
80
90
100
110
120
130
140
150
30H-1
30H-2
30H-3
30H-4

SITE 644 HOLE A CORE 31H CORED INTERVAL 1458.4-1464.4 mbsl; 232.1-238.1 mbsf

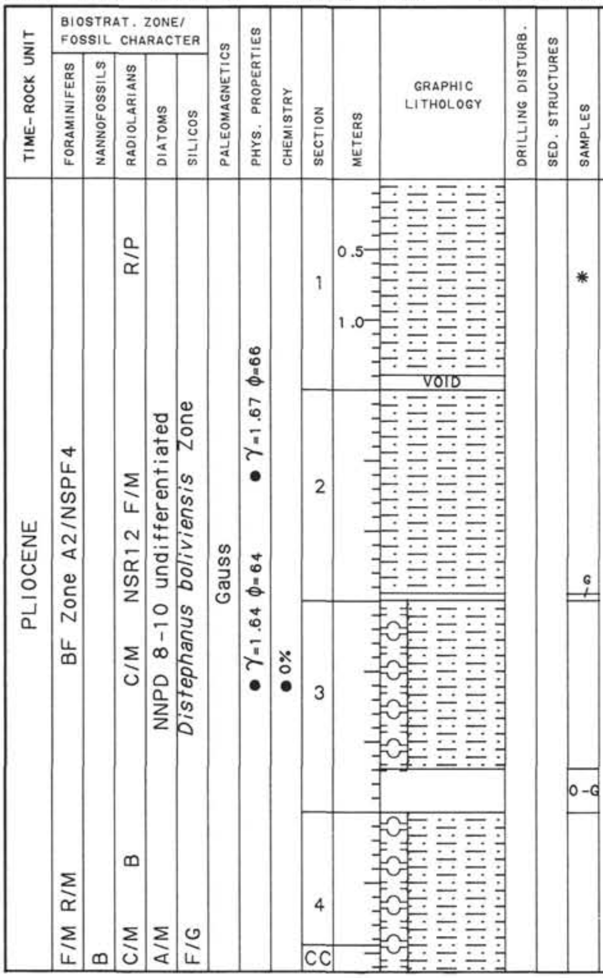

LITHOLOGIC DESCRIPTION

MUD AND SILICEOUS MUD

Section 1, 0–8 and 113–130 cm, are moderately disturbed. Remainder of the core is undisturbed.

Major lithology: Mud and siliceous mud, dark greenish gray (5GY 4/1), with common pyritized burrows, minor mottling and pyrite concretions.

SMEAR SLIDE SUMMARY (%):

	1,70 D	3, 80 D
TEXTURE:		
Sand	—	10
Silt	20	60
Clay	80	30
COMPOSITION:		
Quartz	20	40
Mica	—	1
Clay	80	30
Volcanic glass	—	3
Accessory minerals	—	1
Nannofossils	—	1
Diatoms	—	3
Radiolarians	—	1
Sponge spicules	—	20

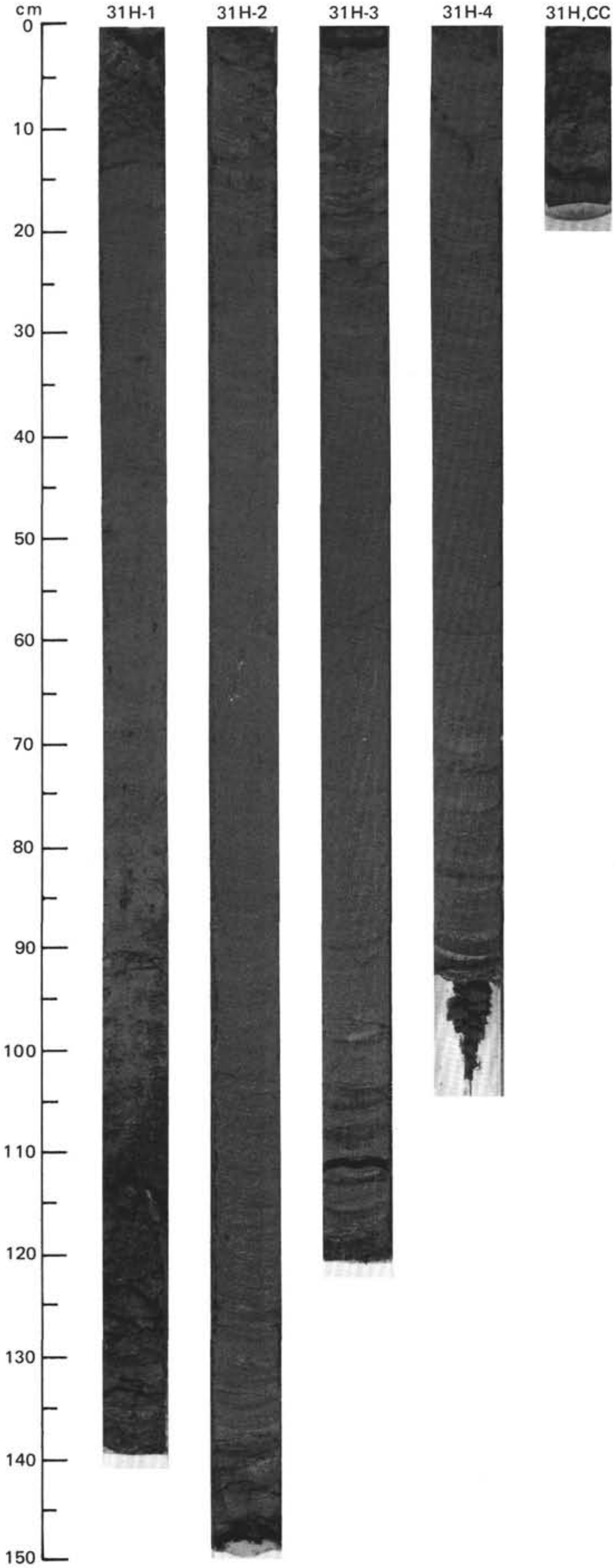
cm
0
10
20
30
40
50
60
70
80
90
100
110
120
130
140
150
31H-1
31H-2
31H-3
31H-4
31H,CC

SITE 644 HOLE A CORE 32H CORED INTERVAL 1464.4-1470 mbsl; 238.1-243.7 mbsf

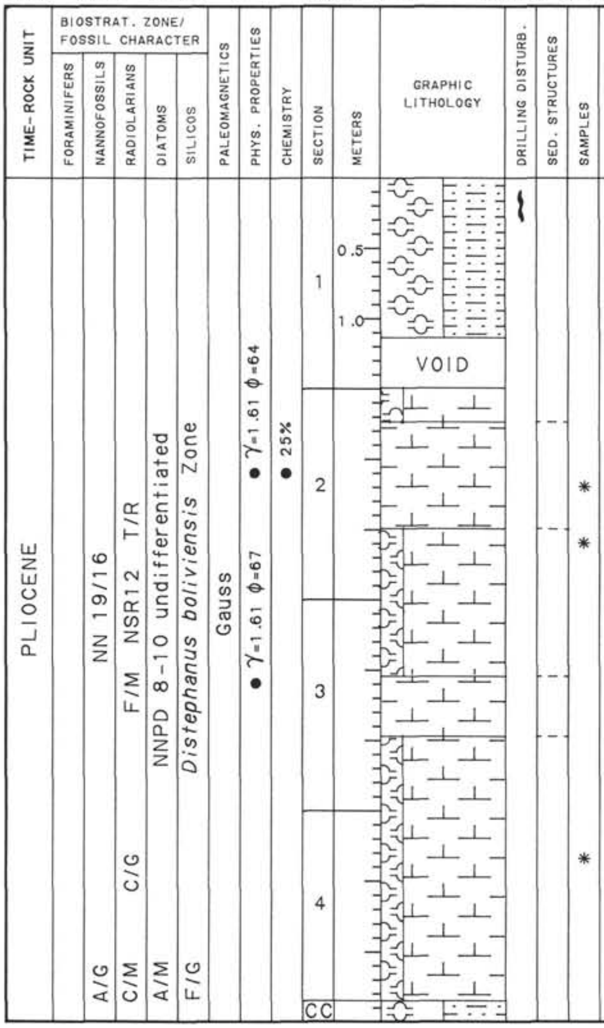

LITHOLOGIC DESCRIPTION

SILICEOUS MUD, NANNOFOSSIL OOZE, AND SILICEOUS NANNOFOSSIL OOZE

Section 1, 0–30 cm, is highly disturbed. Remainder of the core is undisturbed.

Major lithologies:
a. Siliceous mud, dark greenish gray (5GY 4/1), with common pyritized burrows. Section 1 and CC.
b. Siliceous nannofossil ooze, dark greenish gray (5GY 4/1), extensively bioturbated and mottled. Section 2, 0–25 cm; Section 2, 98 cm, to Section 3, 54 cm; Section 3, 97 cm, to Section 4.
c. Nannofossil ooze, greenish gray (5GY 5/1), extensively bioturbated and mottled. Section 22, 25–98 cm; Section 3, 54–97 cm.

SMEAR SLIDE SUMMARY (%):

	2, 70 D	2, 106 D	4, 131 D
TEXTURE:			
Sand	—	—	10
Silt	20	40	40
Clay	80	60	50
COMPOSITION:			
Quartz	5	5	10
Clay	10	20	45
Nannofossils	70	40	—
Diatoms	5	10	15
Sponge spicules	10	25	30

SITE 644 HOLE A CORE 33H CORED INTERVAL 1470-1472.3 mbsl; 243.7-246 mbsf

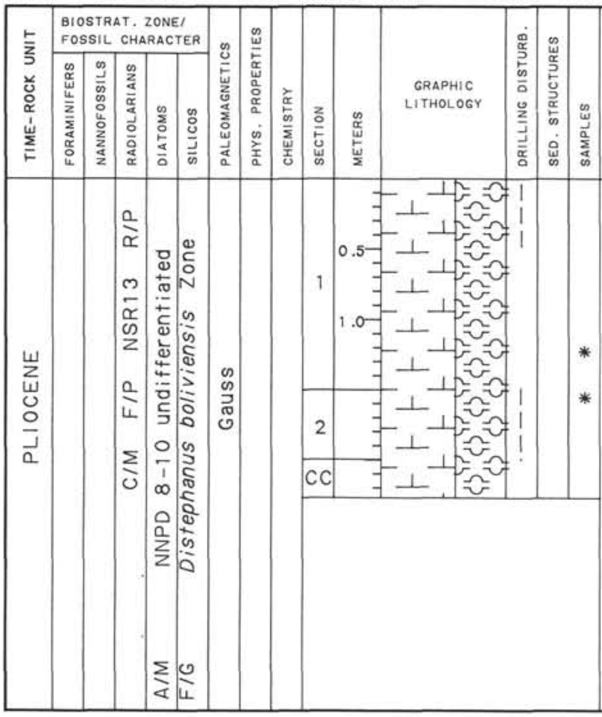

LITHOLOGIC DESCRIPTION

SILICEOUS NANNOFOSSIL OOZE

Section 1, 0–38 cm, is moderately disturbed. Section 2 is slightly disturbed. Remainder of the core is undisturbed.

Major lithology: Siliceous nannofossil ooze, greenish gray (5GY 5/1), and mottled.

SMEAR SLIDE SUMMARY (%):

	1, 122 D	2, 5 D
TEXTURE:		
Silt	30	30
Clay	70	70
COMPOSITION:		
Quartz	5	5
Clay	10	20
Nannofossils	50	50
Diatoms	10	5
Sponge spicules	25	20

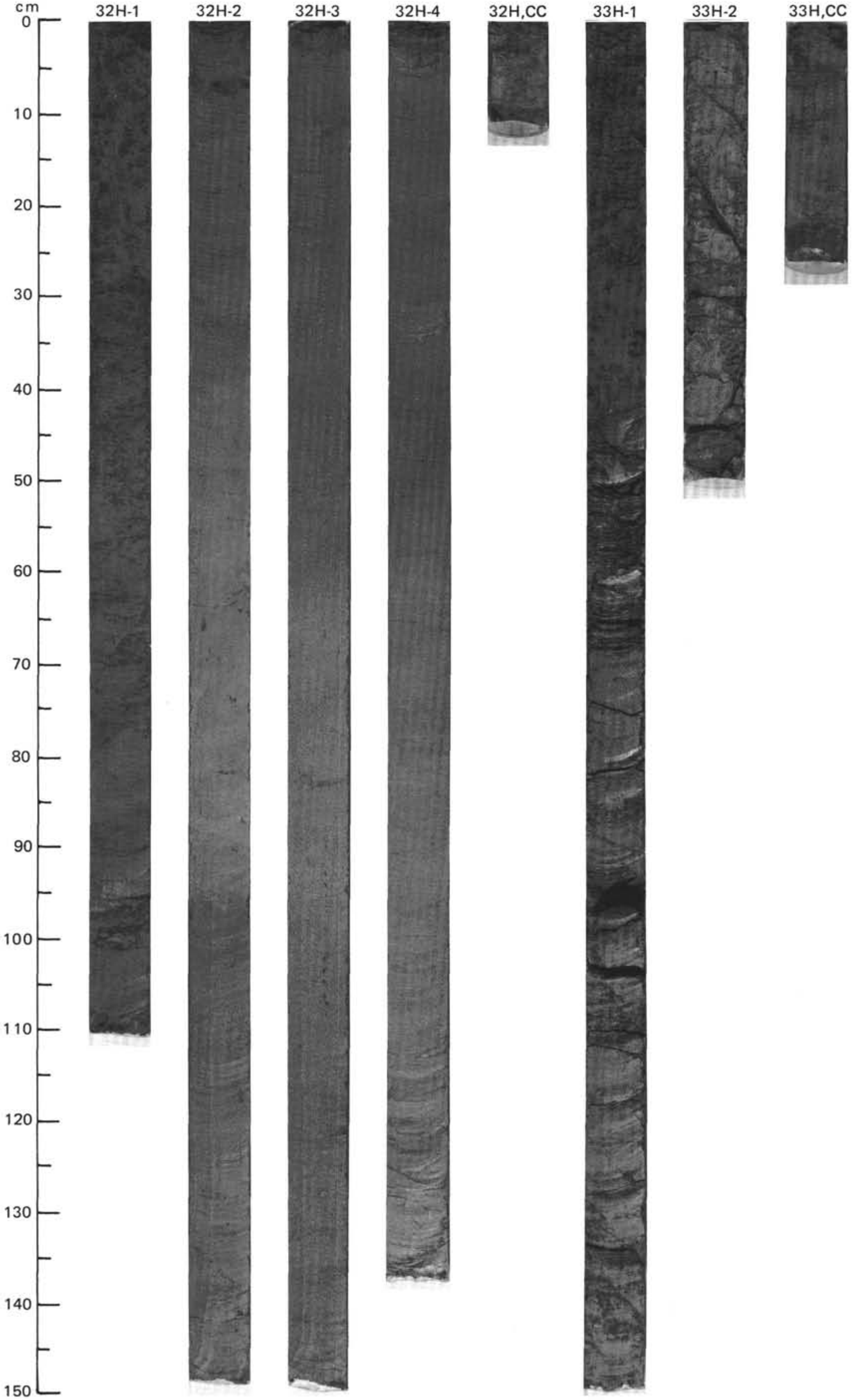
cm
0
10
20
30
40
50
60
70
80
90
100
110
120
130
140
150
32H-1
32H-2
32H-3
32H-4
32H,CC
33H-1
33H-2
33H,CC

SITE 644 HOLE A CORE 34H CORED INTERVAL 1472.3-1479.1 mbsl; 246-252.8 mbsf

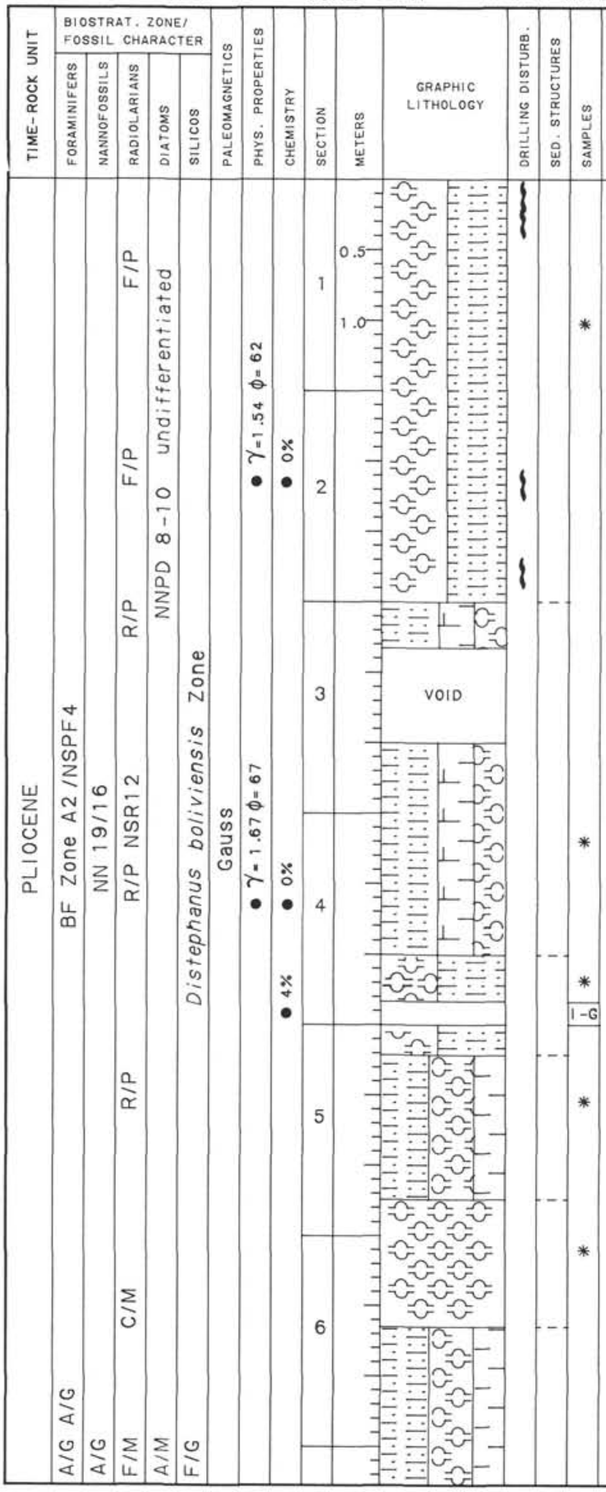

LITHOLOGIC DESCRIPTION

DIATOMACEOUS MUD/SILICEOUS MUD/SILICEOUS OOZE, NANNOFOSSIL SILICEOUS OOZE, AND SILICEOUS NANNOFOSSIL OOZE

Section 1, 0–35 cm, and Section 2, 52–69 and 107–146 cm, are highly disturbed. Remainder of the core is undisturbed.

Major lithologies:
a. Diatomaceous mud/siliceous mud/siliceous ooze, dark greenish gray (5GY 4/1), with minor to common mottling and pyritized burrows. Section 1 to Section 2; Section 4, 101 cm, to Section 5, 125 cm, to Section 6, 66 cm.
b. Nannofossil siliceous ooze, dark greenish gray (5GY 4/1), with common mottling and faint color banding. Section 3 to Section 4, 101 cm.
c. Siliceous nannofossil ooze, greenish gray (5GY 5/1), extensively bioturbated and mottled. Section 5, 20–115 cm; Section 6, 66 cm, to Section 7.

SMEAR SLIDE SUMMARY (%):

	1, 100 D	4, 15 D	4, 116 D	5, 53 D	6, 11 D
TEXTURE:					
Sand	—	—	10	10	—
Silt	70	60	50	40	70
Clay	30	40	40	50	30
COMPOSITION:					
Quartz	20	20	25	15	5
Clay	30	20	35	20	25
Volcanic glass	—	—	3	—	5
Accessory minerals	—	—	2	—	—
Nannofossils	—	20	—	30	—
Diatoms	30	15	10	20	30
Sponge spicules	20	25	25	15	35

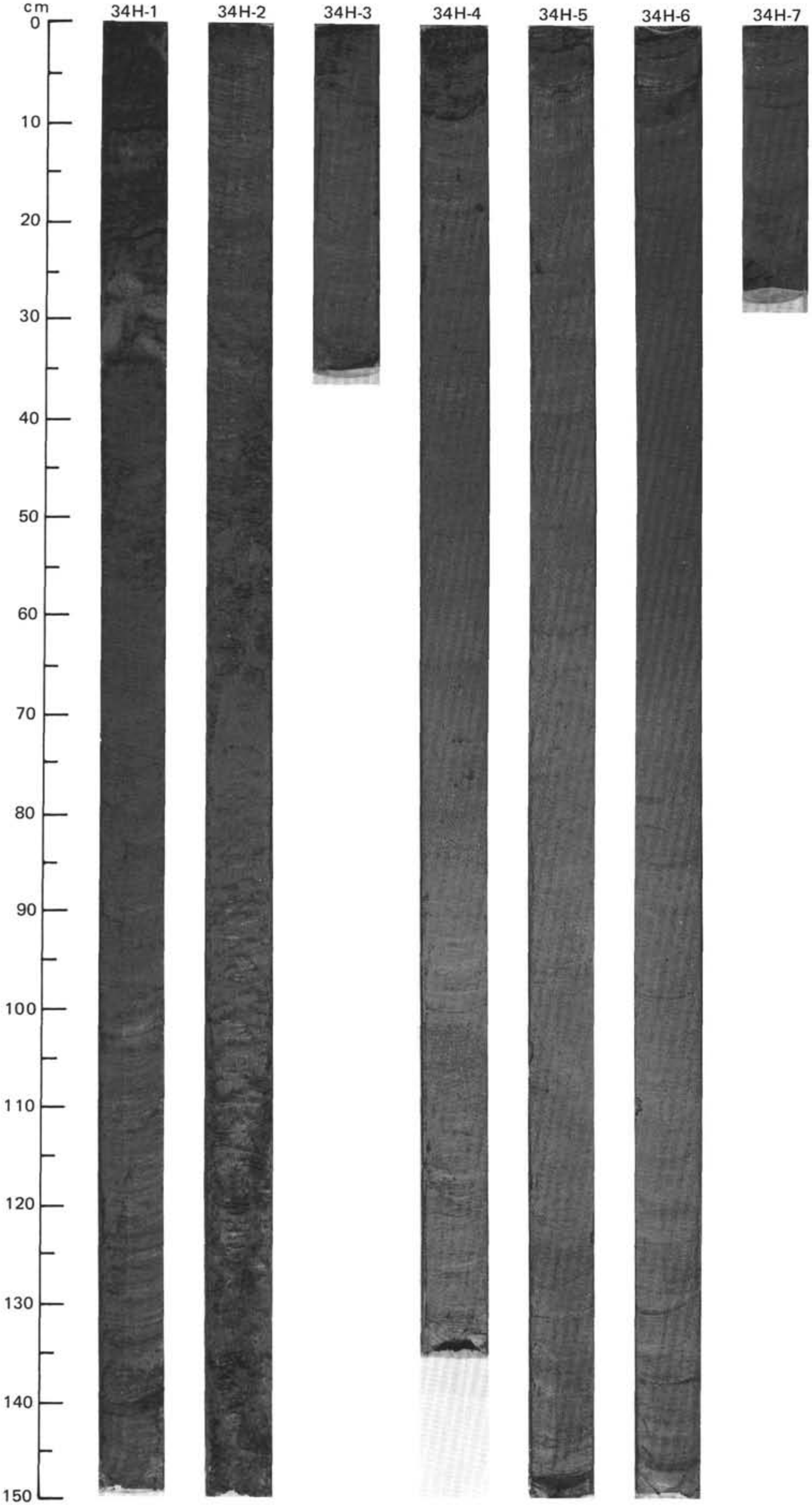
cm
0
10
20
30
40
50
60
70
80
90
100
110
120
130
140
150
34H-1
34H-2
34H-3
34H-4
34H-5
34H-6
34H-7

SITE 644 HOLE B CORE 1H CORED INTERVAL 1225.9-1230.5 mbsl; 0.0-4.6 mbsf

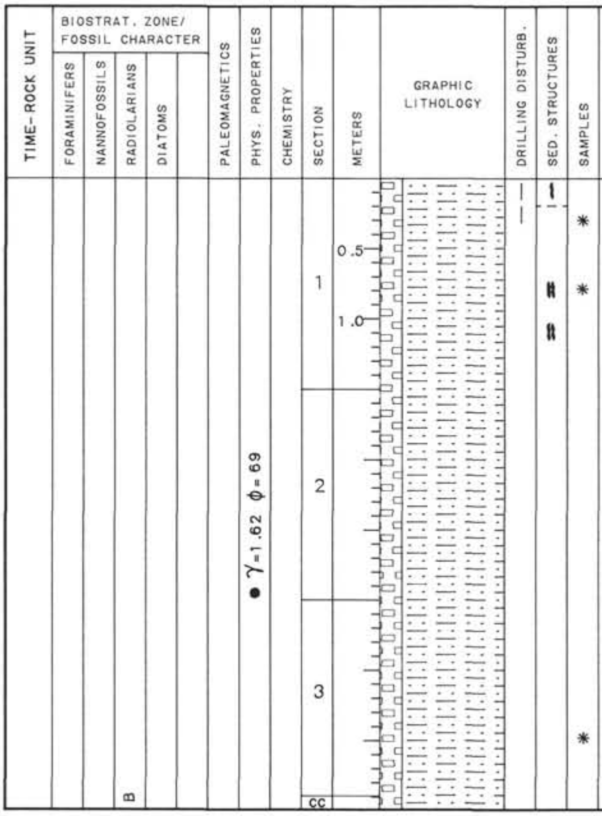

LITHOLOGIC DESCRIPTION

CALCAREOUS MUD

Entire core is undisturbed.

Major lithology: Calcareous mud, dark grayish brown (2.5Y 4/2), with minor mottling and bioturbation throughout.

SMEAR SLIDE SUMMARY (%):

	1, 30 D	1, 83 M	3, 100 D
TEXTURE:			
Sand	10	5	5
Silt	35	25	25
Clay	55	70	70
COMPOSITION:			
Quartz	19	5	3
Feldspar	5	5	—
Clay	55	75	65
Volcanic glass	5	—	—
Calcite/dolomite	20	—	10
Accessory minerals	—	5	2
Foraminifers	Tr	—	—
Nannofossils	10	—	20
Sponge spicules	Tr	—	—

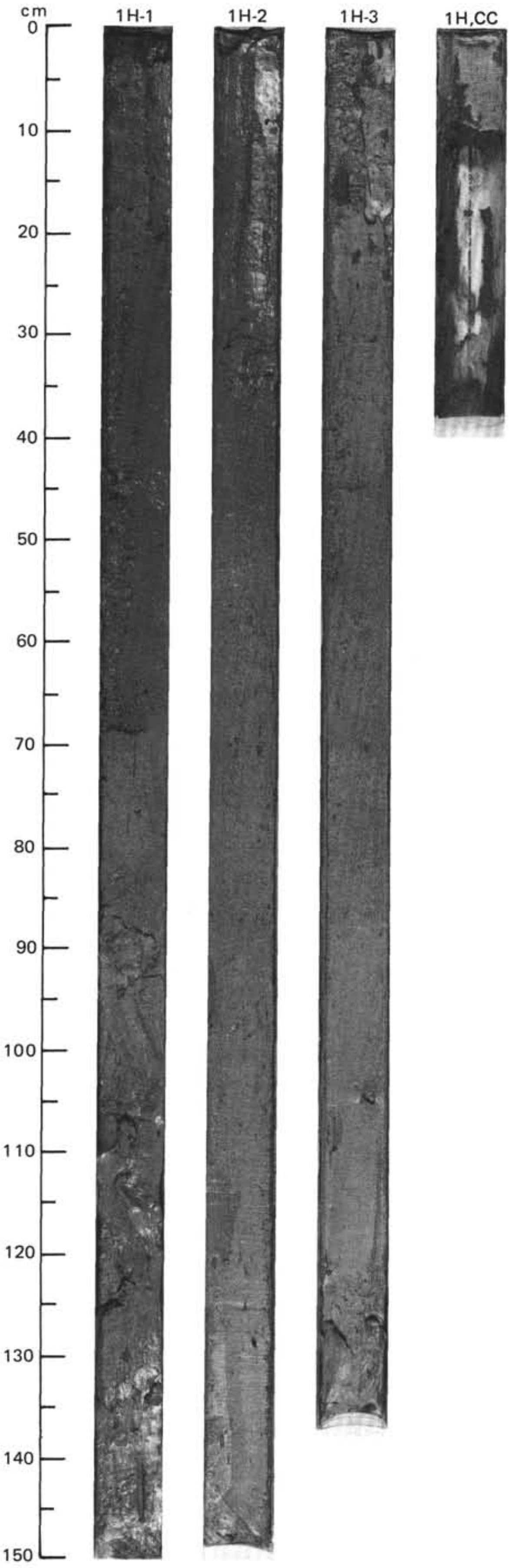
cm
0
10
20
30
40
50
60
70
80
90
100
110
120
130
140
150
1H-1
1H-2
1H-3
1H,CC

SITE 644 HOLE B CORE 2H CORED INTERVAL 1230.5-1240.0 mbsl; 4.6-14.1 mbsf

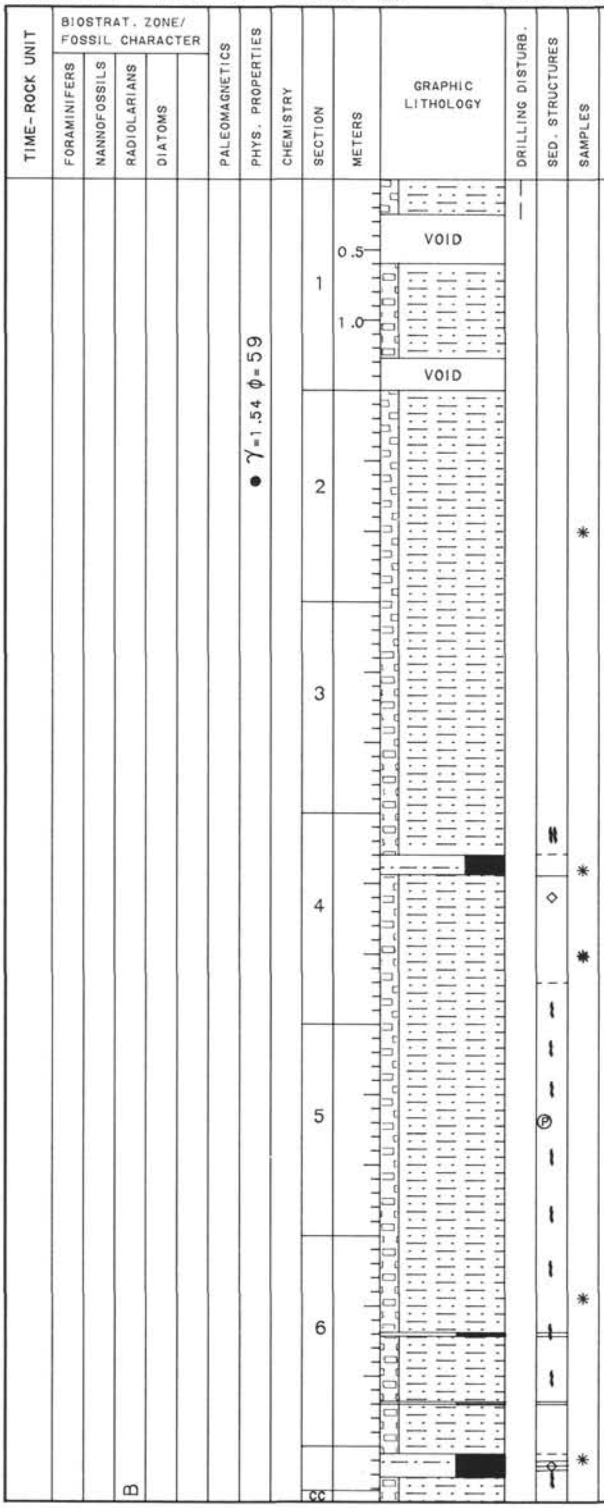

LITHOLOGIC DESCRIPTION

CALCAREOUS MUD TO MUD, AND MUD TO SANDY MUD

Section 1, 0–25 cm, is moderately disturbed; Section 1, 25–60 and 128–150 cm, are voids; remainder of core is undisturbed.

Major lithologies:
a. Calcareous mud to mud, dark grayish brown (2.5Y 4/2) to grayish brown (2.5Y 5/2), with minor to extensive mottling and bioturbation, rare pyrite concretions and dropstones. Section 1 to Section 4, 30 cm; Section 4, 46 cm, to Section 7, 5 cm; Section 7, 22 cm, to CC.
b. Mud to sandy mud, very dark gray (5Y 3/1), with sharp base and gradational top. Section 4, 30–46 cm; Section 7, 5–22 cm.

SMEAR SLIDE SUMMARY (%):

	2, 100 D	4, 40 M	4, 100 D	6, 40 D	7, 10 M
TEXTURE:					
Sand	20	55	5	5	20
Silt	20	20	35	35	25
Clay	60	25	60	60	55
COMPOSITION:					
Quartz	30	60	15	30	25
Feldspar	3	—	—	—	—
Clay	40	30	60	50	65
Volcanic glass	—	5	—	3	7
Calcite/dolomite	5	Tr	5	10	Tr
Accessory minerals	2	—	5	2	Tr
Glauconite	—	—	—	Tr	—
Nannofossils	20	5	15	5	3

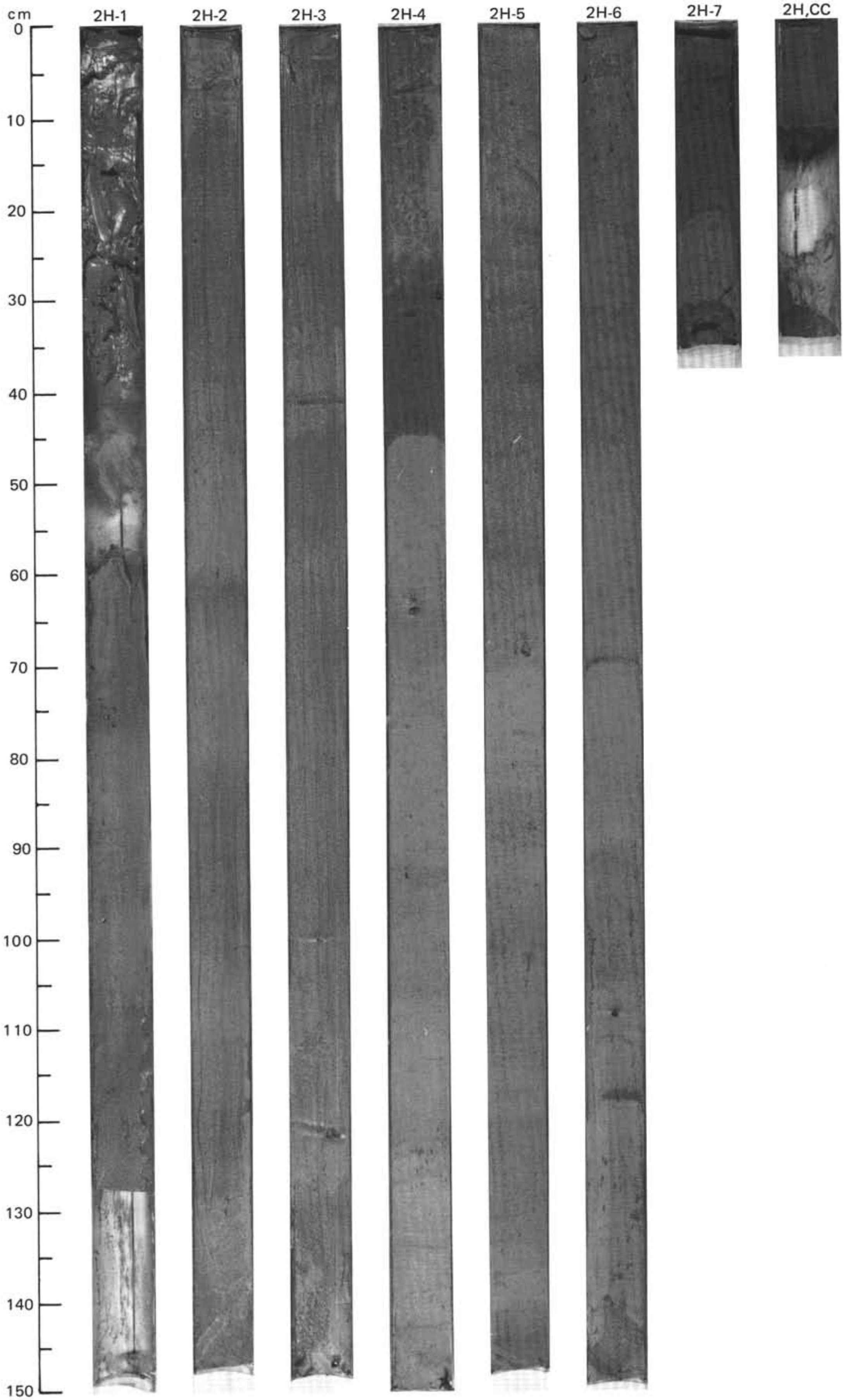
cm
0
10
20
30
40
50
60
70
80
90
100
110
120
130
140
150
2H-1
2H-2
2H-3
2H-4
2H-5
2H-6
2H-7
2H,CC

SITE 644 HOLE B CORE 3H CORED INTERVAL 1240.0-1249.5 mbsl; 14.1-23.6 mbsf

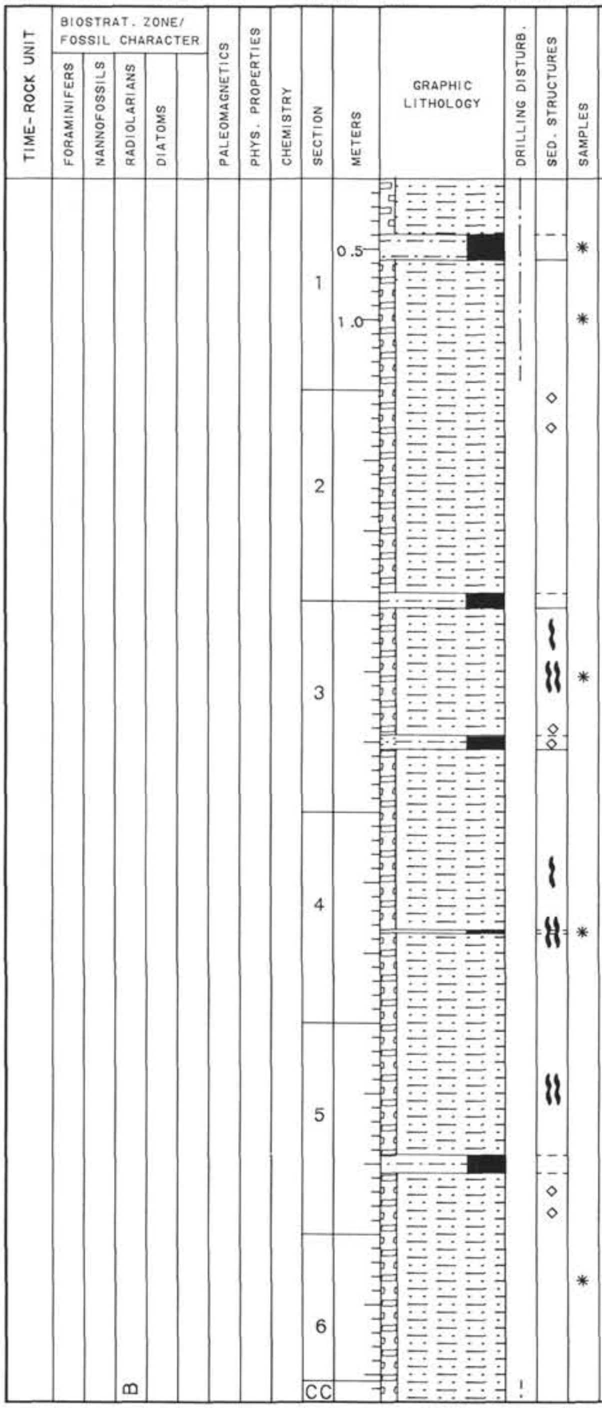

LITHOLOGIC DESCRIPTION

CALCAREOUS MUD TO MUD AND MUD

Section 1 moderately disturbed; remainder of core is undisturbed.

Major lithologies:
a. Calcareous mud to mud, grayish-brown (5Y 5/2) to dark grayish brown (5Y 4/2), with minor pyritized burrows, minor to common bioturbation and mottling, and a few scattered dropstones. Section 1, 0–40 cm; Section 1, 58 cm, to Section 2, 146 cm; Section 3, 3–96 cm; Section 3, 106 cm, to Section 4, 83 cm; Section 4, 84 cm, to Section 5, 96 cm; Section 5, 106 cm, to CC.
b. Mud, very dark gray (5Y 3/1) and sandy, with sharp base and gradational top, scattered large dropstones. Section 1, 40–58 cm; Section 2, 146 cm, to Section 3, 3 cm; Section 3, 96–106 cm; Section 4, 83–84 cm; Section 5, 96–106 cm.

SMEAR SLIDE SUMMARY (%):

	1, 50 M	1, 100 D	3, 50 D	4, 83 M	6, 30 D
TEXTURE:					
Sand	20	3	2	20	35
Silt	30	22	35	20	15
Clay	50	75	63	60	50
COMPOSITION:					
Quartz	25	20	20	35	30
Feldspar	Tr	Tr	—	—	3
Mica	—	—	—	—	2
Clay	47	55	66	50	45
Volcanic glass	5	—	Tr	3	2
Calcite/dolomite	12	15	5	5	15
Accessory minerals:					
Pyrite	5	Tr	2	5	2
Foraminifers	—	—	Tr	—	—
Nannofossils	5	10	5	2	Tr

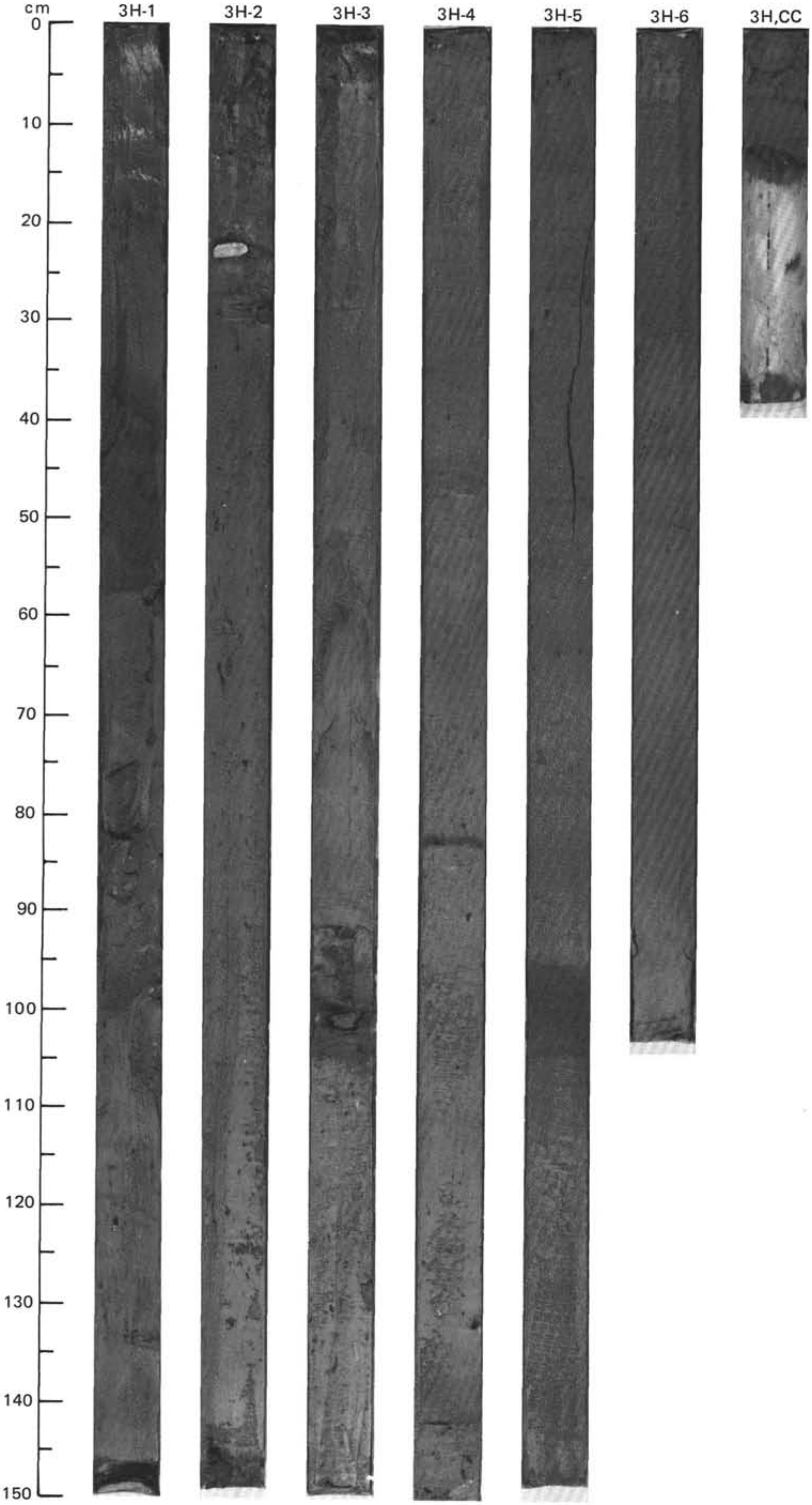
cm
0
10
20
30
40
50
60
70
80
90
100
110
120
130
140
150
3H-1
3H-2
3H-3
3H-4
3H-5
3H-6
3H,CC

SITE 644 HOLE B CORE 4H CORED INTERVAL 1249.5-1259.0 mbsl; 23.6-33.1 mbsf

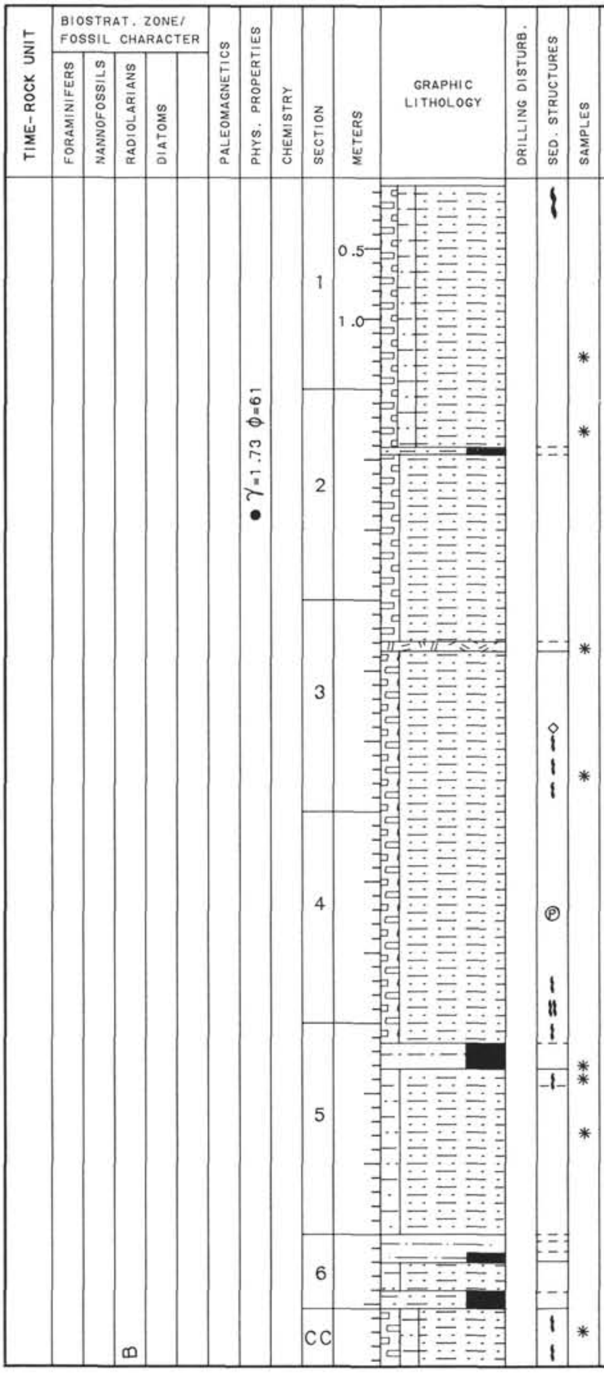

LITHOLOGIC DESCRIPTION

MUD TO CALCAREOUS MUD AND MUD TO SANDY MUD

Section 2, 0–47 cm, is moderately disturbed; remainder of core is undisturbed.

Major lithologies:
a. Mud to calcareous (sandy) mud, grayish-brown (2.5Y 5/2) to dark grayish-brown (2.5Y 4/2) and olive gray (5Y 4/2), with rare to common pyritized burrows and cm-scale bioturbation and mottling. Few scattered dropstones. Section 1 to Section 2, 43 cm; Section 2, 46 cm, to Section 3, 32 cm; Section 3, 35 cm, to Section 5, 15 cm; Section 5, 34–150 cm; Section 6, 6–13 and 20–42 cm; CC.
b. Mud to sandy mud, very dark gray (5Y 3/1), with sharp base, gradational top, and common dropstones. Section 2, 43–46 cm; Section 5, 15–34 cm; Section 6, 0–6, 13–20, and 42–52 cm.

Minor lithology: Volcanic ash, dark olive gray (5Y 3/2). Section 3, 32–35 cm.

SMEAR SLIDE SUMMARY (%):

	1, 130 D	2, 27 M	3, 33 M	3, 125 D	5, 27 M	5, 79 D
TEXTURE:						
Sand	25	2	70	10	30	10
Silt	20	20	15	35	20	30
Clay	55	78	15	55	50	60
COMPOSITION:						
Quartz	20	25	—	20	40	25
Feldspar	Tr	—	—	—	2	—
Mica	3	2	—	—	2	3
Clay	50	68	15	40	48	55
Volcanic glass	—	5	70	3	—	—
Calcite/dolomite	15	—	—	5	—	10
Accessory minerals	Tr	5	15	5	7	2
Glauconite	—	—	—	Tr	Tr	—
Calcareous fragments	10	—	—	—	—	—
Foraminifers	—	—	Tr	2	—	—
Nannofossils	—	5	—	25	—	5
Diatoms	—	—	Tr	—	—	—

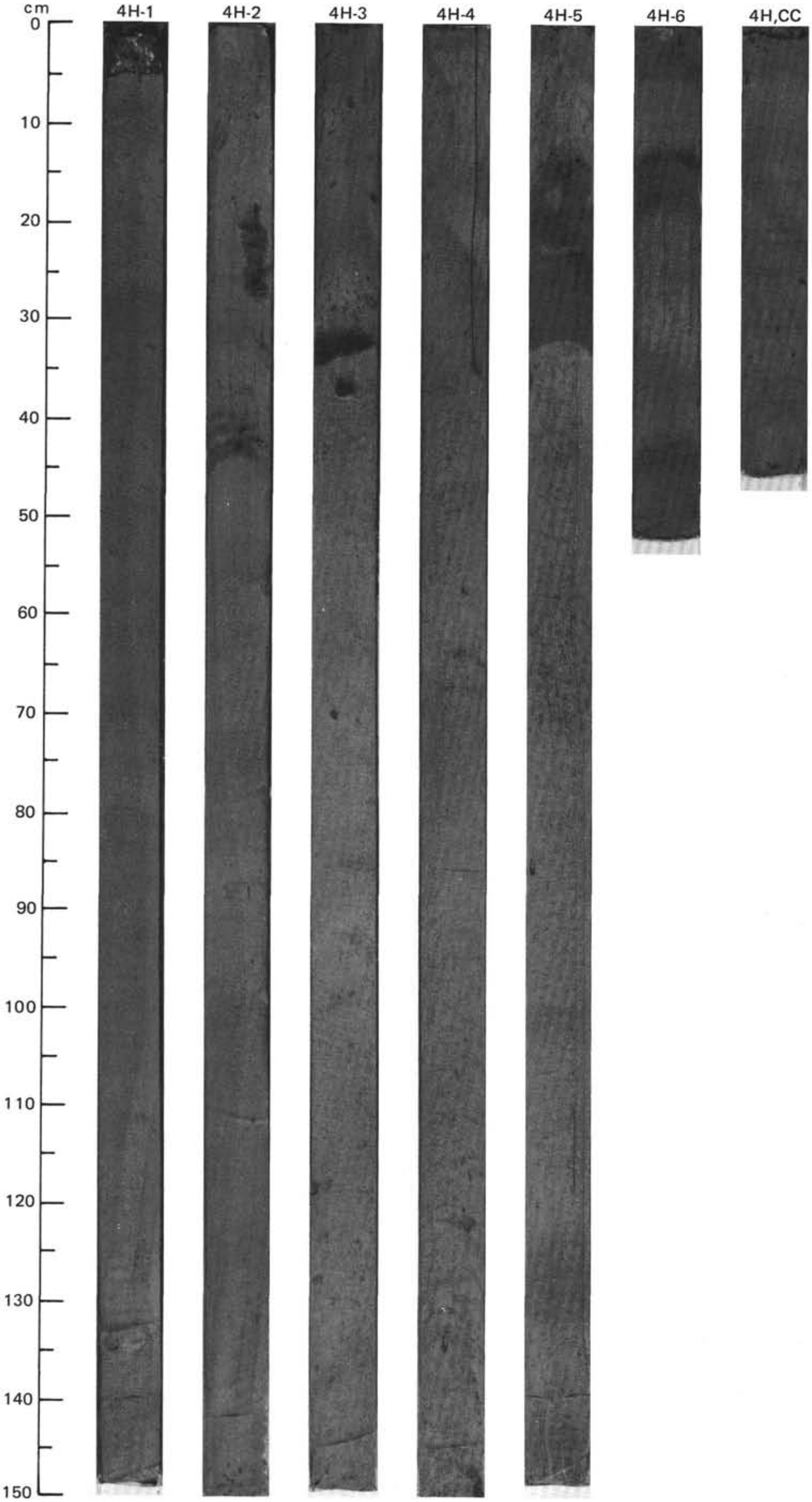
cm
0
10
20
30
40
50
60
70
80
90
100
110
120
130
140
150
4H-1
4H-2
4H-3
4H-4
4H-5
4H-6
4H,CC

SITE 644 HOLE B CORE 5H CORED INTERVAL 1259.0-1268.5 mbsl; 33.1-42.6 mbsf

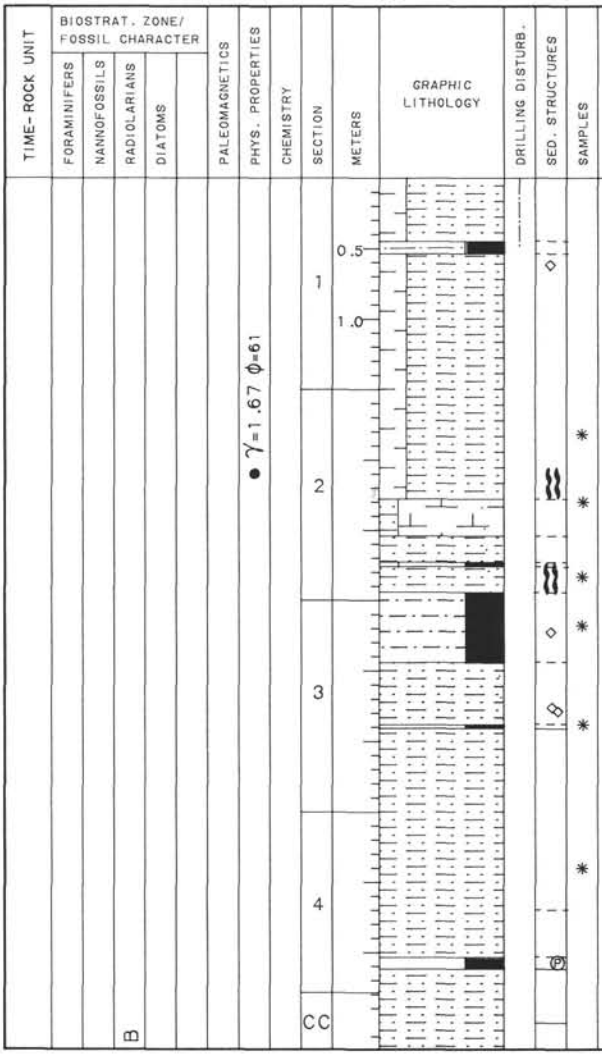

LITHOLOGIC DESCRIPTION

CALCAREOUS MUD TO MUD

Section 1, 0–40 cm, moderately disturbed; remainder of core is undisturbed.

Major lithologies:
a. Calcareous mud to mud, olive gray (5Y 4/2) to dark grayish brown (2.5Y 4/2), with common to abundant pyritized burrows and cm-scale bioturbation/mottling. Scattered dropstones. Section 1, 0–47 cm; Section 1, 51 cm, to Section 2, 79 cm; Section 2, 105–122 and 125–146 cm; Section 3, 47–89 cm; Section 3, 91 cm, to Section 4, 106 cm; Section 4, 112 cm, to CC.
b. Mud, very dark gray (5Y 3/1), slightly sandy, with sharp base and gradational top, rare to common dropstones. Section 1, 47–51 cm; Section 2, 122–125 cm; Section 2, 146 cm, to Section 3, 47 cm; Section 4, 106–112 cm.

Minor lithologies:
a. Calcareous mud to nannofossil ooze, olive gray (5Y 5/2). Section 2, 79–105 cm.
b. Sandy mud, olive gray (5Y 4/2), with pyrite-cemented sandy pebble. Section 3, 89–91 cm.

SMEAR SLIDE SUMMARY (%):

	2, 30 D	2, 80 D	2, 139 M	3,220 D	3, 90 M	4, 40 D
TEXTURE:						
Sand	10	2	30	10	25	5
Silt	30	50	20	20	15	30
Clay	60	48	50	70	60	65
COMPOSITION:						
Quartz	10	5	15	35	10	30
Feldspar	—	—	—	2	—	—
Mica	—	Tr	3	—	Tr	—
Clay	55	15	45	45	55	42
Volcanic glass	—	—	—	—	—	Tr
Calcite/dolomite	3	—	30	3	25	20
Accessory minerals:						
Pyrite	2	Tr	Tr	10	5	2
Glauconite	—	Tr	—	—	—	—
Foraminifers	Tr	—	Tr	—	—	—
Nannofossils	30	75	5	5	5	5

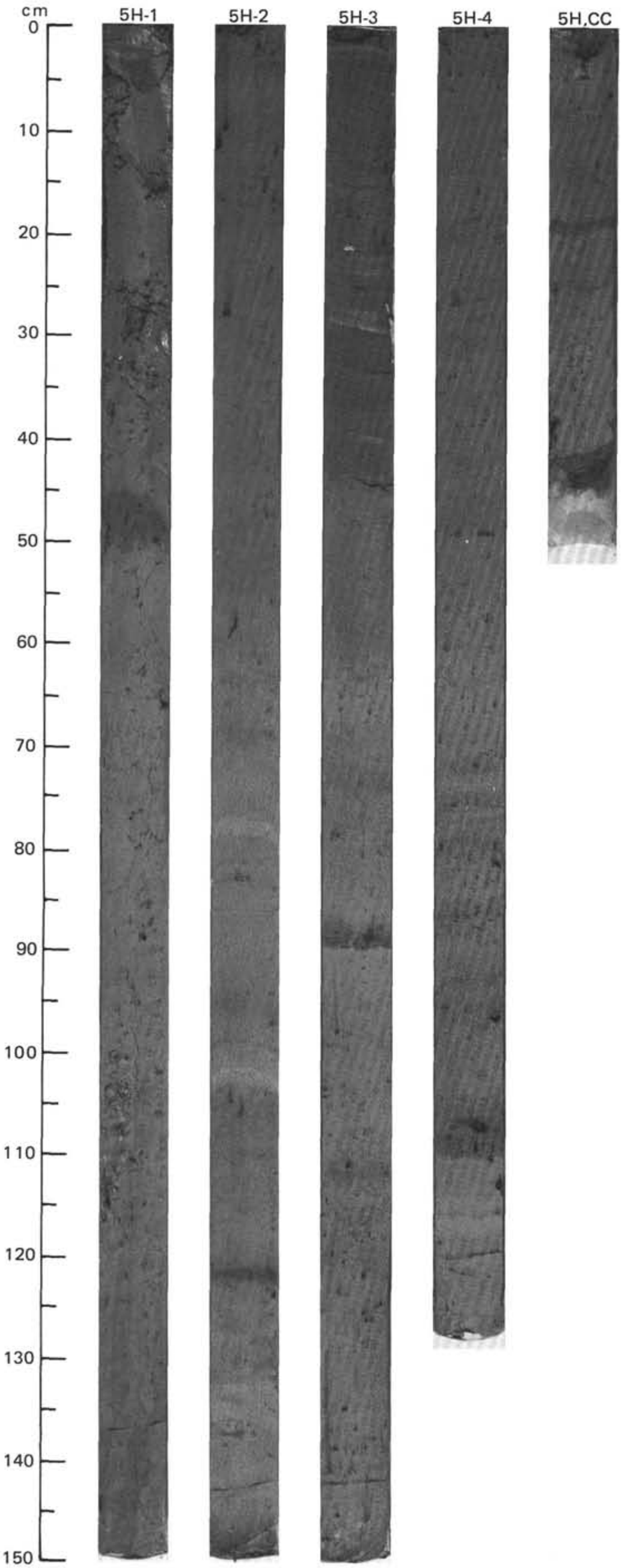
cm
0
10
20
30
40
50
60
70
80
90
100
110
120
130
140
150
5H-1
5H-2
5H-3
5H-4
5H,CC

SITE 644 HOLE B CORE 6H CORED INTERVAL 1271.0-1280.5 mbsl; 42.6-52.1 mbsf

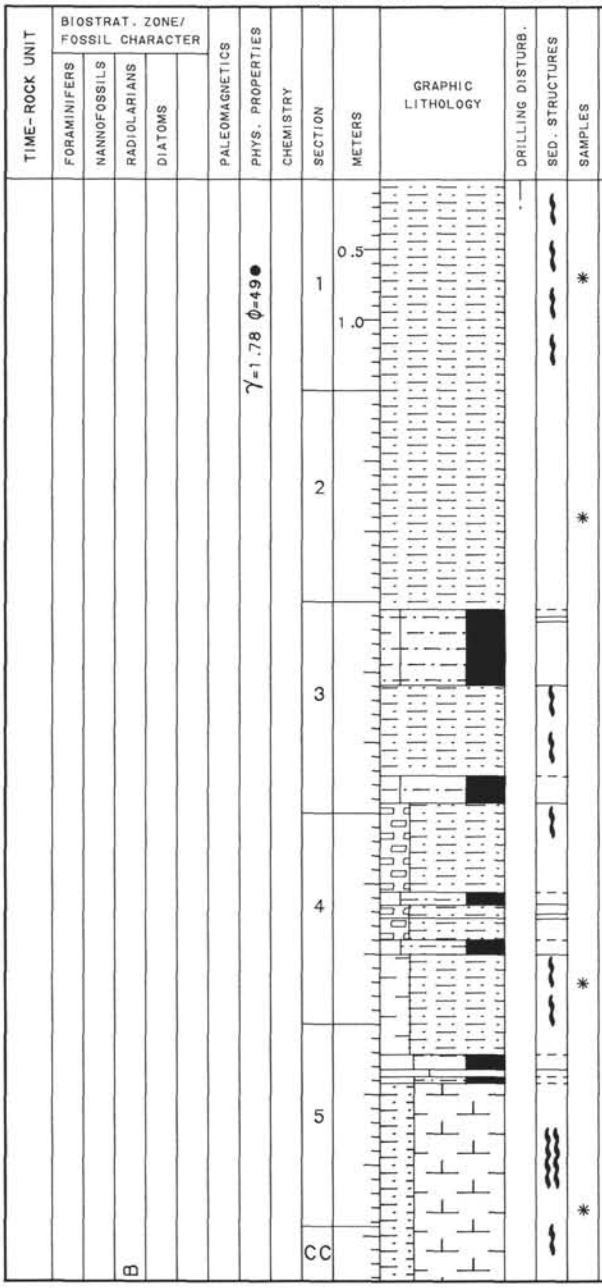

LITHOLOGIC DESCRIPTION

MUD TO CALCAREOUS MUD TO NANNOFOSSIL OOZE, AND MUD

Section 1, 0–15 cm, moderately disturbed; remainder of core is undisturbed.

Major lithologies:
a. Mud to calcareous mud, at some points grading to nannofossil ooze, olive gray (5Y 4/2, 5Y 5/2) to dark grayish brown (2.5Y 4/2). Lithology ranges from uniform appearance to gradationally and indistinctly interbedded and mottled in these colors. Section 1 to Section 3, 6 cm; Section 3, 60–126 cm; Section 3, 143 cm, to Section 4, 57 cm; Section 4, 64–90 cm; Section 4, 99 cm, to Section 5, 23 cm; Section 5, 33–37 cm; and Section 5, 42 cm, to CC.
b. Mud, very dark gray (5Y 3/1) and sandy. Section 3, 126–143 cm; Section 4, 57–64 and 90–99 cm; Section 5, 23–33 and 37–42 cm.

SMEAR SLIDE SUMMARY (%):

	1, 70 D	2, 90 D	3, 20 D	4, 130 D	5, 130 D
TEXTURE:					
Sand	10	5	15	5	5
Silt	25	10	20	20	35
Clay	65	85	65	75	60
COMPOSITION:					
Quartz	20	10	25	10	15
Clay	60	77	57	66	—
Volcanic glass	5	Tr	—	5	4
Calcite/dolomite	5	3	10	3	3
Accessory minerals:					
Pyrite	3	2	3	Tr	Tr
Foraminifers	—	—	—	—	2
Nannofossils	7	7	5	15	75

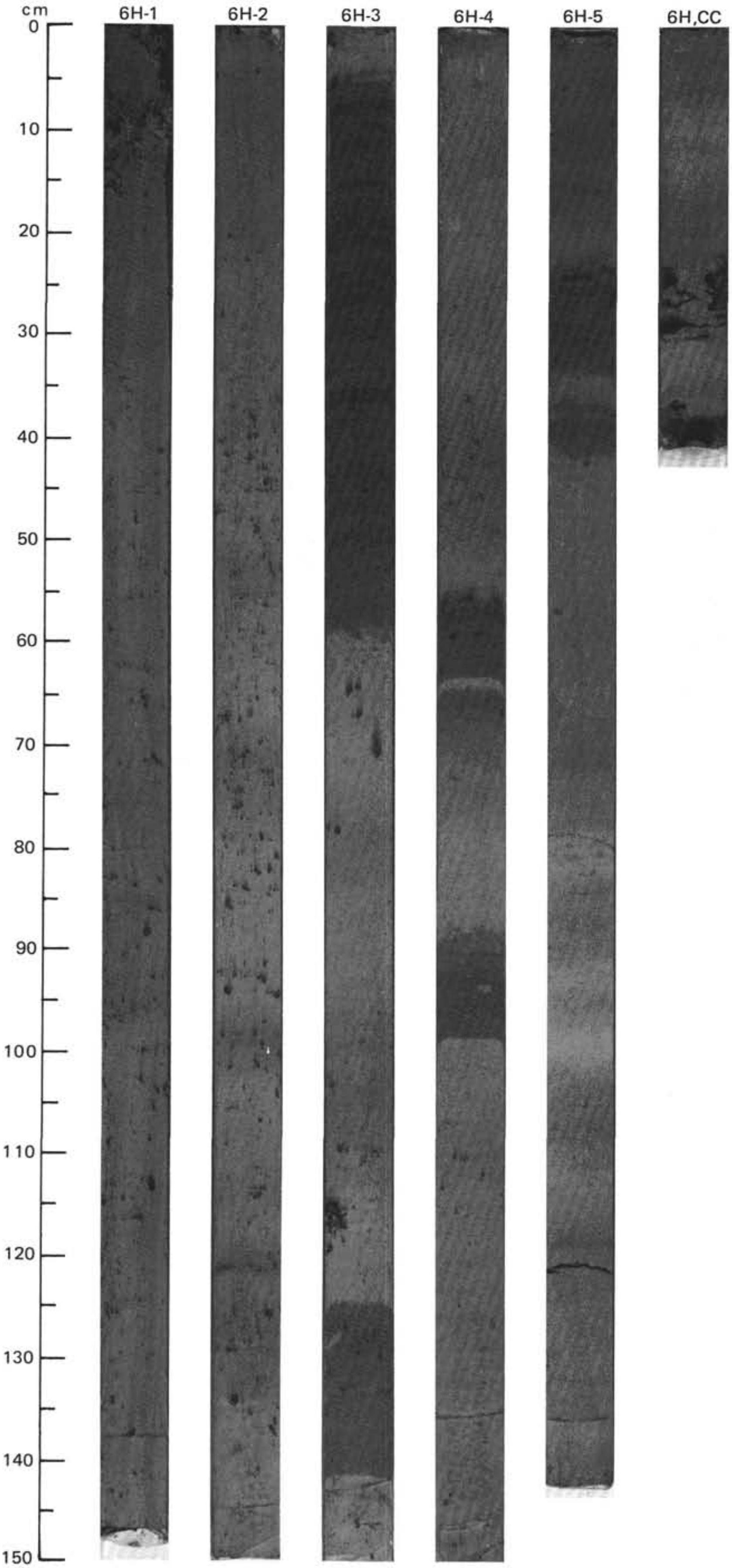
cm
0
10
20
30
40
50
60
70
80
90
100
110
120
130
140
150
6H-1
6H-2
6H-3
6H-4
6H-5
6H,CC

SITE 644 HOLE B CORE 7H CORED INTERVAL 1278.0-1287.5 mbsl; 52.1-61.6 mbsf

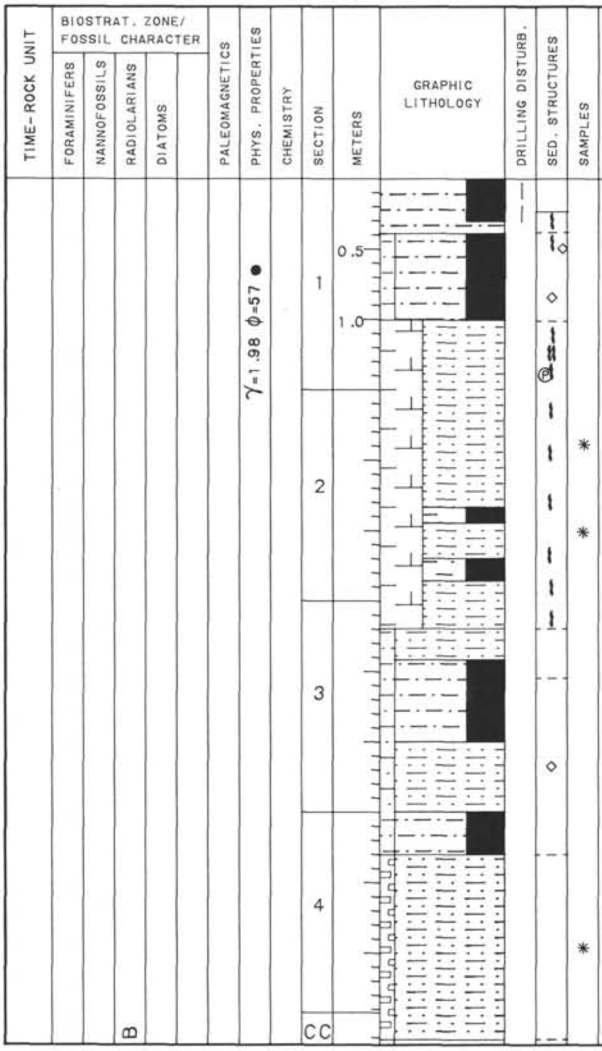

LITHOLOGIC DESCRIPTION

MUD TO CALCAREOUS MUD TO NANNOFOSSIL OOZE, AND MUD

Entire core is undisturbed.

Major lithologies:

a. Mud to calcareous mud, at some points grading to nannofossil ooze, olive gray (5Y 4/2 and 5Y 5/2) and dark grayish brown (2.5Y 4/2) to very dark grayish brown (2.5Y 3/2). Minor to abundant bioturbation and mottling, with minor gradational and indistinct interbedding in these colors. Section 1, 0–39 cm; Section 1, 100 cm, to Section 3, 20 cm; Section 4, 30 cm, to CC, 24 cm.

b. Mud, very dark gray (5Y 3/1) and dark olive gray (5Y 3/2), slightly sandy, with abundant dropstones. Section 1, 39–100 cm; Section 3, 20 cm, to Section 4, 30 cm; CC, 24–26 cm.

SMEAR SLIDE SUMMARY (%):

	2, 37 M	2, 100 D	4, 100 D
TEXTURE:			
Sand	5	15	25
Silt	10	25	30
Clay	85	60	45
COMPOSITION:			
Quartz	5	25	25
Feldspar	—	Tr	—
Mica	—	Tr	—
Clay	—	57	45
Volcanic glass	—	—	Tr
Calcite/dolomite	Tr	3	5
Accessory minerals	Tr	2	Tr
Foraminifers	5	3	3
Nannofossils	88	7	20
Fish remains	—	Tr	—

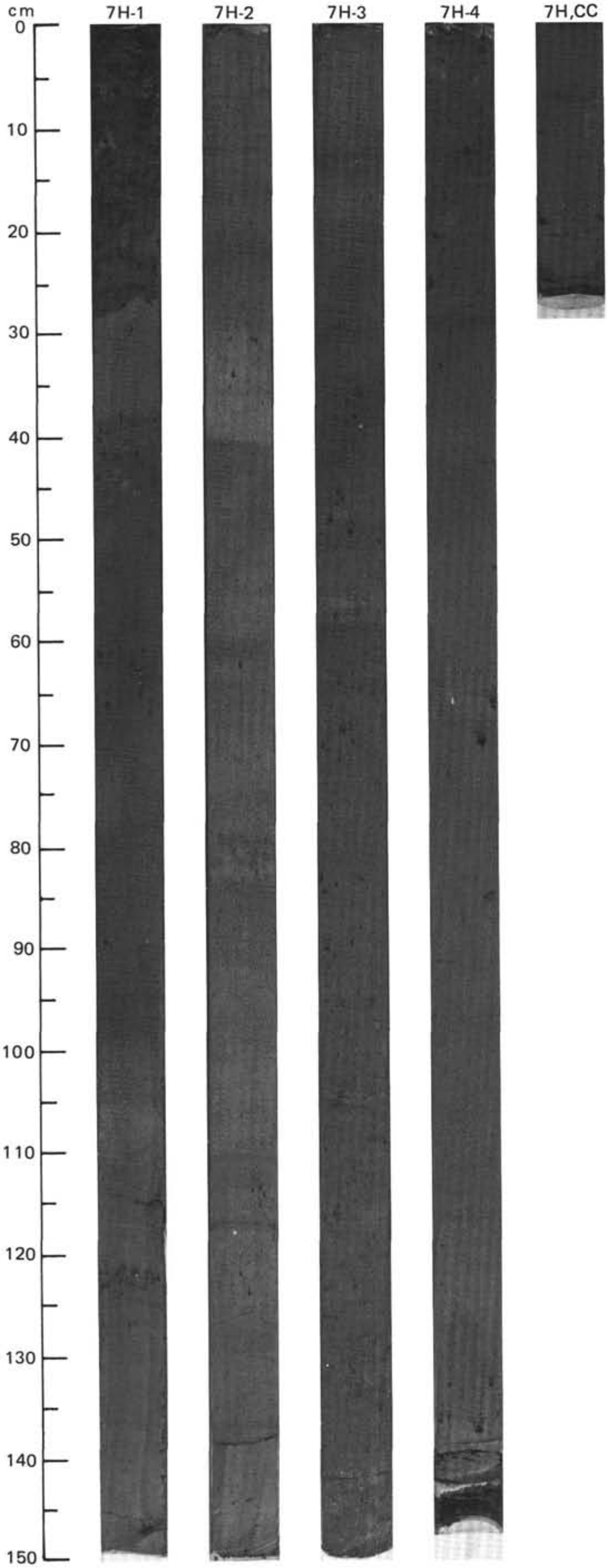
cm
0
10
20
30
40
50
60
70
80
90
100
110
120
130
140
150
7H-1
7H-2
7H-3
7H-4
7H,CC

SITE 644 HOLE B CORE 8H CORED INTERVAL 1287.5-1297.0 mbsl; 61.6-71.1 mbsf

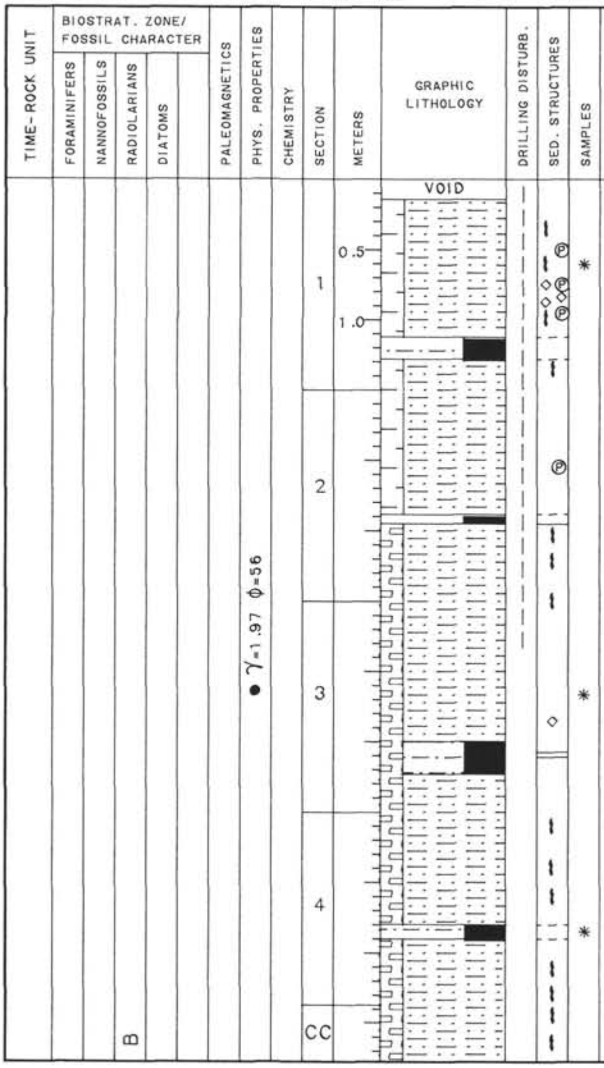

LITHOLOGIC DESCRIPTION

CALCAREOUS MUD AND MUD TO SANDY MUD

Entire core is slightly disturbed.

Major lithologies:
a. Calcareous mud, olive gray (5Y 4/2) to dark grayish brown (2.5Y 4/2), with minor to common pyritized burrows and cm-scale bioturbation/mottling. Section 1, 15–114 cm; Section 1, 128 cm, to Section 2, 89 cm; Section 2, 95 cm, to Section 4, 82 cm; Section 4, 91 cm, to CC.
b. Mud to sandy mud, very dark gray (5Y 3/1), with common small pyrite concretions and dropstones. Section 1, 114–128 cm; Section 2, 89–95 cm; Section 4, 82–91 cm.

SMEAR SLIDE SUMMARY (%):

	1, 58 D	3, 70 D	4, 85 M
TEXTURE:			
Sand	10	5	35
Silt	30	25	20
Clay	60	70	45
COMPOSITION:			
Quartz	20	10	45
Clay	50	70	30
Volcanic glass	Tr	Tr	5
Calcite/dolomite	—	5	10
Accessory minerals:			
Pyrite	3	Tr	5
Foraminifers	Tr	3	—
Nannofossils	25	10	5

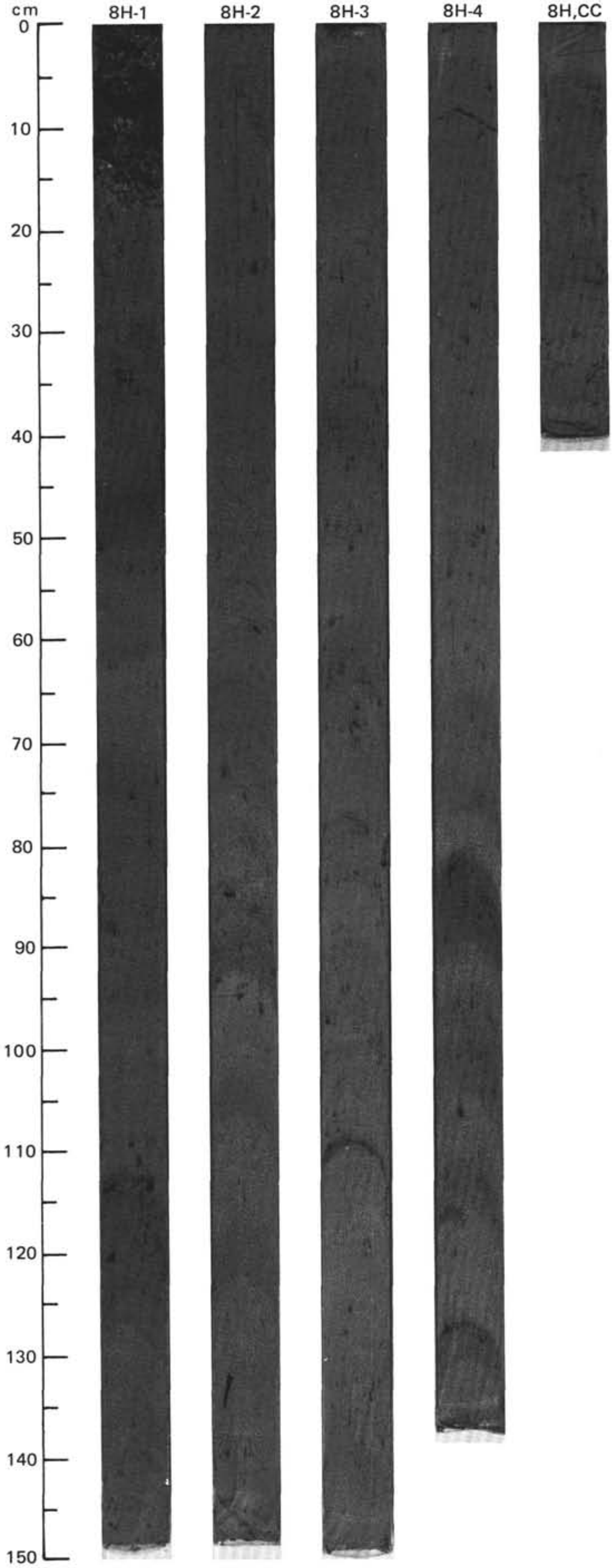
cm
0
10
20
30
40
50
60
70
80
90
100
110
120
130
140
150
8H-1
8H-2
8H-3
8H-4
8H,CC

SITE 644 HOLE B CORE 9H CORED INTERVAL 1297.0-1306.5 mbsl; 71.1-80.6 mbsf

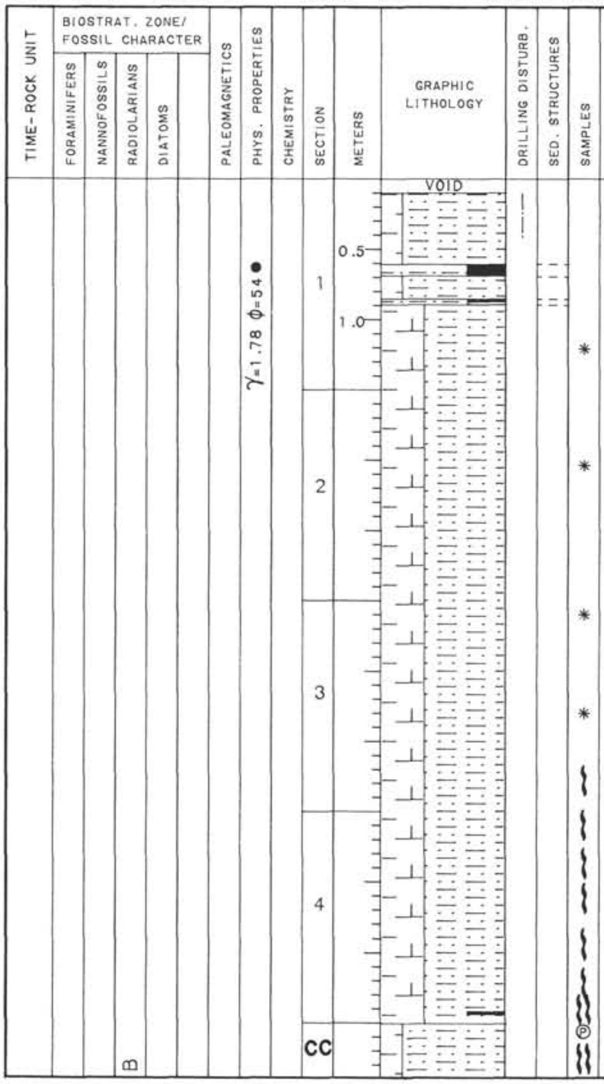

LITHOLOGIC DESCRIPTION

MUD TO MARLY NANNOFOSSIL OOZE

Section 1, 0–41 cm, is moderately disturbed; remainder of core is undisturbed.

Major lithology: Mud to marly nannofossil ooze, olive gray (5Y 4/2 and 5Y 5/2) to dark gray (5Y 4/1), with minor to common pyritized burrows and cm-scale bioturbation/mottling.

Minor lithology: Mud and sandy mud, very dark gray (5Y 3/1), with minor dropstones. Section 1, 63–68 and 87–89 cm.

SMEAR SLIDE SUMMARY (%):

	1, 120 D	2, 55 M	3, 10 D	3, 80 D
TEXTURE:				
Sand	15	20	5	5
Silt	25	15	45	20
Clay	60	65	50	75
COMPOSITION:				
Quartz	20	20	40	15
Clay	10	15	50	65
Volcanic glass	Tr	—	—	—
Calcite/dolomite	5	3	5	10
Accessory minerals:				
Pyrite	3	2	Tr	Tr
Foraminifers	Tr	10	—	—
Nannofossils	60	50	5	10

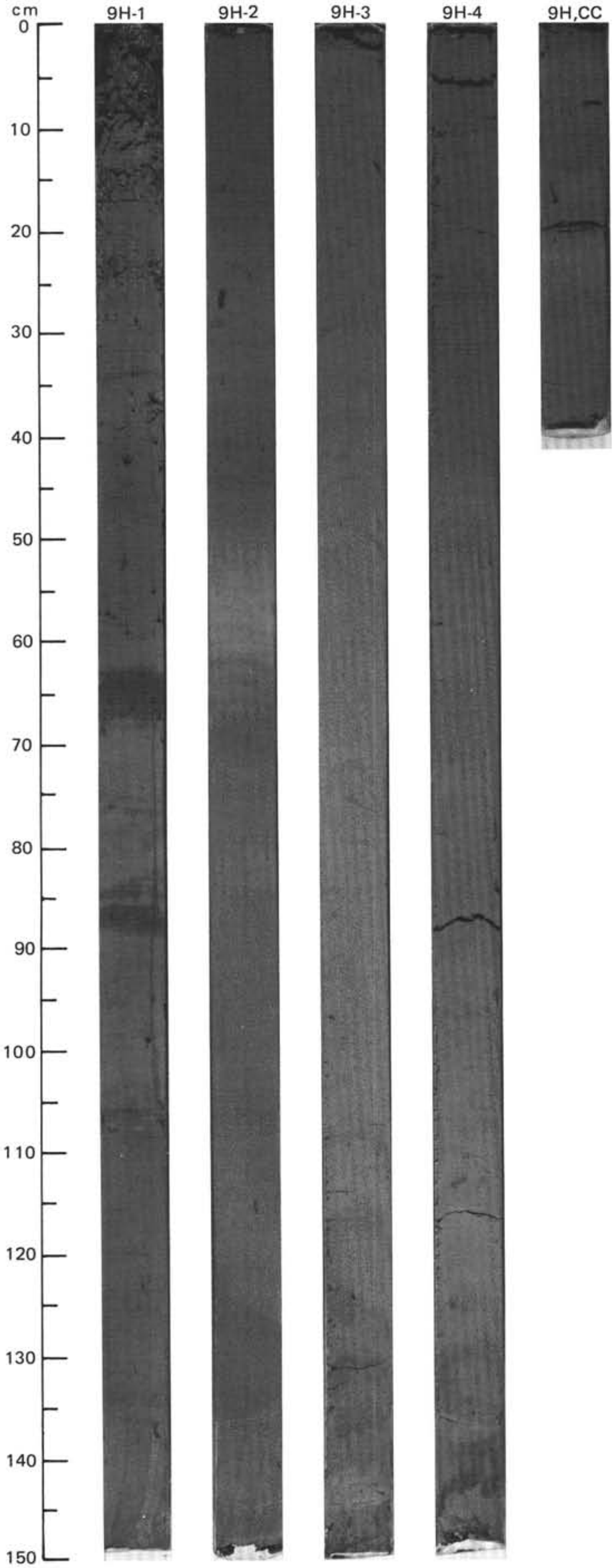
cm
0
10
20
30
40
50
60
70
80
90
100
110
120
130
140
150
9H-1
9H-2
9H-3
9H-4
9H,CC

SITE 644 HOLE B CORE 10H CORED INTERVAL 1306.5-1316.0 mbsl; 80.6-90.1 mbsf

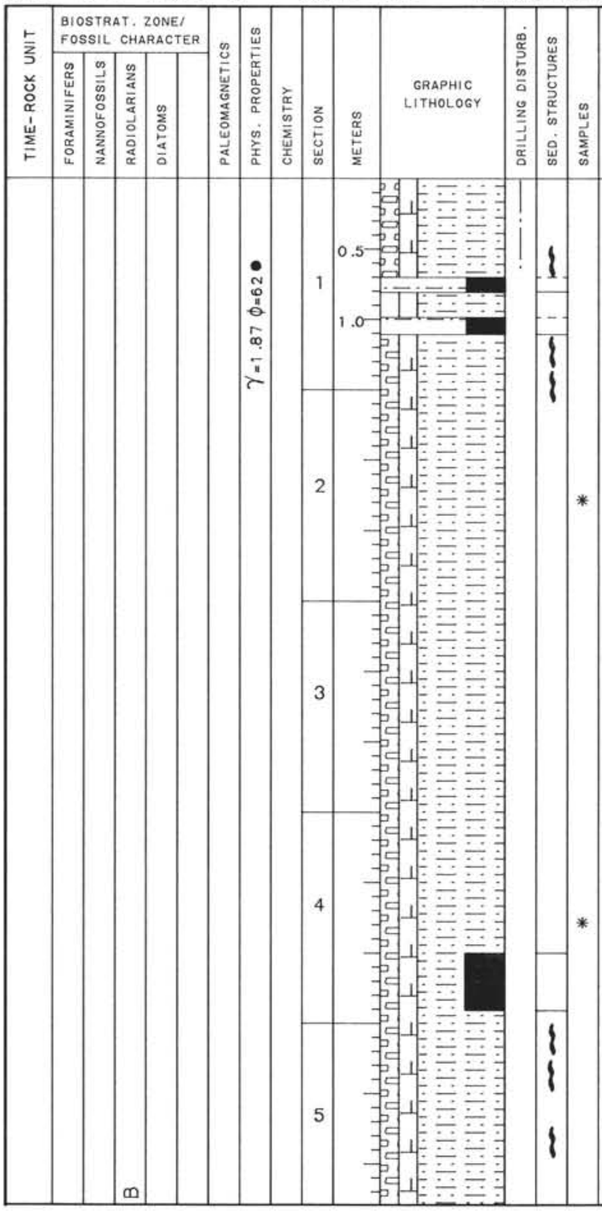

LITHOLOGIC DESCRIPTION

MUD TO CALCAREOUS MUD

Section 1, 0–41 cm, is moderately disturbed; remainder of core is undisturbed.

Major lithology: Mud to calcareous mud, olive gray (5Y 4/2) to dark grayish brown (2.5Y 4/2), with common pyritized burrows and rare to common small pyrite concretions.

Minor lithology: Mud to sandy mud, very dark gray (5Y 3/1), with sharp base and gradational top, common to abundant small pyrite concretions and dropstones. Section 1, 73–83 and 98–111 cm.

SMEAR SLIDE SUMMARY (%):

	2, 75 D	4, 75 D
TEXTURE:		
Sand	30	15
Silt	30	30
Clay	40	55
COMPOSITION:		
Quartz	30	15
Clay	38	42
Volcanic glass	—	5
Calcite/dolomite	20	5
Accessory minerals:		
Pyrite	5	Tr
Nannofossils	7	30
Diatoms	—	Tr
Sponge spicules	—	Tr
Fish remains	—	Tr

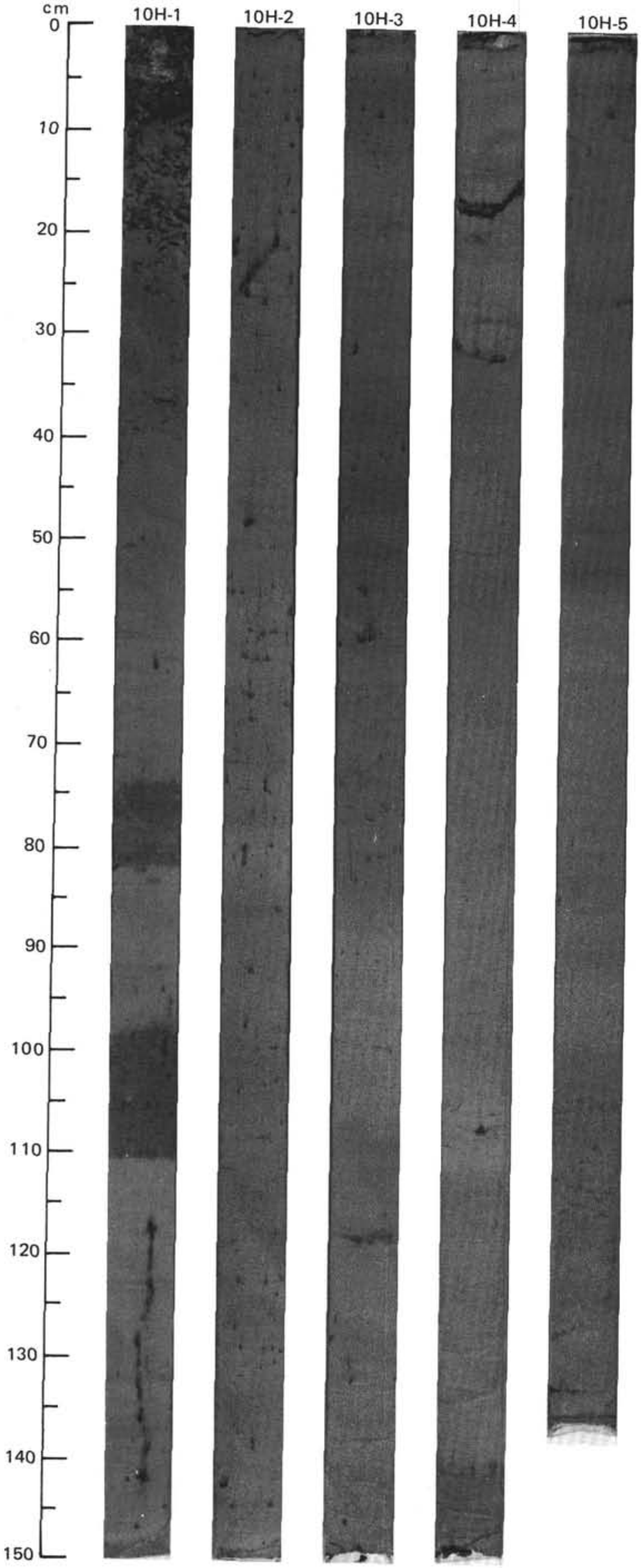
cm
0
10
20
30
40
50
60
70
80
90
100
110
120
130
140
150
10H-1
10H-2
10H-3
10H-4
10H-5

SITE 644 HOLE B CORE 11H CORED INTERVAL 1316.0-1321.8 mbsl; 90.1-95.9 mbsf

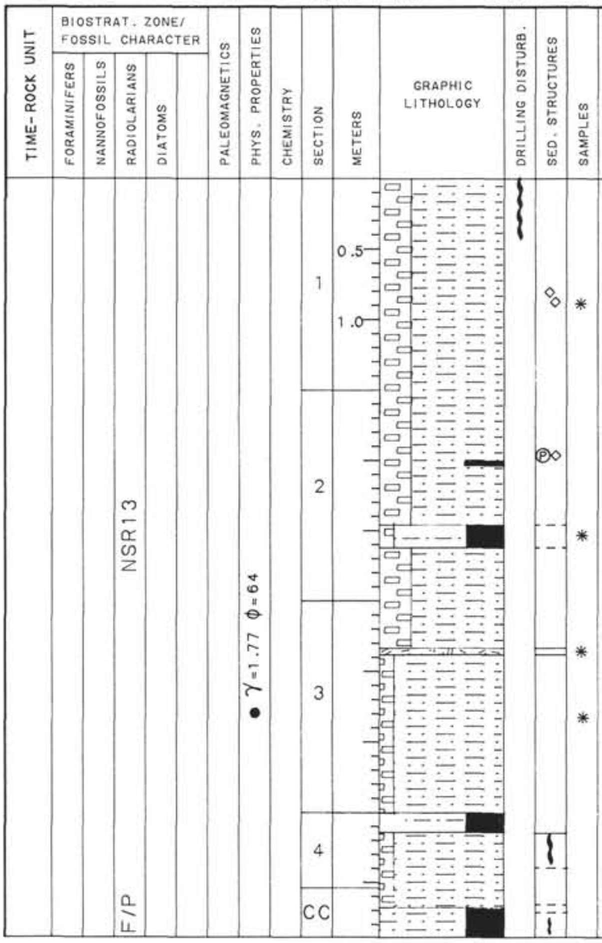

LITHOLOGIC DESCRIPTION

MUD TO CALCAREOUS MUD

Section 1, 0–53 cm, is highly disturbed; remainder of core is undisturbed.

Major lithology: Mud to calcareous mud, olive gray (5Y 4/2) to dark grayish brown (2.5Y 4/2), with rare to common pyritized burrows and cm-scale bioturbation/mottling. Rare dropstones.

Minor lithologies:
a. Mud to sandy mud, very dark gray (5Y 3/1), with minor to common dropstones. Section 2, 98–112 cm; Section 4, 0–14 cm; CC, 18–34 cm.
b. Volcanic ash, light gray (5Y 7/1), with sharp lower and upper contacts. Section 3, 35–39 cm.

SMEAR SLIDE SUMMARY (%):

	1, 135 D	2, 105 M	3, 38 M	3, 80 D
TEXTURE:				
Sand	15	10	90	5
Silt	30	30	10	20
Clay	55	60	—	75
COMPOSITION:				
Quartz	30	20	—	13
Clay	42	55	—	63
Volcanic glass	Tr	—	70	—
Calcite/dolomite	20	15	—	12
Accessory minerals	Tr	5	30	1
Foraminifers	Tr	Tr	—	2
Nannofossils	5	5	—	7
Diatoms	—	—	—	Tr
Fish remains	—	—	—	Tr

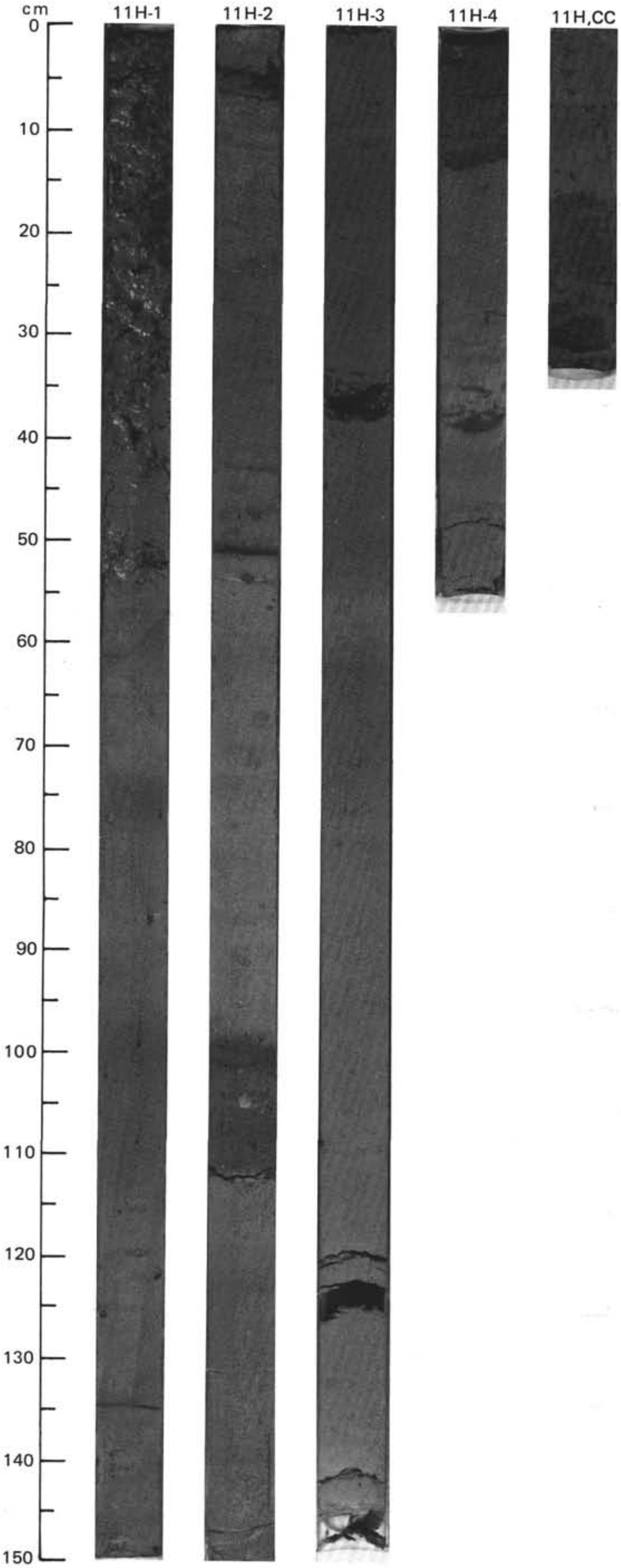
cm
0
10
20
30
40
50
60
70
80
90
100
110
120
130
140
150
11H-1
11H-2
11H-3
11H-4
11H,CC

SITE 644 HOLE B CORE 12H CORED INTERVAL 1321.8-1331.6 mbsl; 95.9-105.7 mbsf

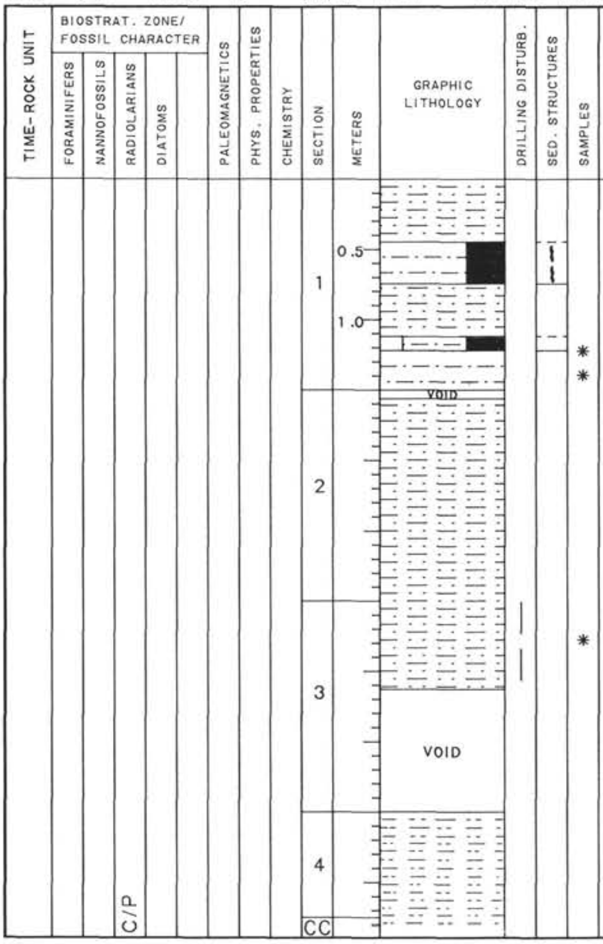

LITHOLOGIC DESCRIPTION

MUD TO SANDY MUD

Section 3 is slightly disturbed; remainder of core is undisturbed.

Major lithology: Mud to sandy mud, olive gray (5Y 4/2) to dark grayish brown (2.5Y 4/2), with minor pyritized burrows. Rare small pyrite concretions in Section 1.

Minor lithology: Mud to sandy mud, very dark gray (5Y 3/1), with sharp base and gradational top, common small pyrite concretions and dropstones. Section 1, 46–74 and 113–123 cm.

SMEAR SLIDE SUMMARY (%):

	1, 120 M	1, 140 D	3, 30 D
TEXTURE:			
Sand	20	35	10
Silt	25	30	20
Clay	55	35	70
COMPOSITION:			
Quartz	30	60	30
Feldspar	3	3	Tr
Rock fragments	Tr	—	—
Clay	48	28	63
Volcanic glass	—	2	—
Calcite/dolomite	15	—	—
Accessory minerals:			
Pyrite	2	2	2
Foraminifers	—	3	Tr
Nannofossils	—	2	—
Diatoms	—	—	2
Sponge spicules	—	—	Tr
Fish remains	Tr	—	—

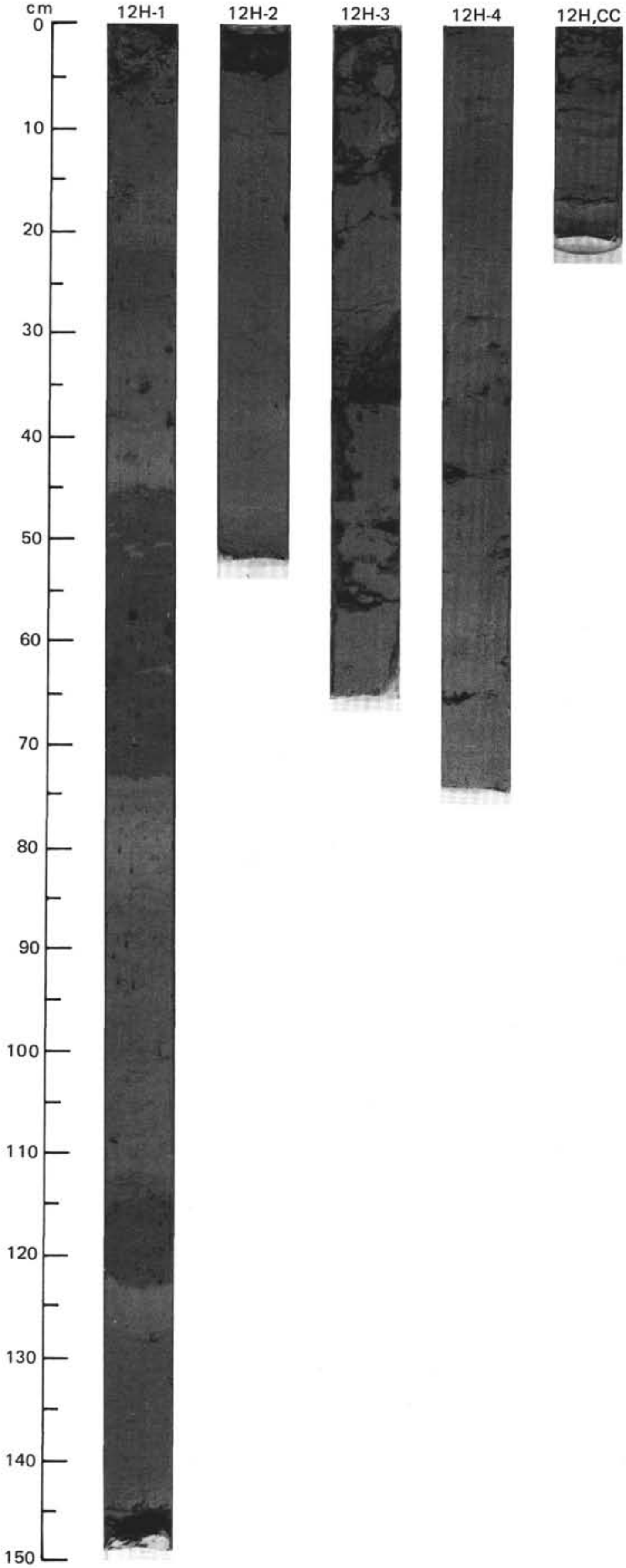
cm
0
10
20
30
40
50
60
70
80
90
100
110
120
130
140
150
12H-1
12H-2
12H-3
12H-4
12H,CC

SITE 644 HOLE B CORE 13H CORED INTERVAL 1331.6-1337.3 mbsl; 105.7-111.4 mbsf

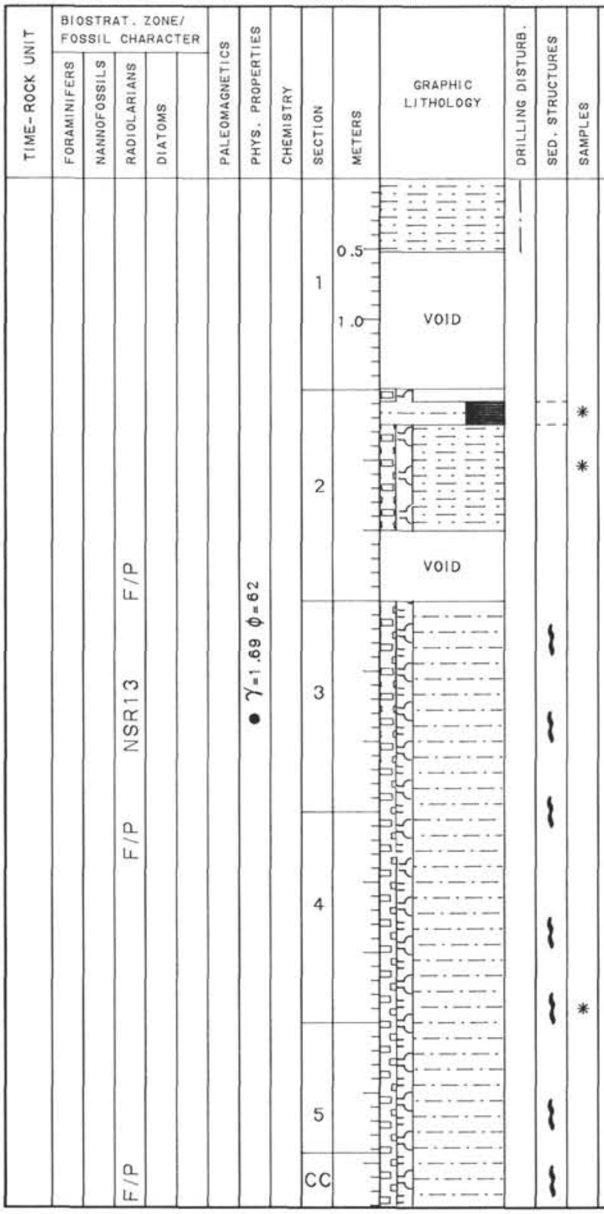

LITHOLOGIC DESCRIPTION

SILICEOUS CALCAREOUS MUD TO SILICEOUS SANDY MUD

Section 1 is moderately disturbed; remainder of core is undisturbed.

Major lithology: Siliceous calcareous to siliceous sandy mud, olive gray (5Y 4/2 and 5Y 5/2), with common to abundant pyritized burrows.

Minor lithology: Mud to sandy mud, very dark gray (5Y 3/1), with dropstone. Section 2, 8–24 cm.

SMEAR SLIDE SUMMARY (%):

	2, 15 M	2, 60 D	4, 140 D
TEXTURE:			
Sand	35	20	30
Silt	20	30	20
Clay	45	50	50
COMPOSITION:			
Quartz	40	25	30
Feldspar	5	Tr	—
Mica	Tr	—	—
Clay	35	45	43
Calcite/dolomite	15	—	10
Accessory minerals:			
Pyrite	3	3	Tr
Glauconite	Tr	Tr	—
Foraminifers	—	5	5
Nannofossils	—	10	Tr
Diatoms	Tr	7	10
Sponge spicules	—	2	—
Silicoflagellates	—	2	—

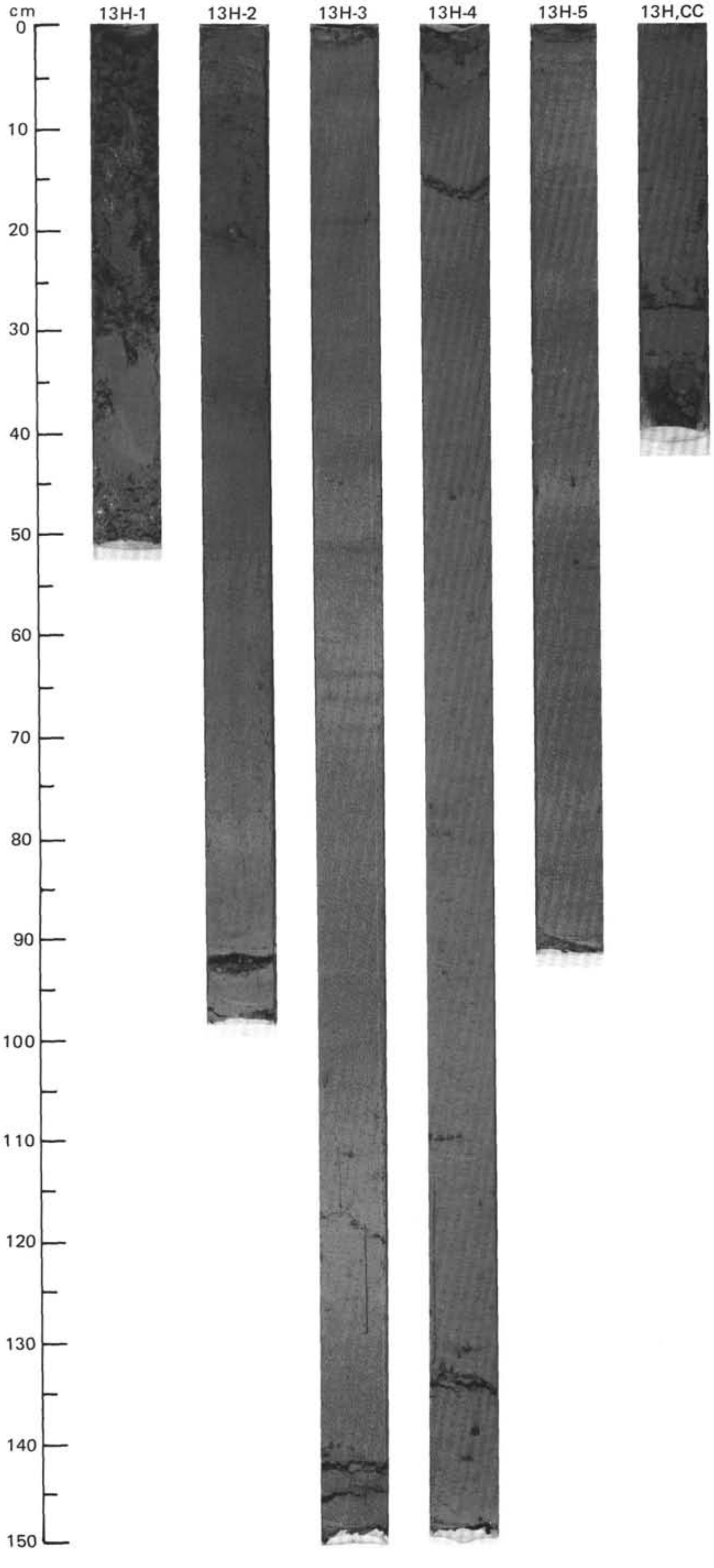
cm
0
10
20
30
40
50
60
70
80
90
100
110
120
130
140
150
13H-1
13H-2
13H-3
13H-4
13H-5
13H,CC

SITE 644 HOLE B CORE 14H CORED INTERVAL 1337.3-1345.1 mbsl; 111.4-119.2 mbsf

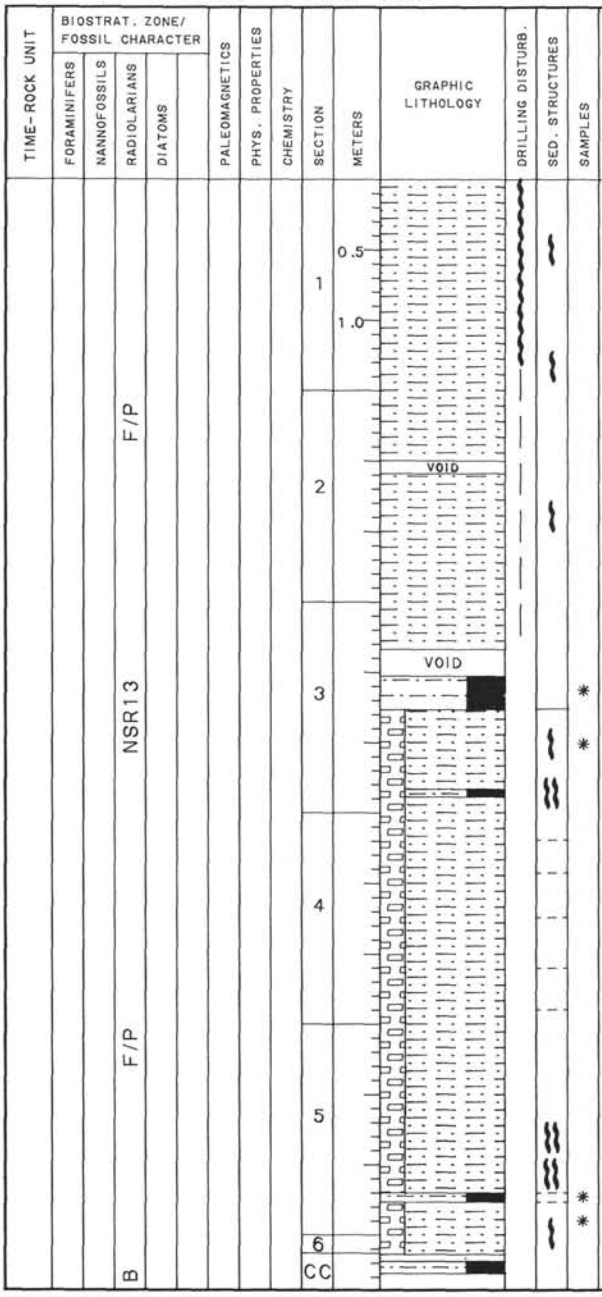

LITHOLOGIC DESCRIPTION

MUD TO CALCAREOUS MUD

Section 1 is very disturbed; Section 2 is slightly disturbed; Section 3, 35–53 cm, is a void; remainder of core is undisturbed.

Major lithology: Mud to calcareous mud, olive gray (5Y 4/2) and dark grayish brown (2.5Y 4/2), with common pyritized burrows and rare to common cm-scale bioturbation/mottling.

Minor lithology: Mud and sandy mud, very dark gray (5Y 3/1), with rare to common small pyrite concretions and dropstones. Section 3, 53–78 cm; Section 5, 123–126 cm; CC, 9–14 cm.

SMEAR SLIDE SUMMARY (%):

	3, 65 M	3, 100 D	5, 120 M	5, 140 D
TEXTURE:				
Sand	30	5	15	10
Silt	20	25	20	25
Clay	50	70	65	65
COMPOSITION:				
Quartz	30	10	20	20
Feldspar	—	—	5	—
Rock fragments	3	—	Tr	—
Mica	2	Tr	Tr	—
Clay	50	64	57	58
Volcanic glass	—	Tr	Tr	—
Calcite/dolomite	7	10	10	10
Accessory minerals:				
Pyrite	2	1	3	2
Glauconite	2	1	Tr	Tr
Foraminifers	3	5	—	Tr
Nannofossils	Tr	7	—	7
Diatoms	—	—	Tr	2

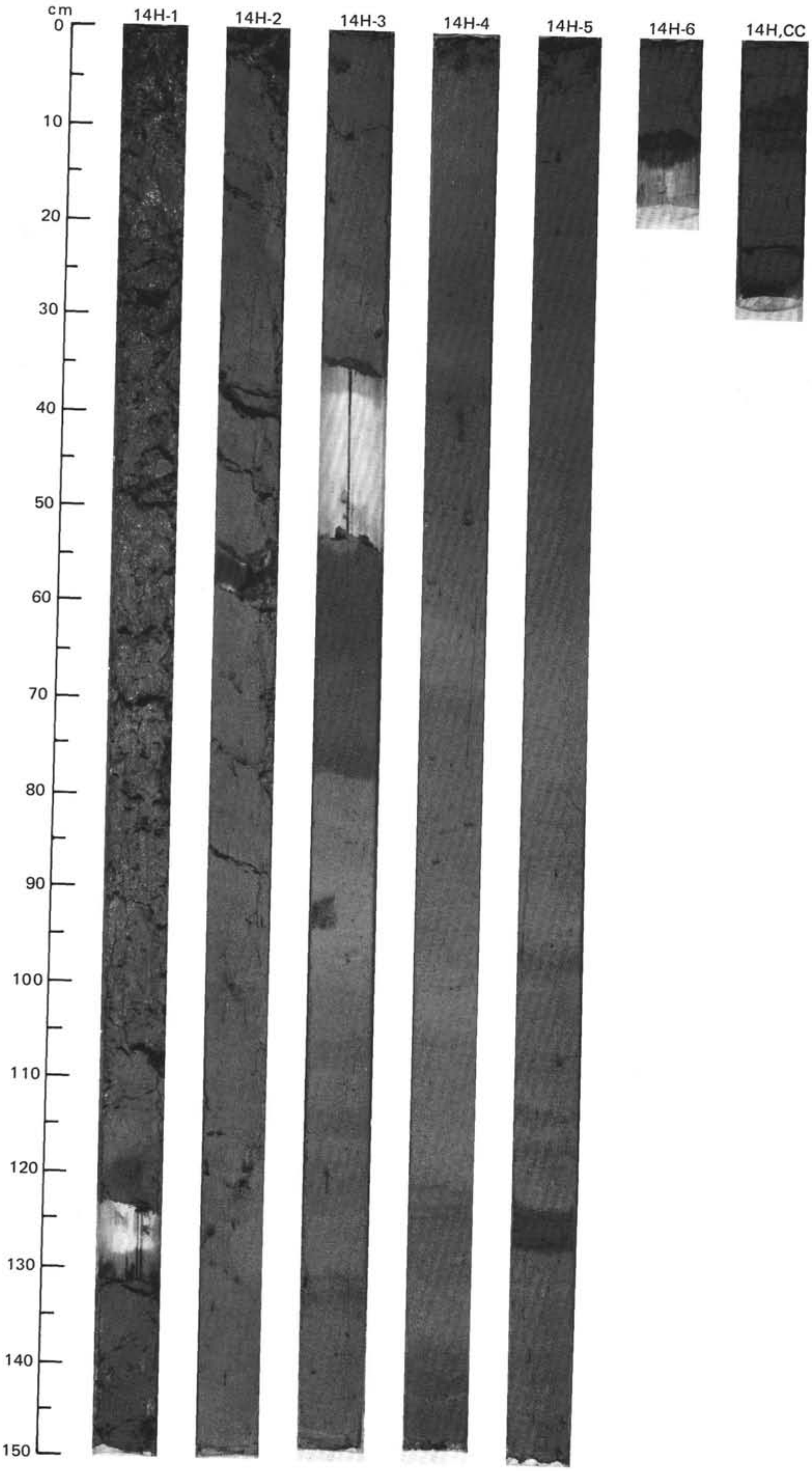
cm
0
10
20
30
40
50
60
70
80
90
100
110
120
130
140
150
14H-1
14H-2
14H-3
14H-4
14H-5
14H-6
14H,CC

SITE 644 HOLE B CORE 15H CORED INTERVAL 1345.1-1353.5 mbsl; 119.2-127.7 mbsf

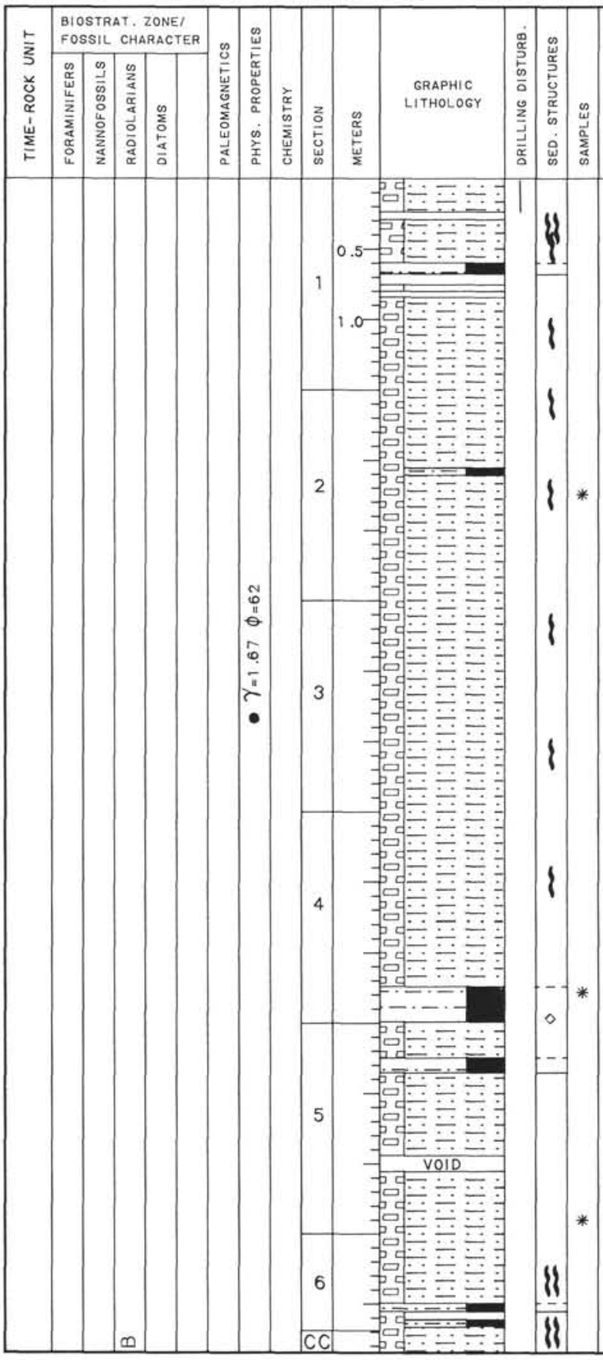

LITHOLOGIC DESCRIPTION

MUD TO CALCAREOUS MUD

Section 1, 0–14 cm, is moderately disturbed; Section 1, 14–29, 69–74, and 80–84 cm, and Section 5, 96–107 cm, are voids; remainder of core is undisturbed.

Major lithology: Mud to calcareous mud, olive gray (5Y 4/2) to dark grayish brown (2.5Y 4/2), with minor to common pyritized burrows and cm-scale bioturbation/mottling. Some gradational and indistinct interbedding of these colors.

Minor lithology: Mud to sandy mud, very dark gray (5Y 3/1), with sharp base and gradational top, minor dropstones. Section 1, 60–67 cm; Section 4, 123–150 cm; Section 5, 25–36 cm; Section 6, 50–55 cm.

SMEAR SLIDE SUMMARY (%):

	2, 75 D	4, 130 D	5, 140 D
TEXTURE:			
Sand	5	15	5
Silt	30	25	25
Clay	65	60	70
COMPOSITION:			
Quartz	15	20	15
Feldspar	—	5	—
Mica	2	—	—
Clay	60	53	62
Volcanic glass	Tr	—	Tr
Calcite/dolomite	10	10	5
Accessory minerals:			
Pyrite	2	3	Tr
Glauconite	—	2	—
Foraminifers	Tr	—	Tr
Nannofossils	7	Tr	10
Diatoms	2	Tr	5

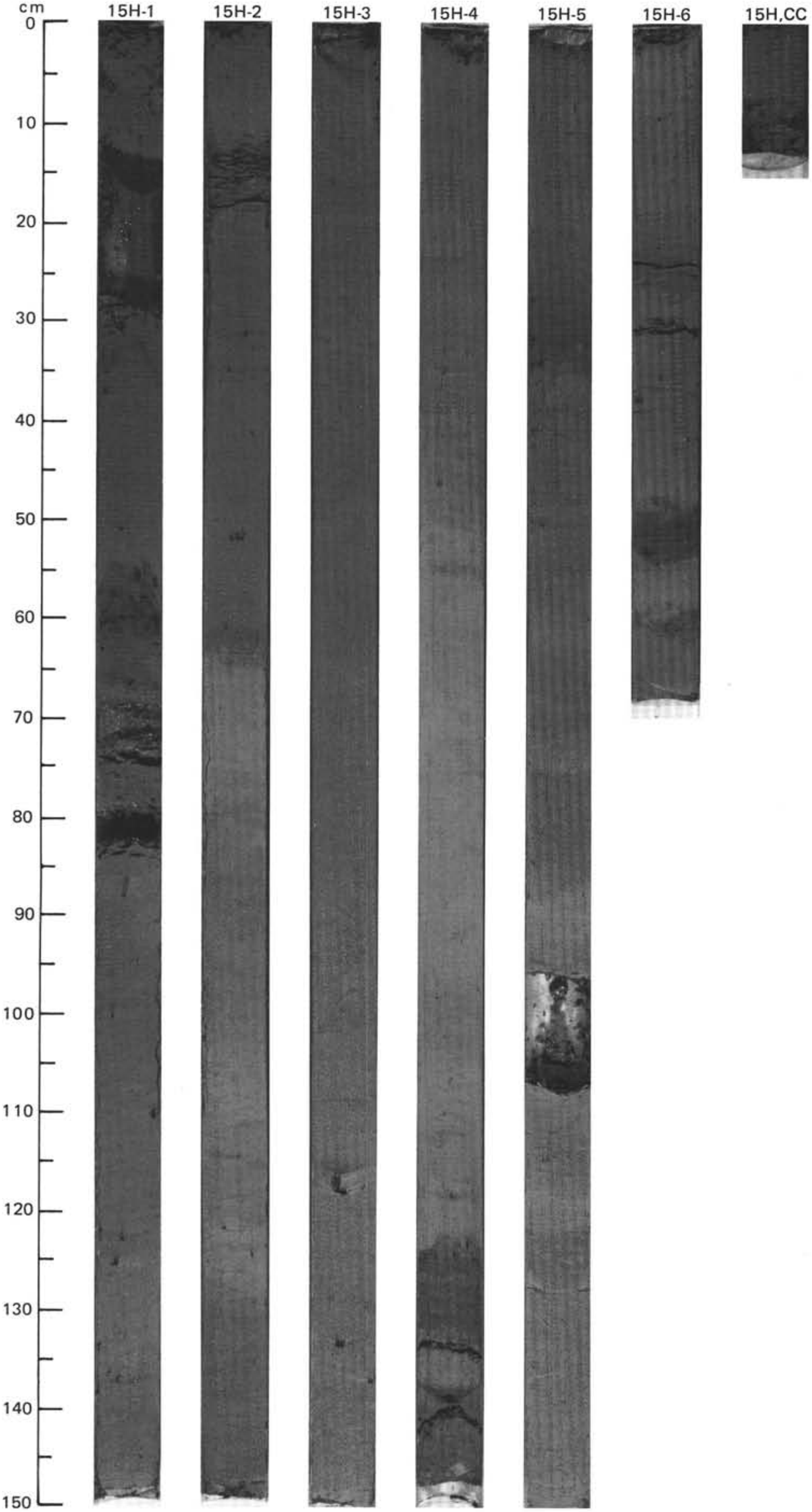
cm
0
10
20
30
40
50
60
70
80
90
100
110
120
130
140
150
15H-1
15H-2
15H-3
15H-4
15H-5
15H-6
15H,CC